THE SYNTHESIS OF URETHANE ACRYLATE RESIN FROM PALM FATTY ACID DISTILLATE AND SOME MECHANICAL PROPERTIES

TEO KIM TECK

FACULTY OF SCIENCE
UNIVERSITY OF MALAYA
KUALA LUMPUR

2020

THE SYNTHESIS OF URETHANE ACRYLATE RESIN FROM PALM FATTY ACID DISTILLATE AND SOME MECHANICAL PROPERTIES

TEO KIM TECK

THESIS SUBMITTED IN FULFILMENT OF THE REQUIREMENTS FOR THE DEGREE OF DOCTOR OF PHILOSOPHY

DEPARTMENT OF CHEMISTRY
FACULTY OF SCIENCE
UNIVERSITI MALAYA
KUALA LUMPUR

2020

UNIVERSITI MALAYA

ORIGINAL LITERARY WORK DECLARATION

Name of Candidate: **TEO KIM TECK**

Matric No.: **SHC130033**

Name of Degree: **DOCTOR OF PHILOSOPHY**

Title of Thesis ("this Work"):

THE SYNTHESIS OF URETHANE ACRYLATE RESIN FROM PALM FATTY ACID DISTILLATE AND SOME MECHANICAL PROPERTIES

Field of Study:

POLYMER CHEMISTRY

I do solemnly and declare that:

(1) I am the sole author/writer of this Work;
(2) This Work is original;
(3) Any use of any work in which copyright exists was done by way of fair dealing and for permitted purposes and any except or extract from or reference to or reproduction of any copyright work has been disclosed expressly and sufficiently and the title of the Work and its authorship have been acknowledged in this Work;
(4) I do not have actual knowledge nor do I ought reasonably to know that the making of this work constitutes an infringement of any copyright work;
(5) I hereby assign all and every rights in the copyright to this Work to the University of Malaya ("UM"), who henceforth shall be owner of the copyright in this Work and that any reproduction or use in any form or by any means whatsoever is prohibited without the written consent of UM having been first had and obtained;
(6) I am fully aware that if in the course of making this Work I have infringed any copyright whether intentionally or otherwise, I may be subject to legal action or any other action as may be determined by UM.

Candidate's Signature Date 5/06/2020

[redacted]

Subscribed and solemnly before,

Witness's Signature Date 5/06/2020

Name:

Designation:

THE SYNTHESIS OF URETHANE ACRYLATE RESIN FROM PALM FATTY ACID DISTILLATE AND SOME MECHANICAL PROPERTIES

ABSTRACT

Depletion of petroleum reserves and increasing environmental concerns have stimulated the efforts to explore materials from readily available, renewable natural resources, such as carbohydrates, oils, fats and proteins. Plant oil and its fatty acids are promising renewable resources to produce environmentally friendly polymeric materials. Palm oil is a major crop in Malaysia and consequently palm fatty acid distillate (PFAD) has been an abundant by-product during the refinery process. PFAD could be a renewable raw material for industrial application. Thus, we develop new PFAD-based acrylate resins UV curable for coatings applications. The resins could be produced by two approaches. Firstly, mixtures of varying amount of PFAD, isophthalic acid, phthalic anhydride, neopentyl glycol and pentaerythritol were reacted to produce hydroxyl terminated macromers. Five macromers with 15, 25, 45, 55 and 70% of PFAD were synthesized. Each macromer was reacted with toluene diisocyanate and 2-hydroxyl ethyl acrylate to produce a UV curable urethane acrylate resin. The content of PFAD has significant influence on the final UV cured film. The urethane acrylate resins with 15–55% PFAD in the macromers, could be UV-cured to form hard films with a T_g of 35–62°C. These resins have potential application for wood coatings. However, urethane acrylate resin with 70% PFAD, cured to form a soft film with $T_g < 30$°C and not useful for coating application. In particular, at around 45% PFAD, the resin could be UV-cured in 60 s to film that has achieved pendulum hardness of 107 s and T_g of 54°C. In the second approach, the influence of different polybasic acids in PFAD-based urethane acrylate resin synthesis was studied. A series of PFAD urethane acrylate resins were synthesized, fixing the PFAD at 45%, and using isophthalic acid (IPA), terephthalic acid (TPA), phthalic anhydride (PA) and adipic acid (AA) as polybasic acid building block. All macromers were formulated with same hydroxyl value at 91 mgKOH/g and polybasic acid equivalent of 0.32 g/mol in 100 g of resin. The results showed that the different structure of polybasic acid has affected the performance of urethane acrylate resin. Generally, aromatic type of polybasic acid can produce higher T_g and hardness of UV cured film. Outstanding mechanical and physical properties such as adhesion, solvent, water, corrosion resistant can be achieved by using aromatic diacids in metal coating application. To a certain extent, good weathering resistance can be achieved on metal coating. Aliphatic type of diacid could impart good flexibility and soft film formation on the PFAD urethane acrylate UV cured film.

Keywords: palm fatty acid distillate (PFAD), urethane acrylate, UV curing, T_g, pendulum hardness

SINTESIS RESIN URETANA AKRILAT DARI DISTILAT ASID LEMAK KELAPA SAWIT DAN BEBERAPA SIFAT MEKANIKAL

ABSTRAK

Kekurangan bahan sumber petrolum dan peningkatan kesedaran mesra alam telah merangsang revolusi dalam menerokai bahan semula jadi yang sedia ada serta boleh diperbaharui seperti karbohidrat, minyak, lemak dan protein. Minyak tumbuhan and asid lemaknya merupakan sumber yang berkesan untuk menghasilkan bahan polimer mesra alam. Kelapa sawit merupakan tanaman utama di Malaysia dan banyak asid lemak sawit distilat (PFAD) telah dihasilkan sebagai produk sampingan semasa proses penapisan minyak kelapa sawit. PFAD menjadi bahan mentah yang boleh diperbaharui untuk applikasi industri. Oleh itu, dalam kajian ini, kami merekabentuk resin akrilat berasaskan PFAD untuk applikasi salutan pengeringan ultraviolet (UV). Resin ini boleh dihasilkan melalui dua cara. Pertamanya, campuran pelbagai jumlah PFAD bertindak balas dengan asid isophatalik, phthalik anhidrida, neopentil glikol and pentaerythritol untuk menghasilkan makromer yang diakhiri dengan hidroksil. Lima makromer dengan kandungan PFAD 15, 25, 45, 55 dan 70% telah disintesis. Setiap makromer dikopolimerkan dengan toluena diisosianat dan 2-hidroksil etil akrilat untuk menghasilkan resin uretana akrilat berasaskan pengeringan UV. Kandungan PFAD mempunyai pengaruh penting dalam filem yang dikeringkan secara UV. Resin makromer uretana akrilat yang mengandungi PFAD 15-55% boleh dikeringkan secara UV untuk menghasilkan filem salutan yang keras dengan T_g dalam linkungan suhu antara 35-62°C. Resin ini mempunyai potensi aplikasi untuk penyalutan kayu. Namun, resin uretana akrilat dengan 70% PFAD, dikeringkan hanya membentuk filem lembut dengan $T_g < 30°C$ dan tidak berguna untuk aplikasi salutan. Secara khususnya, resin dengan kandungan sebanyak 45% PFAD yang dikeringkan secara UV dalam tempoh 60 s telah menghasilkan filem yang menunjukkan kekerasan pendulum sebanyak 107 s dan suhu peralihan kaca (T_g) 54°C. Dalam pendekatan kedua, pengaruh pelbagai asid polibasic dalam resin uretana akrilat berasaskan PFAD telah dikaji. Satu siri resin PFAD uretana akrilat telah disintesis dengan menetapkan PFAD sebanyak 45% dan menggunakan asid isophthalik (IPA), asid terephthalik (TPA), phthalik anhidrida (PA) dan asid adipik (AA) sebagai blok binaan berasaskan polibasic asid. Semua makromer telah diformulasikan dengan nilai hidrosil yang sama iaitu 91 mg KOH/g dan nilai polibasic asid sebanyak 0.32 g/mol dalam 100 g resin. Keputusan kajian menunjukkan struktur asid polibasik yang berlainan telah mempengaruhi prestasi resin uretana akrilat. Secara umum, asid polibasik jenis aromatik boleh menghasilkan filem salutan yang mempunyai T_g dan kekerasan yang tinggi. Sifat-sifat mekanikal dan fizikal yang tinggi seperti lekatan, penahanan ke atas pelarut, air and kakisan boleh dicapai dengan penggunaan diasid jenis aromatik untuk kegunaan salutan logam. Dalam jangkauan tertentu, rintangan cuaca yang baik boleh juga dicapai bagi salutan logam. Diasid jenis alifatik boleh memberikan fleksibiliti dan kelembutan yang baik ke atas filem salutan PFAD uretana akrilat yang dikeringkan secara UV.

Kata kunci: lemak sawit distilat (PFAD), uretana akrilat, UV pemulihan, T_g, kekerasan pendulum

ACKNOWLEDGEMENTS

I express my deepest and sincerest gratitude and utmost appreciation to my supervisor: Professor Dr. Gan Seng Neon and Professor Dr. Aziz Bin Hassan for their generous guidance, support and motivation throughout this study. All patience and help during my candidature and the tireless proofreading efforts for publication works and thesis from both of them are highly appreciated. I learned how to think as a doctor, how to behave professionally, and how to be a scientist from them. I will model myself on both of them as an excellent scientist, professor, mentor, and leader. A very special thanks to Professor Dr. Gan Seng Neon, appreciate his willingness and full support walking through my PhD study even after his retirement.

I thank the staff of Chemistry Department for all their support. I also express appreciation to the former members of Prof. Gan research group; Dr Lee Siang Yin and Dr Nurshafiza for their cooperation and assistant in Prof. Gan's research laboratory work and department.

I reserve a special mention to my beloved family who has been the fundamental base for every success and to whom this work is dedicated, especially my wife, Ms. Tan Bee Swan for her endless support, perseverance and patience throughout my study years. I could not have done this without her support.

Thanks to University Malaya for the financial support through the PPP research grant PG091-2014B.

TABLE OF CONTENTS

CHAPTER 2: LITERATURE REVIEW…….…………………………………….. 66

CHAPTER 3: EXPERIMENTAL………..……………………………………….. 77

CHAPTER 4: RESULTS AND DISCUSSIONS……………………………….. **155**

LIST OF FIGURES

LIST OF TABLES

LIST OF SCHEMES

LIST OF SYMBOLS AND ABBREVIATIONS

cm^{-1}	: Wave number unit of reciprocal centimetres
s	: second
v/v	: volume/volume
w/w	: weight/weight
AA	: Adipic acid
ATR-FTIR	: Attenuated total reflection- Fourier-transform infrared
DSC	: Differential scanning calorimetry
EB	: Electron beam
EEW	: Epoxide equivalent weight
EMM	: Epoxy molar mass
Eqn	: Equation
GPC	: Gel permeation chromatography
2-HEA	: 2-Hydroxyl ethyl acrylate
IPA	: Isophthalic acid
NCO	: Isocyanate group
NPG	: Neopentyl glycol
Tm	: Melting temperature
M-PFAD	: Macromer palm fatty acid distillate
M_w	: Molecular weight
PA	: Phthalic anhydride
PDI	: Polydispersity index
PFAD	: Palm fatty acid distillate
TDI	: Toluene diisocyanate

Tg	: Glass transition temperature
TPA	: Terephthalic acid
TPGDA	: Tripropylene glycol diacrylate
UA	: Urethane acrylate
UV	: Ultra violet
VOC	: Volatile organic compound
WPE	: Weight per epoxide

CHAPTER 1: INTRODUCTION

1.1 An Overview of Surface Coating Technologies

Archaeology has discovered the painting history has been as old as mankind history even in the stone age era. In ancient painting, mankind was using many natural resources such as high mineral content colour stone to draw picture for recording or communication purposes. In the painting evolution timeline, the painting has been evolved from simple natural resources usage to more and more complex surface coating system align with the new technique and discoveries of new coating material. Today, surface coating has become a unique branch of advanced chemical technology industry. We had seen the transformation of manufacturing paint from an art to a science application since twentieth century. The availability of raw materials increased from a few natural extractions, such as linseed oil, turpentine, mineral earth and inorganic colour to a vast range of complex synthetic organic chemicals, which required technical specialists. The development of the surface coatings industry over the last thirty years, has been more rapid than previously. Figures 1.1 and 1.2 attempt to show graphically, as sigmoidal technologically maturity graphs (Roussel, P. A. 1984).

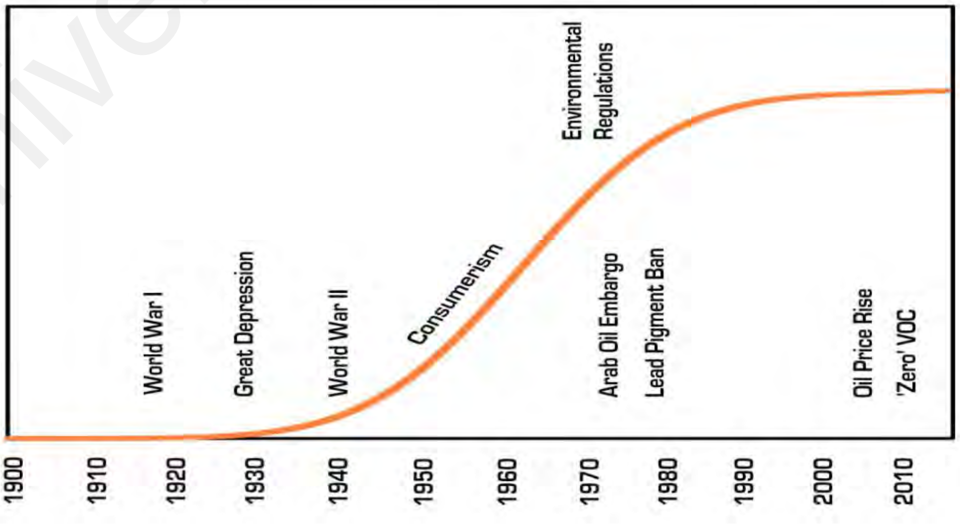

Figure 1.1 The rise of paint technology from the start of the twentieth century. Reproduced from Roussel, P.A. @ Research Management 1984

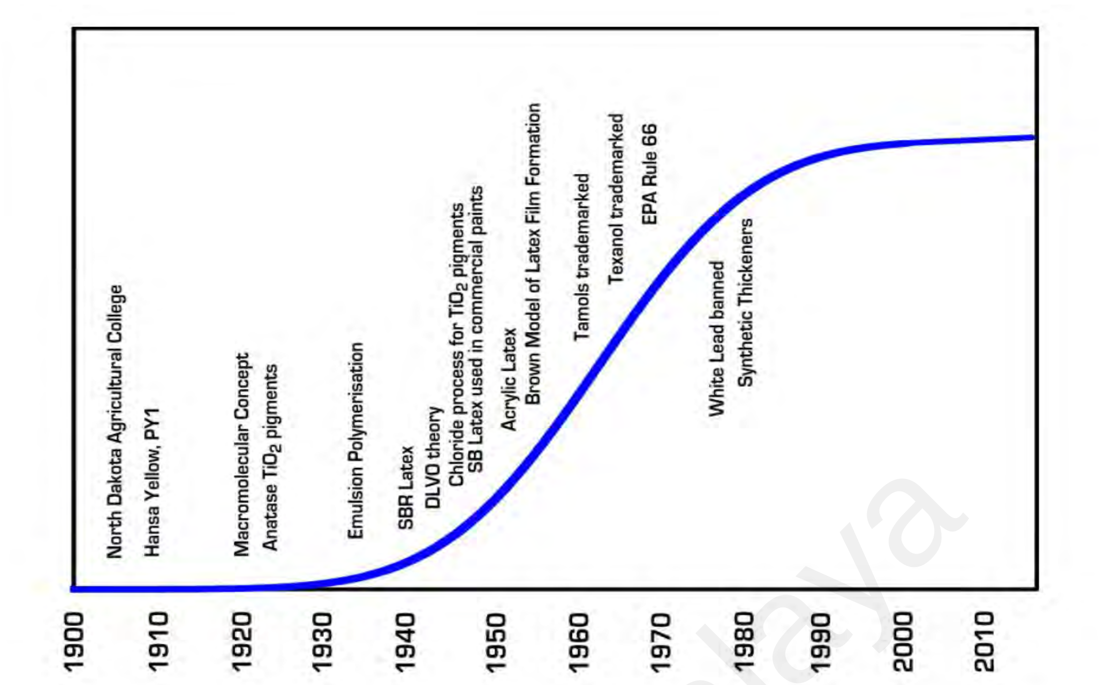

Figure 1.2 Important developments in paint technology from the start of twentieth century. Reproduced from Roussel, P.A. @ Research Management 1984

Whilst paint manufacturers still rely on many natural sources of raw materials during 1930s, crucial development in the science and technology occurred when Hermann Staudinger realized that polymers were very large, covalently bonded molecules or macromolecules (Staudinger, 1920; Morawetz, 1987). The earliest peak of technological changes probably occurred in the 1950s and 1960s, and their effects were felt primarily in the industrial application of coatings intended to provide increasing level of performance. The technology advancement has been progressive for purely synthetic polymer to produce high quality and consistency in supply for industrial application. Align with the technology improvement especially on industrial manufacturing environment, the method of application and curing of coating materials, the nature of substrate and the conditions of use have been more complex than before. Hence, the technology used in creating coatings has never been better than it is today. The development has evolved traditional coating technologies with modern colloidal chemistry to combine many newly available materials in the coating formulation. The technology advancement stream has allowed the coating industry to provide many types of finishes that can meet the required performance, appearance and most recently to meet environmental needs. This is especially true of liquid coatings for the high solid and low VOC formulations for industrial finishes. The method of application and cure conditions have been changed from simple atmospheric oxidation or evaporation of diluent to complex and advanced curing concept. Due to large scale production, many application methods have been developed and applied in modern industries environment such as vacuum coating, electrodeposition, coil coating, curtain coating, electrostatic spray and robotic spray. Due to the different coating film properties required by the industries there are various available processes. The most common being the thermosetting process that uses heat to cure a paint film. Other technologies use chemical reactions to achieve the required film properties, these include the acid catalysed system, polyurethane system and epoxy polyamide or polyamine curing. The continued industrial development and new requirements are driven by environmental concerns, leading to many new coating technologies. These new coating technologies include waterborne (thermosetting emulsion, colloidal dispersion, water-soluble) coatings, high-solids coatings, two-component chemical cross-linking systems, powder coatings and radiation-curable coatings. In principal, the new technologies can be grouped into five major classes: solvent based, water based, electrodeposition, power and radiation cure coatings.

Paint is a colloidal system with pigment or extender suspended in a liquid medium. The liquid medium is mostly composed of binders and solvents. Additives maybe added to achieve special characteristic or overcome some coating defects. The solvent evaporates from the drying film after application, while the binder holds the pigment in the dried film, which adheres to the substrate. Some high quality, high gloss paints are referred to as enamels (Piper, 1965; Schurr, 1981). Historically almost all coatings were employing solvent based formulations. However, since the 1960s a major driving force has been the need to reduce volatile organic compounds (VOC) emissions into the atmosphere. While there have been significant reductions in solvent usage by shifting to the other classes of coatings, another important approach has been to decrease the solvent content by formulating high solid coating~~s~~ systems, which have one major advantage over water-based coatings. They are less susceptible to environmental conditions such as temperature and humidity during the curing phase. High humidity can prevent the water in water-based coating from evaporating, making them impractical in some climates. In general, alkyds, polyesters, acrylic, epoxy, urethane and silicone resins were the principal binders used in solvent based coatings. These binders were diluted with organic solvent to achieve the application viscosity. The formation of films was from simple solvent evaporation, oxidation or chemical crosslinking such as via hydroxyl group of the resin with isocyanate or amino/melamine cross-linkers. The thermoplastic resins were occupying a significant fraction of earlier industrial coating application. The coatings were based on nitrocellulose, thermoplastic acrylic resins or chlorinated resin such as chlorinated rubber and vinyl chloride copolymers. The coatings can be easily dried under ambient conditions or force dry at low heating from 50-80°C. The nitrocellulose lacquer is still used in wood coating industry, the acrylic lacquers were commonly used in auto-refinishing and solution of vinyl and chlorinated rubber coatings continue to be used to some extend in water proofing and heavy-duty coatings application. The increased of coating film performance requirement has limited the usage of thermoplastic coating and resulted in the development of thermosetting coating or chemical cross-linking technologies. These coatings were possible with the development of cross-linkers such as melamine-formaldehyde, polyamine, polyamide and polyisocyanate resin as shown in Figure 1.3. The melamine-formaldehyde can be cross-linked with pendent hydroxyl group in the backbone of resin molecule via acid catalysed reactions at ambient temperature or heat cured at 120-230°C. The polyisocyanate can reacts readily with hydroxyl group of the resin at ambient temperature. Figure 1.3 shows some of the commercial cross-linkers. Due to the high quality of film performance, these coating systems have become major solvent-based system for coating plastic, auto refinishing, wood coating, heavy duty, automotive and many other industrial coating applications.

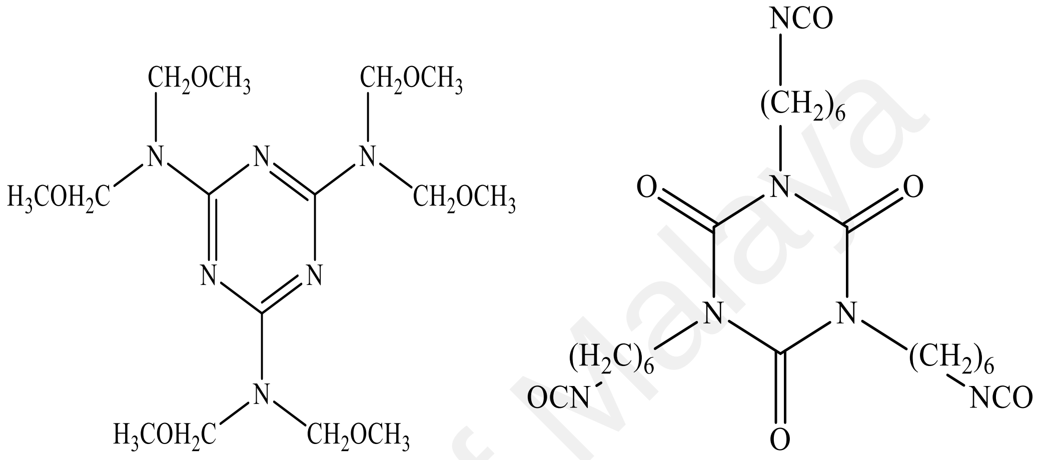

Hexa-methoxy methyl melamine

Isocyanurate of hexa-methylene diisocyanate

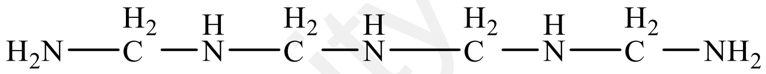

$$H_2N-\overset{H_2}{C}-\overset{H}{N}-\overset{H_2}{C}-\overset{H}{N}-\overset{H_2}{C}-\overset{H}{N}-\overset{H_2}{C}-NH_2$$

Tetraethylenepentamine

Figure 1.3 Chemical structures of some commercially available cross-linkers

Continuous efforts on reducing VOC and the demand for better materials have led to many improvements. The introduction of latex coatings were the major developments in water-based coatings. In 1970, latex paints were successfully introduced for architectural uses and marked the first major step away from solvent based coatings. The two largest classes of water-based coatings are water-reducible coating and latex coatings. In water reducible coating, the resin was not really soluble in water. Most are made from a high solid solution in water miscible solvents of resins with either carboxylic acid groups that are at least partially neutralized with low molecular weight amines. The majority of polymers used in industrial coatings are of the carboxylic acid functional type, and when neutralised with ammonia, they produce quaternary ammonium salts which render them water reducible, as shown in Figure 1.4.

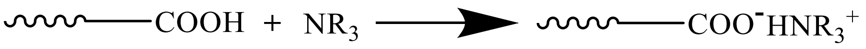

Figure 1.4 Neutralisation of acid functionality

However, polymer chains with basic groups could be neutralised by carboxylic acid such as acetic acid as shown in Figure 1.5.

Figure 1.5 Neutralisation of base functionality

Coatings made with water reducible resins have both advantages and limitations. The main advantage is that using higher molecular weight resin as in conventional thermosetting coating can be possible in the water reducible coating formulation. The resins can be easily cross-linked with melamine formaldehyde to produce cured film performance similar to a conventional thermosetting coating. The window of cure schedule is comparable to that conventional type and problem related to molecular weight and functionality of high solid coating are not encountered. A disadvantage is that the solid content is low. Typically, such coatings are applied by spraying, roller coating or curtain coating at around 20-30% non-volatile by volume. Since only about 20% volatile are organic solvent, the VOC emitted per unit volume of coating excluding water is fairly low. Water reducible coatings are used on large scale in can and metal panel coatings. In automotive, water reducible coating has been successful in topcoat application but the economics were such that solvent based high solid coatings were favoured. In recent water-borne urethane coating development, the water-borne two pack urethane coating has demonstrated adequate pot life for commercial usage (Zeno W. Wicks Jr. et al., 2002).

Latexes have been widely used for many years in decorative paints. In decorative coating formulation, the ingredients are aqueous dispersions. In modern technology, the resin dispersions were prepared via emulsion polymerization. The technology has evolved from a single monomer to a mixture of many acrylic or methyl acrylic monomers and their esters (Otto Rohm,1930). Figure 1.6 show some of the monomers used in acrylic for water-based coatings.

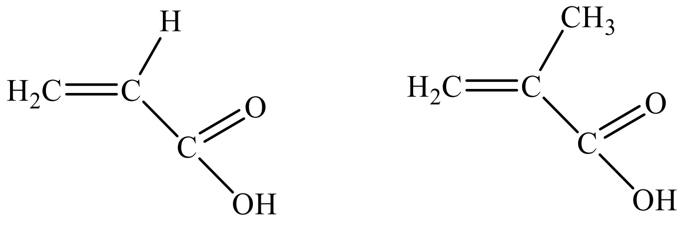

Acrylic acid Methacrylic acid

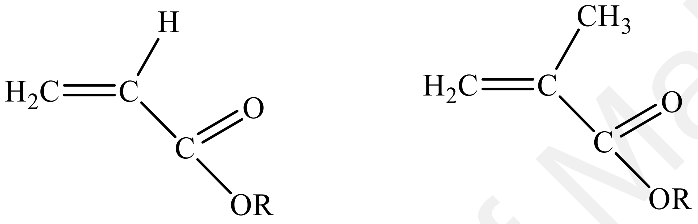

Ester of acrylic acid Ester of methacrylic acid

Where R is;

$-CH_3$	$-CH_2CH_3$	$-CH_2CH_2CH_2CH_3$	$-CH_2CH_2OH$	$-CH_2\text{-}CHOH\text{-}CH_3$
methyl	ethyl	n-butyl	hydroxyl ethyl	2-hydroxyl propyl

Figure 1.6 Chemical structure of acrylic and methacrylic acid and its ester

The latex forms film by coalescence of the polymer particle at temperature higher the Tg of the polymer itself (Eckersley et al., 1990; Kim H.B. et al., 1995). Since the latex paint film is formed by coalescence, there are limitations on the temperature required for good film formation. Another limitation of latex paints is the difficulty in formulating high gloss coatings due the random distribution of pigment particles and latex particles during the evaporation process leading to low gloss film formation. In addition, the presence of surfactant that is not compatible with the latex material will also lead to hazy or blooming film. Poor flow properties have also limited the latex coating in industrial applications. The flocculation of latex particles has resulted in relatively high degree of shear thinning, and in many cases, produced thixotropic characteristic. The emulsion polymerization can produce high molecular weight latexes that enable the coating to achieve excellent mechanical properties of the dried film without requiring further cross-linking reaction.

Rapid industrial manufacturing process has widened the usage of steel in industries such as automobile bodies and parts, tractors and heavy equipment, electrical switch gear, appliances, metal furniture, beverage containers, fasteners, and many other industrial products. The improvement of finding more effective coating's method for these complicated and complex surfaces has led to the development of electrodeposition technologies using electroplating chemistry. Generally, there are two type of electrodeposition: the anionic and cationic systems. The first cathodic electrodeposition coating was patented by BASF AG. PPG Industries Inc. in 1965 and successfully used in automotive industries in 1970 and has become the major electrodeposition coating in modern automotive industry. Figures 1.7 and 1.8 illustrate the principle of anodic and cathodic systems with a micelle particle with its charge bearing stabilising groups, between two electrodes of an electric cell. In anodic system, the negatively charged particle will be attracted to the positively charged anode. The positively charged neutralising amine will be attracted to cathode. At the anode the carboxylic anion will be protonated and with the loss of its ionic character, it will also lose its ability to stabilise the particle in aqueous media. The destabilised particles will precipitate onto the anode surface as a coating film. If the positively charged amine groups are built into the polymer, and low molecular weight carboxylic acids are used as the neutralising species, then the polymer particle would deposit on the cathode as a coating film.

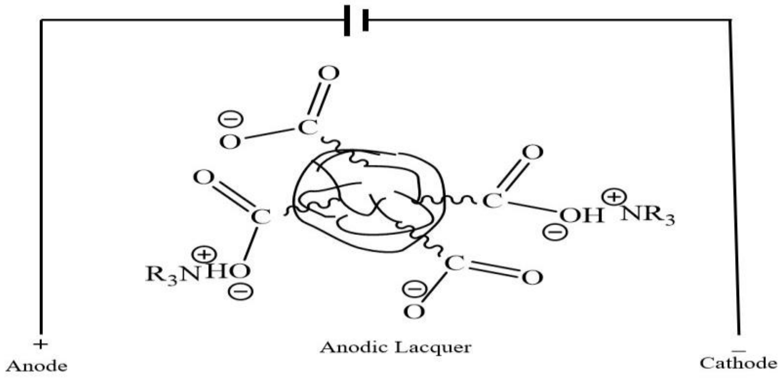

Figure 1.7 Illustration of the principle of anodic electrodeposition coating

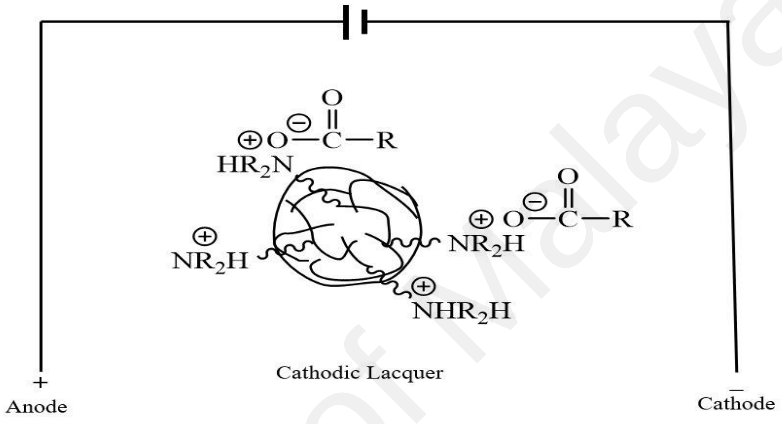

Figure 1.8 Illustration of the principle of cathodic electrodeposition coating

In electrocoating, important factors in spraying application can no longer applied. The polymer chemist has to learn and meet a new set of parameters. Some of the important parameters in electrocoating are throwing power, rupture voltage and rinse sensitivity. During deposition of film, the surface exposed to the electrodeposition changes in resistivity. When the coating started to deposit onto the bare metal, the conductivity of the metal is reduced until at the limit the film is insulating. When the charged particles are no longer attracted to the surface, the particle may move to adjacent area which is non or partially coated. The ability to move away from the electrode and penetrate into space where electrode cannot penetrate is term throwing power. It is well understood that factor which affect the resistivity of the unbaked film will affect throwing power of the formulated coating. To improve the throwing power, the chemist can modify the polymer to be more hydrophobic, e.g. decreasing the water solubility of the polymer backbone by attaching hydrophobic side chain. After depositing a film that has sufficient resistance to stop the flow of electricity and there will be no more deposition take place. The film weight is basically controlled by adjusting the voltage. If, however, the coating is not correctly formulated, it is possible for the resistance of the unbaked film to be broken by the voltage that being applied and this is called rupture voltage. To achieved the right range of deposited film weight, the unbaked film resistance to rupture voltage must be well above the voltages that are to be used to deposit the coating film. One of the important design parameters affecting rupture voltage is the correct choice of type and level of co-solvent. Another factor is degree of neutralisation, the higher amine level will lower the rupture voltages. Having successfully deposited an unbaked film, the film is then rinsed to remove residual coating from the metal substrate before heat curing process. Obviously, the uncured film must not be dissolved in the rinsing and washing process. For example, if the polymers have high acid value, they will remain water sensitive. Also, the right balance of water miscible and immiscible co-solvent in the uncured film will affect water sensitivity and film appearance after rinsing process.

Figure 1.9 shows a schematic diagram of an electrodeposition process system. The object to be coated is hung from a conveyer belt and carried into the dip tank where the coating is electrodeposited. As shown by the diagram, the full system can be automated to reduce labours as required by spraying system. The major advantage of electrocoating is complete coverage of surface regardless of its shape but the system required substrate to be coated must be conductive.

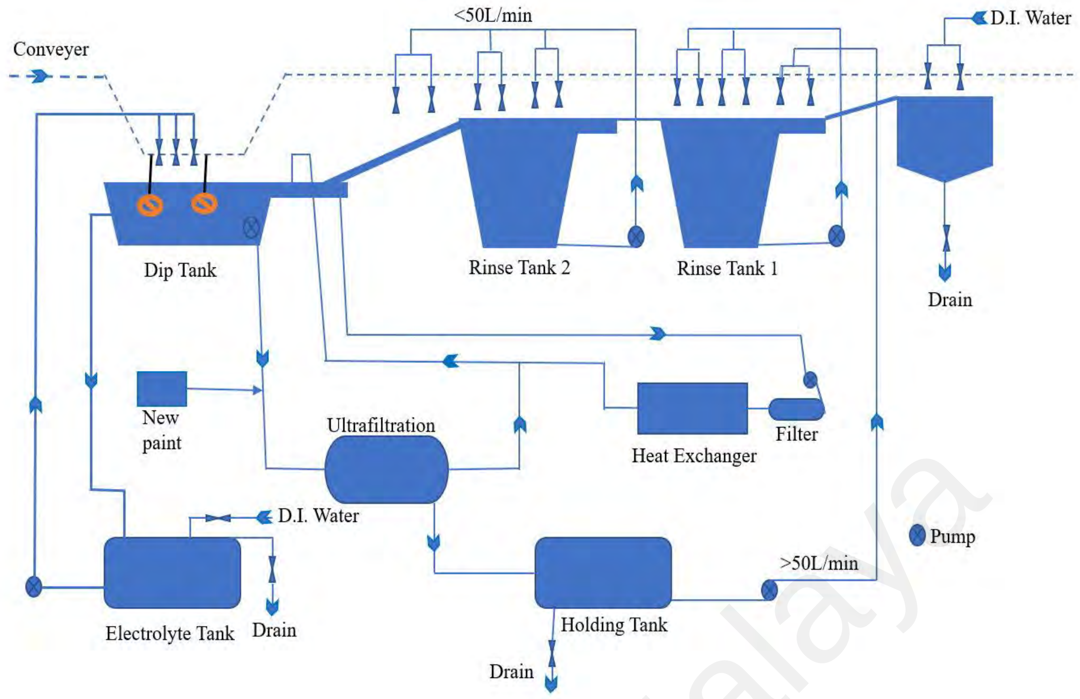

Figure 1.9 A schematic diagram of an electrodeposition process system

Powder coating is a segment of the industrial coatings being developed as part of the progress from the environmental requirement of reduce VOC and clean air standard. The high quality of film performance and environmentally friendliness has made powder coating highly accepted by the metal industry especially in home and office appliances. The heat melting technology was being applied for powder coating film formation process. The solid binder melts upon heating, binds the pigment and results in a pigmented coating cured film upon cooling. The solvent free nature of the finished product has limited the use of raw material in formulating powder coating system. Most of the powders are produced by crushing an extruded melt which means that the final curing composition has to withstand this melting process (Harris S. T., 1976). In powder formulation and production, special attention is needed on some important parameters such as particle size control, melt flow characteristic and resistivity of the formulated coating. In general, powder coatings are applied by fluidized bed or electrostatic spraying. Other application methods include flame spraying, flocking, and in-mould powder coating (Misev T.A., 1991). The coating material, part design and production volume have great influence on the powder coating application method. The type of powder itself must be of a grade suitable for the application equipment (Liberto N., 1996).

The fluidized bed systems typically are used where the desired coating thickness is above 0.13 mm, such as wire products and electrical bus bars. In this system, a fluidized bed of powder coating is generated by forcing air up through a hopper of powder. The system can be either electrostatic or non-electrostatic in application method. In non-electrostatic applications, the part must be preheated so that the powder can be melted and adhered to it as the part passes through the bed. In electrostatic application, the part will transport above the bed and the powder will attract to it by electrostatic charges. In flame spraying method, the powder is propelled through a flame to melt it as it travels toward the object being coated. Successful flame spraying requires control of the powder particles, balancing of coating properties, flame temperature, and powder residence time in the flame (Wicks Z.W. et al., 1994). Currently, spray application of powder can only be done electrostatically. Electrostatic systems fall into two categories which is corona-charging and tribo-charging. In corona-charging system, an electrostatic generator creates an electrostatic field between the gun and the object. Powder sprayed into the field will pick up the electrostatic charge and is attracted to the object along the electric field lines between the electrode and the object. Anyhow, the corona-charging is an inefficient process. Only around 60% of the ions generated actually impart a charge to the powder particles (Wicks Z.W. et al., 1994). In tribo-charging systems, charge is imparted to the powder by friction between the powder and the wall of the spray gun. Polytetrafluoroethylene is typically used for the wall of the spray tube in a tribo-gun. Tribo-charging does not create a large electric potential difference between the gun and the object to be coated. The air flow plays a major role in transferring the powder onto the object. Because there are no significant magnetic field lines between the gun and the object, Faraday cage effects are minimized. Therefore, the tribo-charging system is considered an effective at coating objects with deep recesses (Knobbe A.J., 1996).

Powder coating are divided into two broad categories: Thermoplastic and thermosetting. The thermoplastic powder coatings are based on thermoplastic resin, which flows to form a smooth continuous coating after the heating and cooling process. This resin is basically high molecular weight, tough and resistant polymers that are difficult to grind into very fine particles for necessity spray application. Consequently, thermoplastic coating is used as coating for thickness above 10 mils or 254 μm and are applied by the fluidized-bed technique (Robison T., 1994). The typical thermoplastic resins used in powder coating formulation are polyethylene, polypropylene, polyamide and poly(vinyl chloride) (Wicks Z.W. et al., 1994). Other than the common type of resins, the poly(vinylidene fluoride) type of powder coating has been commonly accepted by high quality architectural coating formulation for impart the excellent outdoor durability and weathering resistance.

Unlike thermoplastic powders, the thermosetting powder is chemically reacted to cross-links between polymer molecules. Thermosetting resin systems are using low molecular weight and solid system that cross-linking during melt-fusion process to form a highly cross-linked polymer film. Their cross-linking nature makes the coating film more resistant to coating breakdown. The binder for the thermosetting formulation consists of primary resin and a cross-linker as shown in Table 1.1.

Table 1.1 Common binder and cross-linker of thermosetting powder coating

Formulation	Primary Resin	Cross-linker
Epoxy	Bis-phenol A or Novalac	Polyamide or phenolic
Hybrid	Acid functional polyester	Bis-phenol A epoxy
Polyester	Acid functional polyester	Triglycidylisocyanurate (TGIC)or hydroxyalkylbisamides
	Hydroxyl functional polyester	Blocked isocyanate or amino resin
Acrylic	Epoxy functional acrylic	Dibasic acid
	Hydroxyl functional acrylic	Blocked isocyanate or amino resin

Advantage derived from its low molecular weight and cross-linking nature, the thermoset powder coating can be applied as thinner coating films at ranging from 0.025-0.10 mm for decorative coating or thicker film ranging from 0.25-0.76 mm for protective coating application. As shown in Table 1.1, the thermoset powder coating is divided into four major classes: epoxy, hybrid, polyester and acrylic. Epoxy coatings are based on bisphenol A (BPA) or novalac resin cross-linked with polyamide or phenolic hardeners. Hybrid coatings also contain BPA resin but cross-linked with carboxylic functional polyester resin. Polyester coating using polyester resin with various cross-linkers that including TGIC, hydroxy alkyl bisamides, and blocked isocyanate or amino resin. Acrylic coating contains acrylic resins with the cross-linkers dibasic acid and blocked isocyanate or amino resin. In addition to the individual classes, various blending of the flour classes sometime called alloys are also being employed (Wicks Z.W. et al., 1994).

1.2 Radiation Curing System

1.2.1 General Overview of Radiation Curing System

The radiation curing technology is utilized the high energy radiation to induce polymerization during curing process. The commonly known radiations and their cured mechanism are summarized in Table 1.2.

Table 1.2 Potential of radiation cure mechanisms

Radiation	Predominant primary cure mechanisms
Electron beam (EB)	Electronic excitation and ionization
Ultraviolet (UV)	Electronic excitation
Infrared	Thermal
Microwave	Thermal
Radio frequency wave (RF)	Thermal

After few decades of technology development, electron beam (EB) and ultraviolet (UV) have become two major sources radiation used by the industry and among these, UV curing is far more widely used. Consequently, any treatment of EB and UV curing will consist of a higher proportion covering the latter, although many of the raw materials may be common to both. Beyond this, specific applications for UV radiation sources have been developed because of the number, cost and flexibility of the UV cure units. Other types of chemistry based on UV irradiation initiating cure have also been developed. Two examples are UV cationic curable systems and thiol/thiolene systems. The advantages and disadvantages of EB and UV curable systems can be compared in many ways and have always been, and will no doubt continue to be the subject of debate. Many of the limitations are a direct consequence of the technology. Table 1.3 contains a simplified general overview of the benefits and drawback of EB and UV curable systems compared with thermally cured solvent based systems.

Table 1.3 Comparison on UV, EB and thermal cured coating system

Factor	**EB**	**UV**	**Thermal**
Commercial			
Capital Cost	-*	+	0*
Energy Consumption	+	0	-
Running Cost (including inert gas)	0	+	-
Formulation Cost (dried film weight)	0	-	+
Space Requirement	0	+	-
Skill Level Requirement	-	0	+
Speed	+	0	-
Technical			
Cross-linked Network	+	0	-
Chemical Resistance	+	0	-
Gloss	+	+	0
Thick Pigmented Films	+	-	+
Thin Pigment Films	-	+	+
Oxygen Inhibition	-	0	+
Damage to Sensitive Substrates	-**	+**	0
Adhesion to Difficult Substrates	+**	0	-
Temperature of cure	+	+	-
Health and Safety			
Fire Hazard	+	+	-
Hazardous Radiation	-	0	+
Environmentally Hazardous Materials	+	+	0
Irritant Raw Materials	-	-	0

** If equivalent throughput and thick coating are considered, EB may be less expensive than a conventional oven.*

*** EB generates less heat than UV, but it has higher energy particles that penetrate to the substrate, which may also improve adhesion by grafting or other mechanisms.*

Other than widely used in wood, paper and plastic industry application, UV curable coating has become important in imaging industry such as electronic and printing plates, which required high precision and fast curing in order to meet their large volume production output. Currently, the substrate coated with UV or EB curable materials is far from complete, but the example listed below illustrates the wide range of everyday objects which now depends on radiation curing. Tag to its advantages, the new applications are constantly being found to expand the list.

Some example of UV curing application,

- Cork Coating
- Dental Bonding
- Glass Fibre Laminates
- Glass Lamination
- Glass Repair
- Magnetic Recording Media
- Medical
- Metal Coating
- Moisture Vapor Barrier Coating
- Optic Fibre Coatings
- Optical Recording Media
- Paper Coatings
- Photopolymers for Printing Plates and Photolithography
- Photoresists for Printed Circuits and Microelectronic
- Photoresists for Photochemical Machining
- Plastic Coatings
- Pressure Sensitive Adhesive
- Printing Inks
- Release Coatings for Paper and Film
- Textile Coatings
- Vinyl Flooring
- Wood Coatings

Equipment for radiation curing is distinctly divided into that for electron beam or ultraviolet. The former generates electrons, which penetrate into the coating, and in so doing, some electrons transfer some of their energy to components of the coatings, which result in ions and free radicals being formed. Electrons are attenuated in air and they can only travel short distances (typically 2.5 to 5 cm). Consequently, they need to be generated in a vacuum. In UV curing, photons electronically excite molecules in a coating, which then generate free radicals or cations. The energies of electron beams are far higher than the energies of photons in UV radiation. This can lead to the generation of X-rays that require electron beam generators to be shielded. Thus, equipment for EB curing is bulkier and more expansive than that for UV curing.

All free radical radiation curable formulations require a proportion of materials containing some degree of unsaturation, usually activated towards polymerization by a neighbouring group. High reactivity of acrylate double bond as compared to other type of unsaturated has made acrylate chemistry widely used in radiation induced free radical polymerization. The earliest UV curing coating was based on styrene and unsaturated polyester system. Prepolymer or oligomers have been synthesized to provide the main properties of the film and the reactive diluents or monomers were made to improve the formulations application feasibility especially in reducing the viscosity. Oligomers or prepolymers are low molecular weight molecules, which are the intermediate of the repeating units of the resulting polymer. For radiation curable systems, these are relatively simple and by normal resin standards, they are well-defined molecules.

Invariably the viscosities of the oligomers or prepolymers are too high for direct incorporation into a coating and it is necessary for a viscosity reducing agent to be incorporated. It is possible to incorporate a reactive (copolymerizable) or a non-reactive (inert) diluent. Solvents are sometimes added, but they have generally evaporated by the time the coating or ink is exposed to radiation. The addition of solvent negates the advantage of a 100% solid, non-flammable (volatile monomer excepted) system and their use should be actively discouraged, unless their addition is vital for application. Failure to remove solvents before polymerization commences can lead to a film with a potential weakness in the position of the solvent molecules. For any free radical reaction to occur, it is necessary for the radiation source to generate free radicals. It is in this respect that

EB and UV systems differ the most. An over simplified comparison between UV and EB curable formulations might be that an EB system is a UV system without the photoinitiator. A schematic representation of the differences is shown in Figure 1.10.

For useful film to be obtained from radiation curable materials, some degree of cure or polymerization and possibly cross-linking must occur. In this purpose, cure can be considered occurred, which produces a film to fulfil the properties required from it. That state may be measured by practical techniques like the thumb twist test, MEK rubs, sand dryness, or analytical techniques like photo DSC or FTIR.

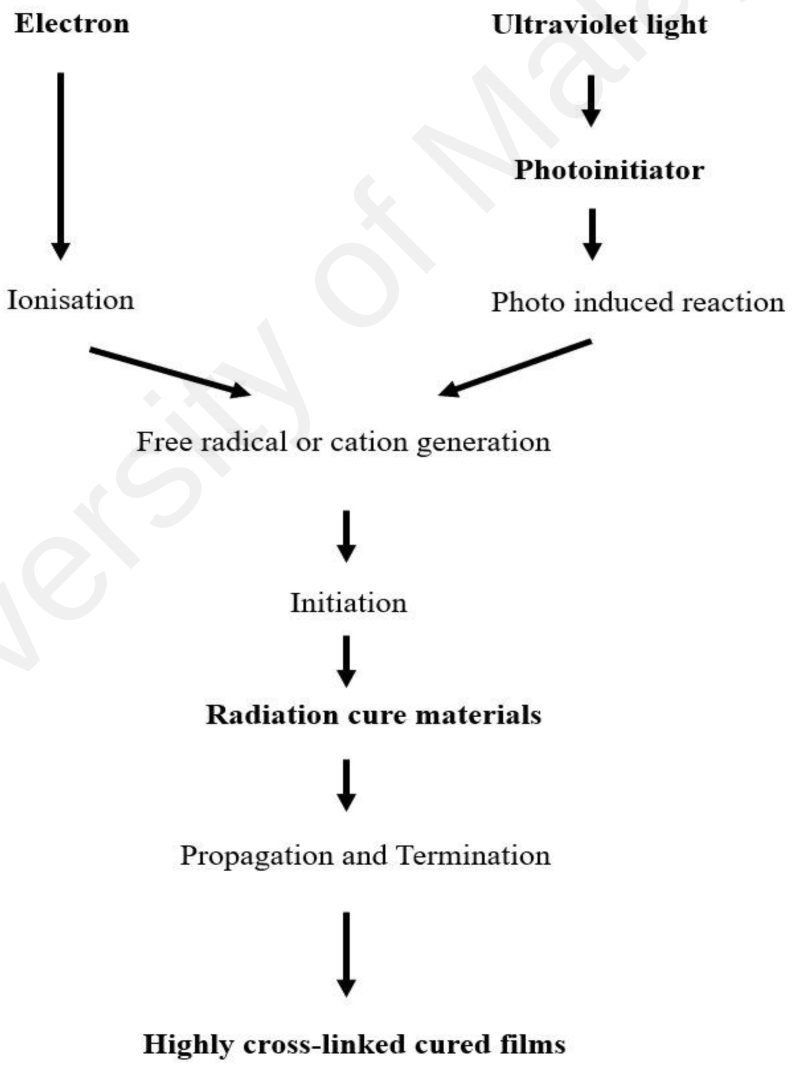

Figure 1.10 Schematic diagram for EB and UV curing process

1.2.2 The Photo-chemistry Reaction

In most UV or visible light photochemical processes, the photosensitive material will be excited by absorbing energy from a photon. To stabilize themselves, the excited material needs to lose its excess energy in one of two ways. The first involves re-radiation of energy and the second a non-radiative energy transition. In both processes, excited states are inter-converted with each other or with the ground state. These processes can be called photophysical processes. In general, the net effect of light energy being absorbed is that light can be converted to light (of different wavelength), heat, or to a potentially chemically reactive moiety.

There are three basic stages in a photoreaction.

A. Absorption of a photon resulting in an electronically excited state.

B. A primary photochemical process, which may involve rearrangements in the electronically excited molecules.

C. A secondary or 'dark' process, which results from the intermediates produced from the primary photochemical process.

Unsaturated oligomer and monomer components in a UV curable system are capable of absorbing UV radiation through their unsaturation. However, the extremely low rate of any subsequent photo-induced polymerization for film formation that has made this process uneconomic and technically unacceptable. Thus, it is necessary to add one or more types of molecules, which undergo photochemical reactions more readily and more efficiently than monomers or oligomers itself. These molecules may act alone or in combination, but the result is the photo-induced initiation of polymerization of the oligomers and monomers. They are molecules of photoinitiators, photosynergists, or photosensitisers, depending upon the role they perform in photoinitiation. Any commercially viable UV process must utilize a photoinitiator system, which is usually present in the formulation, at concentration between 2-15% weight.

The photoinitiator function by absorbing electromagnetic radiation and through either an intermolecular or an intramolecular interaction, it must produce a reactive intermediate. In free radical polymerized system, a free radical is required. In the case of cationic curing, an ion must be generated. The reactive intermediate, which is present in relatively low concentrations compared to polymerizable materials, must cause the wet film to cure. The reactive intermediate initiates reaction between the oligomer and monomer molecules, which then continue to cross-linked and producing a high molecular weight polymer network.

In the case of a UV system, ultraviolet light (wave length within 254-400 nm region) excites a molecule, which in general terms either directly or indirectly leads to the generation of free radicals. These molecules are normally referred to as photoinitiators. In some formulations, a synergist may require to generate a free radical. The following summarizes the major steps in obtaining a final UV cured coating.

Photoinitiators can absorb a photon and become excited and their electronic configuration is altered.

$$\underset{\text{Ground state}}{MX^{\bullet}} \quad + \quad \underset{\text{Photon}}{h\nu} \quad \longrightarrow \quad \underset{\text{Excited state}}{MX^{*}}$$

Figure 1.11 Absorption of photon

The two excited states, of interest to the chemist, are Singlet and Triplet and both refer to electronic spin configuration. A configuration without unpaired electrons is a singlet state and is typical of ground state of most compounds. It is possible for a singlet state to exist as an excited state, because one electron can be promoted to a higher energy level orbital whilst retaining its spin. Thus, the two single electrons at different energy levels of opposite spin remain paired. In a triplet state, there are two unpaired electrons of the same spin. A triplet state cannot be directly formed from a single ground state. The converse is also true. It is necessary for spin inversion or intersystem crossing to occur for a triplet state to be formed. The triplet state has a much longer lifetime than the corresponding singlet state. Thus, the excited triplet state is more stable than the excited singlet state, and having a longer lifetime, it is more likely to react with its surrounding molecules thereby initiating polymerization. In essence, the triplet state produces the most useful photochemical reaction, as far as UV coating is concerned. For most but not all photoinitiators used in UV radiation induced free radical curing technology, carbonyl or activated carbonyl groups are the moieties, which are involved in primary photochemical processes.

The excited state can lose its energy in number of ways. Some do not lead to photoinitiation. Energy can be lost as fluorescence or phosphorescence. The excited molecule returns to its ground state.

$$\underset{\text{Singlet state}}{MX_S^*} \quad - \quad h\nu \longrightarrow \underset{\text{Ground state}}{MX^\bullet}$$

Figure 1.12 Light emitted as fluorescence at singlet state

$$\underset{\text{Triplet State}}{MX_T^*} \quad - \quad h\nu \longrightarrow \underset{\text{Ground state}}{MX^\bullet}$$

Figure 1.13 Light emitted by slow decay as phosphorescence at triplet state

Energy can be lost or transferred to another moiety totally deactivating the excited molecule. If the moiety takes no further part in any reaction, then the moiety has quenched potential photoinitiation.

$$MX_T^* \quad + \quad Q \longrightarrow Q^* \quad + \quad MX^\bullet$$

Triplet Quenching Ground state

Figure 1.14 Quenching process

An excellent quenching molecule is oxygen, which can inhibit potential radiation induced polymerization at all stage. At this stage, the excited molecule is deactivated by oxygen. Later in the polymerization stage, oxygen interferes with the free radicals by trapping them and inhibiting polymerization. As described by Hanrahan M.J. (1990) molecule oxygen is a di-radical with the singlet state being unstable. The triplet state is molecule oxygen's electronic ground state. The di-radical has lacks of energy to initiate polymerization and it is considered stable. However, it readily reacts with existing radicals and goes from its triplet to singlet state, which is unstable and readily reverts back to its di-radical state.

$$MX_T^* \quad + \quad O_{2(T)} \longrightarrow O_{2(S)} \quad + \quad MX^\bullet$$

Triplet state Triplet Singlet Ground state

$$O_{2(S)} \longrightarrow O_{2(T)}$$

Singlet Triplet

Figure 1.15 Oxygen Quenching

Energy also can be transferred to another photoinitiator molecule.

$$MX_T^* \quad + \quad PI\bullet \longrightarrow MX\bullet \quad + \quad PI_T^*$$

Triplet state Ground state Ground state Triplet state

Figure 1.16 Energy transfer to photoinitiator

The photoinitiator can lose its energy by forming free radicals, either directly or indirectly. The direct type fragments into two (or more) species, which are both free radicals, which may or may not initiate polymerization. The fragmentation that gives rise to this type of photoinitiation is commonly called radical cleaving, radical fragmenting or homolytic scission. The α-cleavage take place at the adjacent to the photochemically active carbonyl group. An example of this type of photoinitiator is acetoxy acetophenone.

$$MX_T^* \longrightarrow M\bullet \quad + \quad X\bullet$$

Triplet Free radicals

Figure 1.17 Cleavage process

In the indirect type of photoinitiation, a molecule is photochemically excited will abstracts an H atom either from another molecule or by an intramolecular reaction to form a free radical. The mechanisms involved may be multiple steps and can be very complicated. The two mechanisms are shown below in Figure 1.18 and 1.19. The reaction shown for the amine is considered the most likely one to occur. This photoinitiators is commonly referred to as hydrogen abstractors. Benzophenone is a typical hydrogen abstractor and photosynergists or co-initiators are typically tertiary amines. The co-initiator may form a complex with the excited state benzophenone, thereby enhancing its reactivity. It is possible for photoinitiators to undergo both types of photoinitiation and indeed, many commonly used ones are capable of this. However, there is normally a large difference in the rates for each mechanism and the one predominates will be the mechanism by which the photoinitiator is assumed to react.

There is sometimes confusion about the role amines perform in a UV curable system. They can fulfil at least two functions. The first is the ability to reduce oxygen inhibition by donating hydrogen to a peroxy radical to allow the formation of a new radical. The second function is that of co-initiator or photosynergist. Amines can only act as a photosynergist if they have the correct chemical structure and if a hydrogen abstractor is present. An alternative approach to using free amines is the use of an amine attached to an acrylate prepolymer, which subsequently polymerized into the coating, thereby reducing its extractability or migration from the coating.

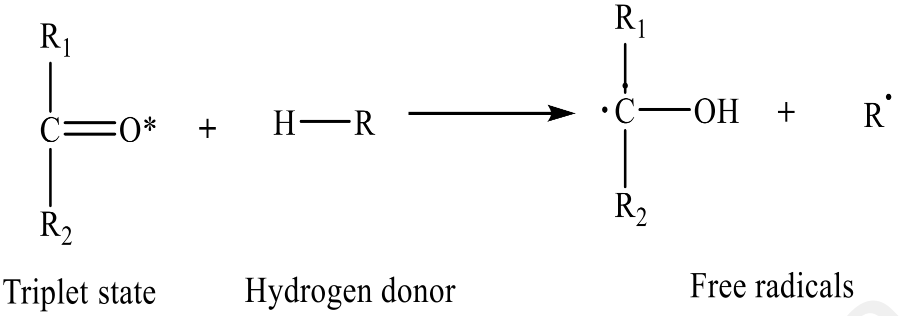

Figure 1.18 Non-amine H abstraction

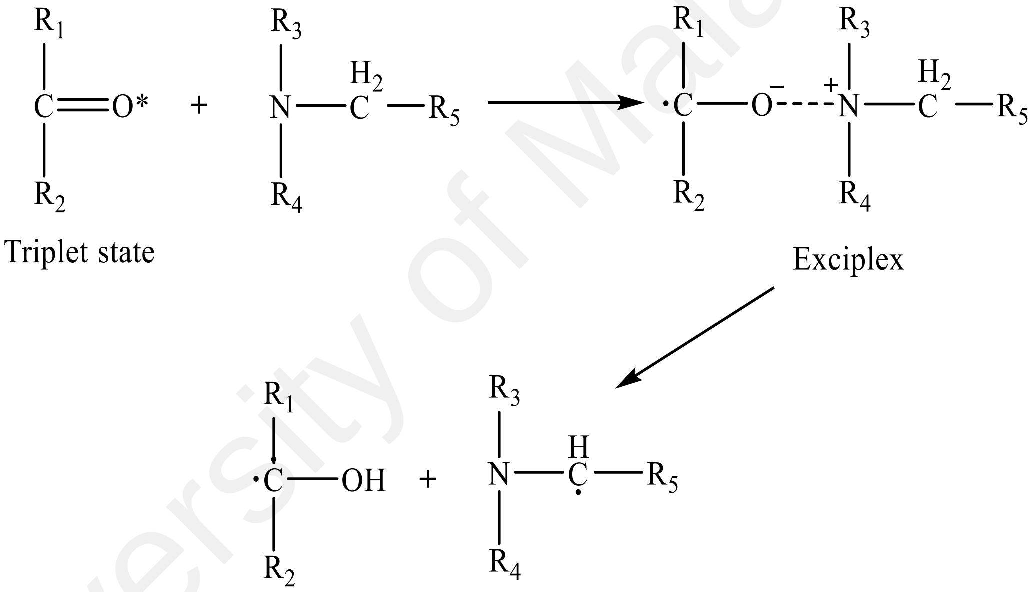

Figure 1.19 Amine H abstraction.

1.2.3 Radiation Induced Free Radical Curing

The reaction of interest for initiating free radical polymerization is the generation of free radicals. The major route is through an excited molecule, degrading or causing degradation. As described earlier, it is also possible for a radical cause by EB irradiation to form a free radical and bypassing the intermediate excited state.

$$XY^{*} \longrightarrow X\bullet + Y\bullet$$

Excited state   Free radicals

Figure 1.20 Free radical generation

As already stated, generating one or more free radicals does not mean that initiation of polymerization will occur. If A• represents a free radical produced by either a direct or indirect UV irradiation or by an electron bean, then recombination can occur.

$$A\bullet + A\bullet \longrightarrow A_2$$

Figure 1.21 Recombination of free radicals

Other than recombination of the free radicals, it is also possible for free radical to be transfer to another molecule.

$$A\bullet + R \longrightarrow A + R\bullet$$

Figure 1.22 Transfer of free radical

In this context, A• has not directly caused a free radical polymerization to commence, although R• may initiate a chain reaction. It is possible for the free radical to terminate a free radical polymerization. If M represents a monomer unit then this reaction can be summarized as:

$$A\bullet + \bullet M_{(m)n} \longrightarrow AM_{(n+1)}$$

Figure 1.23 Termination of free radicals

Pigment, substrate and non-reactive additives, such as waxes can absorb free radicals.

$$A\bullet + \text{Pigment} \longrightarrow \bullet A\text{—Pigment}$$

Figure 1.24 Absorption of free radical by pigment

In some cases, absorption can make the surface more receptive to secondary reactions, so that the absorber is incorporated into the resulting polymer matrix. A major problem which formulators are forced to overcome is oxygen inhibition. This is often referred to as scavenging, because oxygen scavenges for free radicals yielding peroxy radicals.

$$A\bullet \quad + \quad O_2 \longrightarrow A - O - O\bullet$$

Peroxy radical

Figure 1.25 Formation of peroxy radical

The molecular oxygen di-radical is similarly stable and does not initiate polymerization or propagation. It is capable of undergoing a radical transfer reaction, via a hydrogen abstraction route.

$$A - O - O\bullet \quad + \quad HX \longrightarrow X\bullet \quad + \quad AOOH$$

Perox Hydrogen Free
Radical donor radical

Figure 1.26 Radical transfer by hydrogen abstraction

The resulting radical may be capable of initiating polymerization. In this case, oxygen has only caused the formation of another radical and a low molecular weight species. The hydrogen abstraction reaction is one mechanism for mitigating oxygen inhibition and partially explains why amines, however, cannot overcome the problems encountered with oxygen inhibition in EB system.

The peroxy radical prefers reacting with other radicals leading to chain termination or loss of another potentially initiating free radical. The effect of oxygen inhibition on free radicals can be reduced by increasing the concentration of potential free radical generators. A large excess of free radicals then ensures that polymerization commences, but the resulting film can be tacky and have poor cure characteristics due to their low molecular weight resulting from the high concentration of free radicals. Having generated free radicals, polymerization can then proceed by typical free radical scheme as outlined below.

- (I) Generation of an initiating free radical
- (II) Chain initiation
- (III) Chain propagation
- (IV) Chain termination

There are many side reactions occurring during the UV induced polymerization. If the initiating free radical is represented as I• and monomer units as M then the following idealized schemes occur.

$$I\bullet \quad + \quad M \longrightarrow IM\bullet$$

Figure 1.27 Chain initiation

For the resulting film to have beneficial properties, it is necessary for its molecular weight to be increased. This is achieved through chain growth or propagation. The propagation step in an efficient monomer or prepolymer system takes place in many and possibly thousands of times more than the other steps shown. However, growing chains have a limit to size which they can reach and all ultimately undergo some form of chain termination. Chain termination can occur by a variety of mechanisms.

$$IM\bullet \quad + \quad M \longrightarrow IMM\bullet$$

$$IM_nM\bullet \quad + \quad M \longrightarrow IM_{(n+1)}M\bullet$$

Figure 1.28 Chain propagation

$$IM_nM\bullet \quad + \quad IM_mM\bullet \longrightarrow I_2M_{(m+n+1)}$$

Figure 1.29 Chain termination by combination

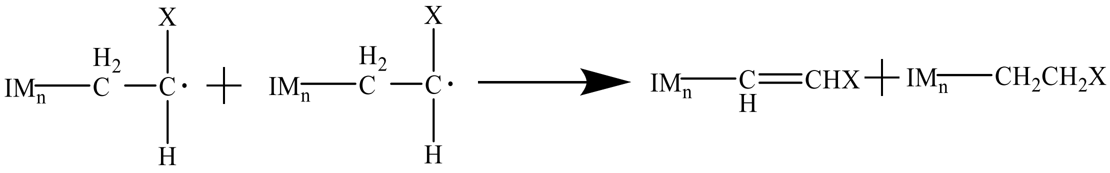

$$IM_n{-}\overset{H_2}{C}{-}\overset{X}{\underset{H}{C}}\cdot + IM_n{-}\overset{H_2}{C}{-}\overset{X}{\underset{H}{C}}\cdot \longrightarrow IM_n{-}\underset{H}{C}{=}CHX + IM_n{-}CH_2CH_2X$$

Figure 1.30 Chain termination by disproportionation

During the radical transfer process, the chain reaction can be terminated and this can occur in many ways.

$$IM_mM\bullet \quad + \quad SX \longrightarrow IM_mMX \quad + \quad S\bullet$$

Figure 1.31 Transfer to a saturated component represented as SX

$$IM_mM\bullet \; + \; I_2 \longrightarrow IM_mMI \quad + \quad I\bullet$$

Figure 1.32 Transfer to an initiator molecule

$$IM_nM\bullet \quad + \quad CH_2{=}\,CHX \longrightarrow IM_{(n+1)}H \quad + \quad CH_2{=}\,CX\bullet$$

Figure 1.33 Transfer to another unsaturated molecule

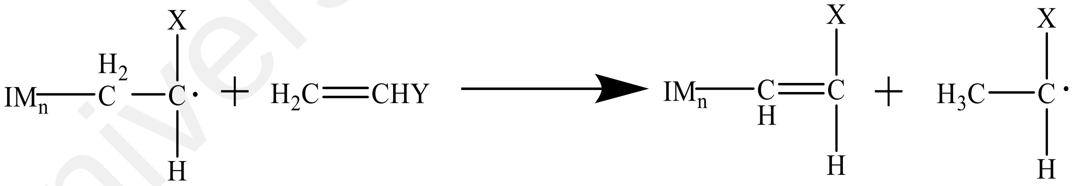

$$IM_n{-}\overset{H_2}{C}{-}\overset{X}{\underset{H}{C}}\cdot + H_2C{=}CHY \longrightarrow IM_n{-}\underset{H}{C}{=}\overset{X}{\underset{H}{C}} + H_3C{-}\overset{X}{\underset{H}{C}}\cdot$$

Figure 1.34 Transfer to a polymer with unsaturation

As shown in Figure 1.31-1.34, the transfer reactions actually do not change the overall free radical concentration. Any of the free radicals generated in the transfer process are capable of initiating a further chain reaction. As a general rule, the higher the numbers of the free radicals present at any instant, the higher the rate of initiation and the lower the overall molecular weight.

1.2.4 Type of UV Cured Resin

1.2.4.1 Introduction

In UV curing formulation, the oligomer or prepolymers used are generally smaller molecular weight than the conventional resins. They normally consist of one or at most few repeat units. Upon polymerized by radiation they can crosslinked to give higher molecular weight structure polymer. The common feature of the UV and EB cure mechanisms is the carbon-carbon double bond functionality that is required for polymerization. Free radical polymerization is the predominant chemistry in practice. The nature of the applications in which UV and EB cure system are found demand a high rate of conversion from unsaturated double bonds in prepolymers and monomers to saturated polymers. The cure reaction must be highly efficient, which means that the propagation step occurs many times for each occurrence of initiation, chain transfer and termination.

Such high efficiency polymerization is achieved using prepolymers with acrylate functionality, or to a lesser extent, methacrylate, allyl, and vinyl functionality. These types of functionality are listed in Figure 1.35 in decreasing order of reactivity.

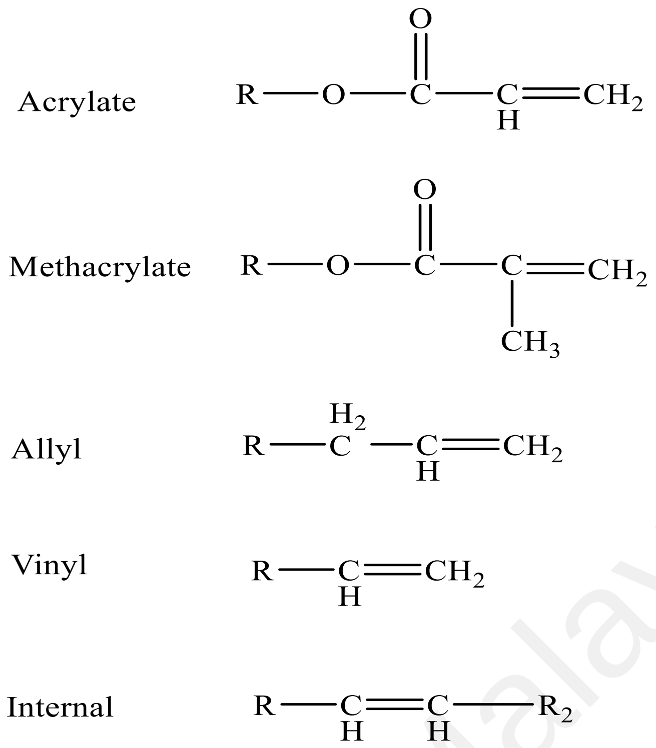

Figure 1.35 Chemical functional in UV resin chemistry

In recent years, the rapid growth of UV curing coating has driven the industry to commercialize large variety of acrylated or methacrylated prepolymer or oligomer to meet the industrial requirements. The design and synthesis of new varieties of acrylate and methacrylate prepolymers still continues on both the laboratory and commercial scales. These both activities fill and also help to create the growing demand for few unsaturated molecules, which upon UV or EB irradiation will give solid, coherent films with new and improved performance properties.

The prepolymers are generally high viscous product which is not possible for direct coating application usage. In most cases, low viscosity monomers or reactive diluents are used to reduce the viscosity of radiation curable formulations. Reactive diluents are preferred to conventional solvents, because the advantages of solvent free and 100% solids systems are retained. These materials can also be used to increase the cure rate of a formulation and increase the crosslinking density of the cured film for improved chemical resistance and hardness.

1.2.4.2 General in UV Resin Synthesis Chemistry

The preparative techniques for the different classes of prepolymer vary from their own chemistry types. Molecular weight of prepolymers are range from a few hundred to a few thousand and it is important to prevent active double bond to polymerize during synthesis and storage. Such can even could cause gelation and loss of product. In a commercial scale production, uncontrollable reaction could result in excessive evolution of heat, which is potentially disastrous for both equipment and personnel. Even if the reaction does not run away, highly exothermic reactions can produce undesirable by products. For example, with acrylated bisphenol a based epoxy resin, degradation of raw materials to toluene and other unwanted products may occur at about 240˚C with much acid fuming (Lee L.H., 1963, Lee & Neville, 1967). Clearly, for large-scale production of prepolymers, it is important the product stability be assured.

Whilst it is necessary to inhibit free radical reaction during manufacture and storage, inhibitor added to stabilize the raw material must not significantly hinder the rapid free radical polymerization once initiated by UV or EB radiation. Two types of inhibitor are commonly used to achieve the proper balance between bulk stability and film reactivity. They can be used alone, or in combination with other inhibitors during synthesis. This is a moderately high temperature inhibitor used at typical processing temperature of 80-130˚C. The other type of inhibitor, sometimes referred to as the "inhibitor cocktail", is included to improve the shelf life of the product. Type of high temperature inhibitor include: hydroquinone, methoxy hydroquinone, p-benzoquinone, phenothiazine, mono-tert-butyl hydroquinone, catechol, p-tert-butyl catchol, 2,5 di-tert-butyl hydroquinone, 2,5 p-dimethyl p-benzoquinone, anthraquinone and 2,6 di-tert-butyl hydroxyl toluene (Chester W. Fitko, 1971). To improve the prepolymer shelf life, p-tert-butyl catechol could be added to the prepolymer upon completion of reaction prior to the packing process.

The presence of oxygen is required for the inhibition efficiency of many of these compounds (Gummeson J.J., 1990) and for many low temperature systems an oxygen blanket alone is claimed to be an effective inhibitor (Joseph Francis Ackerman et al., 1972). Good cooling facilities are also essential to control any exotherms during processing. Air generally provides the source of oxygen. The air or inert gases must be dispersed evenly throughout the mixtures during the synthesis process. Sparge lines must be carefully designed because bubble size and distribution affect the efficiency of inhibitor.

To maintain a low viscosity for efficient mixing during synthesis, the diluents appropriate for the product end use can be initially present or may be added during processing. These may be the common solvents or reactive diluents. In the preparation of oligomers, catalysts are invariably used for at least two purposes. Firstly, they enable reaction at low temperatures and lower reaction temperatures are desirable as already mentioned, to reduce possibility of thermally induced free radical reactions of the carbon-carbon double bonds. Secondly, catalysts can be used to select the desired reaction and to suppress unwanted side reactions. Examples are epoxy-acid rather than epoxy-hydroxyl or epoxy-epoxy reactions, and isocyanate-hydroxyl preferentially to isocyanate-isocyanate or isocyanate-urethane reactions. Whilst predictions can be made about the stability of catalysts, experiments are required to prove their effectiveness, particularly when inhibitors are present whose effects in conjunction with the catalyst may be unknown.

1.2.4.3 Epoxy Acrylate

Structures of some epoxy containing compounds which can be acrylated are given in Figure 1.36. The oligomers of bisphenol-‘A’-diglycidyl ether DGEBA or BADGE contain hydroxyl groups. The relationships between n, molecular weight and physical state are given in Table 1.4 (P.K.T Oldring & Hayward, G. 1995).

Table 1.4 Relationship between Repeat Units and some Properties of DGEBA Epoxy Resins (source from hexion.com)

Value of n	Molecular Weight	Epoxy Equivalent Weight	Melting Point °C
0-1	350-600	170-310	<40*
1-2	600-900	310-475	40-70
2-4	900-1400	475-900	70-100
4-9	1400-2900	900-1750	100-130
9-12	2900-3750	1750-3200	130-150

* Usually liquid at ambient temperature.

Epoxy resins with values of n from 0 to 4 are most commonly acrylated, although a range of 0-20 can be used (Hindley Walker, J. et al., 1965). Care must be exercised when selecting the grade of resin to be acrylated. Some of the liquid grades contain reactive diluents, which are essentially low molecular weight, mono-functional epoxy containing materials. These might be butyl glycidyl ether or phenyl glycidyl ether, which are irritant materials, probably due to the epoxy functionality and their relatively low molecular weight making then mobile. The acrylates of these diluents are also irritant materials and as such, are not generally used for applications where skin contact may occur. For the same reasons, these mobile mono-functional epoxy materials should not be used to scavenge unreacted acrylic acid towards the end of the acrylation process to drive the reaction to completion.

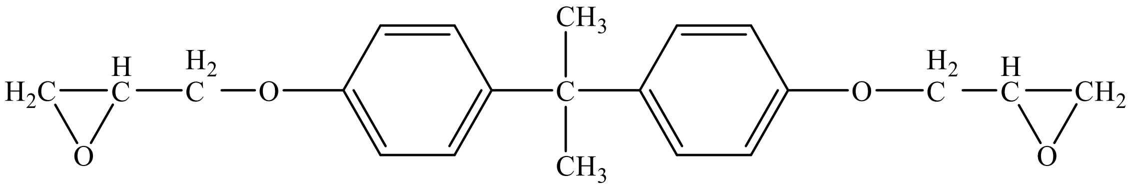

i) Bisphenol A diglycidyl ether

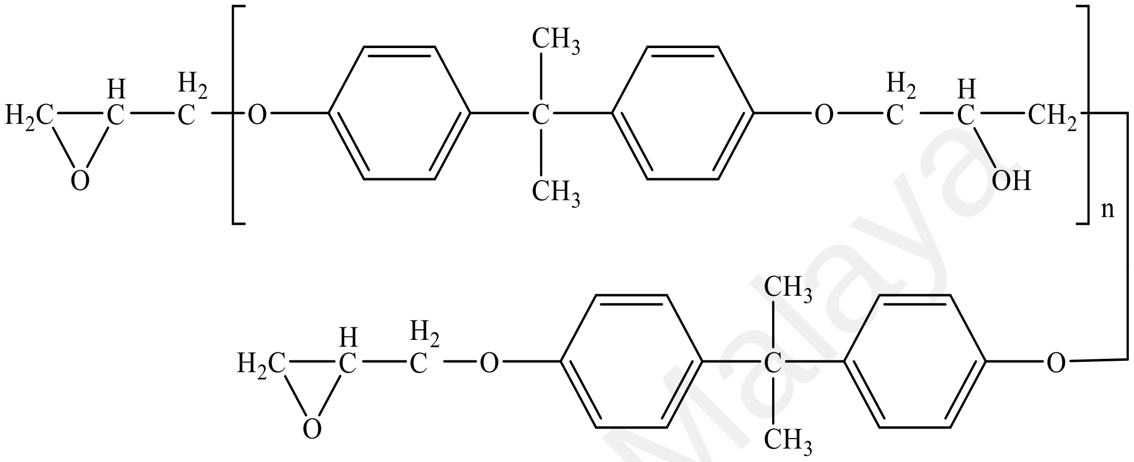

ii) Oligomer of bisphenol A diglycidyl ether

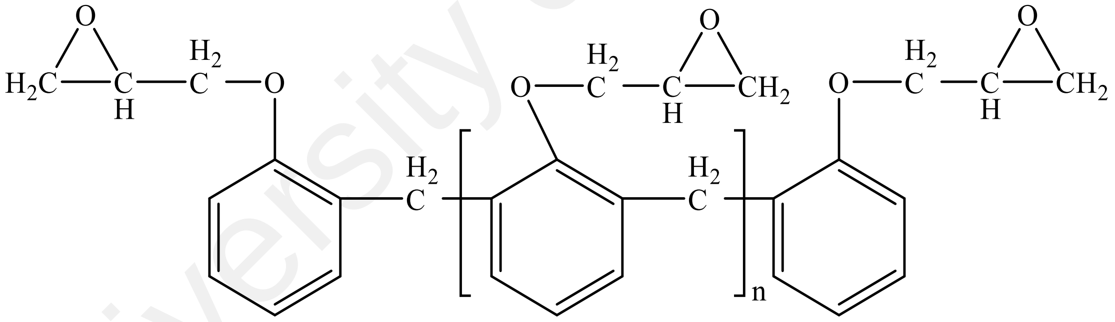

iii) Epoxy novolac

Figure 1.36 Epoxy resin for UV cured synthesis

Whilst the diglycidyl ether of bisphenol 'A' is shown as being di-functional, in reality commercial products consist of mixture of various molecular weights and structures which do not necessary confirm to the idealized structure. There are many ways of expressing the number of epoxy groups per molecule and many of them are interchangeable. The epoxide equivalent weight (EEW) is the weight of resin containing one-gram equivalent of epoxide. The EEW is also referred to as the weight per epoxide

(WPE) or epoxy molar mass (EMM). All three terms are interchangeable and can be considered as a measure of the functionality of the epoxy resin. The EEW needs to be known before acrylation commences to calculate the quantity of acrylic acid to be charged, thereby ensuring complete reaction with minimal residual acid, or epoxy groups.

Epoxy novolac resins are multifunctional and are extremely viscous. They almost certainly require the diluent to reduce their viscosity during processing. Epoxy novolac resins are used in high performance coatings where high temperature resistance and excellent adhesion are required. They also find application in electrical coatings and potting compounds. Thus, it is not surprising that this class of resins is acrylated to utilize their high-performance characteristics.

1.2.4.4 Acrylated Oil

Triglyceride oils used in the coatings and resin industries are derived from plants and trees. Fish oils are also available, but due to odour, they are not generally used. A representation of triglyceride oil is given in Figure 1.37.

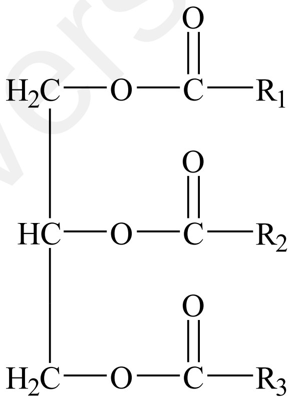

Where R_1, R_2 and R_3 are the hydrocarbon portions of fatty acids.

Figure 1.37 Structure of triglyceride

Oils, being natural products, vary in composition due to climatic and nutrient variations. Indeed, tall oil fatty acid (TOFA) obtained from pine trees grown in Scandinavia is substantially different to that obtained from North America. Differences occur in the fatty acid composition of the triglycerides.

Soya bean oil consists of about 50% linoleic acid (cis-9,cis-12-octadecadienoic acid), 25% oleic acid (cis-9-octadecanoic acid) and about 10% of palmitic (hexadecanoic) and linolenic (cis-,cis-12,cis-15-octadecatrienoic) acids and 5% strearic (octadecanoic) acid (Ivanoc et al., 2010). These fatty acids have between zero and three double bonds. Thus, in soya bean oil there is a high level of unsaturation. No conjugated double bond to be found in soya bean oil fatty acids compositions. The schematic of triglyceride structures with major fatty acids components were shown in Figure 1.38. There are large variations and the structures shown are only representative.

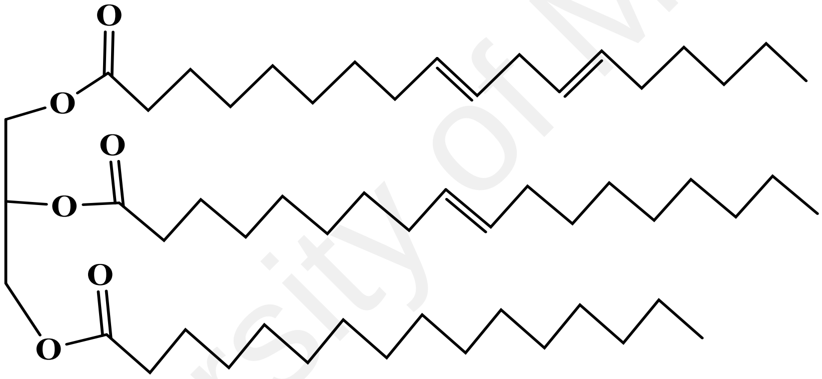

Figure 1.38 Schematic of soya bean oil with major fatty acids composition

The carbon-carbon double bonds can be converted to epoxy groups by reaction with peracid or hydrogen peroxide (Clayton A May, 1988). Epoxidized soya bean oil was used as a stabilizer in PVC formulations, long before its potential as an intermediate in radiation curing was realized. Because of availability and having 90% of market (Clayton A May, 1988). Thus, it is not surprising that this oil is normally selected for acrylation. Epoxidized linseed oil has a higher number of epoxy groups, due to its higher level of unsaturation.

Oils containing epoxy groups, such as epoxidized soya bean oil can be readily acrylated under similar conditions to those used for standard epoxy acrylate manufacture. The reactions, both desirable and undesirable, which occur for epoxy acrylates, also occur during the preparation of acrylate oils. However, the lower degree of unsaturation of the resulting acrylate compared to a DGBEBA based acrylate, reduces the severity of any resulting gel, which should still be avoid by taking similar precautions to those used for epoxy acrylates. Similar catalysts and inhibitors (at similar level) for DGEBA acrylate preparations would be used for epoxidized oil acrylates. Generally, the viscosity of acrylated oil is sufficiently low (20-30 Pa.s) for diluent free preparation and usage.

1.2.4.5 Urethane Acrylate

The formation of urethane acrylate or methacrylate from the reaction of an isocyanate group with the hydroxyl group of an acrylic or methacrylic monomer were shown in Figure 1.39.

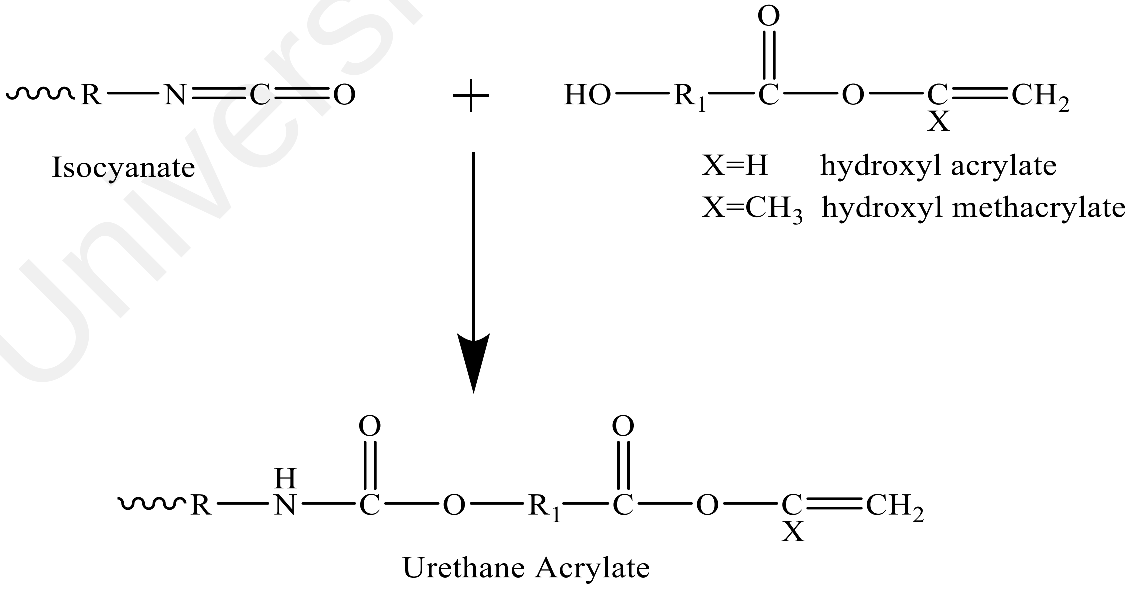

Figure 1.39 Urethane acrylate reaction.

If diisocyanates are utilized, then urethane acrylate with di-functionality may be obtained. The urethane acrylates can be prepared from a large, diverse range of raw materials. Due to the many possible variation in preparation conditions and diverse range of raw materials used, the resulted urethane acrylate oligomers can have very large range of properties in term of resin specification and cured film performance.

The diisocyantes which may be acrylated include toluene diisocyanate (TDI), tetramethoxylxylene diisocyanate (TMXDI), hexamethylene diisocyanate (HMDI), isophorone diisocyanate (IPDI), and its chain isomer, trimethylhexamethylene diisocyanate (TMDI), dicyclohexylmethane diisocyanate (H_{12}MDI), xylene diisocyanate (XDI) and diphenylmethane diisocyanate (MDI). Among the isocyanate monomers, the HMDI and TDI are extremely hazardous and being relatively volatile. To minimize the hazardous of the monomers, oligomers of HMDI and TDI are commercially available. TDI is reacted with triol to give a relatively safe product, which is commercially available as Desmodur L (Product manufactured by Bayer). H_{12}MDI consists of three stereoisomers because of the reduction of the aromatic MDI.

Hydroxy functional monomers used in making urethane acrylate include hydroxyl ethyl acrylate, hydroxyl propyl acrylate (HPA) and hydroxyl ethyl methacrylate (HEMA). The structures of the above starting materials are shown in Figure 1.40a, 1.40b and 1.41. If higher functional polyether or polyester polyols being used, then chain extension is possible. By using this class of polyols, the prepolymers prepared will be vary in functionality and molecular weight with corresponding variations in final film properties (McConnell J.A. et al., 1990). Urethane acrylates probably offer a far wider range of final film properties than any other class of radiation curable oligomers.

(I) Aromatic diisocyanate

Toluene diisocyanate

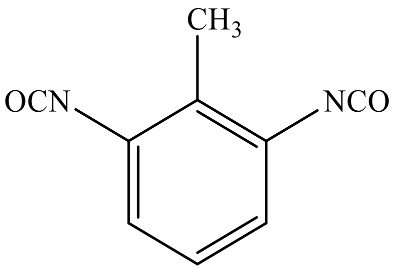

2,6 isomer (20%)

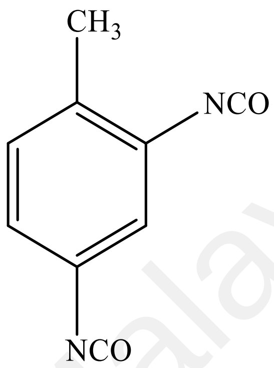

2,4 isomer (80%)

Trimer of TDI

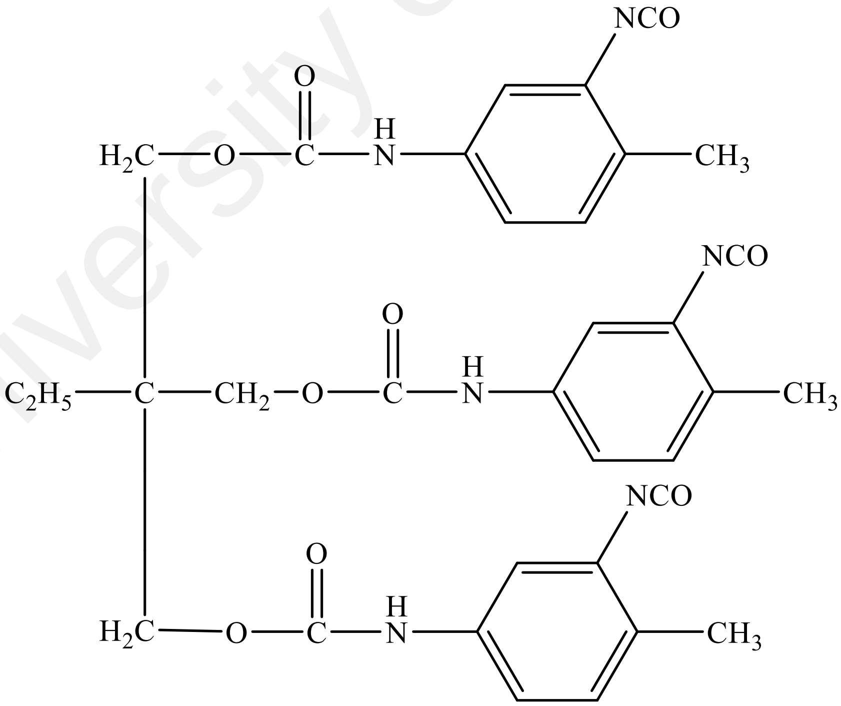

Figure 1.40a Structure of some aromatic isocyanate

(II) Aliphatic Diisocyanate

Tetramethylxylene Diisocyanate (TMXDI)

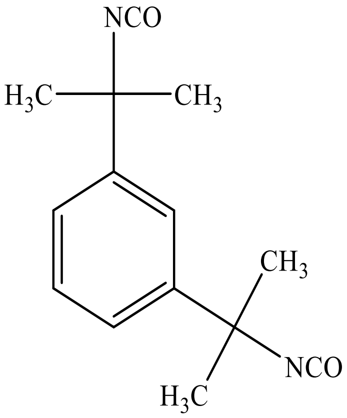

m-TMXDI

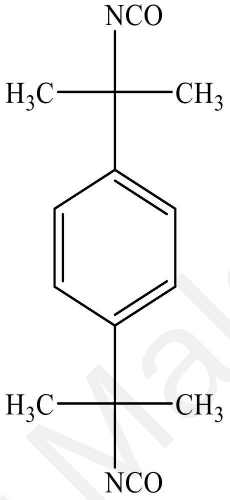

p-TMXDI

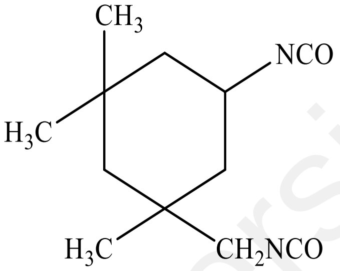

Isophorone Diisocyanate

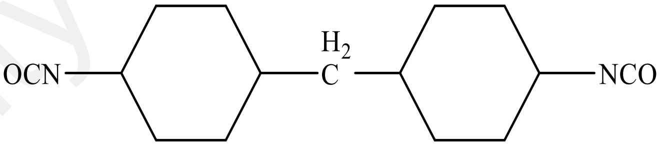

4,4-Dicyclohexylmethane Diisocyanate

$OCN—(CH_2)_6—NCO$

Hexamethylene Diisocyanate (HMDI)

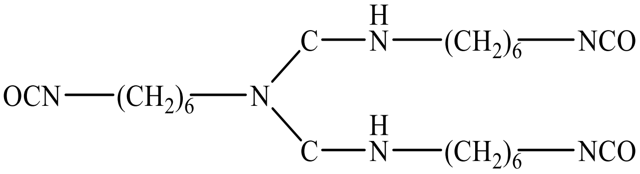

Oligomer of HMDI

Figure 1.40b Structure of some aliphatic isocyanate

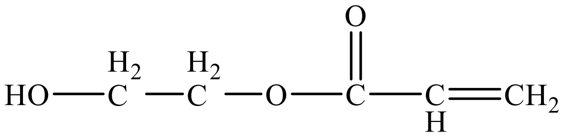

$HO-CH_2-CH_2-O-C(=O)-CH=CH_2$

Hydroxyethyl acrylate (HEA)

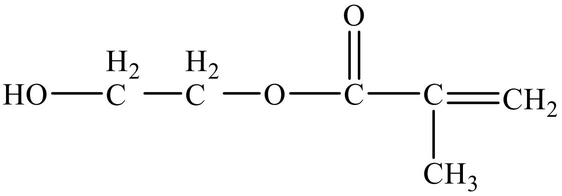

$HO-CH_2-CH_2-O-C(=O)-C(CH_3)=CH_2$

Hydroxyethyl methacrylate (HEMA)

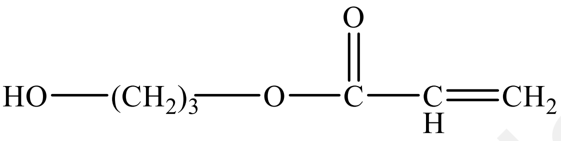

$HO-(CH_2)_3-O-C(=O)-CH=CH_2$

Hydroxypropyl acrylate (HPA)

Figure 1.41 Structure of hydroxyl containing acrylate monomer

1.2.4.6 Multicomponent Urethane Acrylate

Multicomponent urethane acrylate was synthesized using higher hydroxyl functionality polyols. Owing to the complexity of the reactant particularly the polyols, even with identical stoichiometric reaction ratio may yield the final urethane acrylate with significant different properties if the reaction conditions vary. Viscosity is one example of a property that can vary dramatically. Long chain glycol can produce flexible urethane acrylate when reacting with diisocyanate. Aliphatic diol such as polyethelene glycol, polypropylene glycol and carprolactone polyols, are widely used for this purpose, as are polyesters with an excess of hydroxyl groups. As the flexibility increases, the hardness, speed of cure and solvent resistance of the film decrease. A highly branched polyol synthesized from pentaerythritol or NPG can produce a hard urethane acrylate when reacting with diisocyanate.

1.2.4.7 Principle of Urethane Acrylate Synthesis

In principle, there are two chemical pathways can be applied for synthesizing a same urethane acrylate. In the first reaction pathway, the half or partial reacted isocyanate adduct of hydroxyl acrylate or methacrylate was first being produced, then follow by reacting with the polyol compound. In second pathway, the polyol is reacted with the diisocyanate and the resulting product will then proceed with acrylation with hydroxyl acrylate or methacrylate. The two reaction pathways can be summarized as in Figure 1.42.

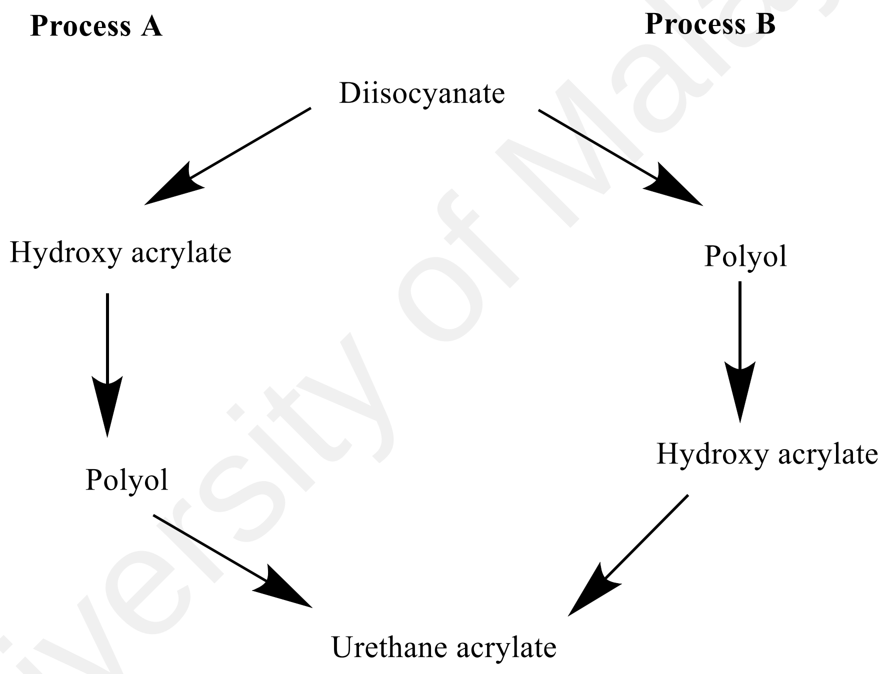

Figure 1.42. Two alternative process routes for urethane acrylate synthesis

Due to the difference in reactivity of the primary, secondary and tertiary hydroxyl in high functionality polyol, and also in asymmetric diisocyanate compounds, the addition order of the reactant into the reaction mixture may have difference impacts to the final urethane acrylate structure. For example, the asymmetric diisocyanate such 2,4 TDI and IPDI, the order of addition is important. For illustration purposes, if 2,4-TDI using process A reaction pathways, the structure I will be the predominant product as shown in Figure

1.43a, whereas structure II become predominates if follow process B reaction order as shown in Figure 1.43b.

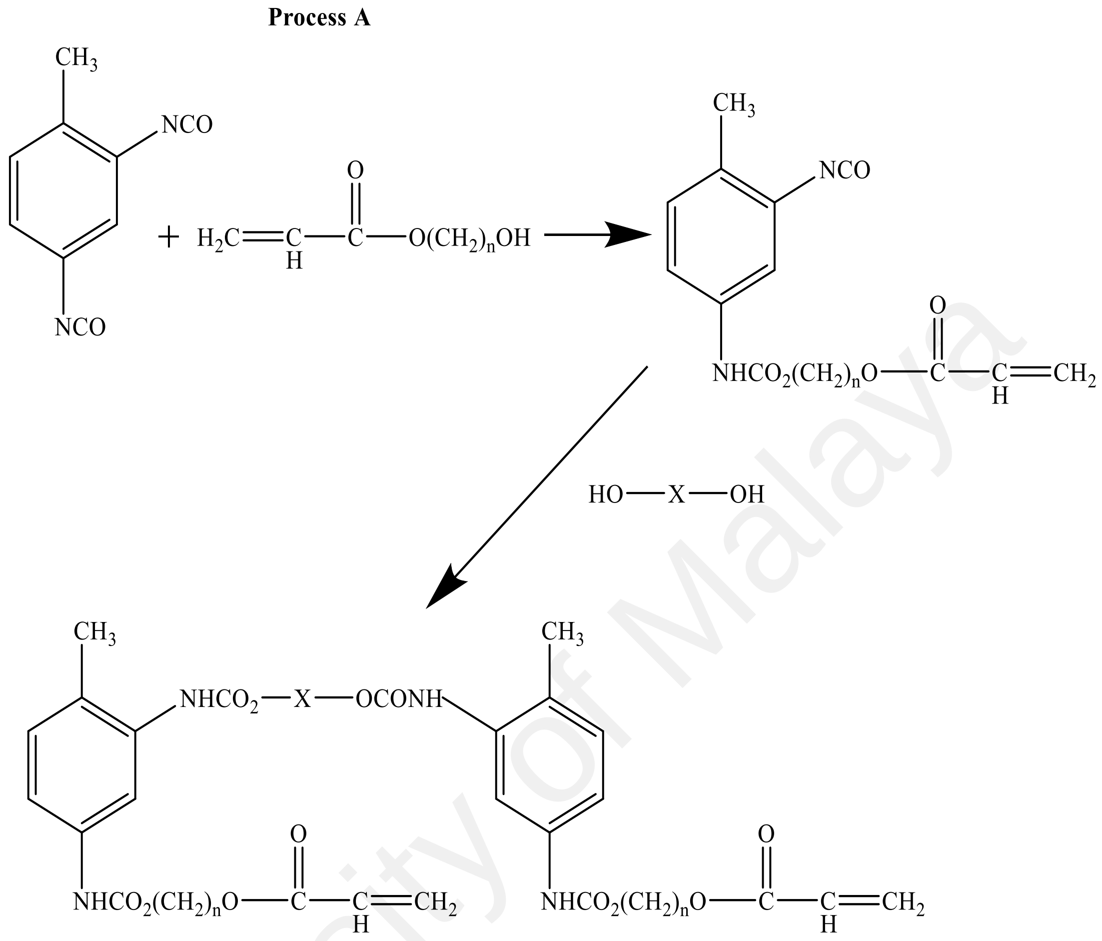

Figure 1.43a Resulting structure I of urethane acrylate from TDI using process A

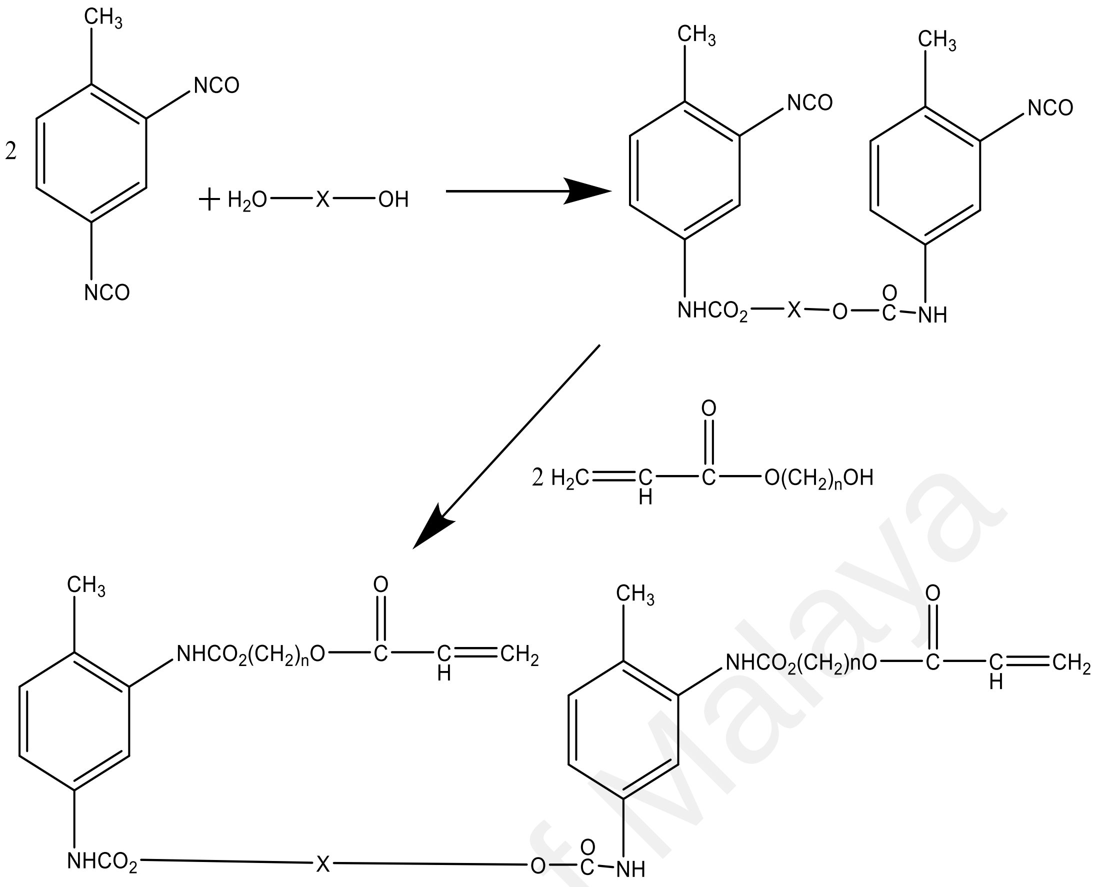

Figure 1.43b Resulting structure II of urethane acrylate from TDI using process B

1.3 Building Block for Alkyd

1.3.1 Introduction of Alkyd

Alkyd resin is a sub-class derived from the convention polyester resin. The key feature differentiates alkyds from other polyester is the presence of monofunctional fatty acids as major part of its composition. Alkyd was the first synthetic polymer being applied in surface coating's technology some 70 years ago ever since its discovery by Roy Kienle of General Electric Co. in 1920. At present alkyd has hold a majority share of the world market for synthetic coating resins, accounting for more than 50% market share of all the resins used in paint industry. The main reasons for their popularity are their cost and versatility of further modification (Oldring P.K.T. et al., 1995). Depletion of petroleum reserves and increasing environmental concerns have stimulated the revolution to explore materials from readily-available, renewable, and inexpensive natural resources, such as carbohydrates, oils, fats, and proteins. Alkyd with the natural occurrence oil or fatty acid as major composition in its resin modification will continue to play noteworthy roles in the development of a sustainable green chemistry. The alkyd reaction is conceded to be the most versatile resin forming reaction ever known. No other resin leads itself to greater internal variation or more useful modification by physical or chemical with other polymers (Oldring P.T.K. et al., 1995, Paul S., 1986). Table 1.5 shows the common polymers used for alkyd modification.

Table 1.5. Polymer commonly used to modify alkyd resin

Physical modification	Chemical modification
Nitrocellulose	Acrylate / methacrylate and their ester
Urea-formaldehyde	Phenolics
Chlorinated rubber	Silicones
Ketonic / Aldehyde resin	Epoxies
Copolymer of vinyl acetate or vinyl Chloride	Isocyanate
Cellulose Acetate Butyrate	Melamine /amino Formaldehyde
	Vinyl monomer

1.3.2 Oil and Fatty Acid

If oil being used as starting material, prior modification of oil is necessary as oil are not directly reactive with other polyester components. The modification of oil molecules will be carried out at the first stage synthesis, called monoglyceride or alcoholysis process. In alcoholysis process, glycerol or other polyol will proceed the transesterification reaction with oil in the molar ratio of 2:1 at reaction temperature of 240-250°C in the presence of a basic catalyst for forming monoglyceride, which capable for further polycondensation reaction. Figure 1.44 illustrate the alcoholysis of oil with glycerol.

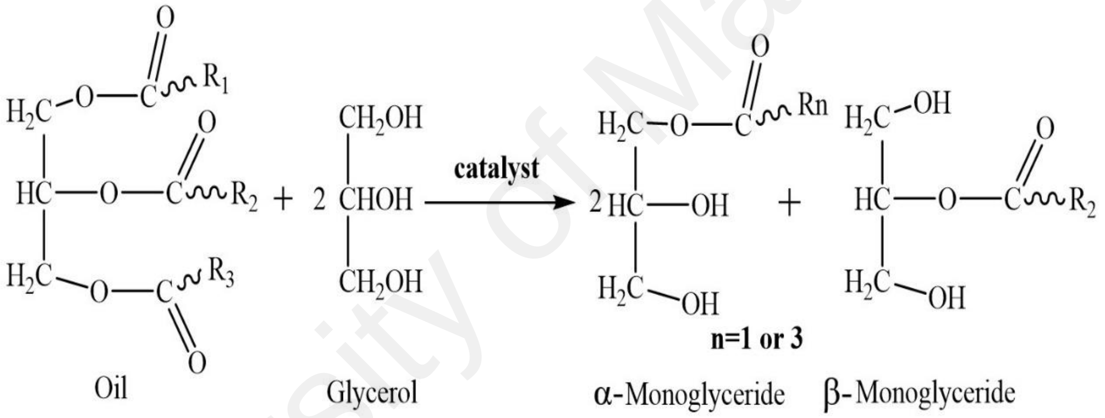

Figure 1.44 Schematic of monoglyceride formation

Preparation of the final resin is carried out by the additional of remaining polyol and dibasic acid for continue the polycondensation reaction stage; in this stage, multiple esterification reactions occur as shown in Figure 1.45 and water formed as a by-product of reaction must be decanted from the reaction vessel.

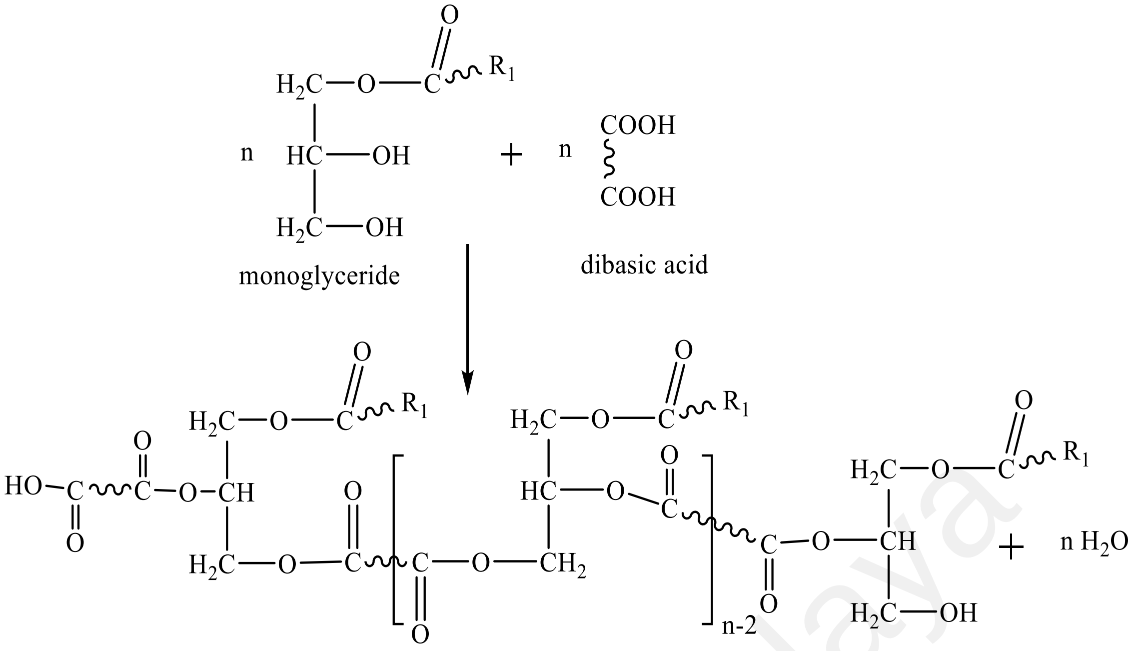

Figure 1.45 Schematic diagram of alkyd formation

The monoglyceride method is commonly practised for long oil alkyd where the oil content above 55%. Whereas, the short and medium oil alkyd were normally synthesized via fatty acid process. In fatty acid process, all ingredients including fatty acid were charged into the reaction vessel at initial stage. The multiple esterification will immediately take place once the reaction temperature reached 180°C before optimum temperature of 230-240°C. Similarly, the water will be produced as by-product and must be decanted out to promote more esterification during the synthesis period.

oil is always made up of a mixture of triglycerides (typically 3 to 5 type), frequently with one or two predominant fatty acid making up 70 – 80% of its composition (Gunstone F., 1996). The degree of unsaturation of a vegetable oil is perhaps the most relevant criteria in alkyd synthesis. In the class of air-dry alkyd, the curing of the alkyd is through the drying of the oil by atmospheric oxidative polymerization through a well-established mechanism (Remy van Gorkum et al., 2005). The unsaturation may also act as a source of other types of polymerization and chemical modification of the synthesized alkyd resins. Figure 1.46 illustrate some of the most common structures of fatty acids present in triglycerides.

When analysing the vegetable oil production, obviously palm oil and soya bean oil were the two major oil being produced worldwide. The Statista research group reported that Palm oil production showing trend of increase and is the largest vegetable oil being produced follow by soya bean oil as shown in Figure 1.47. Even though, palm oil has highest production volume, but both oils were showing quite similar in consumption and there were among the top two highest consumption vegetable oil particularly in food-based product as shown in Figure 1.48. Due to the excellent drying property of soya bean oil as compared to palm oil, the soya bean oil has gained much attention and popular in non-food application particularly in alkyd resin production. But with the abundant volume of palm oil being produce ever year, the potential of using palm oil in alkyd application still highly receptive and positive by the researches where chemical modification can be easily applied on the alkyd resin development. Other than oil itself, many fatty acids can be saponified from palm oil such as palmitic, oleic, stearic and linoleic fatty acid (MPOB, 2019) and this are useful renewable resources for alkyd synthesis via fatty acid process.

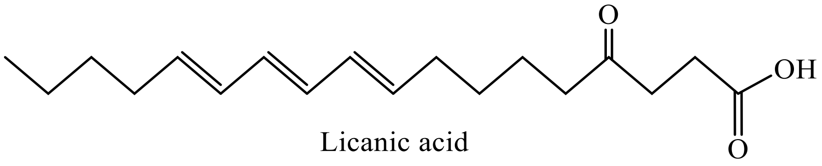

Licanic acid

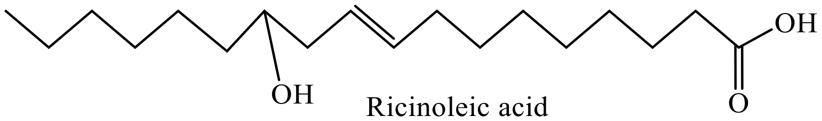

Ricinoleic acid

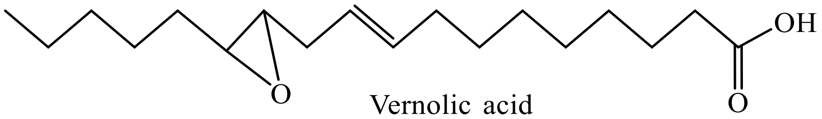

Vernolic acid

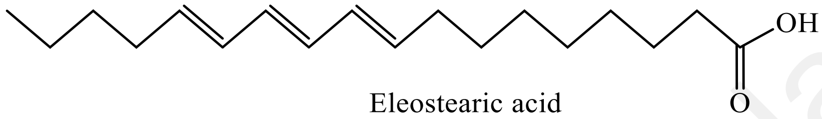

Eleostearic acid

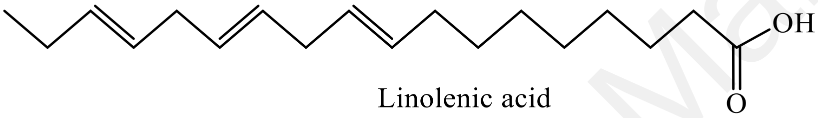

Linolenic acid

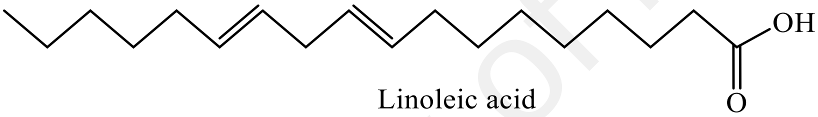

Linoleic acid

Oleic acid

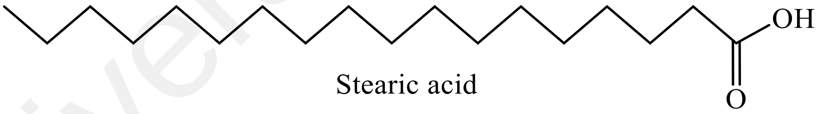

Stearic acid

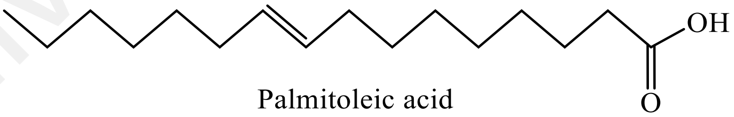

Palmitoleic acid

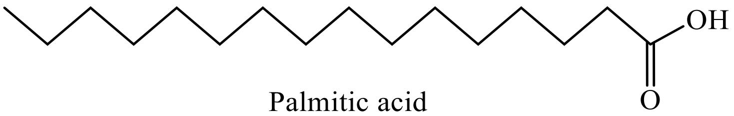

Palmitic acid

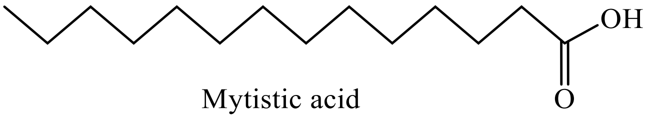

Mytistic acid

Figure 1.46 Structure of some common fatty acid exist in oil composition

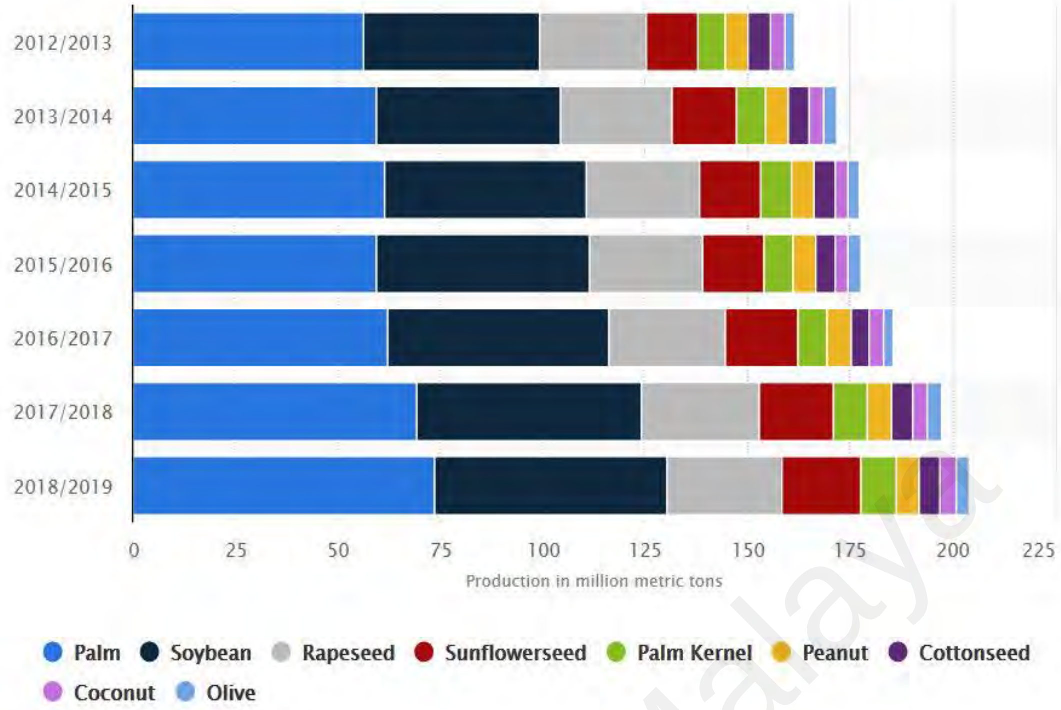

Figure 1.47 Production of major vegetable oils worldwide from 2012/13 to 2018/2019, by type (in million metric tons). Reproduced from Statista research, May 2019 @ www.statista.com

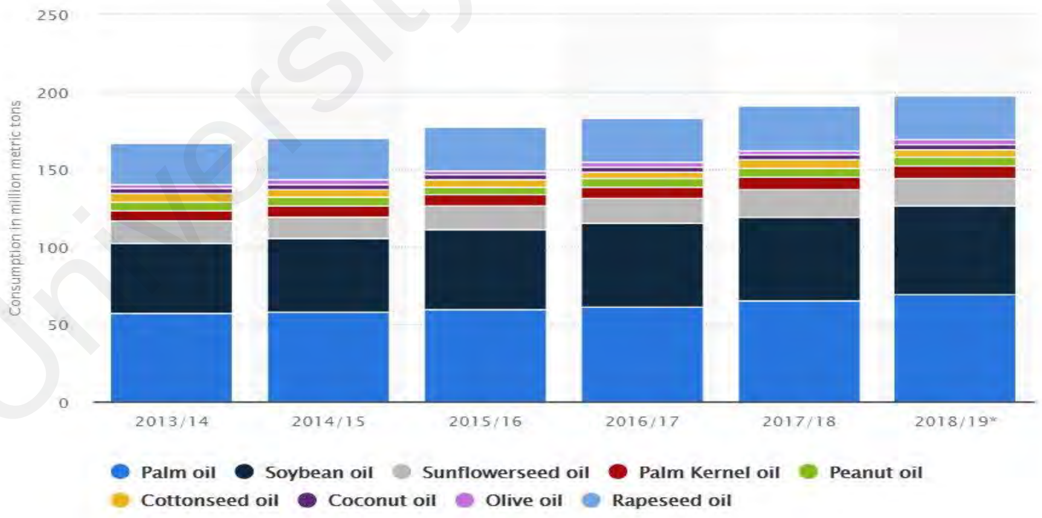

Figure 1.48 Consumption of vegetable oils worldwide from 2013/14 to 2018/2019, by oil type (in million metric tons). Reproduced from Statista research, May 2019 @ www.statista.com

1.3.3 Polyhydric Alcohols

Other than oil or fatty acids as major components in alkyd resin, the resin also derived from polymerization of polyhydric alcohol and polybasic acids. At its earlier stage of resin development after their first discovery, glycerol was the main polyhydric alcohol used in all alkyd synthesis and mainly are for long oil alkyd development. Later development progress has allowed the alkyd to be formulated with higher order of polyhydric alcohol such as in medium or short oil alkyd formulation. In principle, the factor that influence alkyd on their performance are including molecular weight, functionality, degree of branching and structure of polyhydric alcohol or polybasic acid.

Figure 1.49 shows some common polyhydric alcohol used in alkyd or polyester production. In alkyd resin, the type of pendent functionality was mainly hydroxy group (OH) which was derived from the excess of polyhydric alcohol used. The amount of pendant functionality on the alkyd determines the cross-linking density that can be obtained during the curing process of the coating film. In principle, linear polyhydric alcohol such as ethylene glycol, butanediol, hexanediol, etc. will produced alkyd with terminal functionality and resulted a limited cross-link density. As a result, the linear type of alkyd resin will have higher flexibility and low T_g on their cured film properties. Low hardness and poor chemical resistant exhibited by linear type alkyd, mean modification of the resin with other polyol is always required before accepting for actual application need. Using higher order of polyhydric alcohol will increase the branching of alkyd structure. The highly branched alkyd will have higher functionality for better cross-linking density during curing process. Alkyd resin with higher branching always shows increase in viscosity and molecular weight as a result from the higher number of hydroxyl group can be react during polymerization process. Other than functionality and flexibility, good hardness of the alkyd cured film is another important physical property required during designing the alkyd resin. In general, polyhydric alcohol with short chains, cyclic or aromatic rings can produce harder alkyd such neopentyl glycol and bisphenol A.

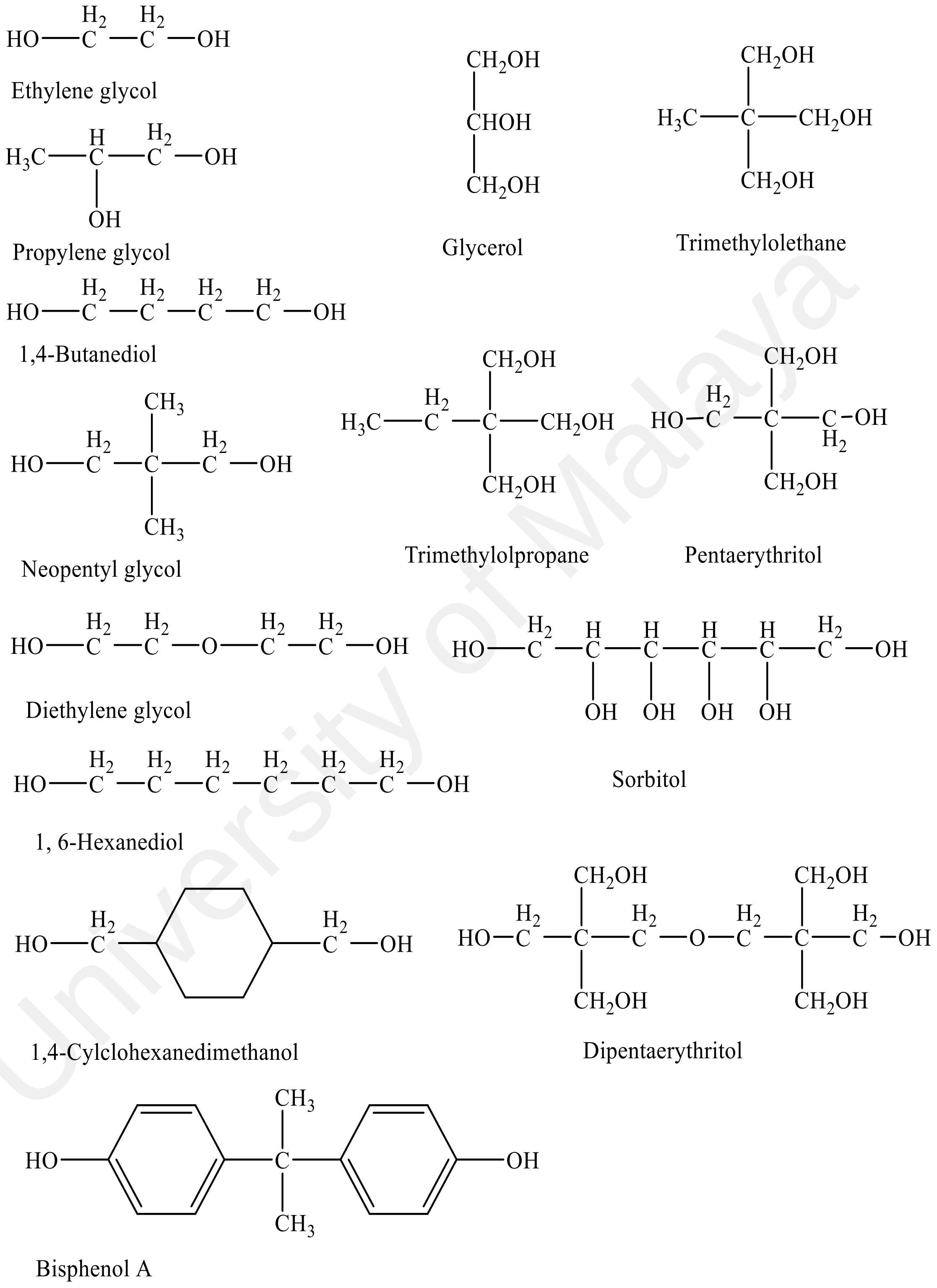

Ethylene glycol

Propylene glycol

Glycerol

Trimethylolethane

1,4-Butanediol

Neopentyl glycol

Trimethylolpropane

Pentaerythritol

Diethylene glycol

Sorbitol

1, 6-Hexanediol

1,4-Cylclohexanedimethanol

Dipentaerythritol

Bisphenol A

Figure 1.49 Common polyhydric alcohols use for alkyd/polyester synthesis

Since alkyd resin was synthesized at high temperature typically at the range of 210-240℃. At such high temperature, side reaction such as etherification might occur where hydroxy-functional species can react with each other to form an ether linkage. In its simplest form the reaction can be represented as follows:

$$R\text{-}OH + R'\text{-}OH \longrightarrow R\text{-}O\text{-}R' + H_2O$$

Figure 1.50 Etherification reaction

The most important result of this reaction is to render hydroxy group unavailable for ester formation, thereby leaving acids in excess. They can have serious repercussion on the tendency of the resin to gel during the later stages of polymerization. The way to counteract this problem is to deliberately add extra polyol. Other than etherification, transesterification is known to occur during alkyd or polyester processing. Normally this is not an important consideration except when producing low molecular weight alkyd or polyester. Carefully selection of esterification catalyst can minimise the transesterification effect particularly for low molecular weight alkyd or polyester synthesis. The reaction can be summarized as follow:

$$R-\overset{\overset{O}{\parallel}}{C}-O-R_1 + R_2-OH \longrightarrow R-\overset{\overset{O}{\parallel}}{C}-O-R_2 + R_1-OH$$

Figure 1.51 Transesterification reaction

1.3.4 Polybasic Acids

Polybasic acids are another important building block for alkyd or polyester resin. Figure 1.52 illustrate some common polybasic acid used in alkyd production. Among the polybasic acids, phthalic anhydride is the main di-basic acid used in alkyd production. The high usage of phthalic anhydride in alkyd polymerization is mainly due to the reactivity of its anhydride group also the aromatic ring which will give alkyd with good hardness and chemical resistance.

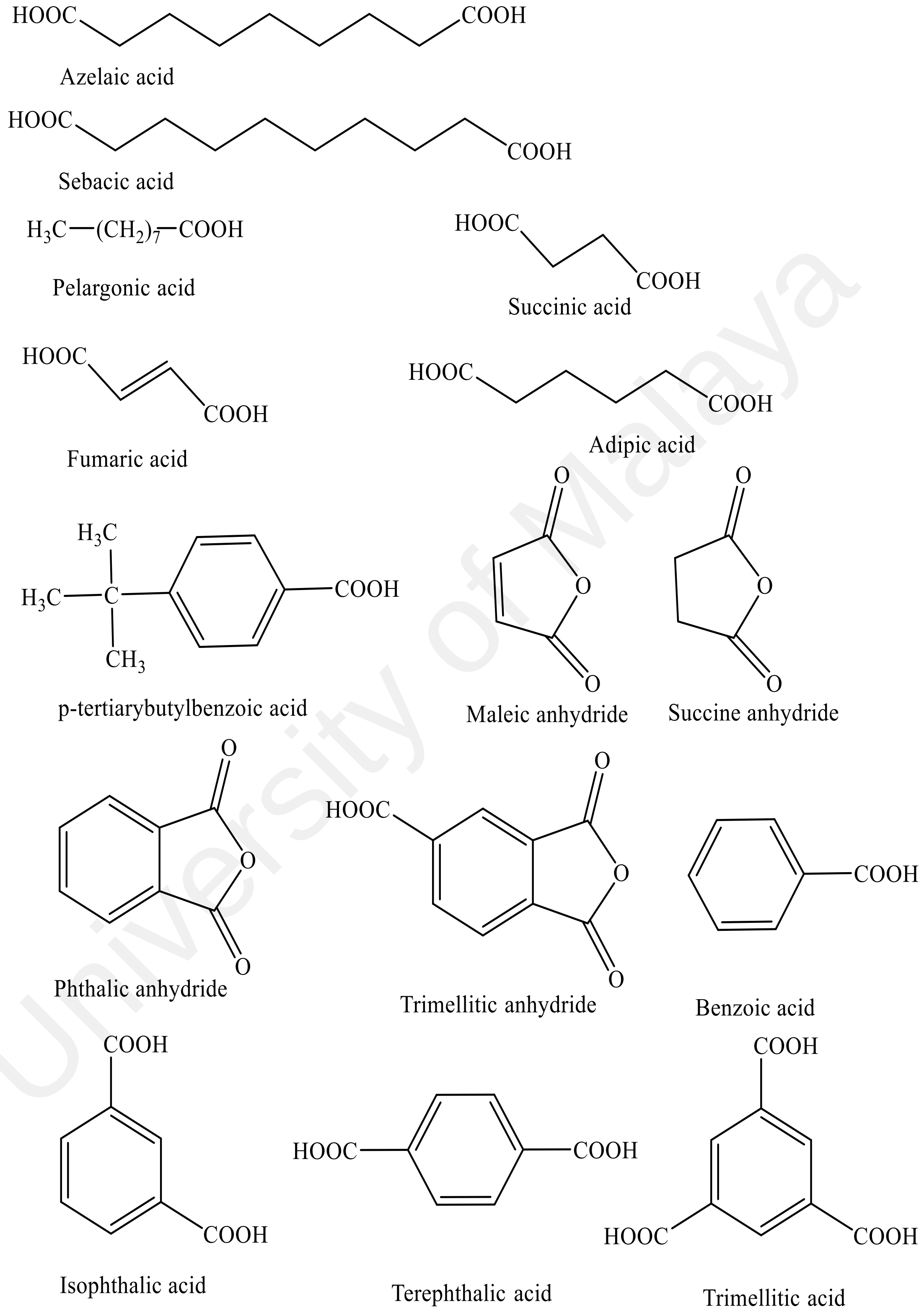

Figure 1.52 Common polybasic acids used in alkyd or polyester synthesis

Phthalic anhydride does not suffer from major solubility problem since the anhydride ring readily open and reacts with polyhydric alcohol to form a half-ester at temperatures as low as 150 °C. Once the half-ester has been formed the phthalic anhydride has effectively been solubilised during the process. Isophthalic and terephthalic acid were used, where improved of film hardness, chemical and heat resistance are required. Terephthalic acid is not soluble in any raw materials of alkyd production and can only be reacted into the alkyd structure by prolong heating at temperature of 240°C or higher. The high process temperature for alkyd process, which may cause the alkyd produced with intense colour or sublimed of other raw material such as phthalic anhydride. To improve the difficulty of processing terephthalic acid in alkyd synthesis, it is commonly used of more soluble dimethyl terephthalate derivative, which can undergo transesterification during polymerization process. Isophthalic acid is more soluble than terephthalic acid but, nonetheless presents processing problems and prolong heating at elevated temperature is often required. The isophthalic acid always used in blend with phthalic anhydride. The isophthalic acid will normally be added into the reactant mixture at earlier stage. The high concentration polyhydric alcohols at beginning process will significantly promote esterification of isophthalic acid and a clear sample after the fusing process at temperature of 240 °C indicating most of the isophthalic acids have been reacted. Then, phthalic anhydride will be added to complete the polymerization by fusion or solvent process.

Other than fatty acid itself, wide range of mono-basic acid are employed commercially. In high functionality alkyd where high order of polyhydric alcohols was used such trimethylolpropane or pentaerythritol. Small amount of benzoic acid will be added to act as the additional chain terminator. In long oil oxidising alkyd where the rapid surface is required, the resin always modified with rosin or rosin ester. The inclusion of rosin acts to improve the drying speed and set for the alkyd. In non-oxidising alkyd, short chain of mono basic acid such as heptanoic acid or nonanoic acid was used to instead of fatty acid for non-yellowing alkyd production.

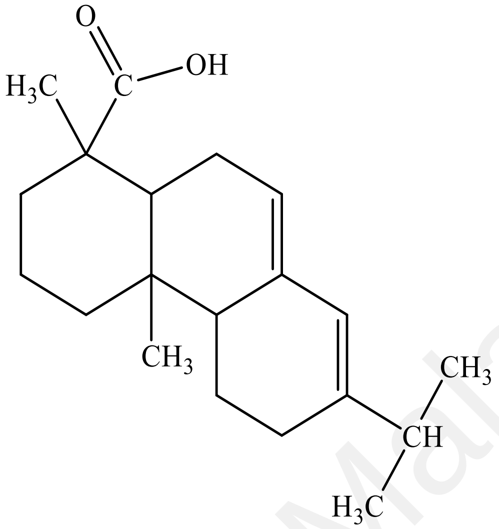

Figure 1.53 Structure of rosin

Maleic anhydride is another important modifier in alkyd synthesis and usually less than 1% of the total solid resin usage. The maleic anhydride is mainly to increase the resin functionality and hence product viscosity at given degree of esterification. The maleic anhydride will react across the double bond of the unsaturated fatty acid present and effectively forming a trifunctional acid which acts as a site for chain branching. To perform such grafting reaction in alkyd synthesis, great care must be taken such as temperature control otherwise gelation can easily occur.

1.4 Wood Coatings

Similar to any other coating technologies, wood coating is one of the important segments in the coating industry that focuses on developing more environment-friendly resins, in comparison to traditional solvent-borne coating system. UV-curable resins offer less VOC, lower energy in the curing process, and shorter curing time always been the interest research focus for all wood coating researches across the world. The worldwide market for Wood Coating is expected to grow at a compound annual growth rate of roughly 5.9%, over the next five years, and will reach 11,700 million US$, in 2023, from 8740 million US$, in 2017 (Global Wood Coating Market, 2018). Malaysia, as one of the ten largest furniture exporters, has provided a very good economic base for the wood coating industry development. Modernization of architectural designs including furniture, has driven the increasing need for improved aesthetic appeal of furniture and other wooden products, making wood coating a very important part of the woodworking industry. In addition, the material needs to be protected against mechanical, physical and chemical attack. The current available technologies include waterborne coatings, high-solids, and UV-cured coatings. There is a noticeable move from the solvent-borne coatings to solvent-free or solvent-reduced materials, driven by the environmental and regulatory demands. Other than conventional waterborne technologies where acrylate/vinyl emulsions are the main binder used, the solvent-borne technology has involved many types of alkyd resin as the main binder in the three major wood coating systems, such as acid catalysed, nitrocellulose and polyurethane. In a high-solid system, UV-curing is the current trend and the focus of development to achieve 100% solidity in a cured coating film.

1.4.1 The Nature of Wood

Due to the wide range of species and naturally occurrence phenomena, the wood substrate has exhibited a very complex structure as a composite material. The understanding of this complexity is playing a key role for a researcher to select or design a suitable coating application on wood substrate. The wood can be generally divided into hard and soft wood, even though there are wide range of wood properties among the species. In term of botanical aspect, the coniferous trees are classified as softwood, and trees with broadleaf were belong to the hardwood category (Dinwoodie, J. M. 1989). Even though, hardwoods are normally harder that softwoods but this is not always so, for example, the physically soft character of balsawood is categorised as hardwood. In term of biological structure, the cell structure was different between hard and softwoods and the cellulose was main components of the wood cover almost 40-50% of the total composition. Lignin is the other components of wood composition, which is built up from phenyl propanol block (Dinwoodie, J. M. 1989). The wood may contain some chemical active and colour extractive compounds. This extractive compound such as stilbenes, tannin and lignans are normally not inert to coating. They might cause coating defects such as staining or loss of drying mechanism in the coating system. The heartwood is located in central area of the body of wood and appears darker than the outer circumference.

Due to the natural occurrence and chemically active nature of the wood compositions, the durability of the coating can be greatly influenced by this characteristic. (Graystone J.A., 2001). It is commonly having different coating performance when carried out the testing on the variability of the wood substrate. Another important characteristic of the wood that the coating chemist must understand is the presence of vessels e.g. pores in oak. This vessel will absorb a large quantity of coating material and transporting water behind the coating, which may cause unevenness or others defects upon drying process. As the wood was built up by a complex organic compound, many chemical treatments are needed prior to the actual industry application to prevent degradation or even fungus growth in order to extend the life spend of the wood product. Chemical treatment of wood substrate will be more difficult particularly the softwood, where their pits or pores may close up after seasoning. Even though wood substrate is a complex material but due to the easy custom design, cutting and the beauty of natural grown wood grain pattern, the wood substrate will continue becoming important material particularly in furniture industry application.

1.4.2 Coating for Wood Substrate

Wood coatings are normally divided into three main coating systems which are topcoat, penetrating stain or sealer and filler or primer coat. Each of the coatings will have its own appearance and performance such as filling and penetrating effect, colouring, protective and decorative purposes. The topcoats are comprising of solvent-based oil or alkyd opaque or transparent glossy, semi-gloss and even matt finishes. The stain is low solid penetrating composition, semi-transparent colouring containing an in-film fungicide formulation. The filler or primer system containing highly pigmented/extender formulation for filling the pores or woodgrain in order to provide a smooth surface and adherent to subsequent coat.

Wood panel applied with primer or filler coating can provide good inter-coat adhesion between subsequent coating system. The primer coating should be able to provide a fully cover and smooth surface, and also to avoid hydrolytically breakdown in order to extend the service life cycle of the coating. The wood primer was normally formulated with vegetable oil and silicate type of extender. The formulated primers must exhibit excellent wetting performance and good mechanical properties such as hardness and flexibility. Primer coating also important to repainting work by covering the damaged area for the new coating application. The high PVC or heavily filled primer compositions will be formulated for this application purpose. The content of pigmentation/extenders in the formulation can be ranging from 35-70% by weight in the total formulation content. Another important function of filler or primer is to provide sanding properties of the coating system. In wood substrate, the wood fibre will be easily stand up due the surface tension contraction during the film drying process and this will affect the surface condition for subsequent coating to be applied. Good sanding property primers and fillers are necessary particularly for industrial wood coating application to ensure high production output in the wood-based industry.

In transparent coating system, a sealer coating has been developed as sub-class of primer to provide a transparent primer coat with good transparency and sanding properties for any clear topcoat system. The sealer is commonly formulated with 5-10% of magnesium silicate powder or zinc stearate for enhancing the sealer's good sanding property. The sealer coating will normally be applied when a semi or full transparent top coating finishing required. In this context, inclusion of colour stain coating is necessary in order to achieve an even distribution of colour on the wood surface for decorative effect. The stain is formulated with very low solid using alkyd or drying oil to ensure good penetrating performance. Recent development also yields the water-based stain using aqueous dispersion polymer as main binder. This development was actually driven by the fulfilment of environmental friendliness target in wood coating industry application.

The topcoat system covers all opaque pigmented and transparent coatings, regardless of sheen, build or system. Other than decorative purposes, the protective functions are the import aspect during development or designing a wood coating formulation, such as to improve the mechanical and chemical resistance of the wood substrate. The high versatility of alkyd and fatty acid modified polyester resins were very popular and commonly used in wood coating formulations. Due to the versatility of alkyd in term of chemical modification, many topcoat's physical and mechanical performance can be achieved by formulating with alkyd resin such as in nitrocellulose, acid catalysed and 2K polyurethane solvent-based coating system. Recent development also involving some UV curable alkyd resin which shows possible of wood coating application (Chittavanich, P. et al., 2012, Narin Thanamongkollit et al., 2012).

1.5 Coatings for Metal Substrate

Steel is the world's most trusted material. It's flexibility and versatility also mean that designers, developers and architects can use it in any number of ways to turn their visions into reality. Though iron has been around for centuries, one of the first major uses of steel for construction purposes was in train stations. In early 20th century, steel buildings become popular. Today, steel is used in many areas such construction, automotive, aerospace and many general appliances. To further widen steel application, technology has uses steel with combination with other construction materials, such as glass, and cold rolled and galvanized for production of flat steel sheet. But the occurrence of corrosion in atmospheric temperature conditions such as pitting and crevice still a serious problem for steel (Hermas, 2008; Okamoto, G. (1978); Schultze, J.W. et al., 2000).

In modern application, many decorative panels have been produced for latest designer with colour and shape. Therefore, the technological advancement on the surface coating in terms of polymer, active pigment or chemical pre-treatment for prevention of corrosion has become an important topic among the coating researches. In addition, other than the decorative effect, the physical and mechanical properties of coatings for metal surface are also important in various applications such high gloss, good adhesion, flexibility, impact resistant, chemical resistant and durability performance. In general, the metal coatings cannot be simply defined as single stream of coating for metal substrate but rather refer to its end used application such as automotive OEM, coil, can, general steel industrial and heavy duty protective and marine usage. The metal coating will be developed according to their individual industrial requirement and specification. Each type of metal coating can present a unique set of painting requirements and performances.

1.5.1 Corrosion of Metal

The most critical factor affecting corrosion is the steel substrate itself (Kearne J.D., 1983). There are large variations in cold rolled steel that can lead to greater or lesser probabilities of corrosion failure. Ferrous hydroxide is produced which, in its hydrated oxide form, is known simply as ‘rust’. Many theories have been invoked to explain corrosion but today electrochemical theories are standard. Iron will rust when it is exposed to oxygen and water. Figure 1.54 shows schematic diagram of the important steps in the rusting of iron. Once exposed to the atmosphere, iron rapidly oxidizes.

$$Fe(s) \longrightarrow Fe^{2+}(aq) + 2e^-$$

The electrons will reduce oxygen in the air in acidic solutions.

$$O_2(g) + 4H^+ + 4e^- \longrightarrow 2H_2O(l)$$

What we call rust is hydrated iron(III) oxide, which forms when iron(II) ions react further with oxygen.

$$4Fe^{2+}(aq) + O_2(g) + (4+2x)H_2O(l) \longrightarrow 2Fe_2O_3.xH_2O(s) + 8H^+$$

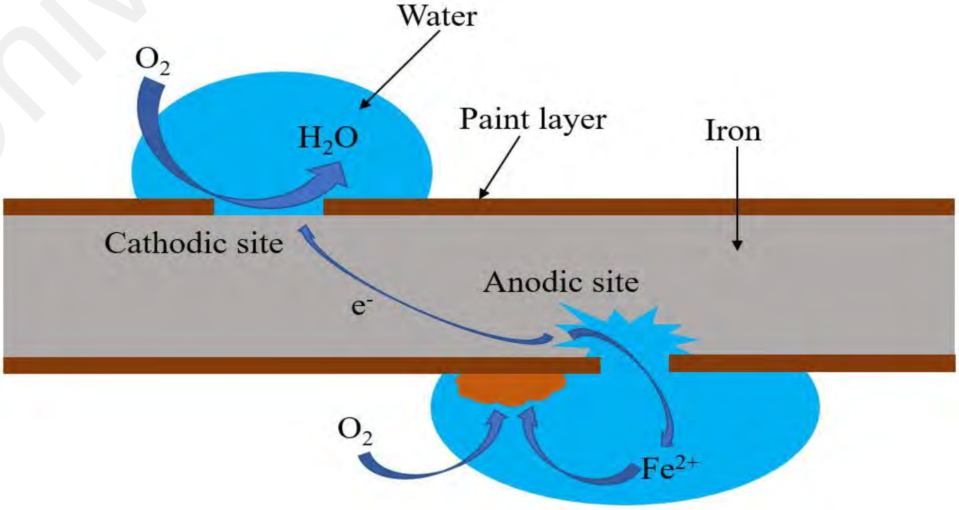

Figure 1.54 Schematic diagram of corrosion phenomenon

In actual condition, the coating defect cause by the corrosion are far more complex than its being defined. Blistering, delamination, undercutting, under-rusting and filiform were common corrosion defects on metal coating systems. The need to protect steel from corrosion, it is important to formulate a good anticorrosion primer coat as compared to topcoat requirement. Along the development, chemist has developed many types of primer formulation in metal coating application, this including etch primer, general purpose primer and zinc rich primer. Etching primers or wash primers are formulated to serve as pre-treatment to promote adhesion especially with non-ferrous metals and subsequently overcoated with a fully pigmented primer is needed (Joseph Edwards, 2007). The general-purpose primers have always been based on various types of resin from alkyd, polyester, epoxy, polyurethane even processed drying oils as primary binder. The complexity of primer formulation is varying from their application and requirement in the individual sectors. The primer is always formulated with magnesium silicate or other similar type of extender at 25-40% by weight in their total formulation to ensure good sanding and anti-corrosion properties. In general coating system, this primer always serves as first coat coverage onto the metal substrate to improve the build or thickness of the coating before applying the subsequent topcoat.

High content of zinc dust in zinc rich primer formulation can provide cathodic protection and galvanizing properties by generating a solid barrier between metal surface and atmospheric moisture (Claus E. Weinell et al., 2007). The type of binder used in zinc rich primer formulation has been used to differentiate the type of zinc rich coatings. Silicate binder was used in inorganic zinc rich primer formulation whereas organic type involves wide range of organic film former such as epoxy, polyurethane, alkyd and etc. The performances of the inorganic and organic zinc rich primer vary as a result from the differences in binder performance (Dr. Llham Ulken et al., 2010). The silicate binder in inorganic zinc rich formulation always shows poorer adhesion to the metal substrate as compared to organic type. Therefore, it is common to have the organic binder formulated into inorganic zinc rich formulation in order to improve its adhesion performance onto the substrate. As the corrosion is unavoidable phenomenon when metal substrate particularly iron still continue being an important substrate for many application, anti-corrosion will remain focus when coating researches continue finding new organic or inorganic coating technologies in coming future.

CHAPTER 2: LITERATURE REVIEW

2.1 Overview of Vegetable Oil and Fatty acids Applications

The exploitation of vegetable oils as raw materials was recorded since 3000 B.C., first for coating applications and soap manufacture, then for progressively wider and more sophisticated applications including inks, plasticizers, alkyd resins, agrochemicals, etc (Verhe R.G. et al., 2004). As expected, this scientific literature is largely complemented by a wide range of patents (Cunningham A. et al, Bussel G.W., 1974; Hodakowski L.E. et al.,1975; Trecker D.J. et al, 1976; Force C.G. et al., 1988).This qualitative and quantitative increase in the realm of materials has been complemented in recent years by the use of vegetable oils for the production of biodiesel. From total vegetable oil production, around 15% was used as precursors to synthesize of new materials. Variety of fatty acids are found in terms of the different chain lengths, the number of carbons, degree of unsaturation sites, position of the unsaturated carbons, and presence of functional groups (e.g., hydroxyl and epoxy), depending on the species and growing conditions (Belgacem and Gandini A., 2008; Islam et al., 2014; Pfister et al., 2011). Among the most interesting chemical modifications of oils or fatty acids, epoxidation occupies a privileged position for the number and variety of studies and applications (Gandini A. 2009). This reaction involves the transformation of C = C alkenyl moieties into oxirane groups using a variety of oxidation systems, for examples, as shown in Scheme 2.1 (Gandini A. 2009). These epoxidized macromonomers have found numerous applications in thermosetting resins using diamines and anhydrides as hardeners, including reinforced nano-hybrid materials and flame retardancy additives. The other mode of activation of the oxirane moieties is through cationic polymerization, which will generate a network for polyfunctional epoxidized glycerides and thermoplastic materials with fatty acids bearing a single epoxy group (Zengshe Liu et al., 2009).

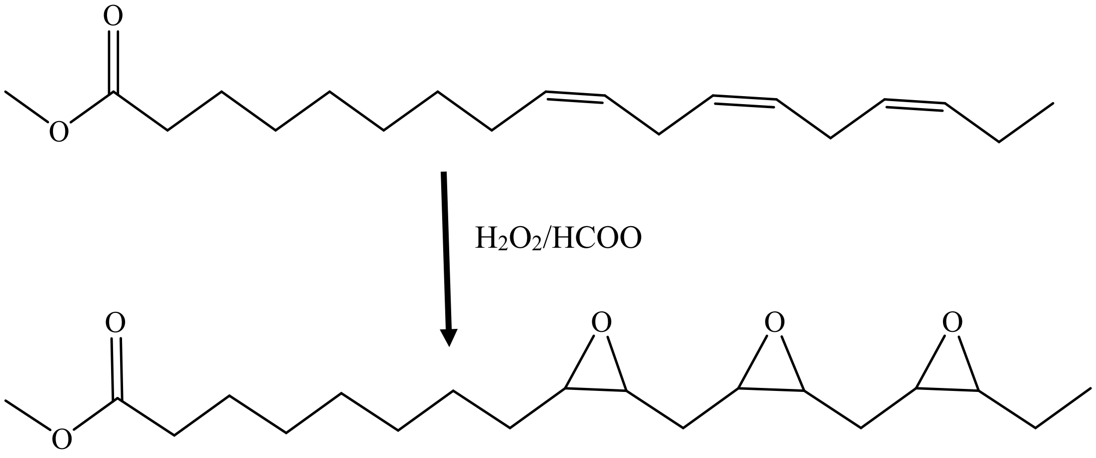

Scheme 2.1 The epoxidation of methyl linolenate by performic acid

The unsaturation sites and ester groups of natural triglycerides can be chemically modified to obtain the reactive functional groups such as epoxides, acrylates, and hydroxyl groups on the fatty acids through using typical synthetic pathways in current polymer industries (Wool and Sun, 2005). Polyols constitute one of the important derivatives of vegetable oil. Better known as oleochemical polyols, they generally consist of long aliphatic chains with various functional groups principally hydroxyls, double bonds, active methylene groups and often –OCH_3, –Cl, –Br, –OCOH and oxirane ring (Sharmin et al., 2007; Akram et al., 2008, 2009, 2010; Vashist et al., 2013; Ghosal et al., 2013; Hazmi et al., 2013). Polyols available in nature mainly comprise of Ricinoleic and Lesquerollic acids, the most abundant constituent (–OH containing) fatty acids of vegetable oil obtained from the seeds of Ricinus Communis or castor oil, respectively. Other examples are Strophanthus, Coriaria, Cardamine Impatiens, Sebastiana Commersoniana and Capparis Zeylanica, which also contain a hydroxyl group bearing fatty acids. These functional groups can undergo various chemical modifications; nonetheless, over the years, research has been focused mainly on the synthesis (involving –OH) and characterization of PU with applications as foams, lubricants, cosmetics, adhesives, plasticizers and coatings. Following appropriate chemical modifications, namely the formation of polyols for the synthesis of polyurethanes (Gan, S.N. et al., 2009) and the insertion of acrylic functions (Scheme 2.2) for photopolymerizable structures (Gan S.N. et al., 2012; P. Chittavanich et al., 2012; Chia-Wai Chang et al., 2013; Aung Min Min et al., 2015). Apart from the above modification, bio-polyester derived from olive oil also has been reported (Shankina, J. et al., 2012).

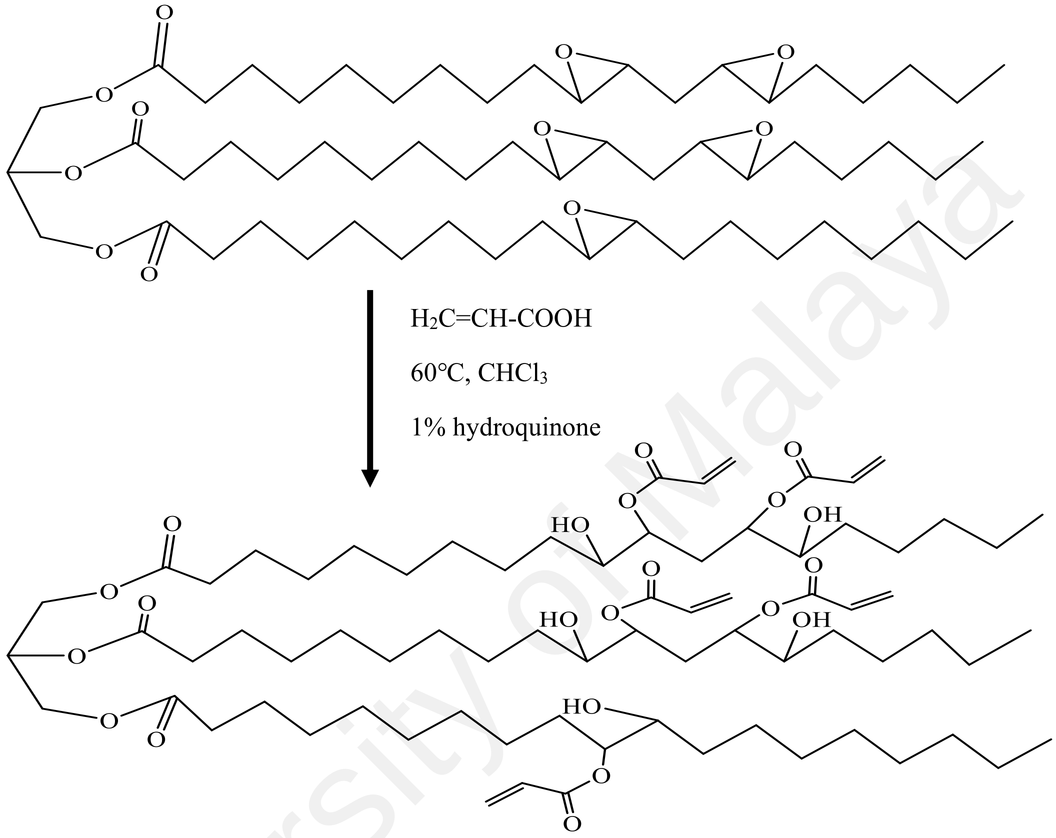

Scheme 2.2 Hydroxylated and acrylated derivative of epoxidized soya bean oil

Other modifications of vegetable oils in polymer chemistry include the introduction of alkenyl functions, the study of novel polyesters and polyethers and the synthesis of semi - interpenetrating networks based on castor oil, and also the production of sebacic acid and 10–undecanoic acid from castor oil (Ogunniyi D.S., 2006). Additionally, the recent application of metathesis reactions to unsaturated fatty acids has opened a novel avenue of exploitation leading to a variety of interesting monomers and polymers, including aliphatic polyesters and polyamides previously derived from petrochemical sources. The vitality of this field is further demonstrated by a continuous search for original ways of exploiting vegetable oils. Examples include self -healing elastomers in which fatty acids play a central role (Montarnal et al., 2008). A thermoplastic resin has been developed by esterification of cellulose with fatty acids (Crepy L et al., 2009). Hojabri L. et al (2009) has successfully synthesized a saturated aliphatic diisocyanate from oleic acid and its subsequent use in the preparation of fully bio-based polyurethanes in conjunction with canola oil-derived polyols. A novel elastomer from the concurrent cationic and ring opening polymerization using linseed oil modification has been studied (Jeong W. et al., 2009).

Polyesteramides is another class of vegetable oil modification. This amide modified alkyds obtained by esterification reaction between vegetable oil, amide diol and an acid/anhydride. They contain repeating ester and amide units in their backbone and possess improved properties over alkyds such as hardness, ease of drying, water vapor resistance and resistance to chemicals, in particular, alkalis (Mahapatra and Karak, 2004; Zafar et al., 2004, 2008; Alam et al., 2009; Chaudhari et al. 2013; Meshram et al. 2013). The presence of ester, amide moieties and pendant (fatty) chains confer synergistic properties of either component to polyesteramides, such as improved chemical resistance, in particular, resistance to alkaline media, thermal stability and imparts flexibility. In addition, fatty chains also serve as functional sites for further modifications. The double bonds and amide groups, as well as extensive hydrogen bonding, influence the mechanical and thermal stability of polyesteramides (Pramanik et al., 2012).

Besides their use in coatings and paints as binders, plant oils and derivatives have also been used as natural corrosion inhibitors. An excellent review has been compiled by Raja and Sethuraman (2008). Srivastava and Sathiyanathan et al. have also reported the use of Ricinus Communis or castor oil for corrosion inhibition of steel in acid media (Srivastava and Srivastava, 1981; Sathiyanathan et al., 2005). Pongamia Glabra and Annona Squamosa have shown corrosion inhibition for steel in acid media (Raja and Sethuraman, 2008). A recent review has appeared on the use of plant oils and derivatives for corrosion inhibition (Dar, 2011). Extracts from leaves and plant oil from seeds of several edible and medicinal plants have also been employed for anticorrosion behaviour against alkaline and acid media as well as chloride ions (Dar, 2011; Lahhit et al., 2011). Here, the anticorrosion activity is attributed to the presence of heterocyclic constituents such as alkaloids, flavonoids, tannins, cellulose, and others.

Plant oil are abundantly available, easy to procure and cost-effective sources of nature. They bear unique natural functional attributes and potential biodegradability as renewable feedstocks for environment friendly materials. Plant oils have found practical applications as biodiesel, lubricants, cutting fluids (metal cutting and forming), coatings and paints along with other applications. Although the use of plant oil in paints and coatings is decades old and well-studied, today emphasis is being laid on research pertaining to the modifications of these materials to introduce novel properties, improved performance coupled with environment friendliness at affordable costs. With persistent and extensive research efforts, vegetable oil coatings may compete well with their petroleum-based counterparts in performance and applications and may establish themselves as ‘‘greener’’ precursors to future environment friendly coatings.

2.1.1 Non-food Application of Palm Oil

While many plant oils have been widely explored in synthetic polymer application, palm oil being the major crop in Southeast Asia particularly in Malaysia has also attracted many researches in the same field of study. Driven by economic and environmental reasons, research and development for alternative sources of PU raw materials have been on-going but previously, only the production of polyol based on renewable materials such as oils/fats and starch have been reported. As a result, in the early 1980s, research on the production of epoxidized palm oil (EPO) was initiated by Malaysian Palm Oil Board for the first generation of polyols from palm oil. (Salmiah et al., 1995). The first generation of palm-based polyols involved conversion of palm oil products to EPO products by using in situ prepared peracids, followed by alcoholysis of the EPO to produce the polyols. Due to the high residue of acid value, which will retard the isocyanate-hydroxyl reaction has led to improvement of second-generation polyol with low acid value and lower viscosity triglyceride-based polyol for PU foam application (Hazimah et al., 2008).

While researches were focused on palm oil-based polyol for PU foam application, exploration of the utilisation of palm oil-based materials as promising, versatile, renewable and biodegradable resources has steered research towards the formulation and development of biodegradable palm-based films and coatings as alternatives to the mineral-based materials. Palm oil, one of the major vegetable oils, falls into the non-drying oil category because of its low iodine value, which is contributed by the relatively large amount of saturated palmitic acid. This means palm oil will not form a coating film upon exposure to air. Issam A. M. et al (2009) has synthesized an alkyd using palm oil, but the drying time was too long in the range of 2-8 days even with cobalt drier in the coating formulation. Nevertheless, to improve the palm oil performance in coating application, this can be done via chemical modification of their functional group such as carboxylic or double bond with other polybasic or polyhydric building block (Alam et al., 2014). A novel water reducible alkyd resin derived from palm stearin fraction with good alkyd/melamine heat cured film performance has been successfully synthesized (Teo, K.T. and Gan S.N., 1997&1999). A higher functionality palm oil fatty acid-based polyol has been reported and find suitable for making two component polyurethane (2K PU) coating formulation (Hoong et al., 2009a). Further research has successfully yielded the air-dry palm oil alkyd via using the dehydration process of palm oil. The reported alkyd made from dehydrated palm oil showed ability of air-drying performance with metal drier as redox catalyst in coating application (Uzoh C. F., 2013). To further strengthen the researchers understanding on polyesterification using palm fatty acid in alkyd synthesis, Shahla Ataei et al (2011) reported that the polyesterfication of palm oleic acid-based alkyd, irrespective of oil length, the alkyd samples follow second order law at the initial stage of polyesterification time with rate constant of order of 10^{-5} g $(\mathrm{mgKOH})^{-1}\mathrm{min}^{-1}$ at initial stage with formation of linear polymer. Branched polymeric chains were formed at subsequent polymerization time.

Other than conventional development of palm oil-based coating, the versatility of palm oil has also drawn attention of researchers in advanced coating technologies such as in UV curable or self-healing coating application. In UV curable coating, much research has focused on the synthesis of epoxidized palm oil acrylate (Cheong et al., 2008; Azam et al., 2001). Most palm oil-based products for UV-curable coating are prepared from epoxidized palm oil (EPO), e.g. cationic photoinitiator-induced UV curing of EPO and cycloaliphatic diepoxide (Rosli et al., 2003). Radiation curable acrylates can be derived from epoxidized palm oil or epoxidized palm olein by reacting them with acrylic acid (Kosheela et al., 2015; Ooi and Hazimah, 2001). Epoxidized palm olein acrylate (EPOLA) has been prepared by reacting EPO with acrylic acid and using trimethylamine as catalyst. Other than epoxidation path, the acrylation pathway has been studied. An UV curable palm strearin based alkyd with methyl methacrylate modification has been reported (Desmond Ang T.C. and Gan S.N., 2012). The hardness of the cured film can be further improved by additional of small amount trifunctional reactive diluent in the coating formulation. Siti Nur Amalina Ramlan and co-workers (2017) has published on palm olein-based UV resin in conductive coating application. The alkyd was modified with maleic acid in order to render it UV curable, then blending with polyaniline to improve the conductivity of the coating. Self-healing polymer or coating has recently getting much focus by the advance material research~~es~~ group throughout the world. Nurshafiza Shahabudin et al (2016) has reported a technology of a microcapsules filled with a palm oil-based alkyd as healing agent for epoxy matrix application. In her work, poly(melamine-urea-formaldehyde) (PMUF) microcapsules containing a palm kernel oil-based alkyd were produced by polymerization of melamine resin, urea and formaldehyde that encapsulated droplets of the suspended alkyd particles. A series of spherical and free-flowing microcapsules with self-healing ability were obtained.

2.1.2 Application of Palm Fatty Acid Distillate

The palm fatty acid distillate (PFAD) is a by-product of the crude palm oil refining process. Malaysian palm oil refineries produce more than 750,000 tonne of PFAD, annually, as a by-product, which is sold at a discounted price, as compared to the RBD (Refined, Bleached and Deodorized) palm oil, at USD200–250 per tonne, for usage in animal feed (Ping B.T.Y. et al., 2009; Nang H.L.L. et al., 2009).

PFAD comprises mainly of free fatty acids, with around 45% palmitic and 33% oleic acid, as the major components, and it has been used in the making of soap and animal feed, and certain oleochemicals. Small amount of vitamin E could be extracted from the PFAD (Gapor, A.B. et al., 1988). Gapor A.M.T. (2000) has developed a process for producing high purity (>90%) squalene from the PFAD. This valuable compound is useful in heath supplements, cosmetics, and in the pharmaceutical industry. In a recent study, the PFAD has been explored as biodiesel feed stock (Kapor, N.Z.A. et al., 2017). Many studies utilize various types of catalysts, such as SO_4^{-2}/TiO_2-SiO_2, and modified Zirconia compounds (Kapor N.Z.A. et al., 2017; Mongkolbovornkij P. et al., 2010; Embong N.H. et al.,2016). Pranali P. Chiplunker et al (2017) has reported the utilization of PFAD-based alkyd resin with sodium lauryl sulfate (SLS) and sodium lauryl ether sulfate (SLES) in the liquid detergent formulation. The PFAD-based alkyd shows defoaming property and having potential application as a foam reducer in detergent for washing machines. Another development of PFAD-based alkyd for conventional air-dry application has been studied (Rochmad et al., 2017). Due to low unsaturation of PFAD, the alkyd could not cure at room temperature and even heat up to 100℃. Therefore, curing of this PFAD based alkyd could only be possible via chemical cross linking such as melamine or amino cross linker with heating conditions. Further review showed that there are yet no reports of PFAD application in advance coating technologies such UV curing application.

2.2 Ultraviolet Light Curing Technology

Most commercial UV curable coatings are based on acrylate chemistry that cures via free radical polymerization. These liquid compositions typically contain a mixture of a reactive oligomer (30 – 60%), one or more reactive monomers (20 – 40%), an UV light-absorbing component (3 – 5%), and one or more additives (<1%). UV curable inks may contain up to 20% pigment. A high pigment content such as used in UV inks typically requires up to 10% of photoinitiator. Generally, three major components are required in the UV-curable coating resins: oligomers/monomers (e.g. acrylates, epoxies, and unsaturated polyesters), reactive diluents, and photo initiator (Sharmin et al., 2015). In general, the binder consists of two types of acrylate esters: acrylate-terminated oligomers and acrylate monomers ranging from mono to hexa- functional type. The monomers serve as reactive diluents. The multi-functional oligomers contribute to a high rate of curing owing to its polyfunctionality and in large measure, exhibit the physical and mechanical properties of the final cured film.

The two principle types of oligomers are derived from epoxy- and isocyanate-functional as starting materials (Holman, R. 1984). Low molecular weight bis-phenol A epoxy resins can be reacted with acrylic acid to yield predominantly difunctional epoxy acrylate derivatives. Epoxidized vegetable oil acrylates have been used where high functionality and lower Tg are desirable (Haiyan Gu et al.,2002). The urethane oligomers are obtained from isocyanate-terminated resins by reacting with 2-hydroxyl ethyl acrylate.

Any hydroxyl terminated resin can be reacted with diisocyanate to produce an isocyanate terminated resin. One of the many advantages of urethane acrylate-based coatings is the different number of oligomers containing urethane groups that can be prepared to meet a wide range of cured film properties. Polyols used to prepare urethane acrylates for UV compositions include polyether, polyesters and alkyd resin (Holman, R. 1984).

The technology of UV curing is commonly applied by the industries on many types of substrate due to energy saving, fast processing rate, low or VOC zero emission (Bongiovanni et al., 2002). In addition, UV-cured polymers generally show better chemical resistance resulted from its high cross-link density (Landry et al., 2008). Materials that are sensitive to heat can be cured by UV-curing method because the radiation process is performed at normal temperature (Sharmin et al., 2015). Ever since the UV-curing flooring coating technology was first introduced in 1980s, 84% of wood flooring coating market was applied by using radiation curing method in 2005 due to the excellent processing benefits (Landry et al., 2010). Even though many industries have already benefit from the technology advancement in UV curing technology application. Today, UV technology still has a limited footprint in the metal coatings market. Throughout so many years of review, some acrylate-based formulations intended as primer for pre-treated hot dip galvanised steel have been reported (Lowe, C. 2004). However, the impact resistance, drawability and salt spray resistance were poor when compared to conventional thermal cured system. Two epoxy acrylate-based coatings for aluminium have been previously discussed (Carroy, A. 1994). It is possible for the coating to have solvent resistance of over 100 MEK double rubs and good adhesion. Metal substrate still remains as important material in many industry applications, and UV curing for metal coating development will still be the focus by many coating researchers in their future studies.

2.3 Objective

The overall purpose of this research was to synthesize UV curable coating materials from renewable and natural resources and investigate their cured film performance in term of chemical and mechanical properties.

The specific research objectives of this study are as below:

1. To synthesize a hydroxyl terminated macromer using PFAD in combination with polybasic acids and polyhydric alcohols. This research focused on finding appropriate composition to produce a macromer which can be used as based resin that could be further modified to UV curable application.
2. To synthesized PFAD-based urethane acrylate by modifying the hydroxyl terminated macromer via chemical reaction with diisocyanate and 2-hyrdoxylethyl acrylate in order to introduce unsaturation (double bond) for UV curing.
3. To characterize the resin using gel permeation chromatography (GPC), Fourier transform infrared spectroscopy and differential scanning calorimetry (DSC) for molecular weight, functional group and glass transition temperature measurement respectively. Acid value (AV) and isocyanate value (NCO) were determined by titration methods. The resin viscosity was measured using Brookfield viscometer.
4. To study the UV curing of the PFAD urethane acrylate by FTIR through monitoring conversion of acrylate double bond at 810 cm^{-1}during UV curing.
5. To evaluate properties of cured film such as gloss, hardness, adhesion to substrate including chemical, mechanical and weathering performance in wood and metal coating application.

CHAPTER 3: EXPERIMENTAL

3.1 Materials

The PFAD was kind gift from Sime Darby Group, Kuala Lumpur, Malaysia. This commercial PFAD was used without further treatment. The 2,2-dimethyl-1,3-propanediol (neopentylglycol, NPG) was purchased from LG Chemical, Yeosu, Korea, 2,2-bis(hydroxylmethyl) 1,3-propanediol (pentaerythritol) from Perstop AB, Malmo, Sweden, phthalic anhydride (PA) from Nanya Plastic, Kaohsiung, Taiwan, purified isophthalic acid (IPA) from MGC Chemical, Tokyo, Japan, terephthalic acid (TPA) from Lotte Chemical, Yeosu, Korea, adipic acid (AA) from Asahi Kasei, Tokyo, Japan, mono-butyl tin oxide from Arkema, Colombes, France, toluene diisocyanate (80/20 TDI) from Covestro AG, Leverkusen, Germany, 2-hydroxy ethyl acrylate (2-HEA) from Osaka Organic Chemical, Osaka, Japan, xylene from Exxonmobil, Leatherhead, USA, Tripropylene glycol diacarylate (TPGDA), and 4-methoxy phenol from Sigma Aldric Chemical, Saint Louis, USA, Speedcure 73 (2-hydroxy-2-methylpropiophenone) from Lambson, Wetherby, UK. Tetrahydrofuran (THF) and other analytical chemicals were from Thermo Fisher Scientific, Waltham, USA. All the Chemicals mentioned were used as received condition without further purification.

3.2 Characterization

3.2.1 Acid Value

Acid value is the amount of KOH in mg required to neutralize the free acids contained in 1 g of sample. This was done according to the procedure of ASTM D974. The reagents required are 0.1N ethanolic potassium hydroxide, 95% ethanol, and 1% phenolphthalein indicator. The solvent used is a mixture of ethanol/toluene at 1:1 ratio by volume.

A suitable amount of test sample was weighed into a flask. In the second flask bring 50 ml of ethanol/toluene mixture with slightly heating and neutralized with 0.1N $KOH_{(ethanolic)}$ using 0.5ml phenolphthalein indicator. The neutralized solvent mixture was then poured into the first flask to dissolved the test sample. The sample mixture was titrated with 0.1N $KOH_{(ethanolic)}$ to the end point when the addition of a single drop of titre produces a slight but definite colour change persisting for at least 15 s. The acid value was calculated using equation 3.1.

$$\text{Acid number (AN)} = \frac{V_{KOH} \times 56.1}{W \times NV} \frac{\text{mgKOH}}{\text{g}} \qquad (\mathbf{3.1})$$

Where:

$V_{(KOH)}$ = volume of KOH required for the titration of sample, mL

W = weight of sample used, g

NV = non-volatile content of sample

3.2.2 Hydroxyl Value

The hydroxyl value was determined accordingly to ASTM D1957-86(2001). Reagents required: (i) acetic anhydride, (ii) n-butyl alcohol, neutralized with 0.5N alcoholic potassium hydroxide (KOH) solution, (iii) 95% (*v/v*) denatured alcohol, (iv) 1% ethanolic phenolphthalein solution, (v) 0.5N ethanolic potassium hydroxide solution, the solution was standardized by titration against standard acid using phenolphthalein as indicator, (vi) pyridine, refluxed with powdered barium oxide and distilled. The fraction at 114-115℃ was collected and used, (vii) water conforming to type 1 of specification D1193, (viii) prepare fresh before use, pyridine-acetic anhydride solution (3:1) (*v:v*).

Procedure: weight 8.0 to 10.0 g of resin in a conical flask and titrate for acid value (A). Prepared 5.0 ml of pyridine-acetic anhydride solution into an empty Erlenmeyer flask for the reagent, add 10 ml of pyridine and neutralized with phenolphthalein, titrate for acid value blank (B). 3.0 to 5.0 g of resin was weighed accurately into another Erlenmeyer flask (V). 5.0 ml of pyridine-acetic anhydride solution (acetylating agent) was added dropwise. Thoroughly mixed the content by gentle swirling. The two specimens of mixture were refluxed with condenser attached with Erlenmeyer flask on an opening steam bath and heat for 1 hour. To each specimen, add 10 ml water through condenser and continue heating for another 10 min. Then, allowed the flask to cool to room temperature with condenser still attached. Add 25 ml of neutralized n-butyl alcohol to each flask in the following manner. About half should be added through condenser, then condenser removed, and remaining alcohol used to wash down the side of the flask. Add 1 ml of phenolphthalein solution to each flask and titrate to faint pink end point with 0.5N ethanolic KOH solution.

The hydroxy value as the number of milligrams of potassium hydroxide equivalent to hydroxyl content of 1 g sample as follow:

$$\text{Hydroxyl value (OHV)} = \frac{\mathrm{B} + \left(\frac{\mathrm{SA}}{\mathrm{C}}\right) - \mathrm{V}}{\mathrm{S}}\ \mathrm{N} \times 56.1 \qquad (\mathbf{3.2})$$

Where:

A = KOH solution required for titration of acid value, ml.

B = KOH solution required for titration of reagent blank, ml.

V = KOH solution required for titration of the acetylated sample, ml.

C = weight of sample for acid value, g

S = weight of sample for acetylation, g

N = normality of KOH solution, N

3.2.3 Isocyanate Value

The isocyanate value is the isocyanate (NCO) content of a urethane intermediate or prepolymer. The test method was done accordingly to ASTM D2572-97. The reagents required: (i) 0.1N hydrochloric acid (HCl) solution, (ii) 0.1N di-butylamine solution, (iii) isopropanol, (iv) dry toluene, (v) bromophenol blue indicator. 0.10 g of test sample was weighted into a dry clean conical flask. Add in 25ml of dry toluene and 25 ml of di-butyl amine solution into the sample flask which was closed with stopper and swirled for 15 min. Then, add 100 ml of isopropanol and continue swirling for 5 min and add in 4-5 drops of bromophenol indication solution and proceed with titration with 0.1N HCl solution to the yellow end point. Also, run a blank titration including all reagents but without sample.

The isocyanate value (IV) was calculated with Eqn 3.3.

$$\text{Isocyanate value (IV)} = \frac{[(\mathrm{V_B} - \mathrm{V_S}) \times \mathrm{N} \times 0.042]}{\mathrm{W} \times \mathrm{NVC}} \times 100\% \qquad (\mathbf{3.3})$$

Where:

V_B = Volume of HCl solution for blank titration, ml

V_S = Volume of HCl solution for sample, ml

N = Normality of HCl solution

W = weight of the sample, g

NVC = non-volatile content of the sample, fraction

3.2.4 Viscosity Measurement

A Brookfield viscometer (model DVI) was used to measure the viscosity of sample at a temperature of 25°C. The sample of macromer was diluted to the targeted oligomer content, with TPGDA or xylene, before viscosity measurement. Figure 3.1 shows the main components of Brookfield viscometer.

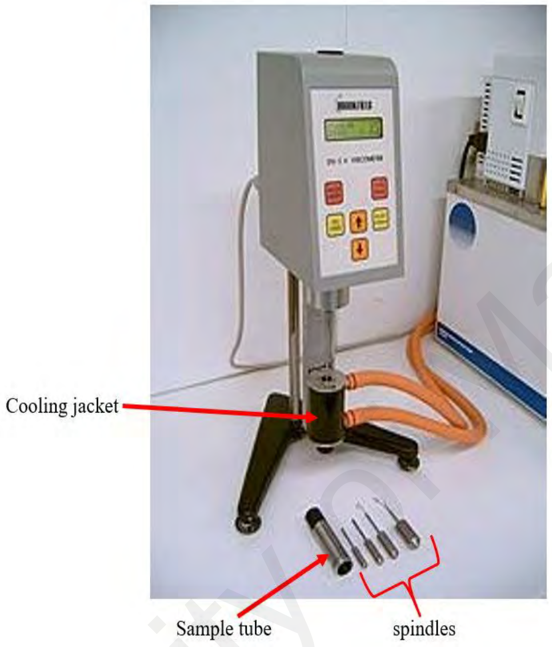

Figure 3.1 Components of Brookfield viscometer

3.2.5 Differential Scanning Calorimetry (DSC)

Differential scanning calorimetry or DSC is a thermal analytical technique. DSC measures the amount of heat absorbed or released by a sample as it is heated, cooled or held at a constant temperature relative to an inert reference. Studying physical transformations or phase transitions is the main purpose of DSC. Melting, crystallization and glass transitions are examples of phase transitions. Energy changes or heat capacity changes are involved in phase transitions (TA instruments, 1997). These changes can be detected by DSC with great sensitivity. When a sample undertakes a phase transition, more or less heat will need to flow into it. This phenomenon is the basic principle that underpins the DSC technique. Requirement of more or less heat flow will depend on the process being exothermic or endothermic. By observing the differences in the heat flow between the sample and the inert reference, DSC instruments are able to measure the amount of heat absorbed or released during phase changes. (Hoh G.W.H. et al., 2003). The majority of DSC instruments are of a heat-flux design. Heat flux is sometimes referred to as heat flow rate intensity. Heat flux is the rate of heat flow through a unit of area per unit of time (TA instruments, 1997). Figure 3.2 shows a schematic heat flux DSC instrument.

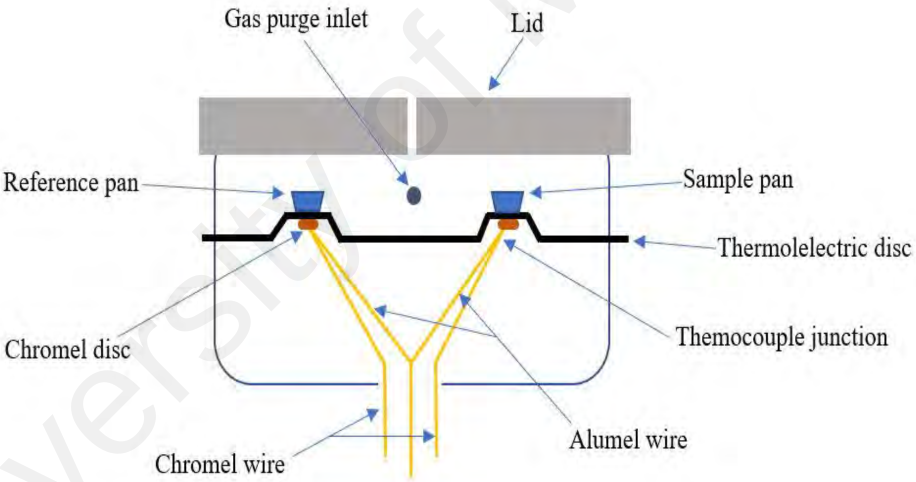

Figure 3.2 Schematic diagram of a heat flux DSC instrument

To make a good thermal contact between the sample and the heat flux plate, flattened and small samples are contained in shallow pans. Balanced heating of the sample and the reference is achieved by using a metal of high thermal conductivity for construction of the furnace. A gas flow is also established in the cell containing the sample and the reference to assist in heat transfer and sweep the volatiles away. The control of the furnace, acquisition of the signal and data processing are fully computerized. The result of a DSC experiment is a curve of heat flow versus temperature as shown in Figure 3.3.

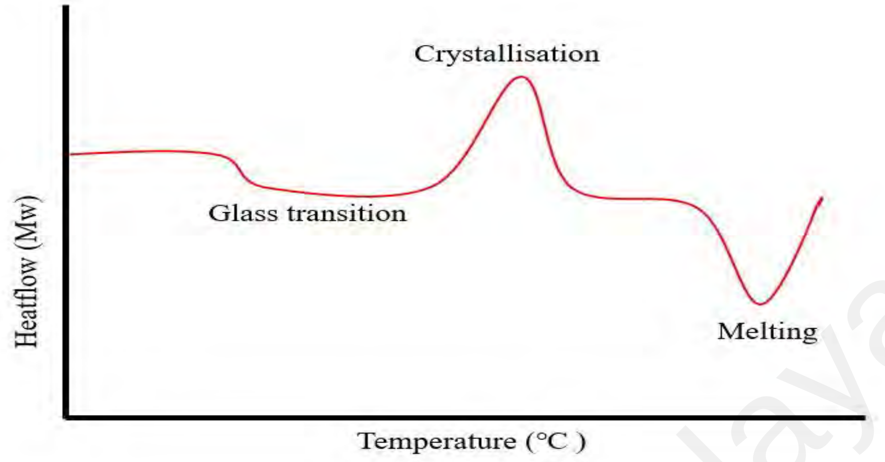

Figure 3.3 Typical DSC curve of a polymer

In terms of polymers, DSC is widely employed to determine the melting temperature (T_m) and the glass transition temperature (T_g). The glass transition temperature is the temperature at which the polymer loses its rigidness or glass-like properties and takes on rubbery characteristics. According to Wilkes G.L. et al (2005) at glass transition temperature the chain of the polymer holds adequate thermal energy that joint and sectional motion of the backbone could occur. Below the glass transition temperature, a motionless but disordered amorphous state exists for the polymer backbone. When a molten polymer is cooled, its free volume decreases. The volume reduction is due to the lack of thermal energy required for chain mobility. At the glass transition temperature, the free volume is reduced to the extent that joint motion of the backbone is almost prohibited. Therefore, any factor which affects the free volume of a polymer will affect its glass transition temperature.

3.2.5.1 Glass Transition Temperature

For determination of the glass transition temperature (Tg) of the sample, the technique of differential scanning calorimetry (DSC) was employed. To determine the Tg of the resin and the cured film, samples were encapsulated in a 40 μL aluminium pan and analysed using the Shimadzu DSC (model DSC-60), at a heating rate of 20 °C min^{-1}.

The synthesised resins were introduced to the differential scanning calorimeter in 100% solid form. In other words, the diluted resin could not be used for differential scanning calorimetry. After the 100% solid resin sample was introduced to the differential scanning calorimeter, initially it was maintained at -50°C for one min with the aid of liquid nitrogen. Then, it was heated from -50°C to 300°C at 20°C/min. The relevant data was then processed and produced as thermograms in which the glass transition temperature, Tg of the resin was calculated by the instrument's software.

3.2.6 Size Exclusion Chromatography (SEC)

Among the factors which greatly influence the properties of polymeric materials inclusive of alkyd resins are molecular weight and molecular weight distribution. For a surface coating resin, sufficient strength and mechanical properties might favour a high molecular weight. But high molecular weights often lead to high melt viscosities which in turn cause drawbacks during both polymerisation and application. By correlation, molecular weight distribution can have a strong effect on the properties of molten polymers from a rheological point of view, with a broader molecular weight distribution leading to a higher melt viscosity (Pilati, F., 1999). The molecules of a polymeric material, even those of a homopolymer with the same repeating unit will show variety of sizes with different weights. For linear polymers, the comprising molecules are of different chain lengths (Paul J Flory, (1971). The molecular weight and the molecular weight distribution of a polymer are determined and described in certain terms. The most important of these include number average molecular weight (M_n), weight average molecular weight (M_w) and polydispersity index which is a measure of the molecular weight distribution. The values of M_n and M_w and the polydispersity index are of great importance, since they affect many of the physical characteristic of a polymer. Some of these properties applicable to surface coating resins including tensile strength, modulus of elasticity, hardness, impact strength, toughness, adhesive strength, cure time, stress-crack resistance, and as mentioned the melt viscosity.

The number average molecular weight is a common method for determination of the molecular weight of polymers. It is determined by measuring the molecular weight of N polymer molecules. The weights are then summed and divided by N

$$M_n = \frac{\sum_i N_i M_i}{\sum_i N_i} \qquad (\mathbf{3.4})$$

An alternative approach towards the molecular weight determination of a polymer is the weight average molecular weight. This is calculated from Eqn 3.5.

$$M_w = \frac{\sum_i N_i M_i^2}{\sum_i N_i M_i} \qquad (\mathbf{3.5})$$

where N_i is the number of molecules of molecular weight M_i (Paul J Flory, 1971).

A measure of the molecular weight distribution of a certain polymer is called polydispersity index. The polydispersity index (PDI) designates the distribution of individual mo1ecular weights in a batch of polymers. The term polydisperse applies to a polymer which exists over a wide range of molecular weights.

The polydispersity index (PDI) is calculated from Eqn 3.6.

$$Polydispersity\ index\ (PDI) = \frac{M_w}{M_n} \qquad (\mathbf{3.6})$$

Where M_w is the weight average molecular weight and M_n is the number average molecular Weight. The value of PDI is greater than one in the majority of cases, but as the polymer chains approach uniform chain length, the value of PDI draws near unity. The polydispersity index mainly depends on the mechanism of polymerisation, the number of reactants present and the reactants ratio. The va1ue of PDI are in the region of two for typical step growth polymerisations.

With advancement in column technologies, gel permeation chromatography or GPC has become the only proven technique for characterising the complete molecular weight distribution of a polymer. GPC can determine M_n, M_w, M_z and the fundamental molecular weight distribution. GPC is a size exclusion chromatographic (SEC) technique in which particles are separated based on their effective solution size which is technically referred to as the hydrodynamic volume. Figure 3.4 shows schematic diagram of a GPC system.

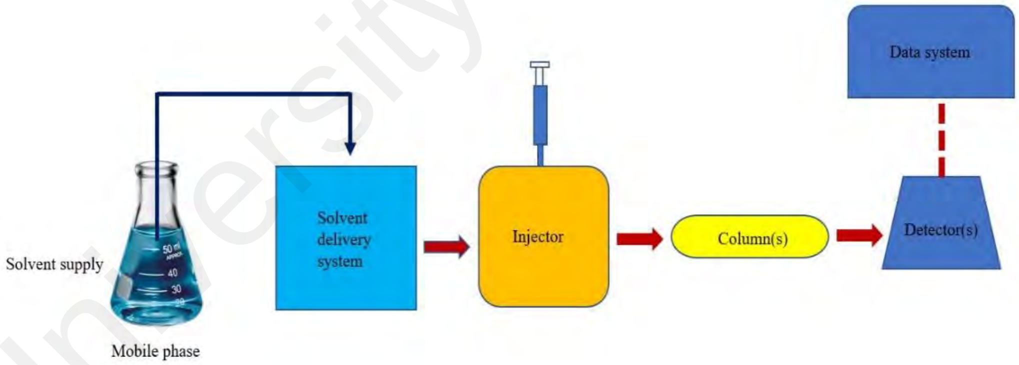

Figure 3.4 Schematic of a basic gel permeation chromatograph system. Reproduced from Waters @ www.waters.com.

Once the sample has been suitably dissolved, it is introduced via an injection mechanism onto a set of columns which act as a molecular filtration system. The columns are packed with a crosslinked gel, for example (-styrene-divinylbenzene copolymer), which contain surface pores. These pores range from small to quite large size and act as the molecular filters mentioned above. The larger size molecules will not fit into the smaller pores. Conversely, the smaller molecules will fit into most of the pores and be retained longer. As a result, the larger molecules will elute first from the system (www.waters.com).

3.2.6.1 Molecular Weight Measurement

Molecular weights of samples were measured by a Shimadzu GPC with tetrahydrofuran as the mobile phase (set at 1.0 ml min^{-1}). Monodisperse polystyrene standards were used for calibration of the column. This instrument provided a variety of information with regard to molecular weight characteristics that included the number average molecular weight (M_n), weight average molecular weight (M_w), and polydispersity index (PDI). 2.0 uL of the sample with concentration of 0.25 g/ml (*w/v*) was injected into the GPC instrument, and eluted with THF at 1 ml/min. The instrument's software provided the processed data in the form of a chromatogram and calculated values of the number average molecular weight, the weight average molecular weight, and the polydispersity index.

3.2.7 Fourier-Transform Infrared Spectroscopy

Infrared spectroscopy is an important technique in organic chemistry to identify the presence of functional groups in a molecule. Also, using the unique of absorption bands to confirm the identity of a pure compound or to detect the presence of specific impurities. Infrared or IR spectroscopy is associated with interpretation of the interaction between the infrared radiation and matter. Infrared radiation is a type of electromagnetic radiation. In terms of frequency, it is within 780 nm to approximately 100,000 nm of the electromagnetic spectra. Organic molecules absorb infrared radiation. The absorption will only take place for specific radiation wave frequencies that correspond to certain energy levels, which will then cause the molecule to vibrate, stretch or bend (Donald L. Pavia et al., 2015). Some of the typical IR molecular motions of a -CH_2 group are shown in Figure 3.5.

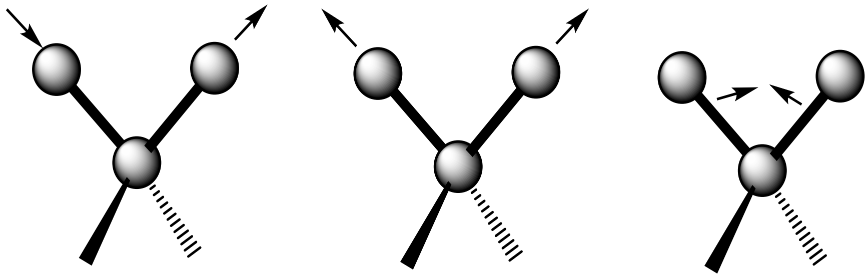

asymmetrical stretching symmetrical strtching scissoring or bending in-plane

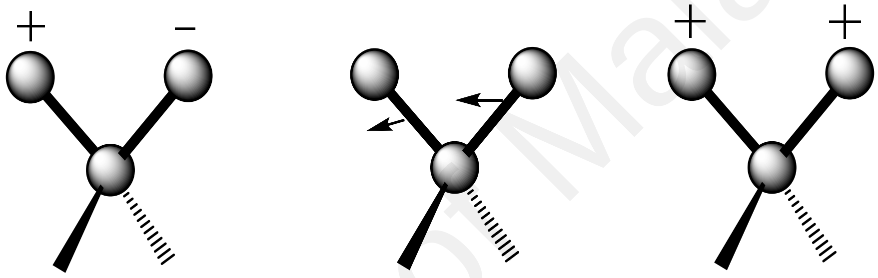

twisting or bending out-of-plane rocking or bending in-plane wagging or bending in-plane

Figure 3.5 IR stretching and bending vibration modes of a -CH_2 group

The vibrating bond of a radiated molecule will absorb the energy only if both the frequency of the radiation and that of the bond itself are the same. When the infrared radiation is absorbed, the magnitude of the vibrations matching that of the infrared light will increase. As a consequence, the bond connecting the two atoms will compress or stretch to a greater extent. By knowing the fact that each infrared radiation frequency corresponds to a certain molecular motion, interpretation of both molecular motions and types of bonds or functional groups present from a molecule's IR spectra is possible. Correlation charts are available in this regard. A summary of general regions of the selected functional groups infrared spectra in which various types of vibrational bands are observed is provided in Figure 3.6.

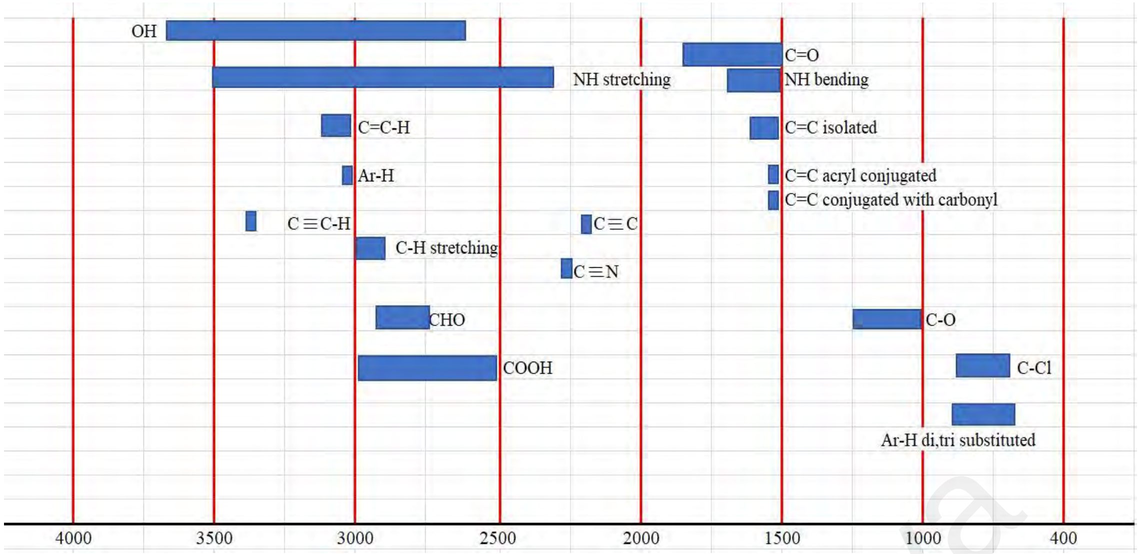

Figure 3.6 Infrared frequencies of selected functional groups

Infrared spectroscopy is commonly employed for characterisation of coating resins particularly in alkyd resin characterization even in curing kinetic study. Among recent research in which resins were characterised and curing kinetic was followed by infrared spectroscopy, those of Choi Joon-Suk et al (2011); Chittavanich, P. et al (2012); Narin Thanamongkollit et al (2012); Min Min Aung et al (2015); Chen Guangxue et al (2016); Yang Xuejuan et al (2017) are worthy of mentioning.

3.2.7.1 Chemical Functionality Identification

FTIR spectra were recorded by using the ATR technique on a Perkin Elmer Spectrum (Perkin Elmer, Waltham, MA, USA). The polymer sample was coated directly onto the ATR diamond plate and the spectrum was recorded. All absorption peak identification was done with FTIR software on their specific wavenumber (cm^{-1}) assigned.

3.2.7.2 UV Curing Kinetic Study

To follow the UV curing, the sample was coated onto a sodium chloride cell and irradiated with UV lamp for the specified time and followed by recording the spectrum using FTIR. The use of Beer-Lambert law allows the determination of the concentration of an absorbing species,

$$A = \varepsilon c l \tag{3.7}$$

Where *A* is the absorbance, *ε* the molar extinction coefficient, *c* the concentration of the absorbing molecules, and *l* the thickness of the test sample. To overcome the effect of different thickness of the sample, a ratio is taken between the absorbance of the targeted group and that of an internal group, in this study, the absorbance at 2930 cm^{-1} (due to C-H stretching) was chosen as the internal standard. The conversion of the acrylate unsaturation is estimated by using Eqn 3.8.

$$\text{Conversion} = \frac{\left[A_{0(810)}/A_{0(2930)}\right] - \left[A_{t(810)}/A_{t(2930)}\right]}{\left[A_{0(810)}/A_{0(2930)}\right]} \times 100\% \tag{3.8}$$

Where:

$A_{0(810)}$ = peak area for absorbance at 810 cm^{-1}at initial.

$A_{0(2930)}$ = peak area for absorbance at 2930 cm^{-1} at initial.

$A_{t(810)}$ = peak area for absorbance at 810 cm^{-1} at t curing time.

$A_{t(2930)}$ = peak area for absorbance at 2930 cm^{-1} at t curing time.

3.2.8 Pendulum Hardness

The hardness of the UV-cured film was measured with the Sheen König pendulum hardness tester (TQCSHEEN, Capelle aan den IJssel, Netherlands), according to ASTM 4366. The tester was used to monitor the surface hardness of the cured film during UV curing. After the UV exposure, the pendulum hardness of the UV cured film surface was measured with respect to the pendulum oscillation time from 6^{o} to 3^{o} at 25±1°C and 50±2 % R.H., as illustrated in Figure 3.7. The pendulum hardness test is based on the principle that the harder a measured surface, the greater the amplitude time of pendulum oscillation. The König pendulum consists of a triangular open framework with an adjustable counterpoise weight and it weighs 200 ± 0.2 g. The pendulum pivots on two bearings of 5 mm diameter that rest on the test surface. The result was recorded as total oscillation or more commonly in total of time in second as unit.

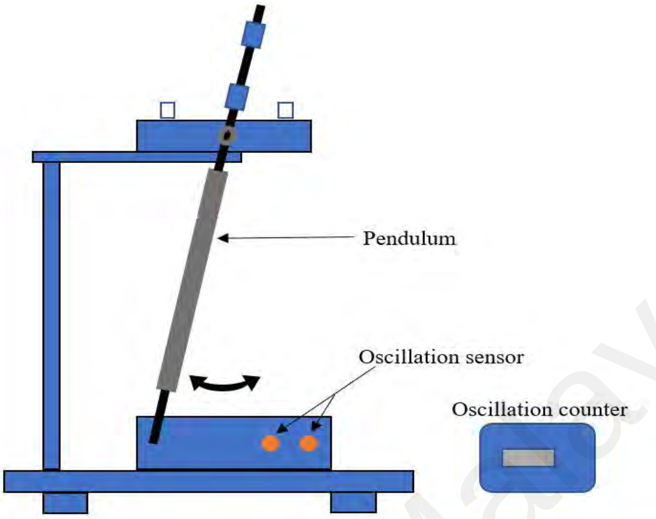

Figure 3.7 Schematic diagram representation of pendulum hardness tester

3.2.9 Pencil Hardness

The hardness of the cured film was measured by pencil hardness accordingly to ASTM D3363. The pencil hardness scale is given below, where 6B denotes the softest and 6H being the hardest:

6B-5B-4B-3B-2B-B-HB-F-H-2H-3H-4H-5H-6H

$\longrightarrow$

Hardness increase

The film hardness determined using the pencil test is a rapid and inexpensive method to determine the film hardness of an organic coating on a substrate, has been used in the coating industry for many years. A coated sample is placed on a firm horizontal surface and the pencil is held firmly against the film at a 45° angle and pushed away from the operator in a 6.5 mm stroke. The hardness was denoted at the grade of pencil just before any un-erase scratches made by a particular pencil grade i.e. if the scratches was made by pencil hardness 2H, the hardness of the coating sample will be denoted at grade H. Figure 3.8 shows pencil hardness tester using 3H pencil tested on a coated wood panel.

Figure 3.8 Pencil hardness tester

3.2.10 Adhesion Performance

The film adhesion was performed according to the ASTM D3359-09 test method B. The test was done by making two cuts/scratch, perpendicular to each other with 1 mm distance, with the appropriate cutter through the coating into the substrate thus making the lattice pattern. After removing the paint flakes, the cut area can be extended by applying standardized adhesive tape parallel to one set of cuts over the lattice pattern and pull it off steadily in 0.5 to 1.0 s. at a 180° within 90 ±30 s. The adhesion performance was assessed and rated as shown in Table 3.1.

Table 3.1 Classification of the adhesion results (Reproduced from TQC cross cut manual, www.tqc.eu)

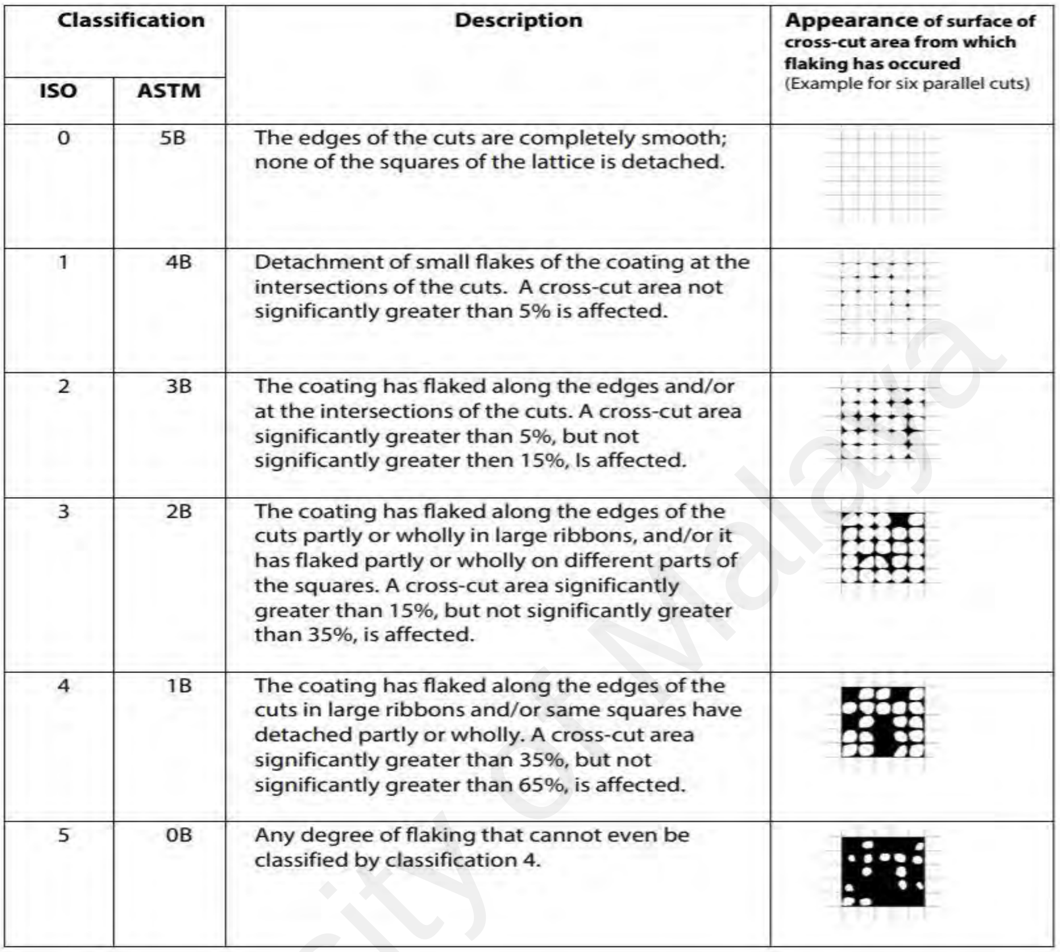

Classification		Description	Appearance of surface of cross-cut area from which flaking has occured (Example for six parallel cuts)
ISO	ASTM		
0	5B	The edges of the cuts are completely smooth; none of the squares of the lattice is detached.	
1	4B	Detachment of small flakes of the coating at the intersections of the cuts. A cross-cut area not significantly greater than 5% is affected.	
2	3B	The coating has flaked along the edges and/or at the intersections of the cuts. A cross-cut area significantly greater than 5%, but not significantly greater then 15%, Is affected.	
3	2B	The coating has flaked along the edges of the cuts partly or wholly in large ribbons, and/or it has flaked partly or wholly on different parts of the squares. A cross-cut area significantly greater than 15%, but not significantly greater than 35%, is affected.	
4	1B	The coating has flaked along the edges of the cuts in large ribbons and/or same squares have detached partly or wholly. A cross-cut area significantly greater than 35%, but not significantly greater than 65%, is affected.	
5	0B	Any degree of flaking that cannot even be classified by classification 4.	

3.2.11 Gloss Measurement

Gloss is a visual impression resulting from surface reflection of light. When more direct light is reflected, the surface would appear glossier. A glossmeter measures the specular reflection. The light intensity is registered over a small range of the reflection angle. The intensity is dependent on the material and the angle of illumination. In case of non-metals (coatings, plastics) the amount of reflected light increases with the increase of the illumination angle. The remaining illuminated light penetrates the material and is absorbed or diffusely scattered dependent on the colour. Metals have a much higher reflection and are less angle dependent than non-metals as illustrated by Figure 3.9. Glossmeters and their handling procedures had to be internationally specified to allow comparison of measurement values. The angle of illumination is of high influence. In order to obtain a clear differentiation over the complete measurement range from high gloss to matte surface, 3 different geometries 20º, 60º and 85º measure angle were normally used by industrial application as shown by Figure 3.10.

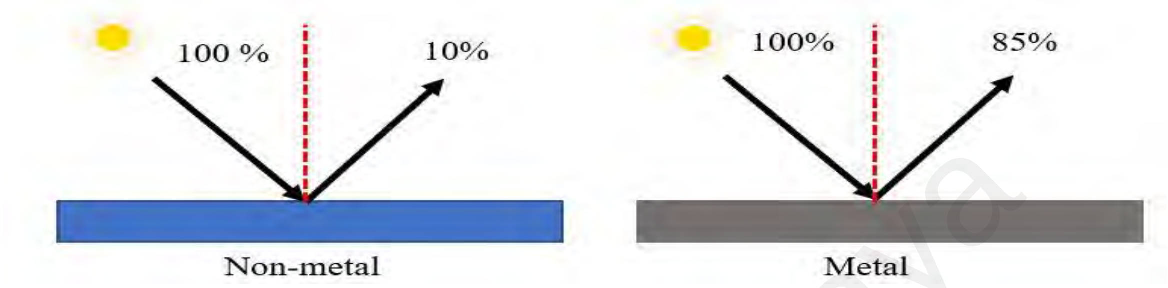

Figure 3.9 Illustration of light reflection on non-metal and metal surface

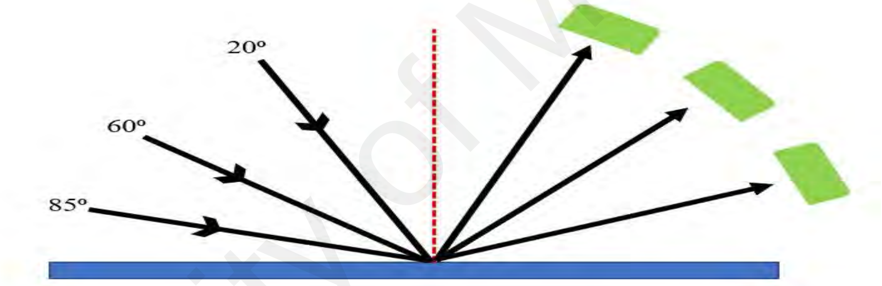

Figure 3.10 Three geometries angle of gloss measurement

The gloss of the cured film was measured with the BYK tri-gloss meter, according to the ASTM D523, for non-metallic substrate. The gloss level was reported as the gloss unit (GU). The measurement results of a glossmeter are related to the amount of reflected light from a black glass standard with a defined refractive index, and not to the amount of incident light. The measurement value for this defined standard is equal to 100 gloss units (calibration). Materials with a higher refractive index can have a measurement value above 100 gloss units (GU), e.g. films. In case of transparent materials, the measurement value can be increased due to multiple reflection in the bulk of the material.

Other than reporting direct gloss measurement reading of a coating surface, gloss retention will normally be calculated as reflection of the coating quality in many coating evaluations particularly in prolong schedule assessment. The calculation was using the equation in Eqn 3.9.

$$\text{Gloss retention} = \frac{\mathrm{GU_t}}{\mathrm{GU_0}} \times 100\% \qquad (\mathbf{3.9})$$

Where,

$\mathrm{GU_t}$ = gloss measurement at schedule (t)

$\mathrm{GU_0}$ = initial gloss measurement

3.2.12 Chemical Resistance of the UV Cured Film

The cured films were subjected to the wood-coating standards of the chemical resistance test. The coating was applied on a rubber wood panel and cured by irradiation, with a UV light, for 60 s. The cured panel was conditioned at room temperature for 1 hour before carrying out the chemical resistance test. Ten milliliters of chemical reagent were dropped onto the film surface and allowed to stand for 24 hours duration. To minimize the evaporation of the reagent, it was covered with a plastic cap. The reagent was then wiped off with a dry clean cloth, and the surface was then dried for 15 min, before making observations and reporting. The reagents used were commonly applied by the Industrial Wood-Coating Standard include coffee, tea, dish washing solution, acetone, cooking oil, 1% (*w*/*w*) ethanol aqueous solution, vinegar {8% *(v*/*v)* acetic acid}, 10% (*w/v*) ammonia solution, 5% (*w*/*v*) sodium hydroxide (NaOH) solution, and 5% (*w*/*v*) hydrochloric (HCl) solution. Figure 3.11 illustrates the chemical test method.

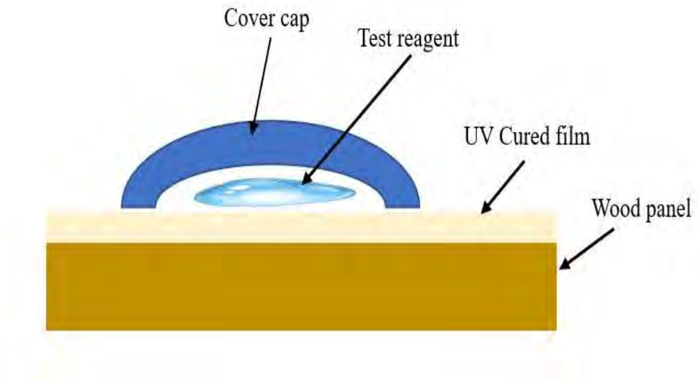

Figure 3.11 Diagrammatic of chemical test method

3.2.13 Resistance of Cracking by Impact Deformation

As coatings (such as paint, varnish, conversion coatings, and related coating products) are subjected to impact damage during their manufacturing and useful life, this test method for impact resistance was found to be useful in predicting coatings' resistances to impact. The purpose of this test is to evaluate the elongation tolerance, resistance to cracking and adhesion of an organic coating upon impact with a predefined weight. In principle, a weight with hemispherical ends falls on the coated side or reverse of a sheet metal specimen fixed onto a corresponding die. The test specimen was fixed into position with the quick release clamp. The weight was lifted to the predefined height set by the adjustable collar device. The weight was then released and the resulting deformation is observed. To create the impact force, a 1.8kg weight was lifted to a 100 cm height and released. The coating adhesion on the deformed area may also be evaluated if required, by the peeling test. Any cracking and chipping of the coating film after the impact test and the peel test are visually observed and reported as the result of the test.

The impact testing was carried out according to ASTM D 2794 procedure using Sheen tubular impact tester model 806/40 for rapidly deforming by impact a coating film and its substrate and for evaluating the effect of such a deformation. Figure 3.12 shows the impact tester used for the evaluation of the coating panel.

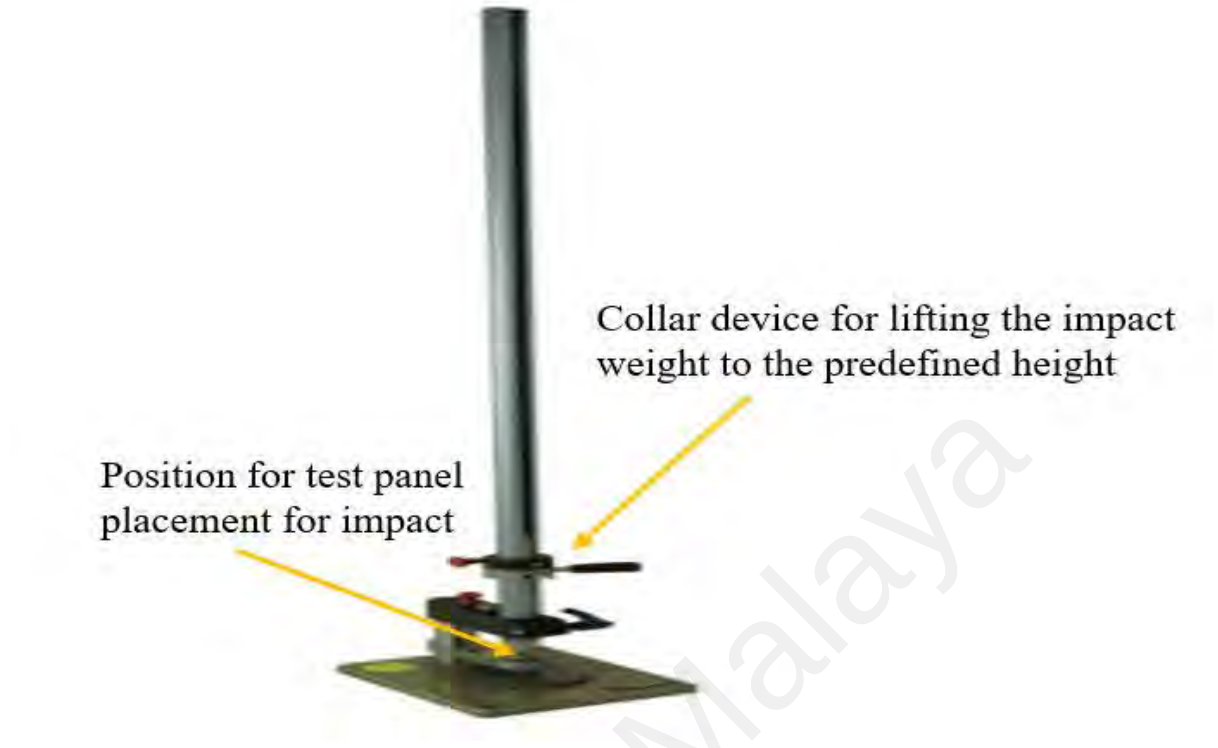

Figure 3.12 Tubular impact tester

3.2.14 Flexibility Test by T-bend Method

The most important test on the quality of precoated metal coating is its flexibility as defined by the T -bend test. The test method was carried out accordance with European Standard EN 13523-Part 7-2014 method. In principle, the purpose of the T -bend test is to evaluate the resistance to cracking of a coating when bent through 135-180°. This test method involves bending the metal coated panel parallel to rolling direction of the coil with the coating on the outside. The bending is carried out through radii between 135-180° over a period of 1-2 s. A close contact has to be maintained between the sample and the wedge to ensure a uniform bend. Any bending device allowing a uniform and smooth bend as such may be used. The minimum bending radius at which the sample panel can be bent without cracking is expressed as the crack resistant radius. The smallest bending radius is stated as OT as shown in Figure 3.13.

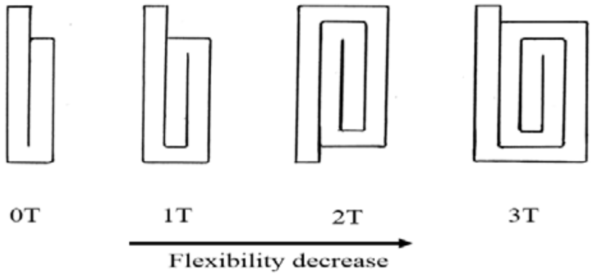

Figure 3.13 Diagrammatic of T-bend radius scale

Bending flexibility by the "T-bend test" is according to ASTM D4145. The painted panels are bent 180° around progressively more thicknesses of metal or larger diameter dies, the end point being when failures no longer occur. The panels are examined at low magnification (5X to 10X) after each bend for fracture of the coating (cracking) and, for loss of adhesion pickoff, by means of a tape pull-off test. When the metal is bent upon itself three times – so that there are two inner layers of the metal separating the outer layers produced by the final bend – the result is a "two-T" radius as shown by Figure 3.13.

3.2.15 Resistance of The Cured Film to MEK Solvent

The purpose of this test is to evaluate the degree of curing of the coating film through its resistance to methyl ethyl ketone (MEK). The test method was carried out accordance with European Standard EN 13523-Part 11-2014 method. In principle, this test method consists of rubbing the coating surface with a test cloth wetted with MEK until the coating begins to be removed. The rubbing is made by longitudinal back and forth rubs (double rubs) with the rubbing length being 5 times the length of the contact area. The contact area must be 100 mm^2 minimum. For preparation, the sample panel has to be cooled down to room temperature after curing and must be of the appropriate size. Procedure wise, the cloth is wetted with MEK and grip onto a hammer sharp tool with 1 kg weight on top and then placed on the sample to be tested. Rubbing speed should be about 1 second per double rub. MEK solvent rubbing test was manually done throughout the test as shown in Figure 3.14.

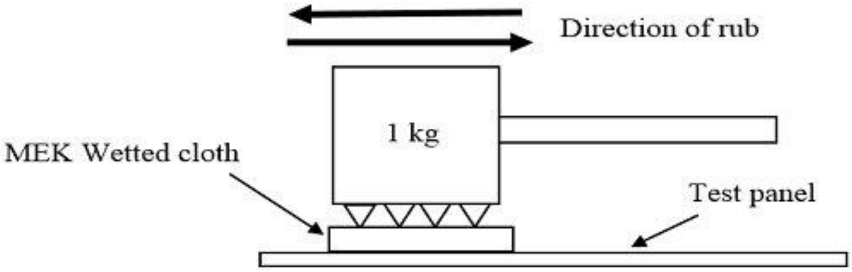

Figure 3.14 Illustration of MEK solvent double rub method

3.2.16 Cured Film Durability by QUV-A Accelerated Weathering Test

Many environmental factors contribute simultaneously to the coating's degradation affecting their life span time. Ultraviolet (UV) radiation, heat, humidity act cooperatively by changing the chemical structure of the polymeric film and its components, i.e. pigment and additives (Wypych, G. 1993 &1999, Jacques, L.F.F. 2000). One of the dominant factors for the coating's degradation is UV radiation (Armstrong, R.D. et al., 1995). Therefore, to understand the durability of the coating film particularly for exterior application still represent one of the most important issue during the development of coating resin. Although the natural weathering is the most direct method to access the durability of the coating film, but the test schedule was rather too time consuming. In order to shorten the development time, the QUV accelerated weathering tester was invented to examine the durability performance of the organic coating film.

The QUV accelerated weathering tester reproduces the damage caused by sunlight and/or rained dew. The testing was carried out in accordance with ASTM D 4587 method. The coated panel was tested using QUV UV chamber with UVA-340nm lamp. The chamber under cycling conditions of eight hours UV radiation at 60ºC follow by 3 hours 45 minutes condensation and spray water for another 15 minutes. This accelerated tester can reproduce the damage that occurs over months or years outdoors, within few days or week. To simulate outdoor weathering, the QUV accelerated tester exposes materials to alternating cycles of UV light and moisture at controlled, elevated temperatures. It simulates the effects of sunlight using special fluorescent UV lamps. It simulates dew and rain with condensing humidity and/or water spray. The test paint film will be monitored on their gloss reduction at specific duration of exposure time. A diagrammatic of QUV accelerated weathering tester was shown in Figure 3.15.

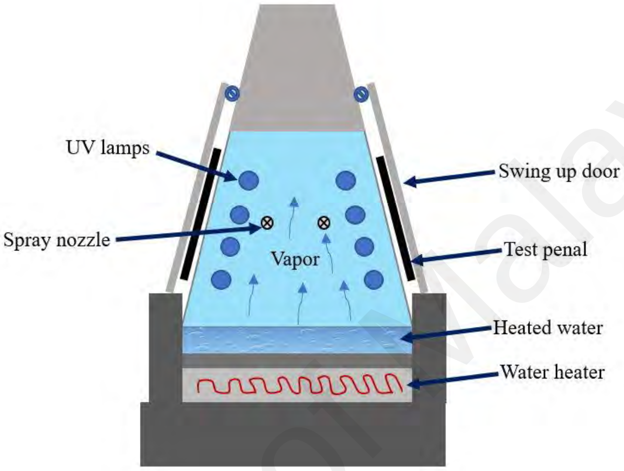

Figure 3.15 Diagrammatic representation of QUV weathering tester

3.2.17 Corrosion Resistance

Corrosion resistance is one of the important measures of the performance of an organic coating. A coated steel sheets that are intended for outdoor structures must have an outstanding resistance against corrosion. One of the more important tests for evaluation of the corrosion resistance of an organic coating is its resistance to salt spray. The purpose of this test is to evaluate the degree of corrosion of a coated steel panel after its exposure to salt solution for a specific period of time. The apparatus of this test consists of a cabinet with a salt solution container and compressed air facilities. This cabinet generates fog of the salt solution by means of one or several spray nozzles. The temperature of the cabinet is maintained at 35±2°C. The compressed air is used for atomisation of the salt solution which is preheated to 50°C. The NaCl solution is prepared to give a concentration of 5%. Sample panels have to be positioned at angles between 15-

25° to the vertical. The flow of the salt fog is adjusted in such a way to ensure that $80cm^2$ of the specimen's horizontal surface collect 1.0-2.0 ml of the condensate per test hour (ECCA, 1996, EN13523-Part 6, 2014).

The backside and edges of the sample panels are protected during the exposure to prevent any corrosive influence from the reverse side on the front side. The front coated side of the coated panel is scored by an appropriate cutting tool. This cut extends only through the top and primer coats and should expose 0.2 mm of the steel substrate. The cut must be of a X-shaped sketch (ECCA, 1996, EN13523-Part 6, 2014). A schematic illustration of the cut profile and dimensions of the specimen is provided in Figure 3.16.

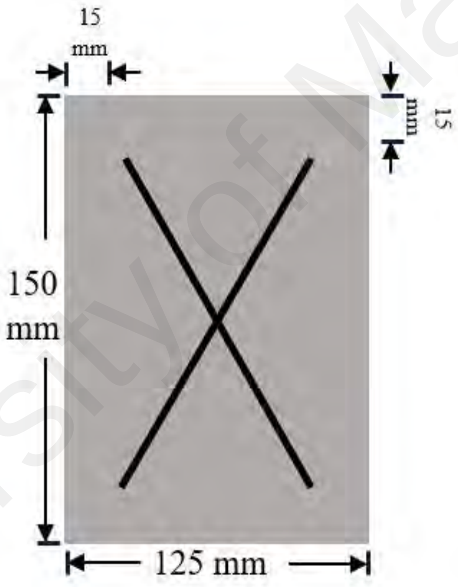

Figure 3.16 Schematic illustration of the cut profile and dimensions of the panel

The accelerated corrosion tests were conducted in accordance to ASTM B117 standard. The ASTM D1654 details the method for evaluation of corrosion performance of painted or coated specimens subject to the salt spray environment dictated in ASTM B117. The rating number of the evaluation results were given as per description in Table 3.2.

Table 3.2 Rating of corrosion as creep based on ASTM B117

Millimetres of Creep	Rating number
Zero	10
Over 0.0-0.5	9
Over 0.5-1.0	8
Over 1.0-2.0	7
Over 2.0-3.0	6
Over 3.0-5.0	5
Over 5.0-7.0	4
Over 7.0-10.0	3
Over 10.0-13.0	2
Over 13.0-16.0	1
Over 16.0	0

3.2.18 Water Resistance by Humidity Cycle Test

Water resistance testing of painted or coated panels is accomplished by placing them in an enclosed chamber containing a heated, saturated mixture of air and water vapor. The temperature of the chamber is maintained at 38°C. At 100% relative humidity, a very small temperature difference between the specimen and the surrounding vapor causes condensation to develop on the specimen. The test panel will be condition at atmospheric temperature for 1 hour before commencing any measurement on the tested surface. Any effects such as gloss change, blistering, loss of adhesion, softening, or embrittlement are observed and reported.

3.3 Design and Development of Urethane Acrylate using PFAD

3.3.1 Design of Hydroxyl Terminated PFAD Macromer (M-PFAD)

The PFAD mainly consist of free fatty acid as per description in section 2.1.2. The high content of fatty acid has provided possibility of using PFAD in alkyd synthesis particularly via direct esterification of fatty acid with other polyhydric alcohols and polybasic acids. In order to modify the resin for possible UV curable properties, the resin must have hydroxyl functionality to react with isocyanate and hydroxyl acrylate monomer to generate side chain containing double bonds. The development of PFAD urethane acrylate would involve more than one steps of polymerization processes, any highly viscosity intermediate should be avoided as it would be unfavourable for the subsequent grafting process. To avoid producing high viscosity resin during synthesis of PFAD alkyd, the formulation was designed to have high hydroxyl functional group as macromer.

3.3.1.1 Reactor used for M-PFAD Synthesis

In general, alkyd process technologies and conditions will be applied on M-PFAD. The reactor with high heating temperature for condensation reaction is required. Figure 3.17 show the diagrammatic of a typical condensation reactor and its important parts attached.

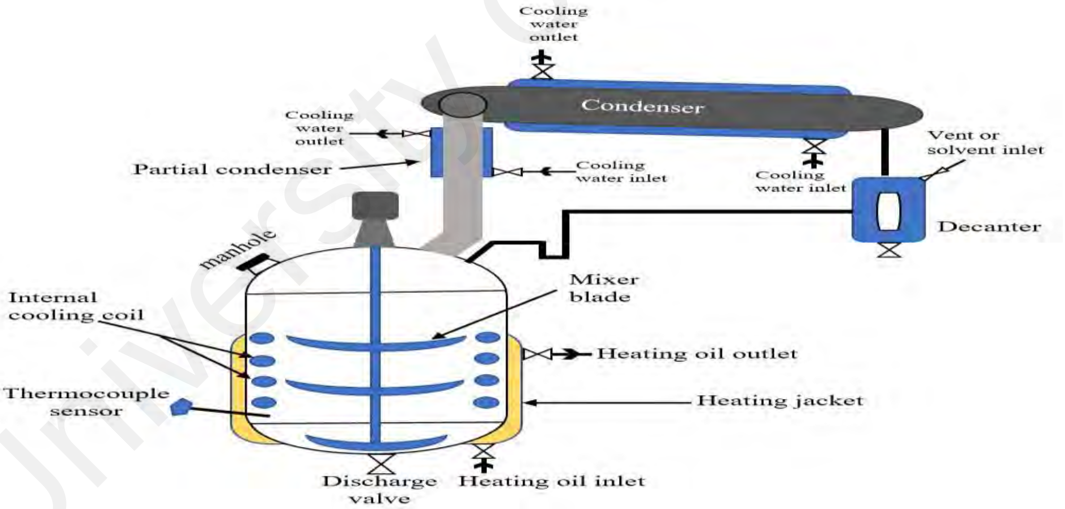

Figure 3.17 Diagrammatic representation of a condensation reactor and its important parts

As shown in the diagram, the reactor was built with a heating system with an efficient stirrer. The reactor is equipped with a vapour release at the top, where lead to partial and main condensers. The main condenser leads to a decanter which enables the collection and measurement of the water produced as a result of the esterification process. The partial condenser directs the water of reaction or the refluxing solvent to the main condenser. The water or refluxing solvent will condense in the main condenser. The water is then separated in the decanter and the refluxing solvent is flowed back to the reactor.

In general, a typical synthesis process of saturated polyester or alkyd resins, usually the polyols are initially added to the reactor and heated until complete meltdown. Depending on the nature of polyols, this initial heat up can be between 50-130°C (Husbands M.J.et al., 1987). Then the polyacids are added and the mixture is heated up to 200-260°C (Tsai C.J et al., 2008, Boyes S.G. et al., 2000). During the second stage of heating up, the polycondensation or the esterification reaction commences. The water produced by the reaction is separated from the reaction mixture at the decanter.

One of the severe phenomena may occur when an alkyd cook become gelation. If the equivalents of acid are greater than the hydroxyl during the initial formulation of an alkyd resin, the resin will gel. Therefore, alkyds are usually formulated with excess hydroxyl. There are also a number of extremely useful approaches that enables the determination of the safe cook of an alkyd formulation. However, even these measures are in place, unexpected gelation will often happen due to the following (Husbands M.J. et al., 1987);

a) loss of glycol or other volatile material through inefficient condensers or inefficient

control of partial condenser's head temperature;

b) temperature of reaction and heat up rate; and

c) other side reactions besides esterification.

However, total care in control during the cooking process especially in terms of viscosity build-up and reduction of acid value. All these factors will provide the best warning to avoid any gelation in an alkyd resin synthesis.

3.3.1.2 Theoretical Evaluation for M-PFAD Formulation

Prior to synthesis of any alkyd system, it is extremely helpful and important to theoretically evaluate the considered formulation by calculating certain parameters. These parameters are calculated from the molecular and equivalent weights of the formulation components and include the following;

1) hydroxyl excess

2) theoretical hydroxyl value

3) theoretical amount of liberated water

4) theoretical yield at acid value = O

5) theoretical yield at acid value =A

6) theoretical molecular weight at a given acid value

7) indication of the tendency of the considered formulation to gel

For the theoretical calculation of the above-mentioned parameters for a designed alkyd formulation, the following definitions have to be considered;

W_i = Total raw material weight input

M_o = Total number of moles of raw materials

E_{COOH} = Total number of equivalent weights of acid

E_{OH} = Total number of equivalent weights of hydroxyl

W_{H20} = Total theoretical liberated water of reaction

The initial development of a hydroxyl terminated PFAD macromer formulation was provided in Table 3.3 and theoretically evaluated. The theoretical parameters. calculated include the amount of liberated water, hydroxyl excess, yield at acid value=O, yield at acid value=10, hydroxyl value, molecular weight at acid value=10 and the tendency to gel.

Table 3.3 Formulation and calculation of M-PFAD

Raw material	W_i	M_w	Eq_{wt}	E_{OH}	E_{COOH}	M_O
PFAD	266.1	287	287		0.93	0.93
Isophthalic acid	177.4	166.1	83.05		2.14	1.07
Phthalic anhydride	224.8	148	74		3.04	1.52
NPG	272.1	104	52	5.23		2.62
Pentaerythritol	59.2	136	34	1.74		0.435
Total	999.6			6.97	6.11	6.58

Based on the total weight input, molecular and equivalent weights of the formulation's polyols and polyacids, the following can be calculated as

W_i= 999.6 g, M_O =6.58, E_{OH} =6.97, E_{COOH} = 6.11

The theoretical weight of liberated water is calculated based on polyacids, since in M-PFAD formulation, the hydroxyl equivalents are always in excess. The liberated water is calculated according to the basic esterification reaction and the number of moles of each acidic component. In esterification reaction, each equivalent of free acid group will liberate one equivalent of water and each anhydride group will liberate half equivalent of water. The total water from M-PFAD formulation with Wi of 999.6 g calculate as follow;

$$W_{H2O} = (0.93 \text{ X } 18 + 2.13 \text{ X } 18 + 3.04 \text{ X } 9) \text{ g}$$

$$= 82.48 \text{ g, where equivalent weight of } H_2O \text{ is } 18.$$

The characteristics of the macromer were calculated based on the equation given as below;

a. Theoretical Yield at AV=0

$$Y_0 = W_i - W_{H_2O} \tag{3.10}$$

b. Theoretical Yield at targeted AV=A

$$Y_A = \frac{56100}{56100-18A} \times Y_0 \qquad (\mathbf{3.11})$$

Where A is targeted acid value

c. Hydroxyl excess

$$\text{Hydroxyl excess} = \frac{E_{OH}}{E_{COOH}} \qquad (\mathbf{3.12})$$

d. Theoretical Hydroxyl value (OHV)

$$OHV = \frac{(E_{OH} - E_{COOH}) \times 56100}{Y_0} \qquad (\mathbf{3.13})$$

e. Theoretical molecular weight at a given acid value

$$M_A = \frac{Y_A}{(M_0 - E_{COOH}) + \frac{(Y_A \times A)}{56100}} \qquad (\mathbf{3.14})$$

f. Indication of the tendency of the considered formulation to gel, use of Patton's Constant

$$\text{Patton's constant (K)} = \frac{M_0}{E_{COOH}} \qquad (\mathbf{3.15})$$

For M-PFAD,

Y_0 = (999.6-82.48) g

=917.12 g

$$Y_{10} = \frac{56100}{56100 - 18(10)} \text{ X } 917.12 \text{ g}$$

= 920.07 g

$$\text{Hydroxyl excess} = \frac{6.97}{6.11}$$

= 1.14

$$\text{OHV} = \frac{(6.97 - 6.11)\ 56100}{917.12}\ \text{mgKOH/g}$$

$$= 53.39\ \text{mgKOH/g}$$

$$M_{10} = \frac{920.07}{(6.58\text{-}6.10) + \frac{(920.07 \text{ X } 10)}{56100}}\ \text{g/mol}$$

$$= 1463.46$$

$$K = \frac{6.58}{6.11}$$

$$= 1.08$$

With regard to the theoretical hydroxyl value and the theoretical molecular weight, it must be stressed that these are only theoretical amounts and are just an indication. The actual hydroxyl value can be determined by standard methods such as ASTM D1957-86. As mentioned in Section 3.2.6, actual molecular weights are determined by size exclusion chromatography. As the Patton's constant is greater than 1, the M-PFAD has theoretical evaluated as a safe cook formulation. However, as mentioned in reactor section, successful cook of the macromer still very much depending on the good adequacy of process control during the synthesis.

3.3.1.3 Procedure of M-PFAD Synthesis

266.1g palm fatty acid distillate and 272.1 g neopentylglycol were charged into a 2L four-necked glass reactor fitted with a decanter and stirrer. The mixture was initially being heated slowly to 100 ºC until all material melted, and subsequently load in 59.2 g pentaerythritol, 177.4 g isophthalic acid, 224.8 g phthalic anhydride and 0.4 g mono-butyl tin oxide and the mixture was stirring during the synthesis process. Heating was continuing slowly until 240 ºC. The polymerization was carried out under fusion process. Water of condensation reactions will be decanted out during the fusion process. Sampling of reaction mixture will be started when reaction temperature reached 190ºC for acid value check and viscosity measurement. For viscosity measurement, the taken sample will be diluted with xylene to 80% solid content before viscosity measurement. The heating process will be stopped, when acid value has dropped below 15 mgKOH/g, and the reactor is allowed to cool down, thus eventually stop the polymerization process. The PFAD macromer was transferred to a storage container at temperature around 100 ºC and the base resin was diluted with TPGDA to 70% PFAD macromer content and is ready for further modification.

3.3.2 Synthesis of PFAD Urethane Acrylate (PFAD-UA)

3.3.2.1 Reactor Used for PFAD-UA Synthesis

To synthesize the PFAD-UA, slow heating rate is adequate for the synthesis purpose. The nitrogen blanketing system is required to avoid unnecessary side reaction of isocyanate with moisture during grafting process. Dry air supply is important, as oxygen is required to activate the inhibitor to prevent homo-polymerization of acrylic monomer during acrylated grafting process. A good cooling system is required for effective cooling during the exothermic grafting reaction process. The cooling system is required to avoid the overheating due to the exothermic nature of the reaction, which might lead to gelling. Since the grafting is not done through one pot reaction, a monomer mixing tank is required and equipped with a dosing pump for controlling the monomer dosing rate. The dosing rate is important factor to control the exotherm of the reaction to ensure the reaction temperature is controlled within the targeted temperature range during the grafting of isocyanate. Figure 3.18 show the reactor and its parts for the grafting process.

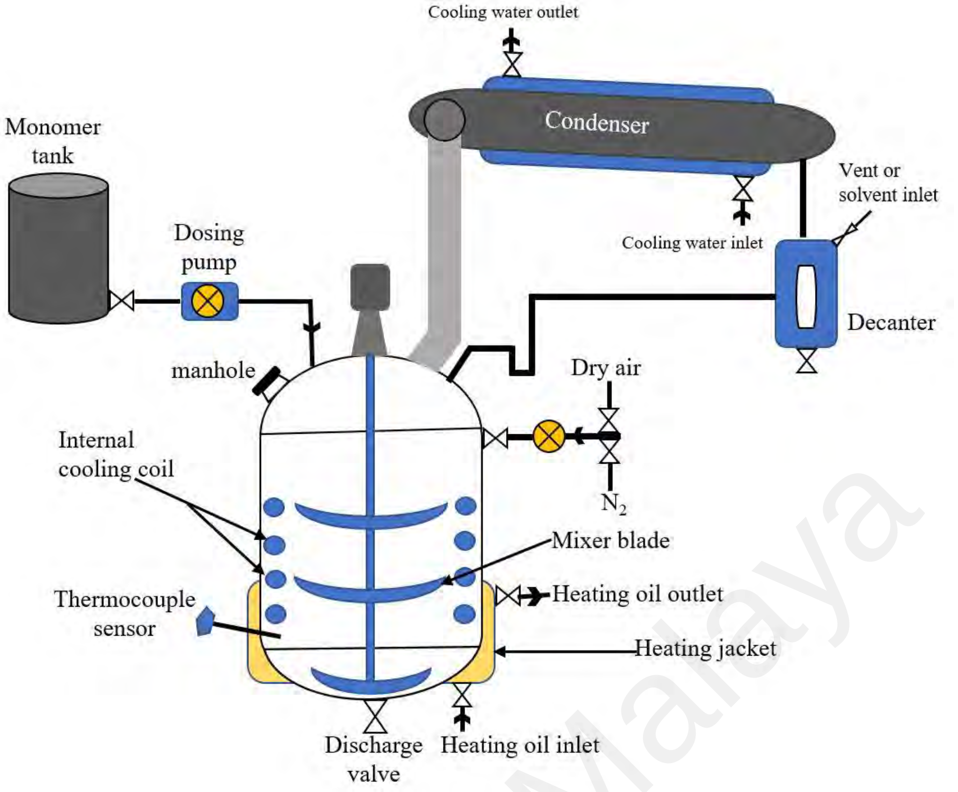

Figure 3.18 Diagrammatic representation of the reactor setup

3.3.2.2 PFAD-UA Formulation Design

The PFAD urethane acrylate was synthesized by copolymerized the M-PFAD with 2-hydroxylethylacrylate (2-HEA) and 2,4-toluenedisiocyanate (TDI). Since the M-PFAD is a polyfunctional polyol and to avoid over cross-linking reaction during isocyanate reaction with the PFAD polyol, the synthesis was adopted with process A as described in section 1.2.4.7. In this case, the TDI adduct of 2-HEA will be synthesized first and then followed by additional of M-PFAD macromer. The 4-methoxy phenol was used as inhibitor to prevent the 2-HEA double bond cross linking during the grafting process. Table 3.4 show the details formulation of PFAD urethane acrylate.

Table 3.4 Formulation of PFAD-UA

Raw material	Weight/g
2-hydroxylethylacrylate	95.9
2,4-toulenediisocyanate	63.4
M-PFAD	840.6
4-methoxy phenol	0.1

From the formulation, theoretical calculation as below;

Total mole (M) calculation;

$$\text{Total mole (M)} = \frac{\text{W}}{\text{M}_\text{w}}\ \text{mol} \qquad (\mathbf{3.16})$$

Where:

W = weight of substance, g.

Mw = molecular weight, g/mol.

Mole of TDI, Mw TDI =174.2 mol

$$M_{TDI} = \frac{95.9}{174.2}\ \text{mol}$$

= 0.55 mol

Mole of 2-HEA, Mw 2-HEA = 116.1 mol

$$M_{HEA} = \frac{63.4}{116.1}\ \text{mol}$$

= 0.55 mol

Since the TDI adduct was reacted with 1:1 mol ratio with 2-HEA, theoretically only one NCO was consumed by 2-HEA as shown by the structure in Figure 3.19.

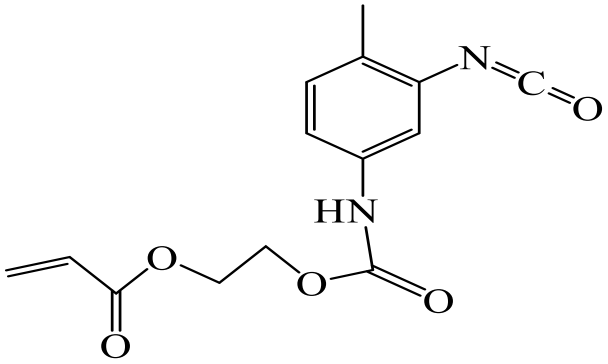

Figure 3.19 plausible structure of mono grafted TDI adduct of 2-HEA

Based on the structure in Figure 3.13, the equivalent weight of the TDI adduct will be 290 g/mol.

The theoretical calculated M-PFAD hydroxyl equivalent weight will be as below;

M-PFAD OHV = 53.39 mgKOH/g

$$\text{Hydroxyl equivalent weight } (\mathrm{E_{OH}}) = \frac{56100}{\mathrm{OHV}}\,\mathrm{g/mol} \qquad (\mathbf{3.17})$$

$$\mathrm{E_{OH(M\text{-}PFAD)}} = \frac{56100}{53.39}\ \mathrm{g/mol}$$

$$= 1050.76\ \mathrm{g/mol}$$

In theory, a maximum molecular weight is reached and those properties associated with molecular weight are optimized when one equivalent of isocyanate reacts with one equivalent of hydroxyl. In this case, full reaction between isocyanate and M-PFAD macromer should be avoided to prevent hardening of the synthesized urethane acrylate before performing coating application by UV curing.

In PFAD-UA formulation, 840.6 g of M-PFAD were used,

$$\text{The number of equivalents in 840.6 g of M-PFAD} = \frac{840.6}{1050.76} \text{ mol}$$

$$= 0.80 \text{ mol}$$

At 1.0 to 1.0, NCO to OH mol ratio, with equivalent of TDI adduct at 290 g/mol;

The amount of TDI adduct = 0.80 X 290 g

= 232 g

Comparing with the actual UA formulation, the total of TDI and 2-HEA is only 159.3g which is around 30 % less than actual requirement on 1:1 NCO:OH, mol ratio. Even though, the formulation was designed with lower cross linking with isocyanate, it must be stressed that these are only theoretical amounts and are just an indication. Proper process control in term of dosing rate, and suitable reaction temperature range have played an important role of successful grafting of the PFAD urethane acrylate.

3.3.2.3 Procedure of PFAD-UA Synthesis

95.9 g of TDI was charged into the reactor equipped with a mechanical stirrer, dropping funnel, a condenser capped with a drying tube, thermometer and a nitrogen inlet. The reactor was heated to 35ºC, 63.4 g 2-HEA and 0.1 g 4-methoxy phenol were activated with dry air for 10 minutes prior added into the reactor. The reactor cooling was applied in order to control the exothermic reaction. The progress of reaction could be monitored by FTIR and also the isocyanate content by titration method. When the isocyanate content has reached half of the initial value, the -OH peak would disappear in the FTIR spectrum. 840.6 g of the PFAD macromer was charged into the reactor. Temperature of the reactor was raised to 97˚C to accelerate the grafting process. The reaction was stopped when the residual isocyanate content was less than 0.05%. TPGDA will be added if necessary and the oligomer is ready for evaluation.

3.4 PFAD-UA UV Curing Development

The PFAD-UA resin was formulated into UV curable clearcoat to proceed for UV curing study including T_g and hardness development on the UV cured film. To evaluate the PFAD-UA in UV curing profile, the kinetic study was followed by FTIR technique as described in section 3.2.7.2.

3.4.1 PFAD-UA Coating Formulation

The UV curable formulation was prepared by mixing the PFAD-UA at 80.00% (*w/w*), speedcure 73 (2-hydroxy-2-methylpropiophenone) at 3.00% (*w/w*) and 17.00% (*w/w*) tripropylene glycol diacrylate (TPGDA). All ingredients were mixed and stir until homogeneous. Figure 3.20 shows the photoinitiator's structure of 2-hydroxy-2-methylpropiophenone and tripropylene glycol diacrylate as reactive diluent.

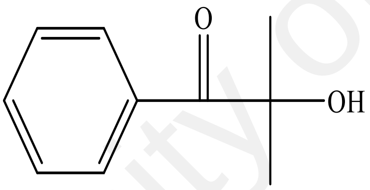

2-hydroxy-2-methylpropiophenone

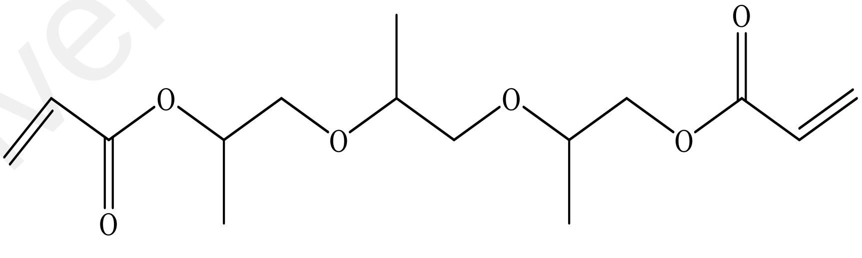

Tripropylene glycol diacrylate

Figure 3.20 Structure of 2-hydroxy-2-2methylpropiophenone and tripropylene glycol diacrylate

3.4.2 Equipment and Procedure of UV Curing

A lab scale UV curing machine was used to performance the UV curing of the PFAD-UA's coating. The UV curing machine was equipped with single mercury vapor lamp with an intensity of 225 mW/cm^2 at an ultraviolet wavelength of 254-365 nm. The machine also equipped with a conveyer which serves to carry the test sample into the curing tuner for UV irradiation purpose. Figure 3.21 shows the diagrammatic representation of the cross section of the UV curing machine.

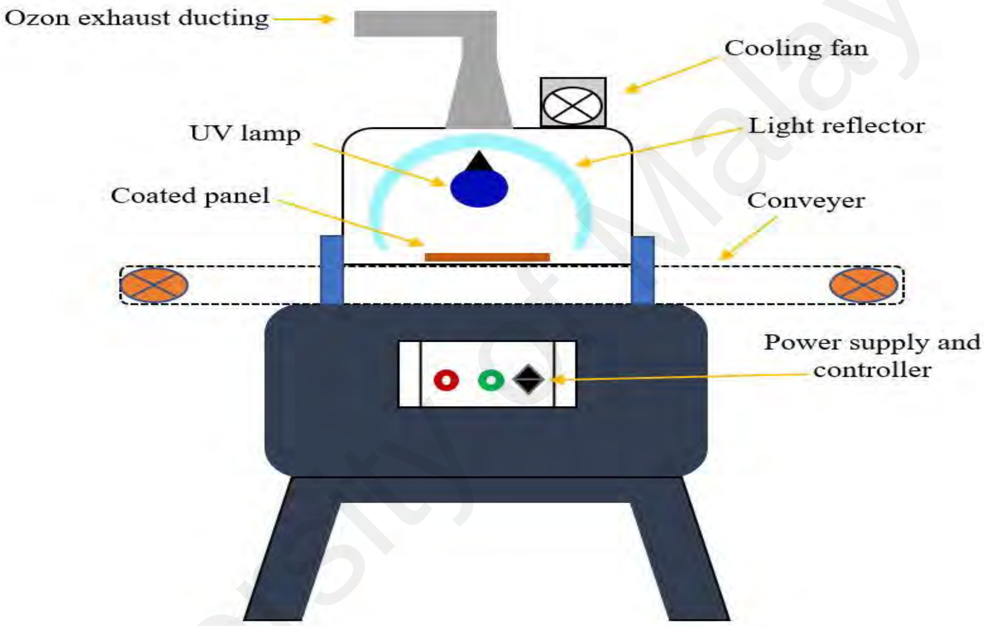

Figure 3.21 Diagrammatic representation of the cross section of the UV curing machine

To perform the UV curing kinetic study, the formulated PFAD-UA's clear coat was cast onto the sodium chloride cell. The coated sample will be delivered by the conveyer into the curing chamber which was then irradiated with the UV light at 10 cm distance from the source at the specified exposure time with 5 s incremental scale until 60 s total exposure time. The spectrum of FTIR on every interval curing time were recorded to measure the reduction peak area of wave number 810 cm^{-1}.

To measure the physical and mechanical performance of UV cured film, the PFAD-UA's clear coat was draw down with bar coater for around 20µm thickness onto a glass panel, wood panel or metal panel. Then, the coated panel will be irradiated according to the targeted curing schedule to produce a UV cured film panel for further film properties investigation purpose. For UV cured film glass transition temperature and pendulum hardness development, similar curing schedule and measurement conditions was used as in the UV curing kinetic study. For the PFAD-UA's cured film physical, chemical and mechanical properties study, the UV cured film was prepared by irradiating the coated panel for 60 s before carried out any measurement or testing on the prepared UV cured film.

3.5 Synthesis of PFAD-UA with Various PFAD Content

In line with the research objective in exploring the PFAD in coating resin application, the research was continued to investigate the influence of PFAD content after successfully developed the PFAD urethane acrylate at first stage of research. Since the project is to discover the maximum and optimum usage of PFAD in the coating resin application, a series of PFAD content ranging from 15 to 70% PFAD content were employed in the macromer formulation. The range chosen was to cover the full range of alkyd's oil length content including short, medium and long oil length. Similar reactor and reaction condition control was used to produce the M-PFAD macromer as described in section 3.3.1.1. The procedure of macromer synthesis followed the description in section 3.3.1.3.

3.5.1 Theoretical Evaluation for Macromers Formulation

All the macromer formulations were theoretically evaluated to obtain a safe cook formulation prior, the commencing the actual synthesis process.

3.5.1.1 Theoretical Evaluation of Macromer (M1)

The M1 formulation was provided in Table 3.5 and theoretically evaluated. The theoretical parameters. calculated include the amount of liberated water, hydroxyl excess, yield at acid value =O, yield at acid value =10, hydroxyl value, molecular weight at acid value =10 and the tendency to gel.

Table 3.5 Formulation of M1

Raw material	W_i	M_w	Eq_{wt}	E_{OH}	E_{COOH}	M_O
PFAD	150.6	287	287		0.53	0.53
Isophthalic acid	180.0	166.1	83.05		2.17	1.08
Phthalic anhydride	269.0	148	74		3.64	1.82
NPG	400.0	104	52	7.69		3.85
Total	999.6			7.69	6.33	7.27

The total water from M1 formulation with W_i of 999.6 g calculated as follow;

$$W_{H2O} = (0.53 \text{ X } 18 + 2.17 \text{ X } 18 + 3.64 \text{ X } 9) \text{ g}$$

$$= 81.17 \text{ g, where equivalent weight of } H_2O \text{ is } 18.$$

The characteristics of the macromer were calculated based on the equation given in section 3.3.1.2 as below;

For M1,

$$Y_0 = (999.6-81.17) \text{ g}$$

$$=918.43 \text{ g}$$

$$Y_{10} = \frac{56100}{56100 - 18(10)} \text{ X } 918.43 \text{ g}$$

$$= 921.38 \text{ g}$$

$$\text{Hydroxyl excess} = \frac{7.69}{6.33}$$

$$= 1.22$$

$$\text{OHV} = \frac{(7.69 - 6.33)\ 56100}{918.43} \text{ mgKOH/g}$$

$$= 83.38 \text{ mgKOH/g}$$

$$M_{10} = \frac{921.39}{(7.27 - 6.33) + \left(\frac{921.39 \text{ X } 10}{56100}\right)} \text{ g/mol}$$

$$= 830.72 \text{ g/mol}$$

$$K = \frac{7.27}{6.33}$$

$$= 1.15$$

As the Patton’s constant is greater than 1, the M1 has theoretical evaluated as a safe cook formulation with OHV at 83.38 mgKOH/g.

3.5.1.2 Theoretical Evaluation of Macromer (M2)

The M2 formulation was provided in Table 3.6 and theoretically evaluated. The theoretical parameters. calculated include the amount of liberated water, hydroxyl excess, yield at acid value=O, yield at acid value=10, hydroxyl value, molecular weight at acid value=10 and the tendency to gel.

Table 3.6 Formulation of M2

Raw material	W_i	M_w	Eq_{wt}	E_{OH}	E_{COOH}	M_O
PFAD	266.1	287	287		0.93	0.93
Isophthalic acid	177.4	166.1	83.05		2.14	1.07
Phthalic anhydride	209.4	148	74		2.83	1.41
NPG	287.5	104	52	5.53		2.76
Pentaerythritol	59.2	136	34	1.74		0.44
Total	999.6			7.27	5.90	6.61

The total water from M2 formulation with W_i of 999.6 g calculated as follow;

W_{H2O} =(0.927 X 18 + 2.14 X 18 + 2.83 X 9) g

= 80.61 g, where equivalent weight of H_2O is 18.

For M2,

Y_0 = (999.6-80.61) g

= 918.99 g

$$Y_{10} = \frac{56100}{56100 - 18(10)} \text{ X } 918.99 \text{ g}$$

= 921.95 g

$$\text{Hydroxyl excess} = \frac{7.27}{5.90}$$

= 1.23

$$\text{OHV} = \frac{(7.27 - 5.90)\ 56100}{918.99}\ \text{mgKOH/g}$$

$$= 84.06\ \text{mgKOH/g}$$

$$M_{10} = \frac{921.95}{(6.61 - 5.90) + \left(\frac{921.95 \text{ X } 10}{56100}\right)}\ \text{g/mol}$$

$$= 1046.29\ \text{g/mol}$$

$$K = \frac{6.61}{5.90}$$

$$= 1.12$$

As the Patton's constant is greater than 1, the M2 has theoretical evaluated as a safe cook formulation with OHV at 84.06 mgKOH/g.

3.5.1.3 Theoretical Evaluation of Macromer (M3)

The M3 formulation was provided in Table 3.7 and theoretically evaluated. The theoretical parameters. calculated include the amount of liberated water, hydroxyl excess, yield at acid value=O, yield at acid value=10, hydroxyl value, molecular weight at acid value=10 and the tendency to gel.

Table 3.7 Formulation of M3

Raw material	W_i	M_w	Eq_{wt}	E_{OH}	E_{COOH}	M_O
PFAD	446.6	287	287		1.56	1.56
Isophthalic acid	160.8	166.1	83.05		1.94	0.97
Phthalic anhydride	99.2	148	74		1.34	0.67
NPG	233.2	104	52	4.48		2.24
Pentaerythritol	59.5	136	34	1.75		0.44
Total	999.3			6.24	4.83	5.87

The total water from M3 formulation with W_i of 999.6 g calculated as follow;

$$W_{H2O} = (1.56 \text{ X } 18 + 1.94 \text{ X } 18 + 1.34 \text{ X } 9) \text{ g}$$

$= 74.92$ g, where equivalent weight of H_2O is 18.

For M3,

$$Y_0 = (999.3\text{-}74.92) \text{ g}$$

$$=924.39 \text{ g}$$

$$Y_{10} = \frac{56100}{56100 - 18(10)} \text{ X } 924.38 \text{ g}$$

$$= 927.36 \text{ g}$$

$$\text{Hydroxyl excess} = \frac{6.24}{4.83}$$

$$= 1.29$$

$$\mathrm{OHV} = \frac{(6.24 - 4.83)\ 56100}{924.38}\ \mathrm{mgKOH/g}$$

$$= 85.16\ \mathrm{mgKOH/g}$$

$$M_{10} = \frac{927.36}{(5.87 - 4.83) + \left(\frac{927.36\ \mathrm{X}\ 10}{56100}\right)}\ \mathrm{g/mol}$$

$$= 768.27\ \mathrm{g/mol}$$

$$K = \frac{5.87}{4.83}$$

$$= 1.22$$

As the Patton's constant is greater than 1, the M3 has theoretical evaluated as a safe cook formulation with OHV at 85.16 mgKOH/g.

3.5.1.4 Theoretical Evaluation of Macromer (M4)

The M4 formulation was provided in table 3.8 and theoretically evaluated. The theoretical parameters. calculated include the amount of liberated water, hydroxyl excess, yield at acid value=O, yield at acid value=10, hydroxyl value, molecular weight at acid value=10 and the tendency to gel.

Table 3.8 Formulation of M4

Raw material	W_i	M_w	Eq_{wt}	E_{OH}	E_{COOH}	M_O
PFAD	546.9	287	287		1.91	1.91
Isophthalic acid	139.2	166.1	83.05		1.68	0.84
Phthalic anhydride	49.7	148	74		0.67	0.34
NPG	203.8	104	52	3.92		1.96
Pentaerythritol	59.7	136	34	1.75		0.44
Total	999.3			5.67	4.25	5.48

The total water from M4 formulation with W_i of 999.6 g calculated as follow;

$$W_{H2O} = (1.91 \text{ X } 18 + 1.68 \text{ X } 18 + 0.67 \text{ X } 9) \text{ g}$$

$$= 70.52 \text{ g, where equivalent weight of } H_2O \text{ is } 18.$$

For M4,

$$Y_0 = (999.3\text{-}70.52) \text{ g}$$

$$=928.79 \text{ g}$$

$$Y_{10} = \frac{56100}{56100 - 18(10)} \text{ X } 928.78 \text{ g}$$

$$= 931.78 \text{ g}$$

$$\text{Hydroxyl excess} = \frac{5.67}{4.25}$$

$$= 1.33$$

$$OHV = \frac{(5.67 - 4.25)\ 56100}{928.78}\ \text{mgKOH/g}$$

$= 85.84$ mgKOH/g

$$M_{10} = \frac{931.78}{(5.48 - 4.25) + \frac{(\underline{931.78 \text{ X } 10})}{56100}}\ \text{g/mol}$$

$= 669.99$ g/mol

$$K = \frac{5.48}{4.25}$$

$= 1.29$

As the Patton’s constant is greater than 1, the M4 has theoretical evaluated as a safe cook formulation with OHV at 85.84 mgKOH/g.

3.5.1.5 Theoretical Evaluation of Macromer (M5)

The M4 formulation was provided in Table 3.9 and theoretically evaluated. The theoretical parameters. calculated include the amount of liberated water, hydroxyl excess, yield at acid value=O, yield at acid value=10, hydroxyl value, molecular weight at acid value=10 and the tendency to gel.

Table 3.9 Formulation of M5

Raw material	W_i	M_w	Eq_{wt}	E_{OH}	E_{COOH}	M_O
PFAD	687.0	287	287		2.39	2.39
Isophthalic acid	50.0	166.1	83.05		0.60	0.30
Phthalic anhydride	40.0	148	74		0.54	0.27
NPG	152.3	104	52	2.93		1.47
Pentaerythritol	70.0	136	34	2.06		0.51
Total	999.3			4.99	3.54	4.94

The total water from M5 formulation with W_i of 999.3 g calculated as follow;

$$W_{H2O} = (2.39 \text{ X } 18 + 0.60 \text{ X } 18 + 0.54 \text{ X } 9) \text{ g}$$

$$= 58.78 \text{ g, where equivalent weight of } H_2O \text{ is } 18.$$

For M5,

$$Y_0 = (999.3\text{-}58.78) \text{ g}$$

$$=940.52 \text{ g}$$

$$Y_{10} = \frac{56100}{56100 - 18(10)} \text{ X } 940.52 \text{ g}$$

$$= 943.55 \text{ g}$$

$$\text{Hydroxyl excess} = \frac{4.99}{3.54}$$

$$= 1.41$$

$$\text{OHV} = \frac{(4.99 - 3.54)\ 56100}{940.52}\ \text{mgKOH/g}$$

$$= 86.63\ \text{mgKOH/g}$$

$$M_{10} = \frac{943.55}{(4.94 - 3.54) + \frac{(943.55 \times 10)}{56100}}\ \text{g/mol}$$

$$= 598.33\ \text{g/mol}$$

$$K = \frac{4.94}{3.54}$$

$$= 1.40$$

As the Patton's constant is greater than 1, the M5 has theoretical evaluated as a safe cook formulation with OHV at 86.63 mgKOH/g.

3.5.1.6 Summary of Macromers Formulation

The macromers designed were named as M1, M2, M3, M4 and M5 according to their PFAD content ranging from 15, 25, 45, 55 to 70% respectively. The formulation and the calculated parameters were tabulated in Table 3.10.

Table 3.10 Summary of composition of M1 to M5 and calculated parameters

Raw Material	Formulation (weight/*g*)				
	M1	**M2**	**M3**	**M4**	**M5**
PFAD	150.6	266.1	446.6	546.9	687.0
NPG	400.0	287.5	233.2	203.8	152.3
Pentaerythritol	-	59.2	59.5	59.7	70.0
Isophthalic acid	180.0	177.4	160.8	139.2	50.0
Phthalic anhydride	269.0	209.4	99.2	49.7	40.0
Mono-butyl tin oxide	0.4	0.4	0.7	0.7	0.7
PFAD in macromer, %	15	25	45	55	70
Y_0 (g)	918.43	918.99	924.38	928.78	940.55
OHV (mgKOH/g)	83.38	84.06	85.16	85.84	86.63
K	1.15	1.12	1.22	1.29	1.40

3.5.2 Synthesis of PFAD Urethane Acrylate (UA) With Various PFAD Content

Each of the synthesized macromer M1 to M5 were copolymerized with TDI and 2-HEA to produce the UA. The designed formulations were tabulated in Table 3.11.

Table 3.11 Composition of UA1 to UA5

Raw Material	**Formulation (weight/*g*)**				
	UA1	**UA2**	**UA3**	**UA4**	**UA5**
TDI	95.9	95.9	95.9	95.9	95.9
2-HEA	63.4	63.4	63.4	63.4	63.4
4-methoxy phenol	0.1	0.1	0.1	0.1	0.1
M1	840.6	-	-	-	-
M2	-	840.6	-	-	-
M3	-	-	840.6	-	-
M4	-	-	-	840.6	-
M5	-	-	-	-	840.6

The theoretical evaluation for UA1 to UA5 calculated as below;

As described in section 3.3.2.2., the equivalent weight of the 2-HEA-TDI adduct was calculated at 290 g/mol.

For UA1,

$OHV_{M1} = 83.38$ mgKOH/g

$$E_{OH(M1)} = \frac{56100}{83.38} \text{ g/mol}$$

$$= 672.82 \text{ g/mol}$$

In UA formulation, 840.6 g of M1 were used,

$$\text{The number of equivalents in 840.6 g of M1} = \frac{840.6}{672.82} \text{ mol}$$

$$= 1.25 \text{ mol}$$

At 1.0 to 1.0, NCO to OH mol ratio, with equivalent of TDI adduct at 290 g/mol;

The amount of TDI adduct = 1.25 X 290 g

= 362.50 g

For UA2,

OHV_{M2}= 84.06 mgKOH/g

$$E_{OH(M2)} = \frac{56100}{84.06} \text{ g/mol}$$

$$= 667.38 \text{ g/mol}$$

In UA formulation, 840.6 g of M2 were used,

$$\text{The number of equivalents in 840.6 g of M2} = \frac{840.6}{667.38} \text{ mol}$$

$$= 1.26 \text{ mol}$$

At 1.0 to 1.0, NCO to OH mol ratio, with equivalent of TDI adduct at 290 g/mol;

The amount of TDI adduct = 1.26 X 290 g

= 365.40 g

For UA3,

OHV_{M3}= 85.16 mgKOH/g

$$E_{OH(M3)} = \frac{56100}{85.16} \text{ g/mol}$$

$$= 658.76 \text{ g/mol}$$

In UA formulation, 840.6 g of M3 were used,

$$\text{The number of equivalents in 840.6 g of M3} = \frac{840.6}{658.76}\ \text{mol}$$

$$= 1.28\ \text{mol}$$

At 1.0 to 1.0, NCO to OH mol ratio, with equivalent of TDI adduct at 290 g/mol;

The amount of TDI adduct = 1.28 X 290 g

= 371.20 g

For UA4,

OHV_{M4}= 85.84 mgKOH/g

$$E_{OH(M4)} = \frac{56100}{85.84}\ \text{g/mol}$$

$$= 653.54\ \text{g/mol}$$

In UA formulation, 840.6 g of M4 were used,

$$\text{The number of equivalents in 840.6 g of M4} = \frac{840.6}{653.54}\ \text{mol}$$

$$= 1.29\ \text{mol}$$

At 1.0 to 1.0, NCO to OH mol ratio, with equivalent of TDI adduct at 290 g/mol;

The amount of TDI adduct = 1.29 X 290 g

= 374.10 g

For UA5,

OHV_{M5} = 86.63 mgKOH/g

$$E_{OH(M5)} = \frac{56100}{86.63}\ \text{g/mol}$$

$$= 647.58\ \text{g/mol}$$

In UA formulation, 840.6 g of M5 were used,

$$\text{The number of equivalents in 840.6 g of M5} = \frac{840.6}{647.58}\ \text{mol}$$

$$= 1.30\ \text{mol}$$

At 1.0 to 1.0, NCO to OH mol ratio, with equivalent of TDI adduct at 290 g/mol;

$$\text{The amount of TDI adduct} = 1.30 \times 290\ \text{g}$$

$$= 377.00\ \text{g}$$

The actual amount of TDI and 2-HEA as copolymerization reactants for all formulations were only 159.3 g of which less than the actual theoretical calculation requirement on 1:1 NCO:OH, mol ratio and the fully cross-linked urethane reaction can be avoided when all reactant of TDI and 2-HEA has been fully consumed. The formulation of UA1 to UA5 were theoretically evaluated as safe cook formulations, aside from carefully controlling the important process parameters.

3.5.3 Evaluation of UA in Wood Coating Application

In woodworking industry, the wooden substrate was the main component particularly in furniture industry. Due to the complexity of wooden composition and poor physical properties, the substrate needs to be protected against the mechanical, physical and chemical attacked and this has made the wood coating very important in woodworking industry. Malaysia, as one of the ten largest furniture exporters, has provided a very good economic base for the wood coating industry development and also provide a good reason for the PFAD urethane acrylate to be evaluated in wood coating performance. In this regard, the mechanical, physical test and chemical resistant test were employed on the UV cured film of five PFAD urethane acrylate derived from various PFAD content.

3.5.3.1 Wood Coating Panel Preparation

Due to the differences in chemical and physical properties as compared to metal or plastic substrates, the coating systems involved were very much different from those for metal or plastic. As described in section 1.4.2., the wood coating finishes consist of three major coating system which to serve for different coating purposes. The three-coating system are wood filler, wood sealer and topcoat clear or colour. On wooden surface, naturally the wood grain or pores are being observed on the wood substrate. To apply the coating on such surface, this morphology appearance needs to be taken care before any topcoat finishes can be applied. In this study, the rubber wood panels were used for evaluating the physical and mechanical performance of the UV cured PFAD urethane acrylate coating. To prepare the coated wood panel in this project, the filler and sealer coating were being formulated with the PFAD urethane acrylate synthesized. Table 3.12 and 3.13 show the formulation of filler and sealer coat for wood panel preparation before applied the topcoat finishes.

Table 3.12 Wood filler formulation

Raw material	**% (*w/w*)**
PFAD urethane acrylate	20.00
Polygel GA801 W40	4.00
Defoamer	1.00
Silica powder 325 mesh	40.00
Koalin clay	10.00
Speedcure 73	5.00
TPGDA	20.00

Other than PFAD urethane acrylate as binder in the formulation, many other commercial ingredients were used to formulate the filler. The Polygel GA801W40 is the commercial thixotropic resin for controlling the rheology of the filler particularly for anti-settling performance. The silica powder and kaolin to serve as extender powder for filling purpose. The defoamer was used to break the bubble during the process or application of filler.

The application of filler is different for any other conventional coating where the filler should be applied by wiping instead of spraying. The filler is applied in circular motion by wiping with a clean cloth directly onto the bare wood surface. Upon the full coverage of the bare wood surface, the excess of filler will be wiped off to obtain a smooth filled surface. The filler coating will be then UV cured at the schedule irradiation time, and proceed with sanding using sand paper grade 350 to obtain a smooth surface. Repeating the above steps for another filler coat to obtain a fully filled surface. Figure 3.22 shows the schematic representation of filler application motion and Figure 3.23 shows the diagrammatic representation of the filled and sanded wood surface.

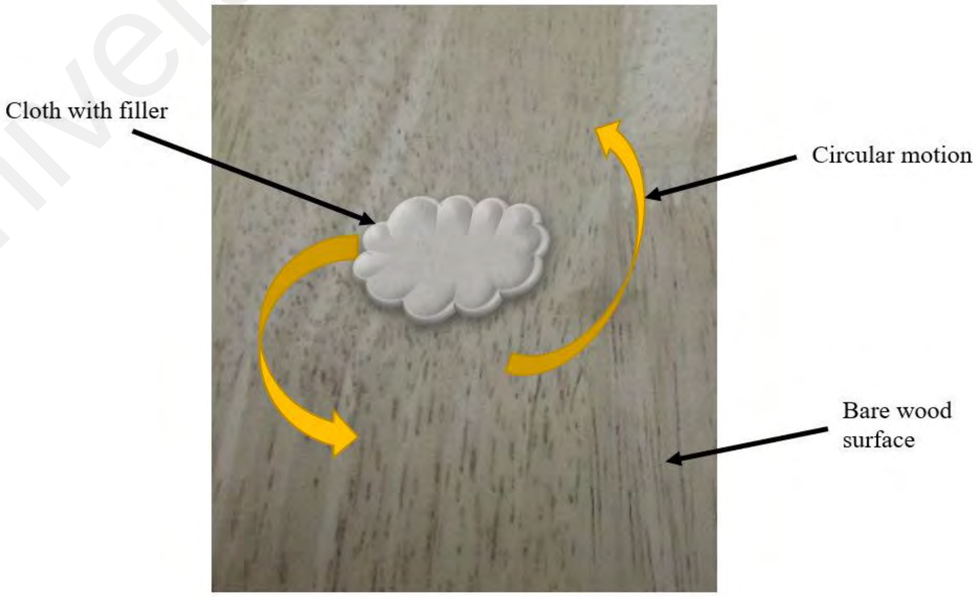

Figure 3.22 Schematic representation of filler application motion

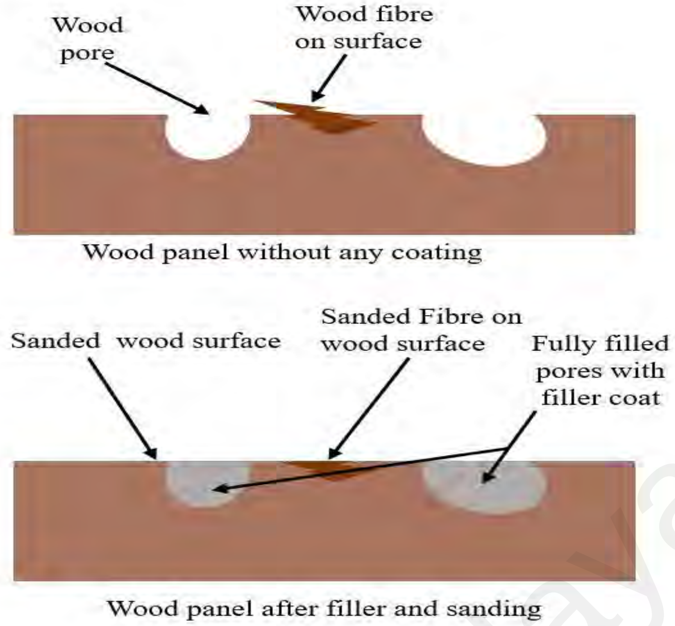

Figure 3.23 The illustration of wood panel surface after filler coat and sanding

In wood coating, the filler coat will normally function as pores filling coating rather than providing a whole smooth surface for subsequent topcoat application. To achieve the fully coated surface, the sealer coat needs to be applied. Based on its function and coverage, the sealer formulation will provide more binding effect than the filler coat, with condition that a reasonable amount of sanding powders was used for sanding purposes. Table 3.13 show the typical sealer formulation using PFAD urethane acrylate resin synthesized.

Table 3.13 Sealer coat formulation

Raw material	**% (*w/w*)**
PFAD urethane acrylate	60.00
Polygel GA813 X60	3.00
Defoamer	0.30
Micronized talc powder	15.00
Levelling additive	0.30
Speedcure 73	5.00
TPGDA	16.40

Similarly, to filler formulation, other commercial ingredients also being used. The Polygel GA813 X60 is another type of thixotropic resin to control the rheology of sealer. In order to enhance the resin rich content and good flow requirement after application, the formulation added the levelling additive to improve the levelling and good flow for a better coverage. Again, the defoamer is required for bubble breaking and deaeration purpose during application process. To apply the sealer coat, normally roller, curtain or spray method can be employed. The sealer coat also required sanding after UV curing process in order to obtain a well coverage and smooth surface for subsequent topcoat application. Figure 3.24 show the illustration of wood panel before and after the filler and sealer coat application.

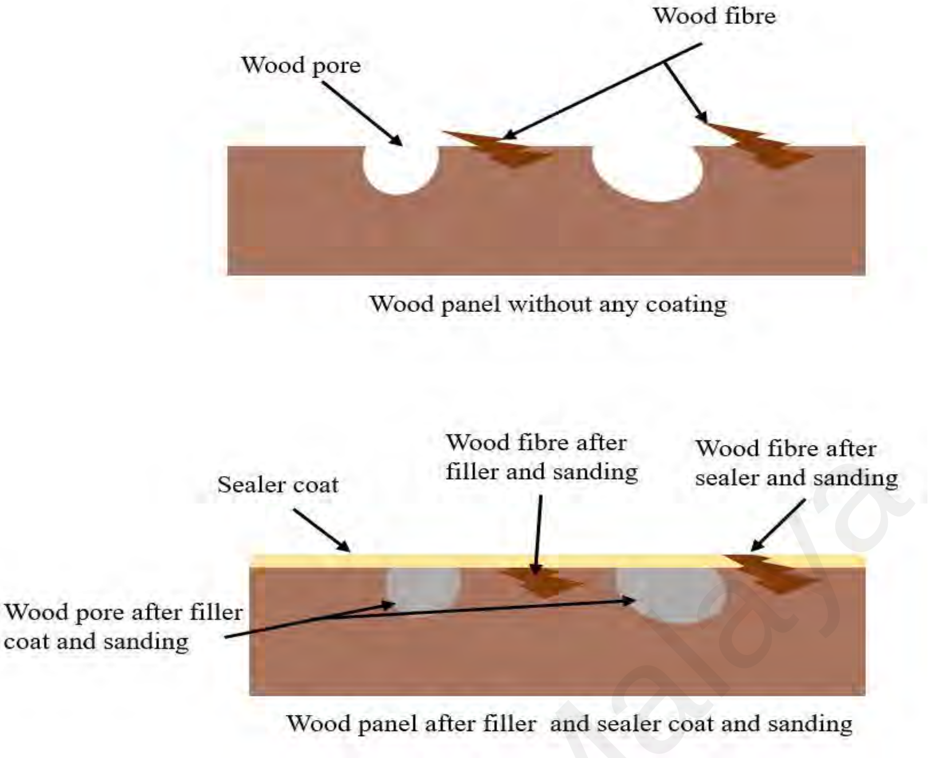

Figure 3.24 Illustration of wood panel before and after completion of filler and sealer coat

After completion of sealer coat, the wood panel is ready for any topcoat application. In this study, the sealer coated panel will be applied with the PFAD urethane acrylate clear coat as per description in section 3.4.1 and UV cured accordingly to the schedule set in individual test conditions. Figure 3.25 shows the complete wood finishes system on a standard bare wood panel.

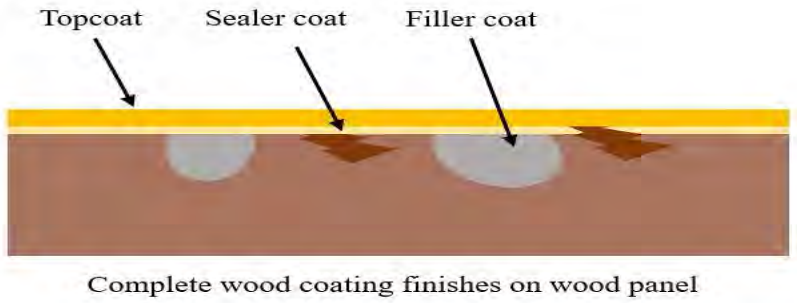

Figure 3.25 Illustration of a complete wood coating finishes

3.6 Synthesis of UA with Various Dicarboxylic Acid

Since the PFAD urethane acrylate was derived from the hydroxyl terminated macromer which was based on alkyd type of synthesis pathway. As per alkyd formulation discussed in section 1.3, alkyd is made from esterification of fatty acid with polyhydric alcohol and polybasic acid. Due to the limitation of mono functional of PFAD in alkyd polymerization, the study on the understanding of other polybasic acids building block become crucial and important. For synthesizing the PFAD hydroxyl terminated macromer, inclusion of other polybasic acids is necessary. Therefore, to further strengthen the use of PFAD in urethane acrylate synthesis application, the project has extended into investigating the effect of different polybasic acids building block particularly dicarboxylic acid in PFAD urethane acrylate synthesis.

3.6.1 Synthesis of Hydroxyl Terminated Macromer with Various Dicarboxylic Acid

To investigate and produce the PFAD hydroxyl terminated macromer with various dicarboxylic acids, four common commercially available dicarboxylic acids were chosen. Adipic acid (AA), isophthalic acid (IPA), terephthalic acid (TPA) and phthalic anhydride (PA) were the chosen dicarboxylic acids used in the PFAD macromers synthesis which represented the aliphatic, aromatic and anhydride type of dicarboxylic acids in the study. The chosen acids have showed extensive usage for different properties in many polyester polymerizations for various industry application such as plastic, fibre glass, PU foam and many other automotive and medical parts/devices application. The study is targeted to provide more data of understanding the PFAD urethane acrylate synthesis in term of physical, chemical and mechanical properties by using different polybasic acids building block. This study will also provide the base information for future modification and development to suit the various possible industry's needs.

For results consistency and good formulation design control, the fatty acid was formulated at 44-46 % range depending on the theoretical calculation on individual acids used. All macromers were using same dicarboxylic acid equivalent at 0.32 g/mol in 100 g of resin and hydroxyl value of 91 mgKOH/g based on 100% (*w/w*) calculated resin formulation.

3.6.2 Theoretical Evaluation of Macromer using Various Dicarboxylic Acid

3.6.2.1 Theoretical Evaluation of Macromer Using Adipic Acid (M-AA)

Similar theoretical evaluation parameters applied as per description in section 3.3.1.2. Table 3.14 shows the formulation of PFAD macromer using adipic acid.

Table 3.14 Formulation of M-AA

Raw material	W_i	M_w	Eq_{wt}	E_{OH}	E_{COOH}	M_O
PFAD	460.2	287	287		1.60	1.60
Adipic acid	240.0	146	73		3.29	1.64
NPG	237.8	104	52	4.57		2.29
Pentaerythritol	61.3	136	34	1.80		0.45
Total	999.3			6.38	4.89	5.98

The total water from M-AA formulation with W_i of 999.3 g calculate as follow;

W_{H2O} =(1.60 X 18 + 3.29X 18) g ,where equivalent weight of H_2O is 18.

= 88.04 g

For M-AA,

Y_0 = (999.3-88.04) g

=911.96 g

$$Y_{10} = \frac{56100}{56100 - 18(10)} \text{ X } 911.96 \text{ g}$$

$$= 914.19 \text{ g}$$

$$\text{Hydroxyl excess} = \frac{6.38}{4.89}$$

$$= 1.30$$

$$\text{OHV} = \frac{(6.38 - 4.89)\ 56100}{911.26} \text{ mgKOH/g}$$

$$= 91.41 \text{ mgKOH/g}$$

$$M_{10} = \frac{914.89}{(5.98 - 4.89) + \left(\frac{914.89 \text{ X } 10}{56100}\right)} \text{ g/mol}$$

$$= 824.41 \text{ g/mol}$$

$$K = \frac{5.98}{4.89}$$

$$= 1.22$$

As the Patton’s constant is greater than 1, the M1 has theoretically evaluated as a safe cook formulation with OHV at 91.41 mgKOH/g.

3.6.2.2 Theoretical Evaluation of Macromer Using Terephthalic Acid (M-TPA)

Table 3.15 shows the formulation of PFAD macromer using terephthalic acid.

Table 3.15 Formulation of M-TPA

Raw material	W_i	M_w	Eq_{wt}	E_{OH}	E_{COOH}	M_O
PFAD	440.0	287	287		1.53	1.53
Terephthalic acid	267.0	166.1	83.05		3.21	1.61
NPG	232.0	104	52	4.46		2.23
Pentaerythritol	60.3	136	34	1.77		0.44
Total	999.3			6.24	4.75	5.81

The total water from M-TPA formulation with W_i of 999.3 g calculate as follow;

W_{H2O} = (1.53 X 18 + 3.21 X 18) g, where equivalent weight of H_2O is 18.

= 85.46 g

For M-TPA,

Y_0 = (999.3-85.46) g

=913.84 g

$$Y_{10} = \frac{56100}{56100 - 18(10)} \text{ X } 913.84 \text{ g}$$

= 916.78 g

$$\text{Hydroxyl excess} = \frac{6.24}{4.75}$$

$$= 1.31$$

$$\text{OHV} = \frac{(6.24 - 4.75)\ 56100}{913.84}\ \text{mgKOH/g}$$

$$= 91.29\ \text{mgKOH/g}$$

$$M_{10} = \frac{916.77}{(5.81 - 4.75) \quad + \quad \left(\frac{916.77 \text{ X } 10}{56100}\right)}\ \text{g/mol}$$

$$= 745.28\ \text{g/mol}$$

$$K = \frac{5.81}{4.75}$$

$$= 1.22$$

As the Patton's constant is greater than 1, the M-TPA has theoretical evaluated as a safe cook formulation with OHV at 91.29 mgKOH/g

3.6.2.3 Theoretical Evaluation of Macromer Using Isophthalic Acid (M-IPA)

Table 3.16 shows the formulation of PFAD macromer using isophthalic acid.

Table 3.16 Formulation of M-IPA

Raw material	W_i	M_w	Eq_{wt}	E_{OH}	E_{COOH}	M_O
PFAD	440.0	287	287		1.53	1.53
Isophthalic acid	267.0	166.1	83.05		3.21	1.61
NPG	232.0	104	52	4.46		2.23
Pentaerythritol	60.3	136	34	1.77		0.44
Total	999.3			6.24	4.75	5.81

The total water from M-IPA formulation with W_i of 999.3 g calculate as follow;

W_{H2O} = (1.53 X 18 + 3.21 X 18) g, where equivalent weight of H_2O is 18.

= 85.46 g

For M-IPA,

Y_0 = (999.3-85.46) g

=913.84 g

$$Y_{10} = \frac{56100}{56100 - 18(10)} X\ 913.84\ g$$

= 916.78 g

$$\text{Hydroxyl excess} = \frac{6.24}{4.75}$$

= 1.3132

$$\text{OHV} = \frac{(6.24 - 4.75)\ 56100}{913.84}\ \text{mgKOH/g}$$

$$= 91.29\ \text{mgKOH/g}$$

$$M_{10} = \frac{916.77}{(5.81 - 4.75) + \left(\frac{916.77 \times 10}{56100}\right)}\ \text{g/mol}$$

$$= 745.28\ \text{g/mol}$$

$$K = \frac{5.81}{4.75}$$

$$= 1.22$$

As the Patton's constant is greater than 1, the M1 has theoretical evaluated as a safe cook formulation with OHV at 91.29 mgKOH/g.

3.6.2.4 Theoretical Evaluation of Macromer Using Phthalic Anhydride (M-PA)

Table 3.17 shows the formulation of PFAD macromer using phthalic anhydride.

Table 3.17 Formulation of M-PA

Raw material	W_i	M_w	Eq_{wt}	E_{OH}	E_{COOH}	M_O
PFAD	460.2	287	287		1.60	1.60
Phthalic anhydride	240.0	148	74		3.24	1.62
NPG	237.8	104	52	4.57		2.29
Pentaerythritol	61.3	136	34	1.80		0.45
Total	999.3			6.38	4.85	5.96

The total water from M-PA formulation with W_i of 999.3 g calculate as follow;

W_{H2O} =(1.60 X 18 + 3.24 X 9) g ,where equivalent weight of H_2O is 18.

= 58.05 g

The characteristics of the macromer were calculated based on the equation given in section 3.3.1.2 as below;

For M-PA,

Y_0 = (999.3-58.05) g

=941.25 g

$$Y_{10} = \frac{56100}{56100 - 18(10)} \text{X } 941.25 \text{ g}$$

= 944.28 g

$$\text{Hydroxyl excess} = \frac{6.38}{4.85}$$

= 1.32

$$\text{OHV} = \frac{(6.38 - 4.85)\ 56100}{941.25} \text{mgKOH/g}$$

= 91.15 mgKOH/g

$$M_{10} = \frac{944.98}{(5.96 - 4.85) + \left(\frac{944.25 \text{ X } 10}{56100}\right)} \text{ g/mol}$$

= 735.43 g/mol

$$K = \frac{5.96}{4.85}$$

$$= 1.23$$

As the Patton's constant is greater than 1, the M1 has theoretical evaluated as a safe cook formulation with OHV at 91.08 mgKOH/g.

3.6.2.5 Summary of Macromers Formulation Using Various Dicarboxylic Acid

The macromers designed were named as M-AA, M-PA, M-IPA and M-TPA according to their dicarboxylic acid building block used respectively. The formulations and the calculated parameters were tabulated in Table 3.18.

Table 3.18 Summary of composition of M-AA, M-IPA, M-TPA and M-PA

Raw Material	**Formulation (weight/*g*)**			
	M-AA	**M-IPA**	**M-TPA**	**M-PA**
PFAD	460.2	440.0	440.0	460.2
NPG	237.8	232.0	232.0	237.8
Pentaerythritol	61.3	60.3	60.3	61.3
Isophthalic acid	-	267.0	-	-
Terephthalic acid	-	-	267.0	-
Phthalic anhydride	-	-	-	240.0
Adipic acid	240.0	-	-	-
Mono-butyl tin oxide	0.7	0.7	0.7	0.7
PFAD in macromer, %	46	44	44	46
Y_0 (g)	911.96	913.84	913.84	941.25
OHV (mgKOH/g)	91.41	91.29	91.29	91.15
K	1.22	1.22	1.22	1.23
Acid equivalent (g/mol)	3.29	3.21	3.21	3.24

3.6.3 Synthesis of UA with Various Dicarboxylic Acid

Same technique of synthesis and reaction conditions as per described in section 3.3.2.2. and 3.3.2.3 were employed in the synthesis of PFAD urethane acrylate using different dicarboxylic acids building block. The formulations were tabulated in Table 3.19.

Table 3.19 Formulation of UA derived from different dicarboxylic acids

Raw Material	**Formulation (weight/*g*)**			
	UA-AA	**UA-TPA**	**UA-IPA**	**UA-PA**
TDI	95.9	95.9	95.9	95.9
2-HEA	63.4	63.4	63.4	63.4
4-methoxy phenol	0.1	0.1	0.1	0.1
M-AA	840.6	-	-	-
M-TPA	-	840.6	-	-
M-IPA	-	-	840.6	-
M-PA	-	-	-	840.6

The theoretical evaluation for UA-AA, UA-TPA, UA-IPA and UA-PA calculated as below;

As described in section 3.3.2.2., the equivalent weight of the 2-HEA-TDI adduct was calculated at 290 g/mol

For UA-AA,

$OHV_{M\text{-}AA}$= 91.34 mgKOH/g

$$E_{OH(M1)} = \frac{56100}{91.34} \text{ g/mol}$$

= 614.19 g/mol

In UA formulation, 840.6 g of M-AA were used,

$$\text{The number of equivalents in 840.6 g of M-AA} = \frac{840.6}{614.19} \text{ mol}$$

= 1.37 mol

At 1.0 to 1.0, NCO to OH mol ratio, with equivalent of TDI adduct at 290 g/mol;

The amount of TDI adduct = 1.37 X 290 g

= 397.30 g

For UA-TPA,

OHV_{M2} = 91.29 mgKOH/g

$$E_{OH(M2)} = \frac{56100}{91.29} \text{ g/mol}$$

= 614.53 g/mol

In UA formulation, 840.6 g of M-TPA were used,

$$\text{The number of equivalents in 840.6 g of M-TPA} = \frac{840.6}{614.53} \text{ mol}$$

= 1.37 mol

At 1.0 to 1.0, NCO to OH mol ratio, with equivalent of TDI adduct at 290 g/mol;

The amount of TDI adduct = 1.37 X 290 g

= 397.30 g

For UA-IPA,

$OHV_{M3} = 91.29$ mgKOH/g

$$E_{OH(M3)} = \frac{56100}{91.29} \text{ g/mol}$$

= 614.53 g/mol

In UA formulation, 840.6 g of M-IPA were used,

$$\text{The number of equivalents in 840.6 g of M-IPA} = \frac{840.6}{614.53} \text{ mol}$$

= 1.37 mol

At 1.0 to 1.0, NCO to OH mol ratio, with equivalent of TDI adduct at 290 g/mol;

The amount of TDI adduct = 1.37 X 290 g

= 397.30 g

For UA-PA,

$OHV_{M4} = 91.08$ mgKOH/g

$$E_{OH(M4)} = \frac{56100}{91.08} \text{ g/mol}$$

= 615.94 g/mol

In UA formulation, 840.6 g of M-PA were used,

$$\text{The number of equivalents in 840.6 g of M-PA} = \frac{840.6}{615.94} \text{ mol}$$

$$= 1.36 \text{ mol}$$

At 1.0 to 1.0, NCO to OH mol ratio, with equivalent of TDI adduct at 290 g/mol;

The amount of TDI adduct = 1.36 X 290 g

= 394.4 g

The actual amount of TDI and 2-HEA as copolymerization reactants for all formulations were only 159.3 g of which less than the actual theoretical calculation requirement on 1:1 NCO:OH, mol ratio and the fully cross-linked urethane reaction can be avoided when all reactant of TDI and 2-HEA has been fully consumed. All UAs derived from different dicarboxylic acid were theoretically evaluated as safe cook, aside from carefully controlling the other important process parameter.

3.7 The Performance of UA UV Cured Film in Metal Coating Application

The mechanical, chemical and physical test were carried out on the PFAD urethane acrylate UV cured film derived from four dicarboxylic acids according to the test method described from section 3.2.8 to 3.2.17. All the clear coats were formulated according to formulation designed in section 3.4.1 using similar UV curing condition as described in section 3.4.2. The PFAD urethane acrylate synthesized were only evaluated as topcoat application. The metal panel used was a pre-coated with a polyester/ melamine stoving primer obtained from the local metal panel producer and the UA's clear coat were applied directly on top of the primer, then follow by UV curing process.

3.7.1 Mechanical, Chemical and Physical Tests on Metal Coating Application

As described in section 1.5, good mechanical and outstanding adhesion are the important requirement of a metal coating. Six coating's performance tests were employed for the UV cured film derived from the four dicarboxylic acids. In this regard, the UV cured film was evaluated on its film properties according to the test methods of resistance to cracking on bending, MEK solvent rubbing test, resistance to rapid deformation, cured film durability, resistance to humidity and resistance to salt spray. In addition to the above test criteria, the pencil hardness also being determined on the UV cured film.

3.7.1.1 UV Cured Film Flexibility Performance By T-bend Method

Other than structurer usage of metal substrate, the metal has wide used in many industrial applications such as coil, can, appliances and automotive parts formation. Because of the industrial processes which may involve the coating subjected to bending, deep drawing and shape forming of the pre-coated panel, the metal coating's flexibility is one of the important qualities as defined by the T-bend test as described in section 3.2.14.

After the application and UV curing of the coating, the coated panel has to be prepared as following;

1) the coating under the test should always be at the outside of the bend.

2) only flat strip should be used, in such a size that the required bending process can be executed.

3) the coating surface shall be free of oil and other matter that can influence the flexibility or interfere with the observation for cracking or adhesion.

4) the samples can be measured as soon as the cured coating is cooled down to room temperature.

5) immediately after bending, the coated panel must be examined with a x10 magnifier for any cracking.

6) because of possible burrs, one should ignore up to 5 mm on extreme edges of the coated panel.

The bending method is selected according to the size of the coated panel, either folding or mandrel method can be used. In this case, the folding method was selected on the UV cured panel. Figure 3.26 illustrate the schematic of the folding and full bending by mechanical or hydraulic press machine.

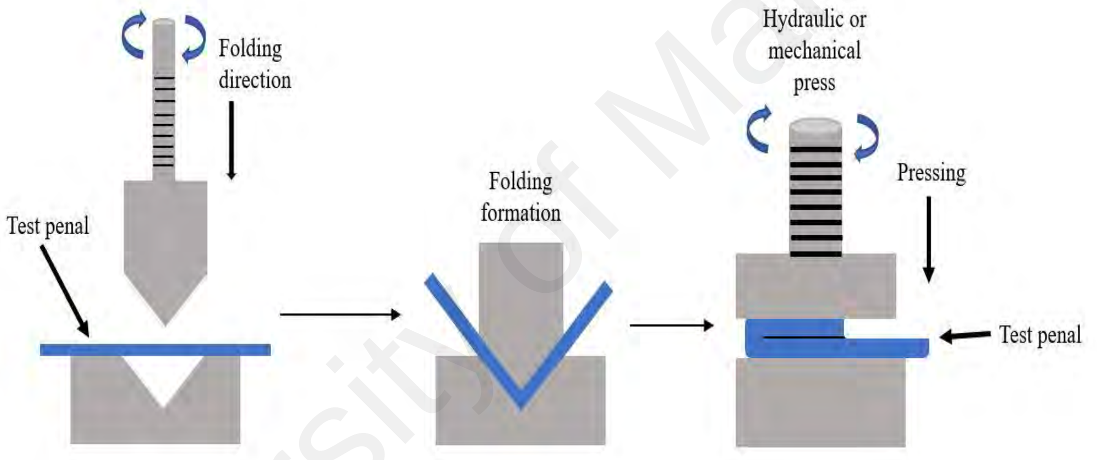

Figure 3.26 The schematic diagram representation of a panel bending procedure

The mechanical or hydraulic press was used to press down the folded panel ensure a complete bending of the coated panel is obtained prior evaluation of the adhesion and cracking defect

3.7.1.2 Cracking Resistance of the UV Cured Film by Impact Deformation

The elongation tolerance, resistance to cracking and adhesion of the four UA's UV cured film were evaluated by using a tubular impact tester described in section 3.2.13. The coated panel is fixed into position with the quick release clamp as shown in Figure 3.6. The weight is lifted to the predefined height set by the adjustable collar device. The weight is then released and the resulting deformation is observed. The coating adhesion on the deformed area may also be evaluated if required by the peeling test. The back sides of the sample panel are subjected to the impact. The peel test must be carried out on the coating area deformed as the result of the impact on the backside of the coated panel by means of adhesive tape. Any cracking and chipping of the coating film after the impact and the peel tests are visually observed and reported as the result of the test.

3.7.1.3 Solvent Resistance of the UV Cured Film

The degree of curing of the four PFAD urethane acrylate UV cured films were evaluated through its resistance to MEK (methyl ethyl ketone) solvent described in section 3.2.15. In principle, the test method consists of rubbing the coating surface with a cloth impregnated with MEK. Evaluation is based on colour change, blistering, cracking and gloss reduction which was noticeable after the rubbing test schedule. Rossi et al (2007) and Perou A.L. et al (1997) also used the same method for evaluating the degree of curing and chemical resistance of coil coating systems.

The rubbing is made by longitudinal back and forth rubs (double rubs) with the rubbing length being 5 times the length of the contact area. The contact area must be 100 mm^2 minimum. A cotton type test cloth was used for this test. For preparation, the test panel was cooled down to room temperature after curing prior the rubbing test. The test cloth must remain wet throughout the whole rubbing procedure. At the point where the coating begins to be removed and the material underneath can be seen, the rubbing must stop. The result of the test is expressed as the number of double rubs by which the coating film was removed.

3.7.1.4 Durability of UV Cured Film

The durability of the four UA's UV cured film were evaluated using accelerated weathering test against UV light and humidity resistance as described in section 3.2.16.

All UV cured panel will be condition at room temperature for 24 hours before subjected to accelerated weathering test schedule. The total test schedule was targeted to expose the UV cured film for 1500 hours of QUV exposure. The gloss measurement and appearance observation of the test panels were carried out at every 100 hours of exposure interval. All test panel will be cleaning with a dry clean cloth and conditioning at room temperature for 1 hour before carried out any measurement.

3.7.1.5 Performance of Corrosion Resistance of the UV Cured Film

The performance of the corrosion resistance of the UA's clear coating were evaluated by a salt spray method as described in section 3.2.17. Similarly, to QUV test panel, the coated panel also undergo for 24 hours room temperature conditioning before subjected to salt spray test. To avoid the influence of corrosion on the uncoated surface, the uncoated surface was protected and fully covered by using adhesive plastic tape including all the side edges. The panel was prepared according to the description in Figure 3.10 with the cross cut on the coated film. The coated panel was subjected to 720 hours test schedule. The observation and measurement of gloss were carried out at every 24 hours of test interval. The test panel will be cleaned with a dry clean cloth and also subjected to conditioning at room temperature for 1 hour before carried out any measurement on the coating. The extent of creep and blistering in millimetres from the X-shaped cuts after the predefined exposure duration is reported as the test result rated using the rating given in Table 3.2.

3.7.1.6 Performance of Water Resistance of the UV Cured Film

The performance of the water resistance of the UV cured film was evaluated by using humidity cycle test method as per described in section 3.2.18. The test panels were prepared according to the similar condition in QUV testing described in section 3.7.1.4. A total of 720 hours cycle exposure was scheduled for all test panels. To carried any test or measurement, the test panels have to clean with dry clean cloth and conditioning for 1 hours before any measurement applied. The gloss measurement was recorded at every 24 hours interval. The adhesion and pencil hardness for the UV cured film were determined at initial and final stage of the test schedule.

CHAPTER 4: RESULTS AND DISCUSSION

4.1 Design and Development of PFAD Urethane Acrylate

The PFAD urethane acrylate resin was developed by designing a hydroxyl terminated macromer, then co-polymerizing with TDI and 2-HEA. The macromer was produced by reacting with NPG and pentaerythritol and polybasic acids phthalic anhydride and isophthalic acid. The purpose of grafting the TDI and 2-HEA onto the macromer backbone was to introduce the double bond for the resin to become UV curable.

4.1.1 Synthesis of Hydroxyl Terminated Macromer (M-PFAD)

The composition of the macromer synthesized during this stage of study are provided in Table 3.3. The plausible structure of M-PFAD is showed in Scheme 4.1.

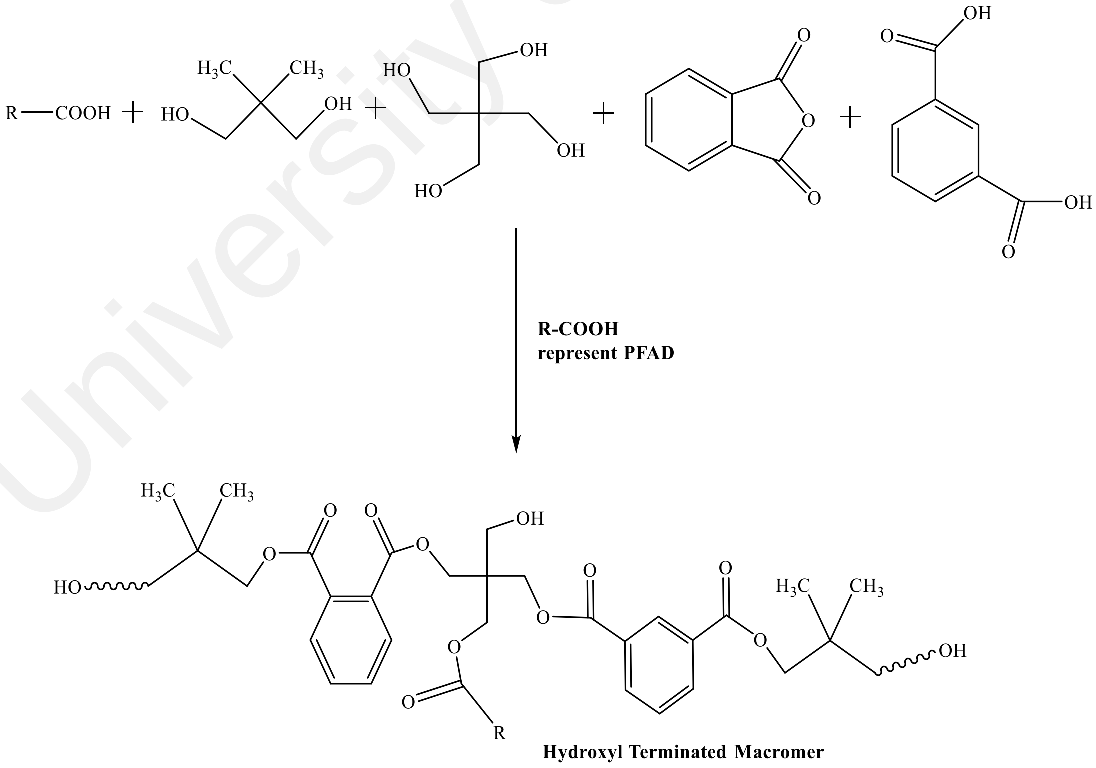

Scheme 4.1. Plausible structure of PFAD macromer

4.1.1.1 Acid Value and Molecular Weight Analysis

The changes of acid value and molecular weight during M-PFAD synthesis were measured and determined according to method described in section 3.2.1 and 3.2.6. The reactions proceed with decrease in acid value and increase in molecular weight with the reaction time as shown in Figure 4.1. The macromer had M_w = 2800 dalton at acid value of 18.0 mgKOH/g. The acid value has decreased slowly, with the reaction of carboxylic groups with hydroxyl group, the M_w has increased and finally attained 6800 dalton when the acid value was reduced to 9.8 mgKOH/g.

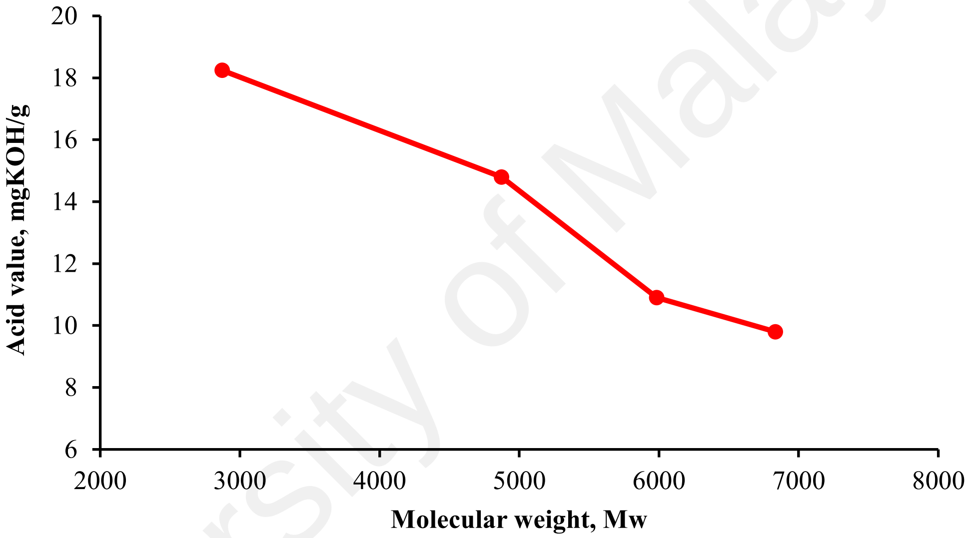

Figure 4.1 Acid value versus molecular weight during macromer synthesis

4.1.1.2 FTIR analysis of M-PFAD

The FTIR spectrum of M-PFAD is shown in Figure 4.1. The feed compositions of the M-PFAD was given in Table 3.3. Peak assigments for the FTIR spectrum are provided in Table 4.1.

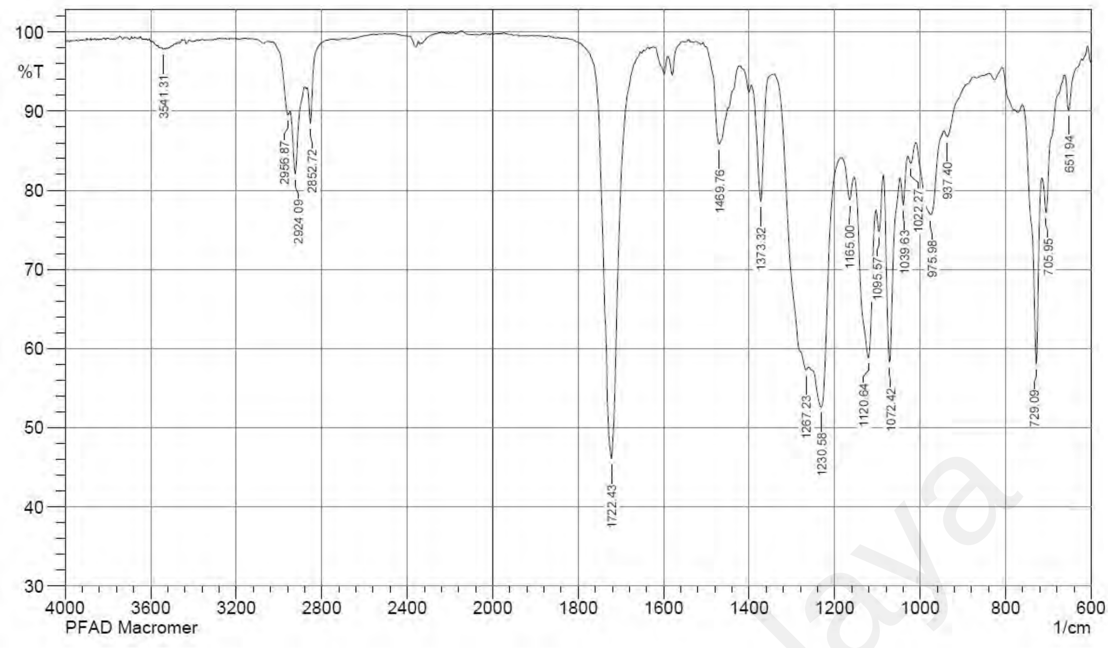

Figure 4.2 FTIR spectrum of the PFAD hydroxyl terminated macromer

Table 4.1 Assignment for the FTIR spectrum for M-PFAD

Wave number (cm^{-1})	**Assignment**
3541	O-H stretch, weak
2956 -2857	C-H stretch, weak
1722	C=O stretch, strong
1599 -1579	C=C stretch, weak
1469	$-CH_2-$ bending, weak
1373	$-CH_3$ bending, medium
1267 -1039	C-O bending, strong
975	C-O-H out of plane bending, medium
729 -705	C-H out of plane bending of di-substituted benzene ring, strong

The weak and broad peaks at 3541cm^{-1} is the hydroxyl stretching vibration. The weak peak between 2857 -2956 cm^{-1} is the stretching of C-H. The strong absorption peaks centered at 1722 cm^{-1} is the carbonyl (C=O) stretching of the ester linkages that were present in the polymeric backbone of tM-PFAD. The weak peaks within 1579 -1599 cm^{-1} is due to C=C stretching. Such groups are due to the aromatic ring of isophthalic acid and phthalic anhydride moieties. The weak and broad peaks centered at 1469 cm^{-1} is assigned to methylene (-CH$_2$-) bending. The medium peaks centered at 1373 cm^{-1} is assigned to methyl (-CH$_3$) bending, The strong peaks between 1039 -1267 cm^{-1} is assigned to C-O group of the ester linkages. The absorption peaks centered at 975 cm^{-1} is assigned to the carboxyl functionality. The strong peak between 705 -729 cm^{-1} was due to out of plane bending of C-H in the meta di-substituted benzene ring of isophthalate moieties.

The final properties of the PFAD macromer are summarized in Table 4.2.

Table 4.2 The final properties of PFAD macromer

Macromer Content, %	70.0
Active diluents TPGDA, %	30.0
Viscosity@ 25°C	70.0 poise
Acid value, mgKOH/g	9.8
Molecular weight, M_w	6800 dalton
Polydispersity, PDI	3.24

4.1.2 Synthesis of PFAD Urethane Acrylate (PFAD-UA)

The M-PFAD was reacted with TDI and 2-HEA. TDI contains –NCO at ortho and para positions, and the para-NCO is 8 times more reactive than ortho-NCO at temperature below 30˚C (Webster G, 1997; Lu W.H. et al., 2006). The adduct of TDI and 2HEA was first produced at temperature below 30˚C. The consumption of NCO was being monitored through the reduction of peak at 2270 cm^{-1} in the FTIR spectrum and also with titration method. The plausible reaction path of PFAD-UA formation is shown in Scheme 4.2.

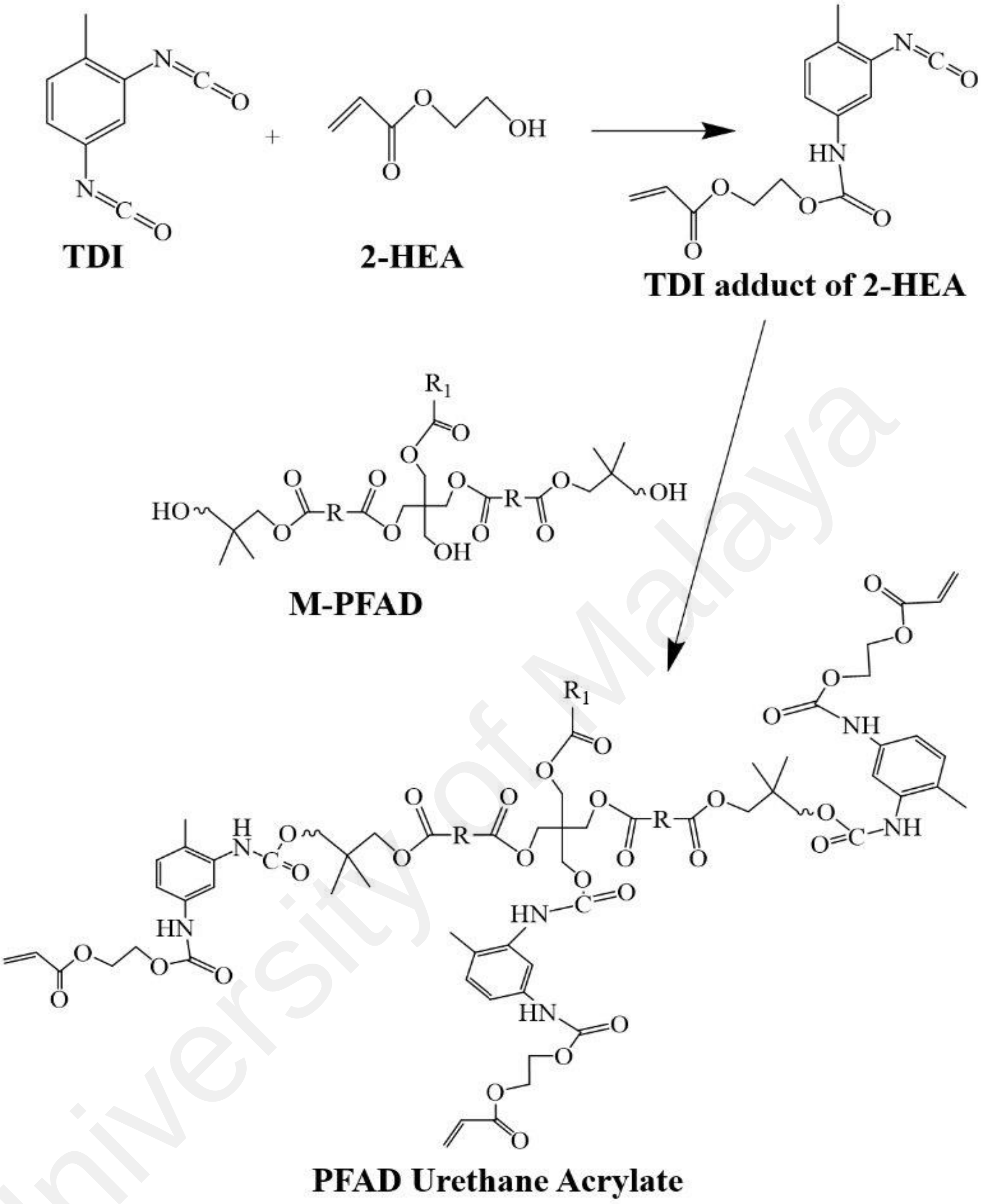

Scheme 4.2 Plausible reaction and structure of PFAD urethane acrylate

4.1.2.1 NCO Content Analysis for PFAD-UA

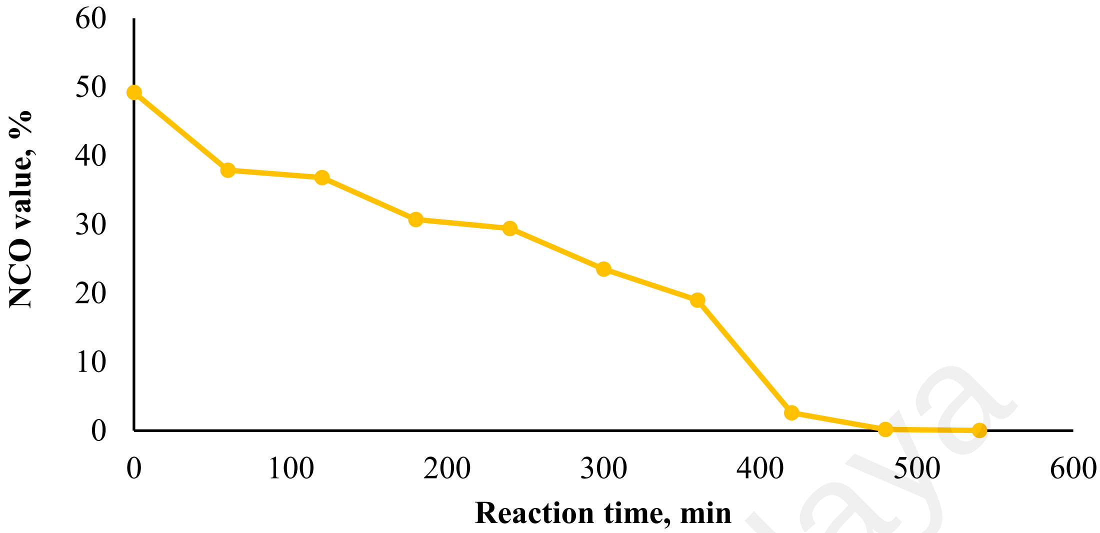

Figure 4.3 NCO value during synthesis of PFAD urethane acrylate

Figure 4.3 shows the change in NCO fraction with reaction time during the synthesis of PFAD-UA. The reduction of NCO content was due to the reaction between the hydroxyl group and isocyanate during the grafting process. At initial stage, the isocyanate would presumably react faster with hydroxyl group in 2-HEA, then further react with pendent hydroxyl group at M-PFAD. The initial NCO of 49.2% has reduced gradually and reached 2.6% after 420 min. Further 120 min was needed to reduce the NCO value to 0.03%, due to low mobility of reactants as viscosity has built up to more than 1000 poise during the grafting reaction.

The grafting reaction was also followed by FTIR technique on the reduction of NCO peaks centered at 2270 cm^{-1}. Figure 4.4. shows the overlaid of NCO peaks spectra at different reaction time and the NCO peak area reduction can be seen at reaction time 360, 420 and 480 min show continue reduction of NCO, which was resulted from the NCO reaction between hydroxyl functionality of the M-PFAD. All NCO groups were consumed at the end of the reaction time of 540 min and the traces of NCO couldn't be detected by FTIR in the final FTIR spectrum in Figure 4.4.

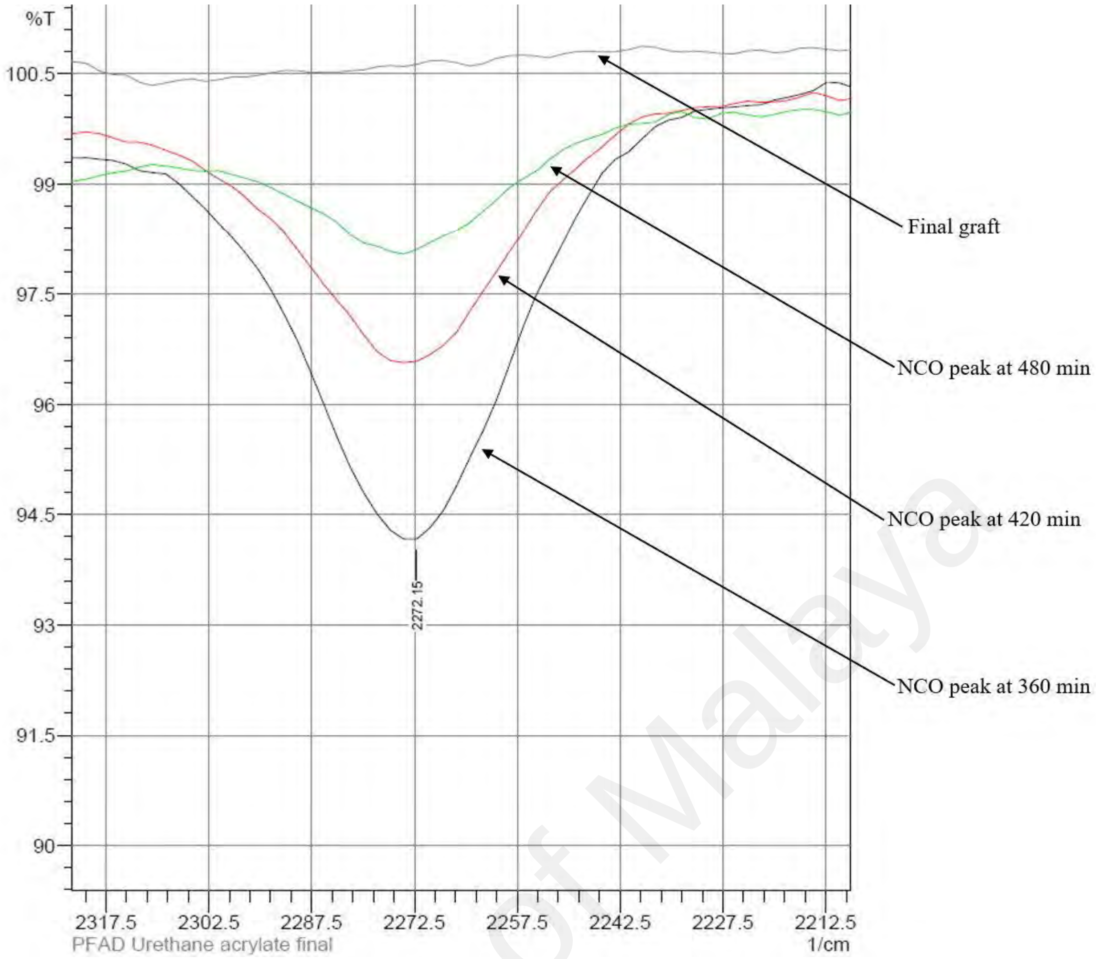

Figure 4.4 Overlaid of FTIR spectra of NCO peak at 2272 cm^{-1} during grafting reaction

4.1.2.2 FTIR Analysis of PFAD-UA

Figure 4.6 shows the overlaid FTIR spectra of the M-PFAD and PFAD-UA. The summaries of the peak's assignment between M-PFAD and PFAD-UA were provided in Table 4.3.

Table 4.3 Comparison of FTIR peaks between M-PFAD and PFAD-UA

Wave number(cm^{-1})	**Assignment in M-PFAD**	**Assignment in PFAD-UA**
3541	O-H stretch, weak	Absent
3336	Absent	NH stretch, weak
2956 -2857	C-H stretch, weak	C-H stretch, weak
1722	C=O stretch, strong	C=O stretch, strong
1599 -1579	C=C stretch, weak	C=C stretch, weak
1531	Absent	NH deformation, medium
1469	$-CH_2-$ bending, weak	$-CH_2-$ bending, weak
1406	Absent	$–CH_2=CH-R$ scissoring bending
1373	$-CH_3$ bending, medium	$-CH_3$ bending, medium
1267 -1039	C-O bending, strong	C-O bending, strong
975	C-O-H out of plane bending, medium	C-O-H out of plane bending, medium
810	Absent	C=C out of plane deformation of acrylate double bond
729 -705	C-H out of plane bending of di-substituted benzene ring, strong	C-H out of plane bending of di-substituted benzene ring, strong

M-PFAD and PFAD-UA similar peaks in the spectra except the new peak at 3336, 1531, 1406 and 810 cm^{-1} in PFAD-UA, while and peak at 3541 cm^{-1} was not found in PFAD-UA.

The shift of peak at 3541 to 3336 cm^{-1} was due to formation of urethane linkage resulted from the reaction of -OH and -NCO groups. This is supported by the emergence of NH deformation at 1531 cm^{-1}. Figure 4.5 illustrated the formation of urethane linkage during the synthesis of PFAD-UA resin.

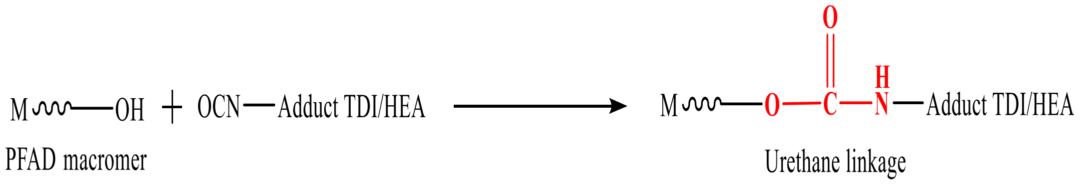

Figure 4.5 Illustration of the urethane linkage formation in PFAD-UA

The peak at 810 cm^{-1} is attributed to the out of plane deformation of the C=C of the vinyl moieties of the acrylate groups and was supported by the absorption peak at 1406 cm^{-1} for –CH$_2$=CH-R scissoring bending.

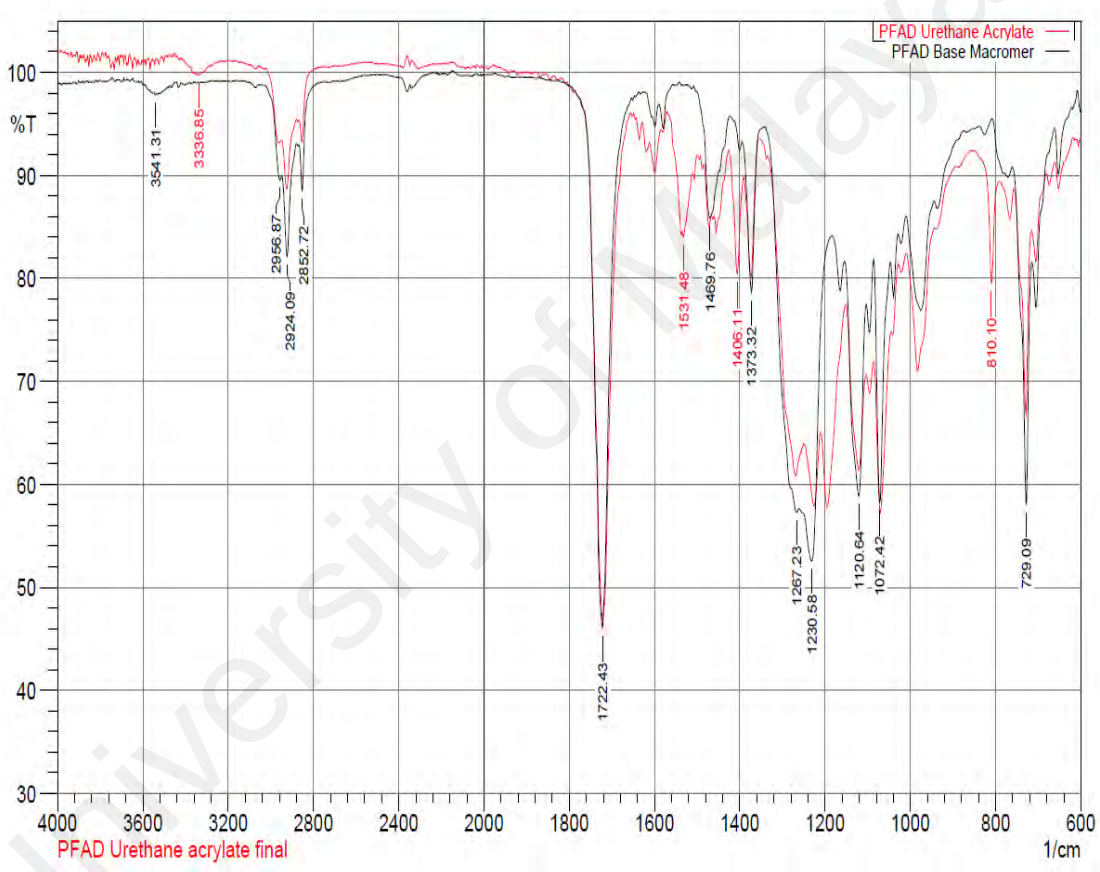

Figure 4.6 Overlaid FTIR spectra of PFAD macromer and urethane acrylate

The molecular weight of polymer relative to polystyrene standards were determined by GPC. The M$_w$ of PFAD-UA was 12500 dalton while the M-PFAD was recorded at 6800 dalton as shown by the GPC chromatogram in Figure 4.7. The increase is due to the reactions of the M-PFAD with TDI and 2-EHA. Properties of the PFAD-UA are summarized in Table 4.4.

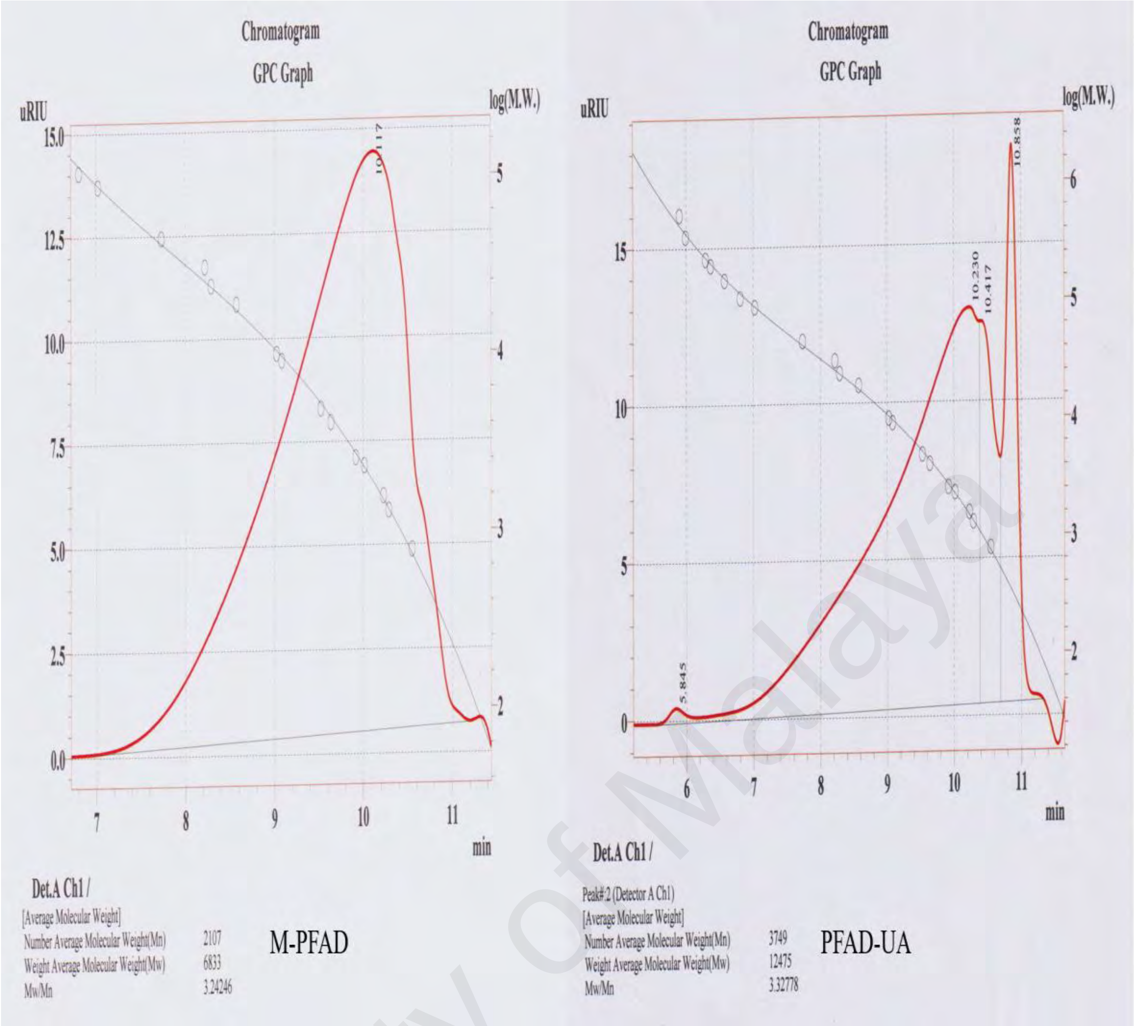

Figure 4.7 Chromatogram of PFAD urethane acrylate and macromer

Table 4.4 Properties of PFAD urethane acrylate oligomer

Oligomer content, %	70.0
Active diluents TPGDA %	30.0
Viscosity@ 25°C	>1000 poise
Acid value, mgKOH/g	9.8
TDI value, %	0.03
Molecular weight, M_w	12500 dalton
Polydispersity, PDI	3.33

4.1.3 UV Irradiation Curing of PFAD-UA

The UV curing of PFAD-UA using the clear coat formulation provided in section 3.4.1 was followed by FTIR. The reaction was monitored on the reduction of peak area of the acrylate double bond at 810 cm^{-1} and the conversion of the acrylate unsaturation was calculated by using Eqn 3.8. Figure 4.8 shows the overlaid FTIR spectra of the peak absorption 810 cm^{-1} at various selected curing time. The change in peak area versus the curing time is shown in Figure 4.9.

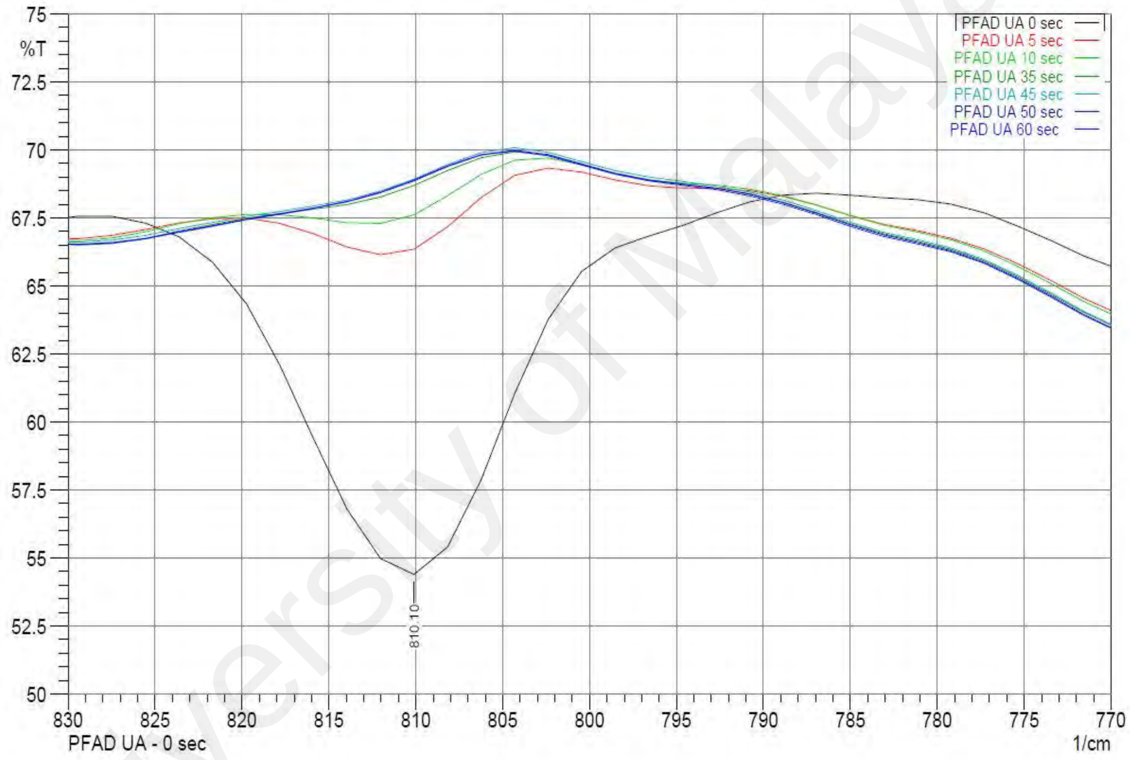

Figure 4.8 Overlaid peak at 810 cm^{-1} at different UV curing time

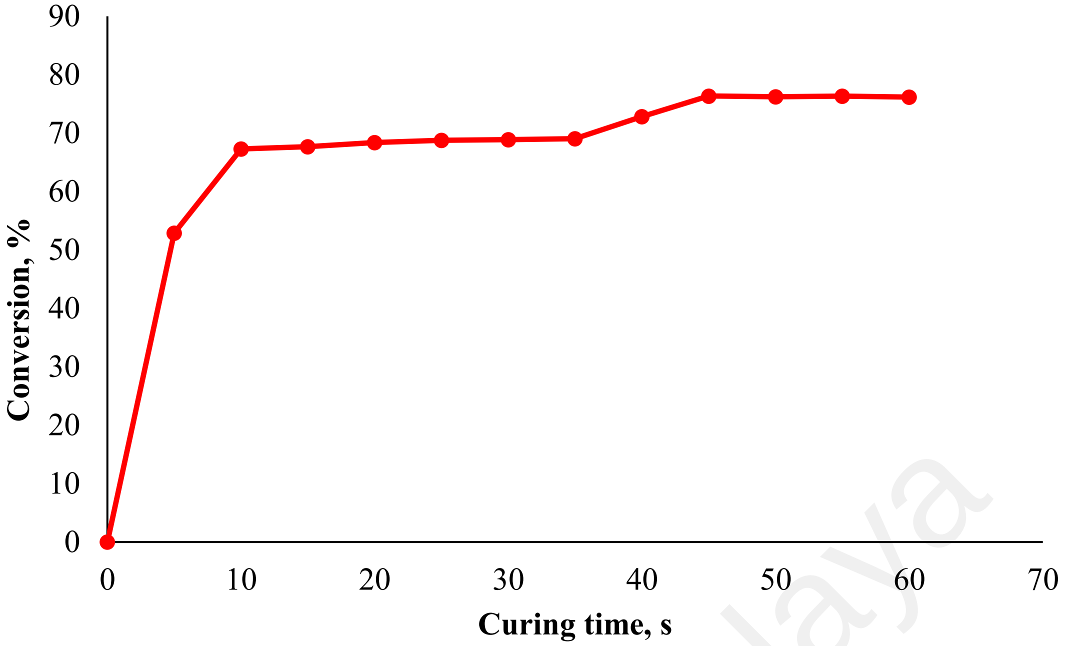

Figure 4.9 Conversion of peak area 810 cm^{-1} versus UV curing time for PFAD-UA

When the PFAD-UA clear coat was exposed to UV irradiation, the photoinitiator generated free radicals to start the cross-linking reaction of the double bonds in PFAD-UA. FTIR spectrum showed that the peak at 810 cm^{-1} decreased as the double bond was consumed during the reaction. Figure 4.9 shows a fast-initial conversion of 53% after 5 s. The conversion reached 70% after 10 s and subsequently slowed down due to viscosity increase, which reduce the mobility of the remaining reactive groups. Finally, the conversion achieved 76% after 45 s and remain constant until 60 s.

4.1.4 T_g Development of the PFAD-UA UV Cured Film

The change in T_g of the PFAD-UA's clear coat at various UV curing time was measured by using DSC method. Figure 4.10 shows the trend of the T_g at different curing time.

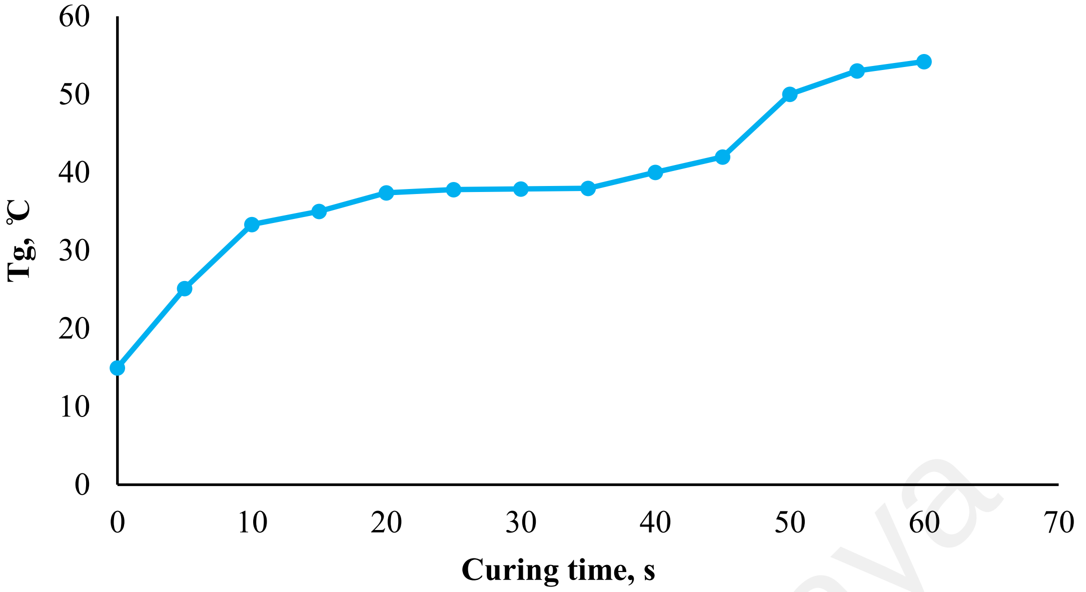

Figure 4.10 T_g development of PFAD-UA UV cured film at various curing time

T_g has shown an increasing trend with UV exposure time as shown in Figure 4.10. This observation has supported occurrence of crosslinking reaction, which have resulted in changes in mechanical and chemical properties of PFAD-UA resin. The initial tacky PFAD-UA resin was transformed into hard and non-tacky film after the UV irradiation. The radical cross-linking reaction has produced a highly crosslinked film with higher T_g.

The T_g has increased rapidly from 15.0˚C to 33.0˚C after 10 s of UV exposure. Subsequently, the T_g has increased slowly to 40℃ after 40 s. Longer exposure has increased the film T_g to 54˚C after 60 s, presumably the heat built up during prolonged exposure could have assisted the reaction to proceed. Figure 4.11 shows the initial and final thermograms of T_g measurement on the PFAD-UA resin.

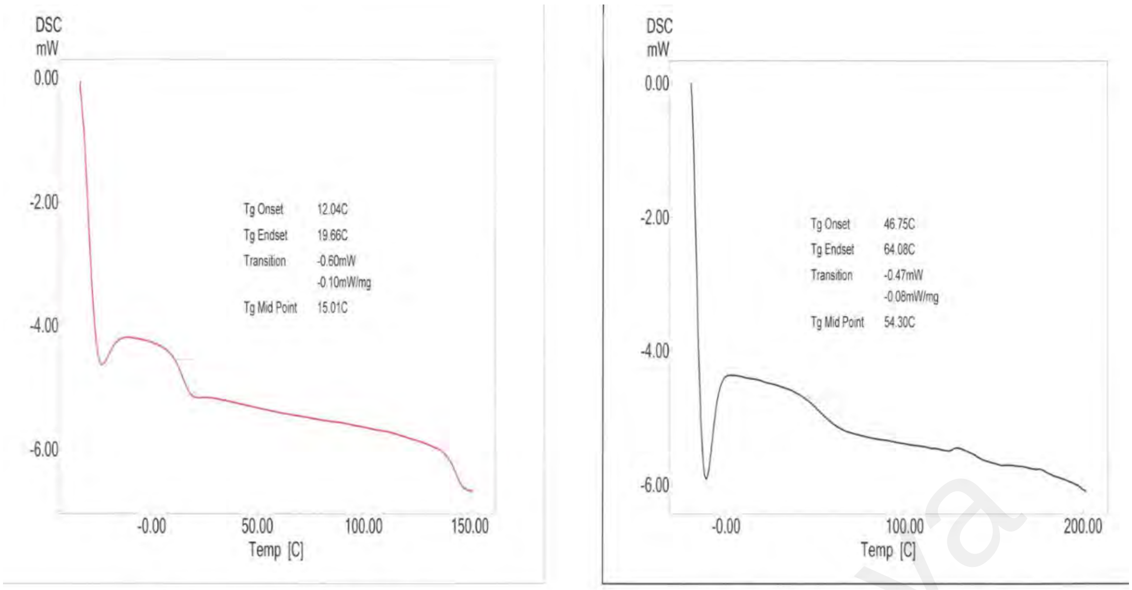

PFAD-UA before UV curing

PFAD-UA after 60s of UV curing

Figure 4.11 Thermogram of PFAD-UA initial and final T_g after 60 s of UV curing

4.1.5 Pendulum Hardness Development of the PFAD-UA UV Cured Film

The hardness of the UV cured film was measured by Sheen König pendulum hardness tester. Figure 4.12 shown the hardness during the UV curing process.

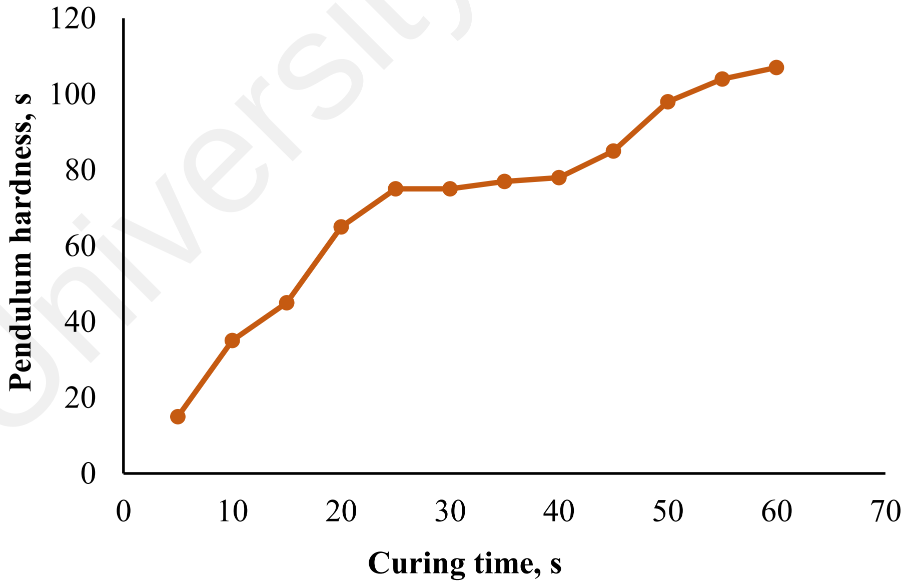

Figure 4.12 Pendulum hardness of the PFAD urethane acrylate UV cured film.

Film hardness has increased due to higher cross-linking density. The cross-linking reactions were expected to occur at faster rate at the initial stage due to the better mobility and higher concentration of available double bonds. This is in agreement with the observed film hardness increasing at higher initial rate from 15 to 75 s within the first 25 s. Subsequently the film hardness has not changed during 30 to 40 s. Prolonged exposure has caused heat built up and the film shows another increase to 107 s after 60 s of UV exposure.

4.2 Synthesis of PFAD Urethane Acrylate with Various PFAD Content

The PFAD content used in the M-PFAD formulation has followed the alkyd oil content's range of short oil (oil/fatty acid content below 40%), medium oil (oil/fatty acid content 40-60%) and long oil (above 60% oil/fatty acid). The M-PFAD were designated as M1, M2, M3, M4 and M5 and formulated with PFAD content at 15.1, 26.7, 44.7, 54.7 and 68.7% respectively. The compositions are shown in Table 3.10.

4.2.1 Synthesis of M1 to M5

4.2.1.1 Acid Value and Molecular Weight Analysis for M1 to M5

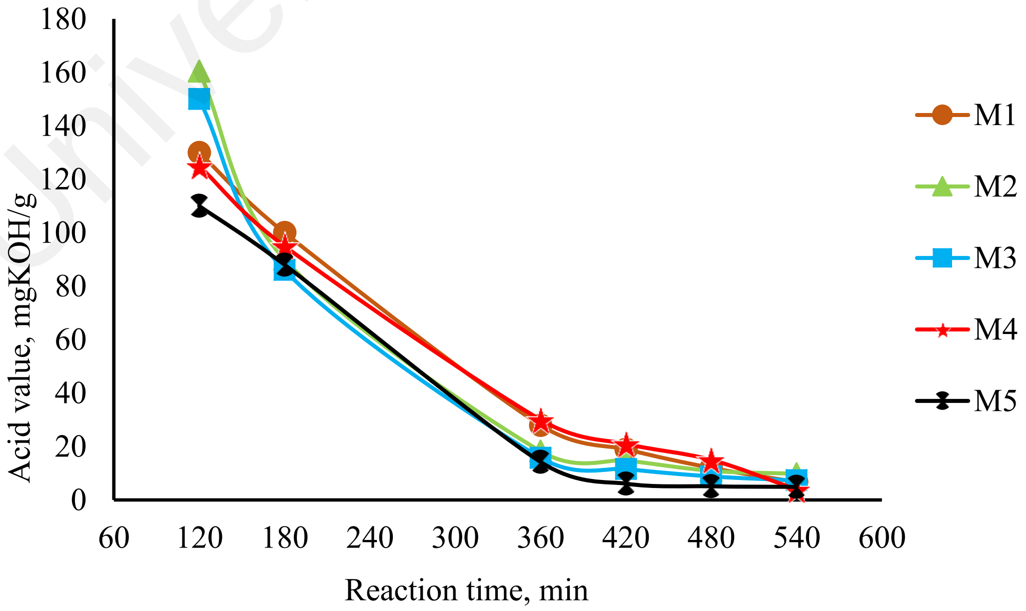

Figure 4.13 Acid value as function of reaction time

Figure 4.13 shows the change in acid values, with reaction time, during the synthesis of the macromers. With reference to Table 3.10, the PFAD content in an increasing order is M1 < M2 < M3 < M4 < M5, and all the macromers showed a similar reaction trend, being fast at the initial stage from 120–360 min, and reached a constant AV, after 420 min. Between 180–360 min, the acid value of all macromers decreased at comparable rates, all of them reached a minimum <10 mgKOH/g.

The M_w of each macromer is shown in Table 4.5. Figure 4.14a, b and c show the chromatogram of M1 to M5. Molecular weight of the alkyd resin is known to be affected by its oil-length (Patton T.C., 1962). In this case, from M1 to M3, with PFAD content increases from 15% to 45%, the M_w showed an increasing trend, from 2300 to 7900 dalton. However, for the M4 and the M5, at PFAD content of 55% and 70%, respectively, the M_w had dropped to around 2600 dalton. In this series of study, the macromer had attained the highest M_w, with M3 containing 45% PFAD, at 7900 dalton.

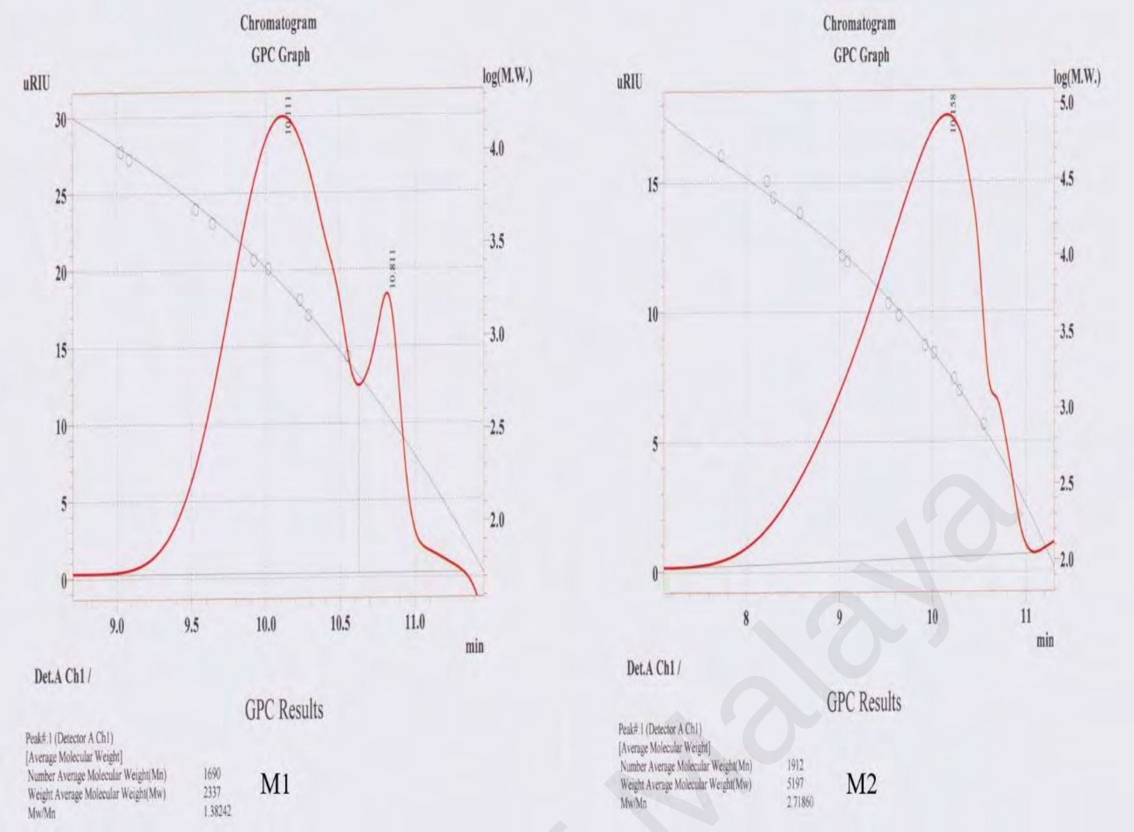

GPC Results

Peak#:1 (Detector A Ch1)
[Average Molecular Weight]
Number Average Molecular Weight(Mn) 1690
Weight Average Molecular Weight(Mw) 2337
Mw/Mn 1.38242

GPC Results

Peak#:1 (Detector A Ch1)
[Average Molecular Weight]
Number Average Molecular Weight(Mn) 1912
Weight Average Molecular Weight(Mw) 5197
Mw/Mn 2.71860

Figure 4.14a GPC Chromatogram of M1 and M2

GPC Results

Peak#:1 (Detector A Ch1)
[Average Molecular Weight]
Number Average Molecular Weight(Mn) 3474
Weight Average Molecular Weight(Mw) 7939
Mw/Mn 2.28499

GPC Results

Peak#:1 (Detector A Ch1)
[Average Molecular Weight]
Number Average Molecular Weight(Mn) 1650
Weight Average Molecular Weight(Mw) 2883
Mw/Mn 1.74707

Figure 4.14b GPC Chromatogram of M3 and M4

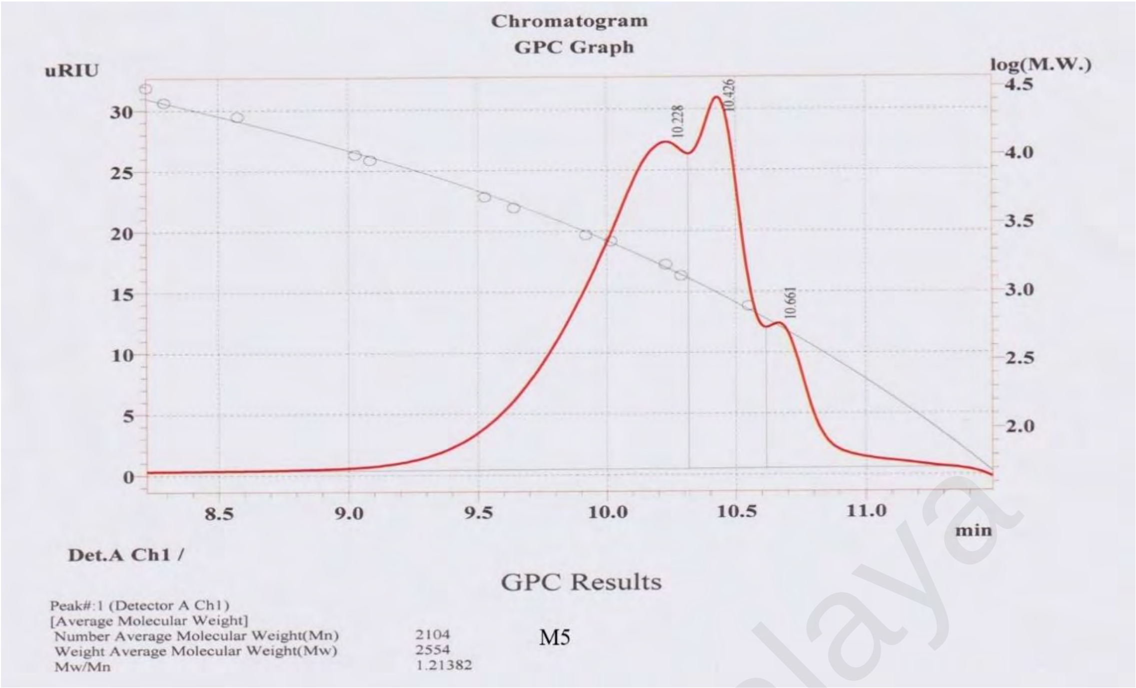

```
Peak#:1 (Detector A Ch1)
[Average Molecular Weight]
 Number Average Molecular Weight(Mn)          2104
 Weight Average Molecular Weight(Mw)          2554
 Mw/Mn                                        1.21382
```

Figure 4.14c GPC Chromatogram of M5

Table 4.5 Molecular weight (M_W) of the five macromers

Formulation	Molecular Weight (dalton)	Polydispersity, PDI
M1	2300	1.38
M2	5200	2.72
M3	7900	2.28
M4	2900	1.75
M5	2600	1.21

Alkyd of short oil-length has a fatty acid content of 20–40%, and the polymerization was mainly controlled by the polyhydric alcohol and the polybasic acid used. According to Patton alkyd formulation (Patton T.C., 1962), the optimum properties of alkyd is achieved when higher order of functionality reactants content was within the range of 45-55%, which will be predominated in the alkyd polymerization reaction. However, when the fatty acid content exceeded 55% as in the range of long oil alkyd, the termination reaction by the mono-functional fatty acid, has become predominant during the esterification process, and could resulted in lower molecular weight resin synthesized.

4.2.1.2 FTIR Analysis of M1 to M5

The FTIR spectra of M1 to M5 are shown in Figure 4.15 and 4.16. The feed compositions of the M-PFAD macromers were provided in Table 3.10.

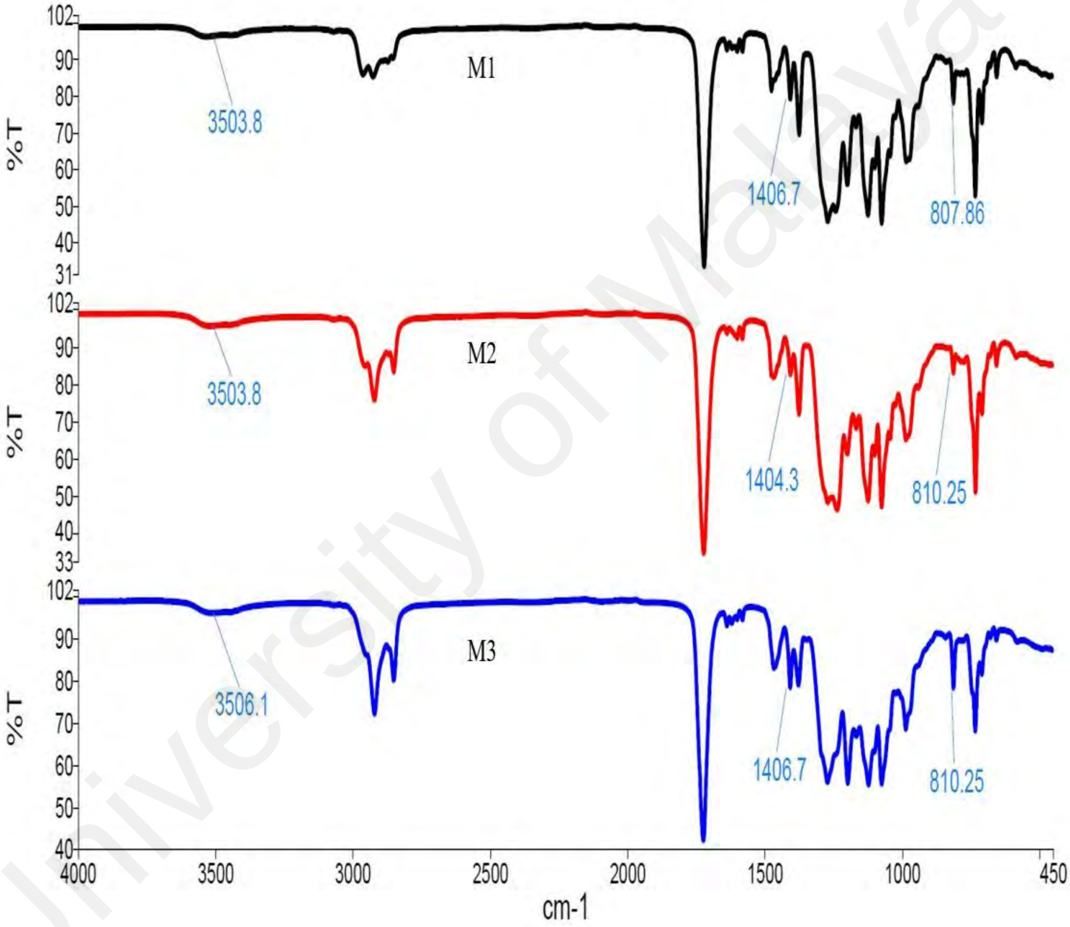

Figure 4.15 FTIR spectra for M1, M2 and M3

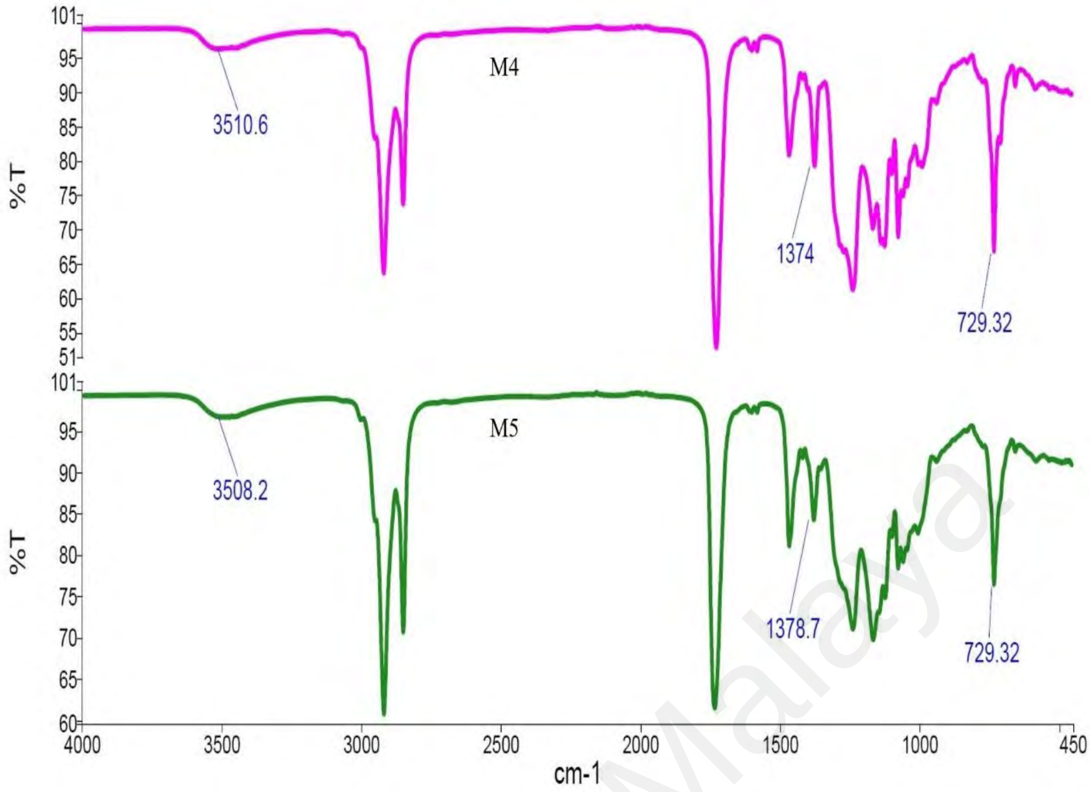

Figure 4.16 FTIR spectra of M4 and M5

It could be seen that the peaks of M1 to M5 show similar peaks due to the resemblance of the functional groups of the macromer. In Figure 4.15 and 4.16 the hydroxyl groups (-OH) of the polyols are seen as weak stretching at 3504 cm^{-1}. The weak peaks at 2853–2922 cm^{-1} were associated with the symmetric and asymmetric stretchings of the C–H. The weak $–CH_2$ bending was observed at 1409 cm^{-1} and the $–CH_3$ bending at 1375 cm^{-1} can be observed for all macromer's spectrum. Other peaks included the strong stretching of –C=O, at 1723 cm^{-1}, and the C–O–C stretching at 1120–1230 cm^{-1}. In Figure 4.14, the M1, M2, and M3, the $–CH_2$=CH–R of scissoring bending at 1409 and 809 cm^{-1} out of plane deformation of acrylate double bond, were contributed by the TPGDA diluents. The dilution of these three macromers were necessary as the macromers have high viscosity and could not be used for the subsequent grafting process. Figure 4.16 shows the spectra of M4 and M5, which were not diluted with TPGDA, hence the acrylate peak was not observed.

4.2.2 Synthesis of UA1 to UA5

The feed composition of UA1 to UA5 were provided in Table 3.11. Each macromer was copolymerized with TDI and 2-HEA to produce the PFAD-UA resin. The plausible structure of PFAD-UA is shown in Scheme 4.3.

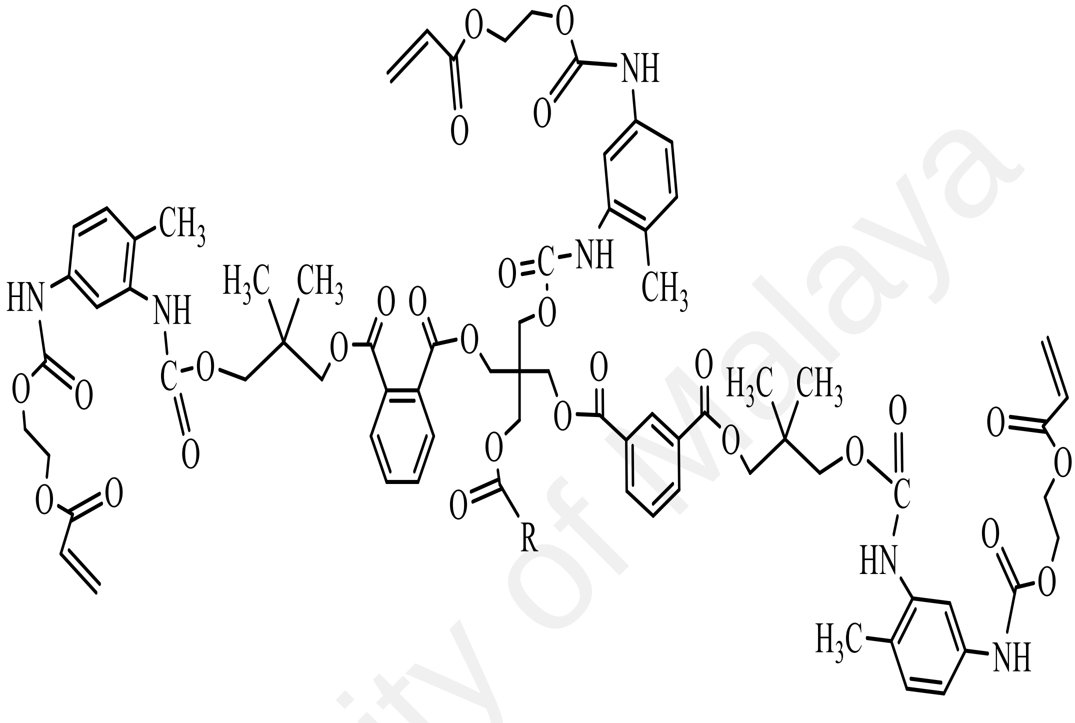

Scheme 4.3 The plausible structure of PFAD-UA

4.2.2.1 NCO Content Analysis for UA1 to UA5

Figure 4.17 show the reduction of NCO content during grafting process as resulted from the reaction of isocyanate with hydroxyl functionality of 2-HEA and PFAD macromers.

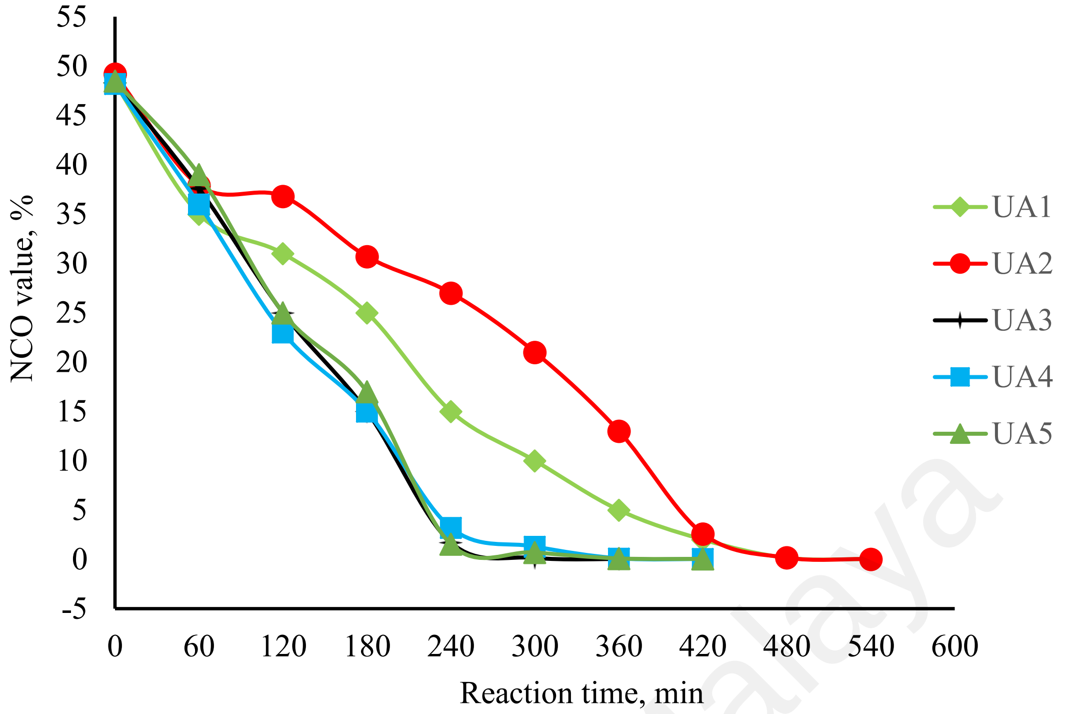

Figure 4.17 The NCO values during the synthesis of UA1 to UA5

The initial 49.2% of NCO had decreased, gradually, and reached 0.05% at the end of the reaction. At time intervals of 120 min, UA1 and UA2 showed a slower rate of formation, as compared to the UA3, UA4, and UA5, presumably due to the effect of viscosity. The high viscosities of M1 and M2 had reduced the mobility of reactive groups, and resulted in a slower reaction rate, to form UA1 and UA2, respectively. The low viscosities of M3, M4, and M5 provided a higher mobility medium for the TDI adduct to react, as clearly reflected in the faster decrease of the NCO value, particularly at time of 60–240 min.

4.2.2.2 FTIR Analysis of UA1 to UA5

The undiluted M4 was used to compare with UA4. Figure 4.18 show the comparison FTIR spectrum between M4 and UA4.

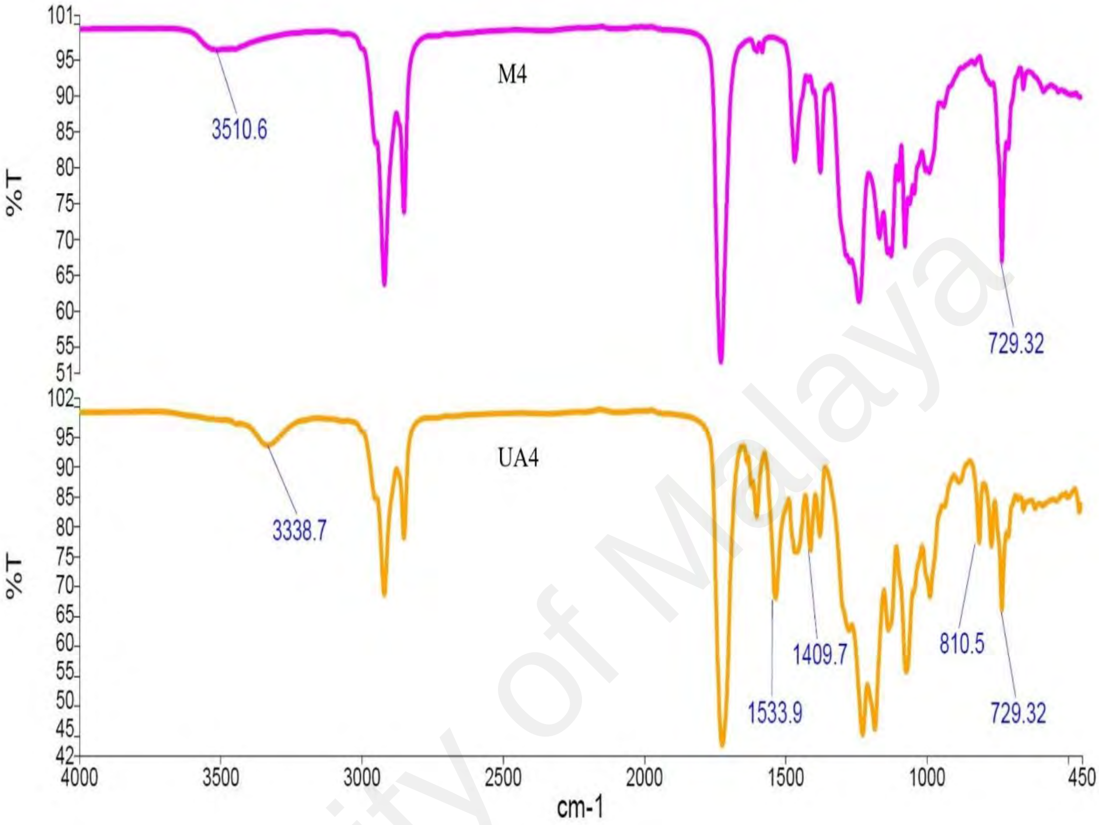

Figure 4.18 Comparison of FTIR spectra between M4 and UA4

The reaction between the hydroxyl group with isocyanate can be identified from the change of OH peaks at 3504 cm^{-1} to NH at 3332 cm^{-1} during urethane formation. The NH deformation at 1534 cm^{-1} was observed. The peak centred at 809 cm^{-1} in UA4 was associated with acrylate double bond bending, this was not observed for M4.

Each spectrum has the NH stretching at 3333 cm^{-1} and NH deformation at 1534 cm^{-1} from the formation of urethane linkage after the isocyanate grafting reaction. Identification of peaks at 809 cm^{-1} on all UA has confirmed the successful of introducing the acrylate double bond onto the UA backbone.

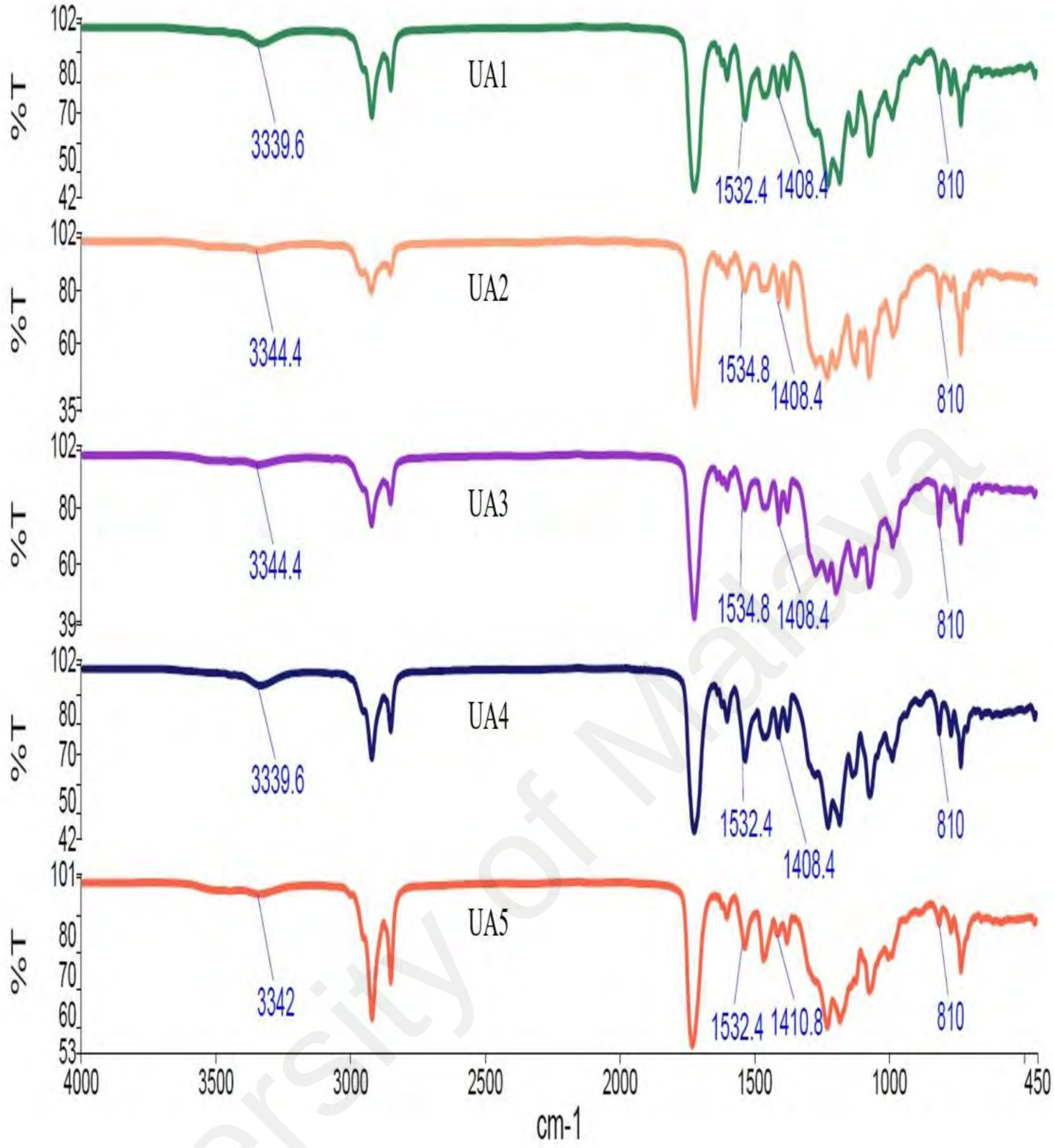

Figure 4.19 FTIR spectra of UA1, UA2, UA3, UA4 and UA5

The GPC chromatogram shown in Figure 4.20 has confirmed that the M_w of the UA was higher than its macromer. The increase was due to the further reactions of the macromer with a TDI and a 2-HEA adduct. The final properties of UA1 to UA5 are summarized in Table 4.6

GPC Results

Peak#:1 (Detector A Ch1)
[Average Molecular Weight]
Number Average Molecular Weight(Mn) 2541
Weight Average Molecular Weight(Mw) 4141
Mw/Mn 1.62989

UA1

Peak#:3 (Detector A Ch1)
[Average Molecular Weight]
Number Average Molecular Weight(Mn) 2685
Weight Average Molecular Weight(Mw) 7490
Mw/Mn 2.78982

UA2

Figure 4.20a GPC chromatogram of UA1 and UA2

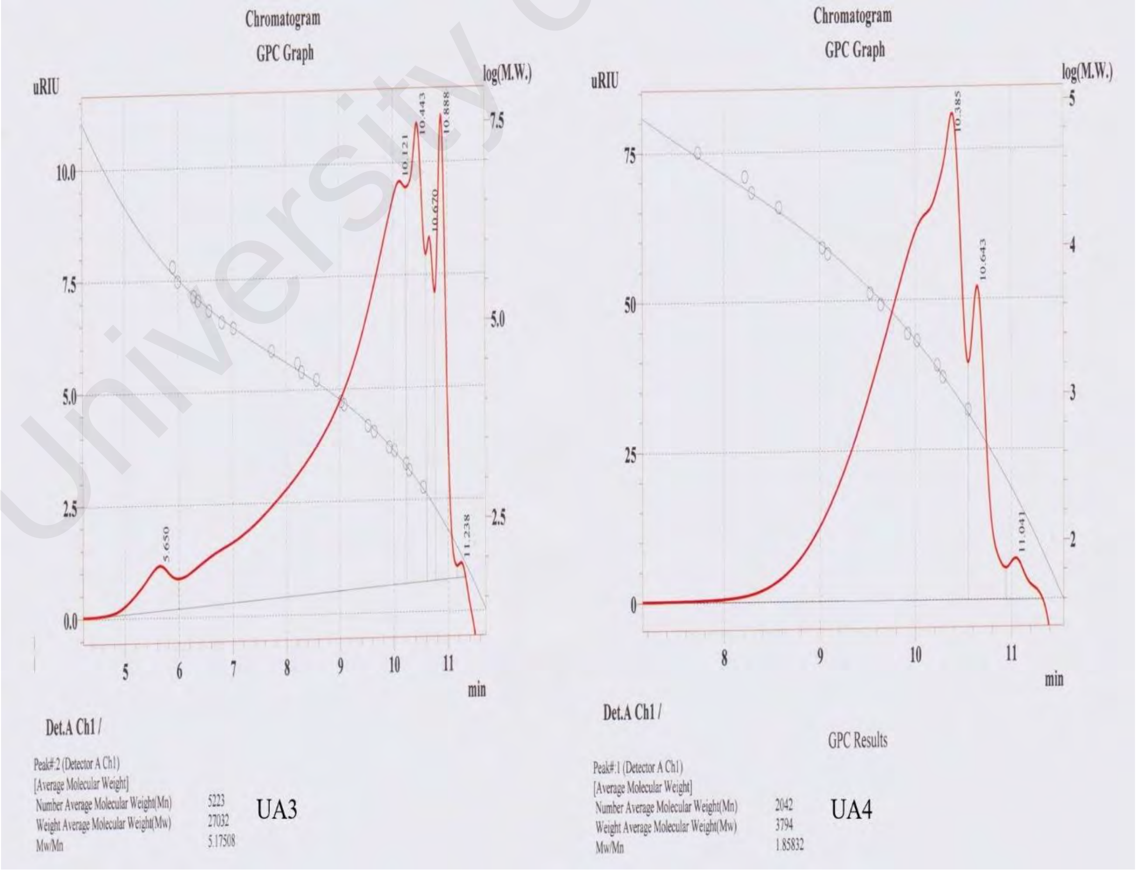

Peak#:2 (Detector A Ch1)
[Average Molecular Weight]
Number Average Molecular Weight(Mn) 5223
Weight Average Molecular Weight(Mw) 27032
Mw/Mn 5.17508

UA3

GPC Results

Peak#:1 (Detector A Ch1)
[Average Molecular Weight]
Number Average Molecular Weight(Mn) 2042
Weight Average Molecular Weight(Mw) 3794
Mw/Mn 1.85832

UA4

Figure 4.20b GPC chromatogram of UA3 and UA4

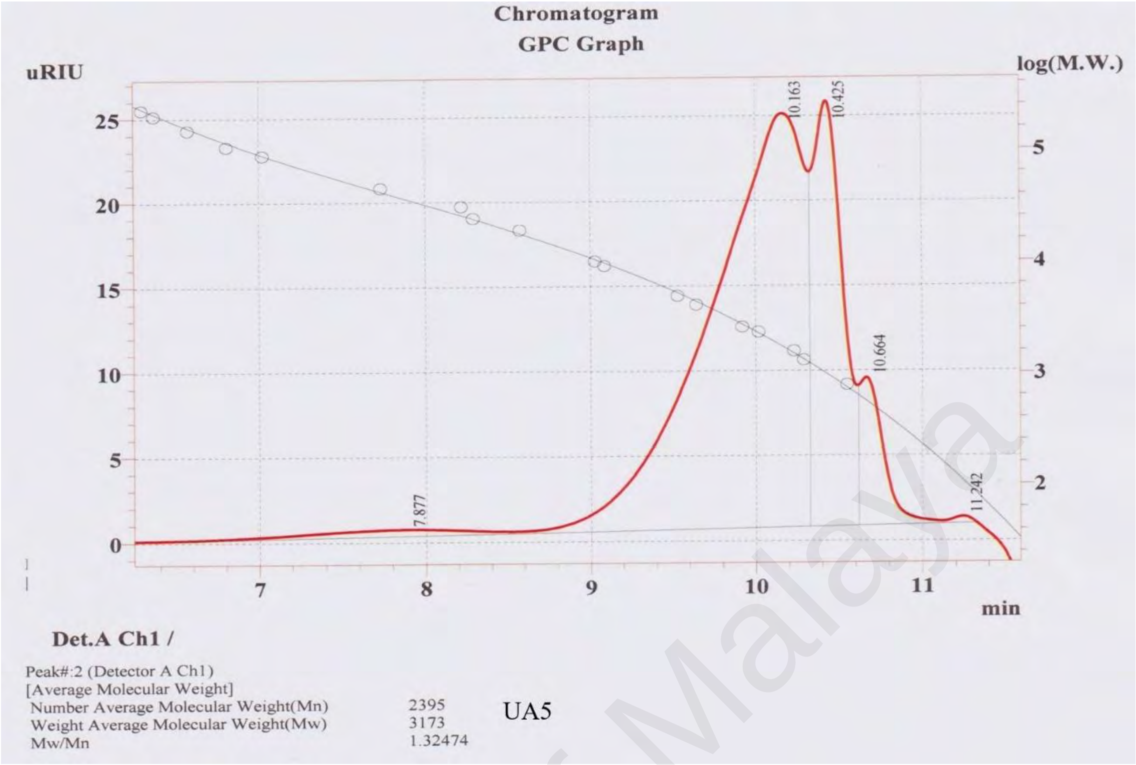

```
Peak#:2 (Detector A Ch1)
[Average Molecular Weight]
 Number Average Molecular Weight(Mn)          2395
 Weight Average Molecular Weight(Mw)          3173
 Mw/Mn                                        1.32474
```

Figure 4.20c GPC chromatogram of UA5

Table 4.6 Final properties of UA1 to UA5

Description	UA1	UA2	UA3	UA4	UA5
Oligomer content/%	70.0	70.0	70.0	70.0	70.0
Reactive diluent/%	30.0	30.0	30.0	30.0	30.0
Viscosity @25°C/poise	pasty	pasty	pasty	850	165
Acid value/mgKOHg^{-1}	6.7	9.8	7.3	3.9	4.9
TDI value/%	0.02	0.03	0.04	0.04	0.05
Molecular weight (M_w)/dalton	4100	7500	27000	3800	3200
Polydispersity/PDI	1.63	2.79	5.18	1.86	1.32

4.2.3 T_g Analysis of the UA1 to UA5's UV Cured Films

Figure 4.21 shows the DSC thermograms of UA 1 to UA5 at initial stages and after UV curing. Figure 4.22 shows the change in the T_g of the cured film, at different curing times. Generally, all formulations show rapid photopolymerization at 5 to 20 s UV exposure. Subsequently, curing has slowed down as the acrylate double bond was used up. The curing reaction was accompanied by an increase in viscosity, which would reduce the mobility of the reactants with the effect of reducing the rate of reaction. As shown in Figure 4.22, the PFAD content in the UA has a great influence on the T_g of the cured-film. Generally, the T_g was reduced with a higher PFAD content. The UA5 film showed the lowest T_g (29 °C), after 60 s of UV irradiation. The UA3 film had a higher T_g value, among the UA2 to UA5. In case of the UA1, its highly reactive polyester backbone had a predominant contribution to the T_g, thus, the UA1 had attained the highest T_g (63 °C), as compared to the other four.

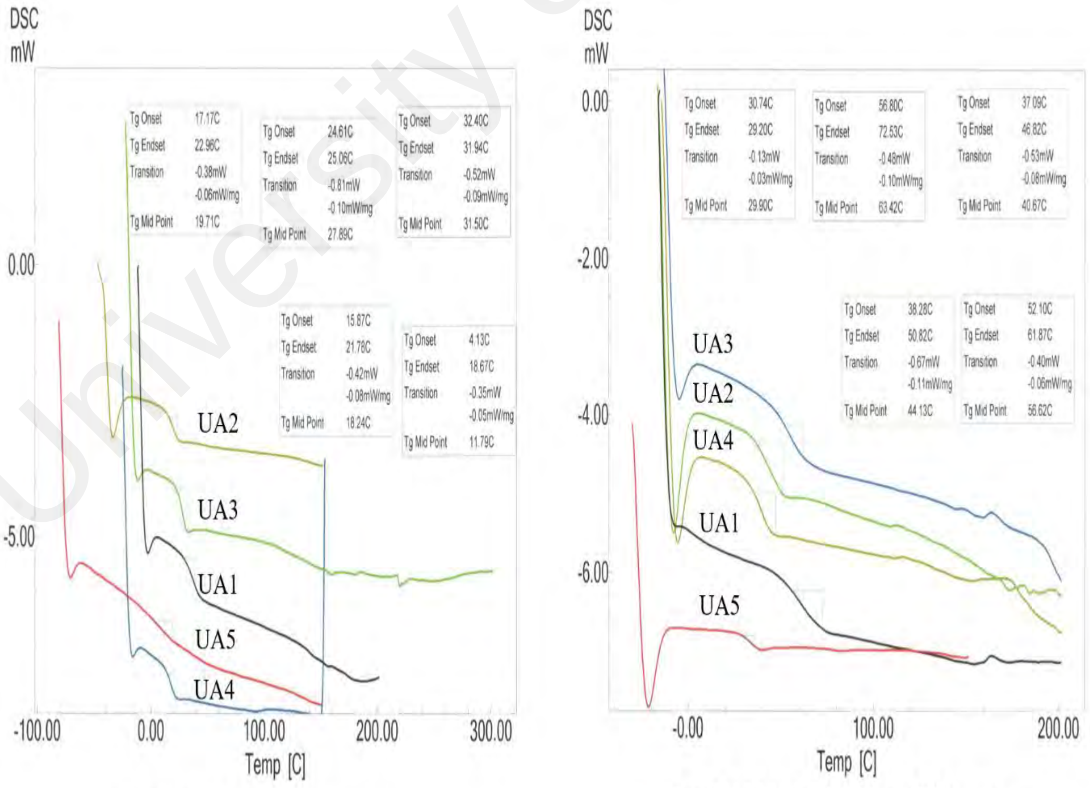

Tg of UA1 to 5 before UV curing

Tg of UA1 to 5 After 60 s of UV curing

Figure 4.21 T_g of UA1 to UA5 before and after 60 s of UV curing

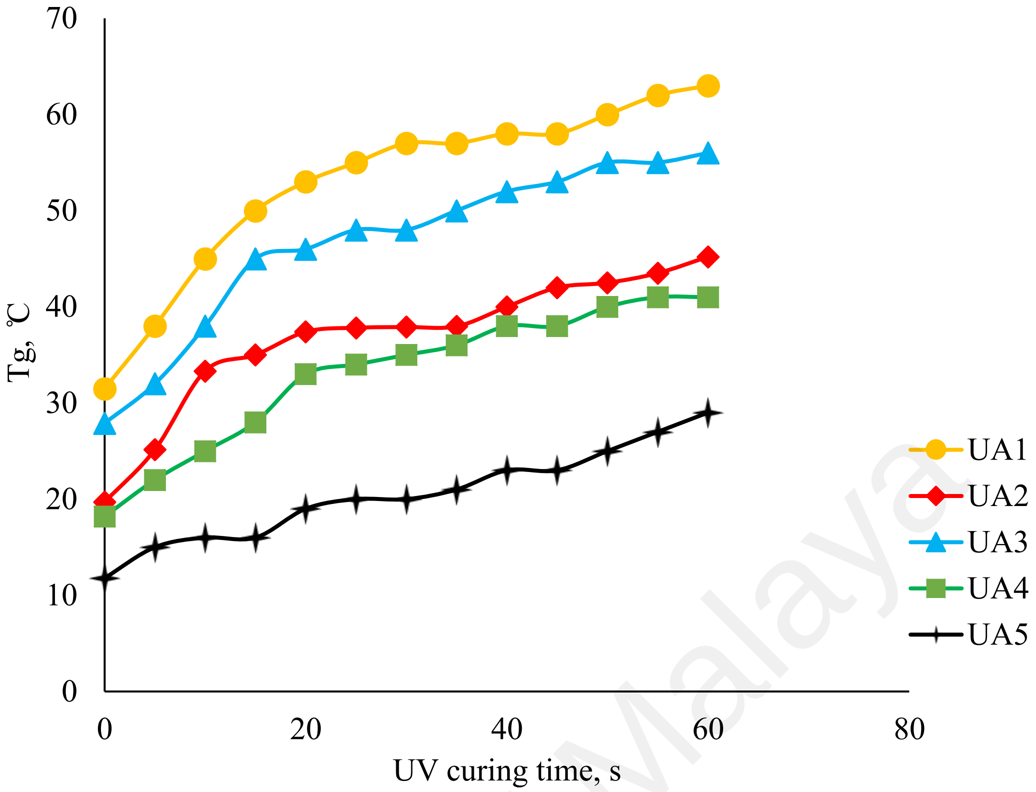

Figure 4.22 T_g of the UA UV Cured film at different UV curing times

4.2.4 Pendulum Hardness Analysis of the UA1 to UA5 UV Cured Film

The film at different stages of UV curing was subjected to the pendulum hardness test by using the Sheen Konig pendulum tester, according to the ASTM 4366. The results are shown in Figure 4.23.

Only four resins (UA1 to UA4) had films with a measurable hardness during the UV-curing from 5–60 s. The film of UA5 was very soft, as reflected by its low-film T_g (<30 °C). In general, the hardness, as well as the T_g of the cured film, had increased during the photo-induced crosslinking process. Similar to the T_g property, the hardness of the film was influenced by the PFAD content. Thus, UA1 with the lowest PFAD content and more reactive polyester backbone had showed a good hardness development, as compared to the others three and achieved the final pendulum hardness of 118 s. As PFAD content increased, the UA3 showed optimum cured film properties and achieved the final film hardness of 111 s. On the other hand, UA2 and UA4 showed quite similar hardness, after 5 s of UV curing time, but subsequently the hardness development of UA2 increased faster than the UA4, from 10 to 30 s. At 30 s, UA2 and UA4 had achieved pendulum hardness of 77 s and 49 s, respectively, and the final pendulum hardness 88 s and 55 s, respectively. Presumably the difference was due to the M_w, where UA2 had a higher M_w of 7500 dalton, as compared to UA4, at M_w of 3800 dalton.

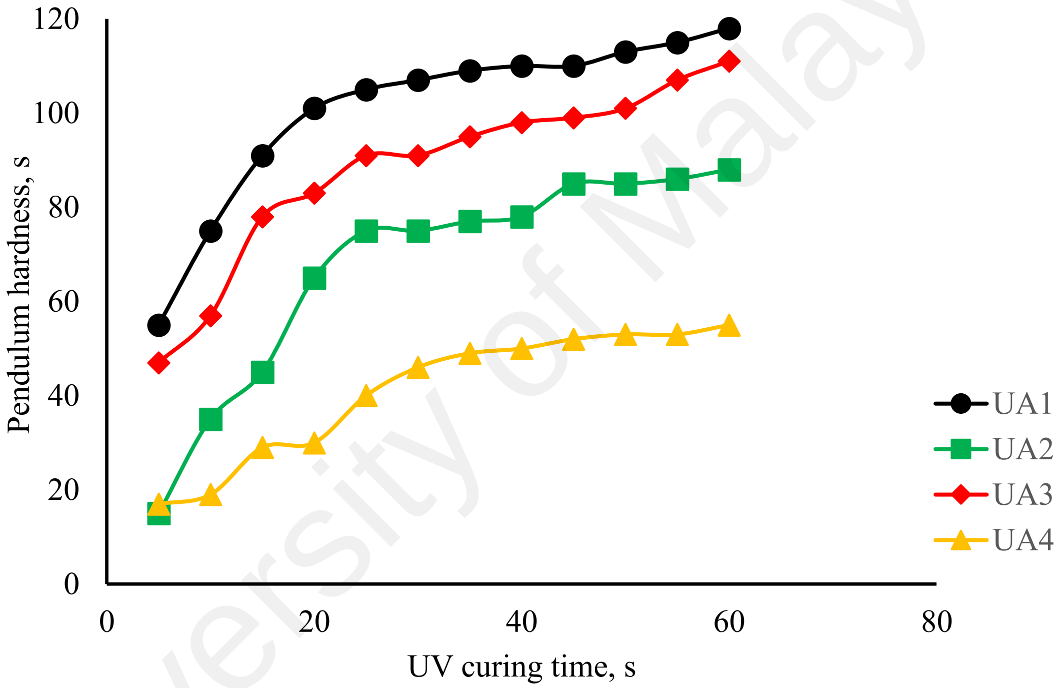

Figure 4.23 Pendulum hardness of the UA UV cured film at various UV curing times

4.2.5 Performance of UA1 to UA5 in Wood Coating Application

The clear coats of the UA1 to UA5 UV were formulated using formulation as described in section 3.4.1. Rubber wood selected for the testing was based on the availability and common substrate used in the local industry. To produce a smooth UV cured topcoat, the wood panel was coated with UV cured filler and sealer coating using the formulation provided in Table 3.12 and 3.13.

4.2.5.1 Observation of the UV Cured Filler and Sealer Coating

As shown in Figure 4.24, the filler coating formulated with UA, demonstrated a good penetrating property and managed to fill the wood pores. As illustrated in Figure 4.25, the filler has showed good UV cured performance by providing an easy sanding property with only powdery sanding dust without any sticky uncured resin residue.

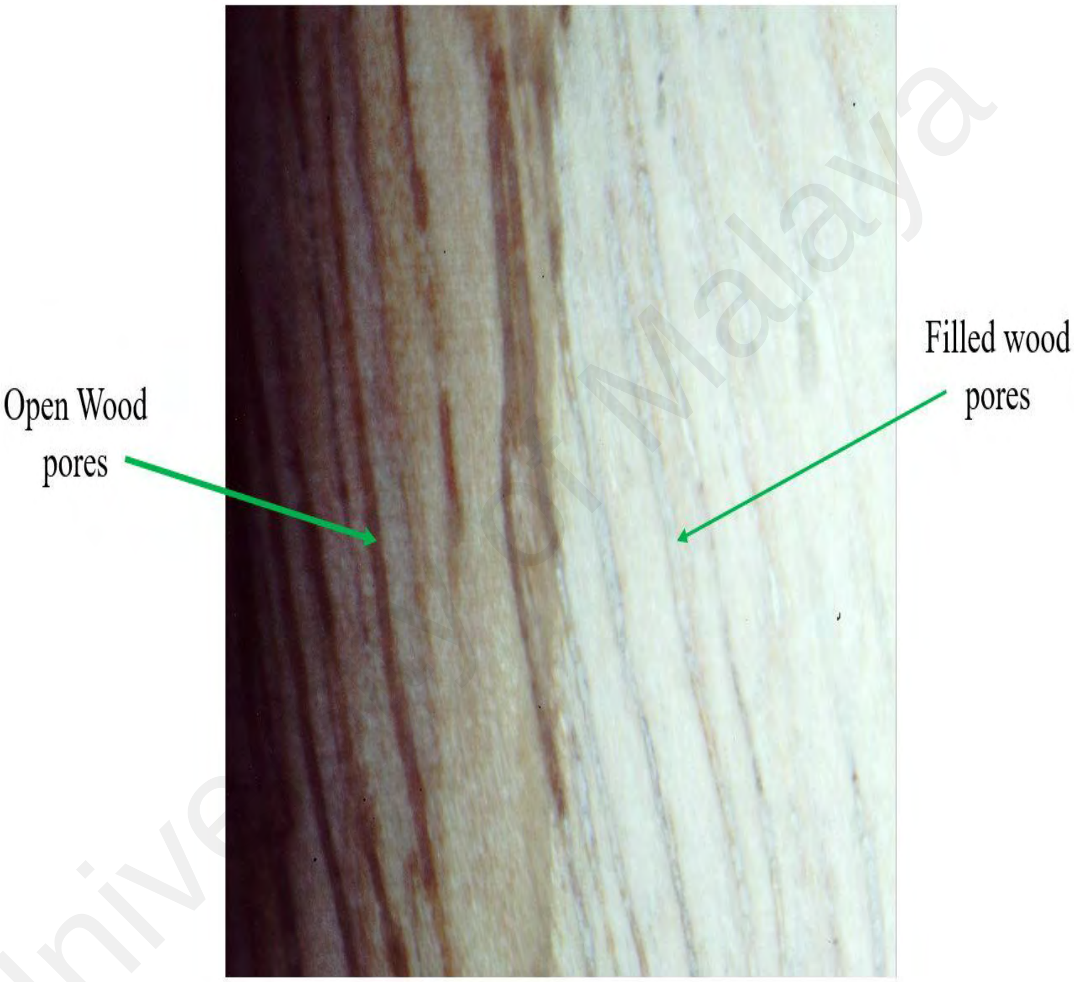

Figure 4.24 Comparison of the bare wood and filler coated wood panel

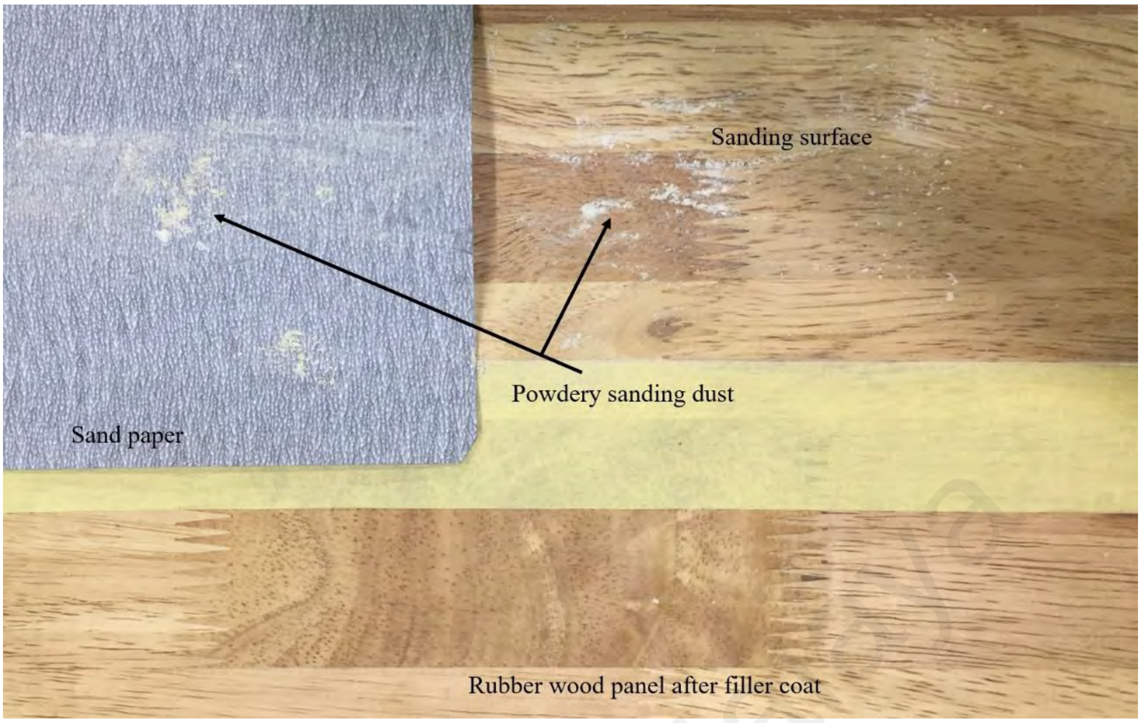

Figure 4.25 Illustration of sanding property of the PFAD-UA based UV cured filler

Figure 4.26 shows the wood panel coated with sealer coating after the filler coating treatment. The coated surface has shown a smooth surface. A good UV curing performance has been demonstrated by the sealer coat by giving good sanding property as shown in Figure 4.27. The good film properties of the sealer coating such as good substrate wetting, levelling and good UV cured properties were important factor to ensure the topcoat performance has minimum impact on its film performance particularly the film adhesion performance.

Figure 4.26 Comparison of bare wood surface with filler and sealer coated wood panel

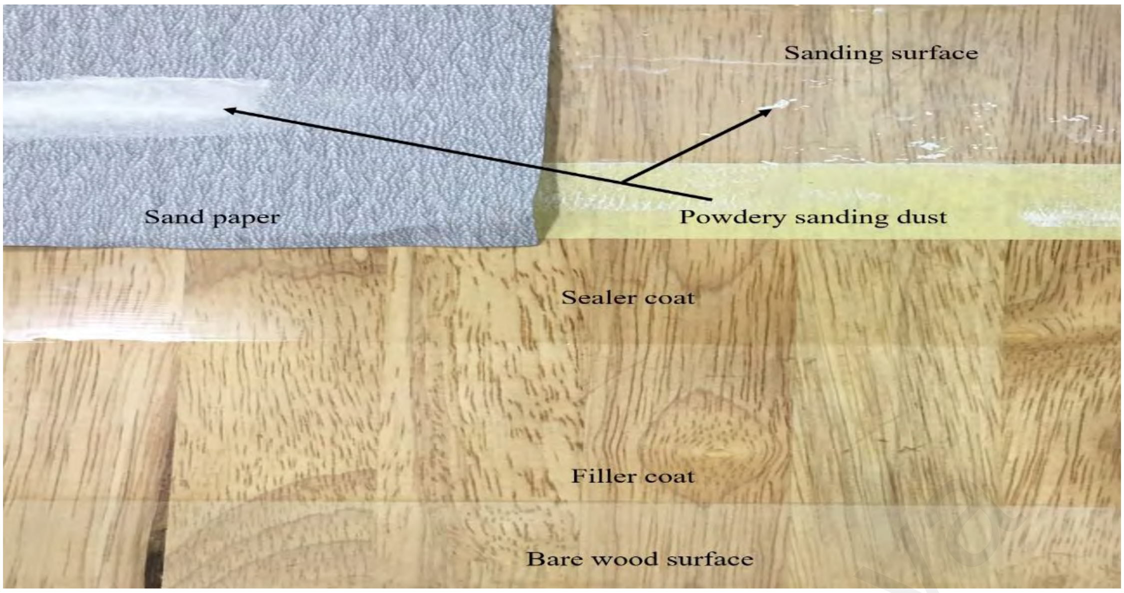

Figure 4.27 Illustration of sanding property of PFAD-UA based sealer

4.2.5.2 Chemical Resistance of Cured Films

For all UA1 to UA4 UV cured film physical properties including film appearance were measured recorded according to test method descripted in section 3.2.9 to 3.2.11. The film chemical resistance was tested with the reagents commonly applied by the Industrial Wood-Coating Standard include coffee, tea, dish washing solution, acetone, cooking oil, 1% (*w/w*) ethanol aqueous solution, vinegar (8% (*v/v)* acetic acid), 10% (*w/v*) ammonia solution, 5% (*w/v*) sodium hydroxide (NaOH) solution and 5% (*w/v*) hydrochloric (HCl) solution. The film properties UA1 to 4 after 24 hours of aging including appearance, adhesion and mechanical properties were reported. UA5 (70% PFAD) formed soft and tacky film and was excluded from the tests due to unable to performance any physical measurement and chemical test on the tacky film.

4.2.5.2.1 Initial UV Cured Performance

The cured film performances include appearance, 60^{o} gloss measurement, substrate adhesion and pencil hardness. The initial cured film properties and appearance are summarized in Table 4.7 for discussion.

Table 4.7 The initial UV cured film properties

Properties	**UA1**	**UA2**	**UA3**	**UA4**	**UA5**
Film appearance	Glossy	Glossy	Glossy	Glossy	Tacky
60° Gloss unit (GU)	97.1	93.4	92.9	93.3	NA
Crosshatch adhesion	5B	5B	5B	5B	NA
Pencil hardness	H	F	H	HB	NA

Results from Table 4.7 shows that all cured films had good physical properties except the UA5 that remained tacky. UA1 to UA4 showed a glossy appearance with 93–97 GU. All cured films had excellent adhesion onto wood panel. In the pencil hardness scale, UA1 and UA3 showed a hardness of H, followed by UA2 of F and UA4 of HB.

.

4.2.5.2.2 Chemical Resistance of UA1 to UA5's UV Cured Film After Chemical Aging

The appearance of UV cured films after aging are reported in Table 4.8 and the films' adhesions and pencil hardness were reported in Table 4.9.

Table 4.8 Appearance of the UV cured films after 24 hours of chemical aging

Chemical Test	UA1	UA2	UA3	UA4
Coffee	UC	UC	UC	UC
Tea	UC	UC	UC	UC
Dish washing solution	UC	UC	UC	Fading and whitish mark
Acetone	UC	UC	UC	UC
Cooking oil	UC	UC	UC	UC
1% ethanol aqueous solution	UC	UC	UC	UC
Vinegar	UC	UC	UC	Slight fading
10% ammonia solution	UC	UC	UC	Slight fading
5% NaOH solution	Fading and whitish mark	Fading and whitish mark	Fading and whitish mark	Fading and whitish mark
5% HCL solution.	UC	UC	UC	Slight fading

UC = unchanged.

In Table 4.8, the cured films of UA1, UA2, and UA3 exhibited a good chemical resistance with an unchanged film appearance, after 24 h aging, with almost all the chemicals. Generally, the films showed a poor alkaline-resistance. Fading and whitish marks were observed on the cured film when testing was done with a 5% NaOH solution. UA4 (55% PFAD) and UA5 (70% PFAD) showed poorer film properties, as compared to UA1, UA2, and UA3. Fading and whitish marks were observed on the wood panels, for tests using the dish-washing solution and a 5% NaOH solution. The UA4-cured film showed slight fading in vinegar, 10% ammonia solution, and 5% HCL solution aging test.

The poor NaOH resistance of all UA cured film could be due to the fatty acid ester linkage in the UA backbone, which was undergo alkaline hydrolysis. The higher the content of PFAD in the UA backbone, the easier for alkaline hydrolysis to occur as reflected by UA4, where the film was also affected by disc washing solution and 10% ammonia solution. In addition, higher PFAD content has also weakened the film against acid hydrolysis and resulted in fading of the cured film appearance.

Table 4.9 shows the results of adhesion and pencil hardness tests performed on the all-cured film, after 24 h chemical aging test. For the films of UA1, UA2, and UA3, results for crosshatch adhesion and pencil hardness remained perfect, except for those after the 5% NaOH solution aging. In the case of the pencil hardness test, films of the UA1, UA2, and UA3 were not affected after the chemical aging, except for the 5% NaOH solution. Their hardness remains unchanged at the initial values of H, F, and H, for the UA1, UA2, and UA3, respectively. The UA4 film showed a significant reduction in performance, especially in the 5% NaOH and in the dish-washing solution. The cured film adhesion had reduced to grade 2B and 3B and a hardness of 3B and 2B were recorded, after aging with the 5% NaOH solution and the dish-washing solution, respectively. A slight reduction of film properties was observed in vinegar, 10% ammonia solution, and a 5% HCl solution, for the UA4. The crosshatch adhesion had dropped one grade lower than its initial value and the pencil hardness was recorded at B, for these three chemical aging tests.

Table 4.9 The adhesion and pencil hardness of UA1 to UA4 after 24 hours chemical aging

Chemical Test	UA1		UA2		UA3		UA4	
	Crosshatch Adhesion	Pencil Hardness	Crosshatch Adhesion	Pencil Hardness	Crosshatch Adhesion	Pencil Hardness	Crosshatch Adhesion	Pencil Hardness
Coffee	5B	H	5B	F	5B	H	5B	HB
Tea	5B	H	5B	F	5B	H	5B	HB
Dish wash solution	5B	H	5B	F	5B	H	3B	2B
Acetone	5B	H	5B	F	5B	H	5B	HB
Cooking oil	5B	H	5B	F	5B	H	5B	HB
1% ethanol solution	5B	H	5B	F	5B	H	5B	HB
Vinegar	5B	H	5B	F	5B	H	4B	B
10% ammonia solution	5B	H	5B	F	5B	H	4B	B
5% NaOH solution	3B	HB	3B	B	3B	HB	2B	3B
5% HCL solution	5B	H	5B	F	5B	H	4B	B

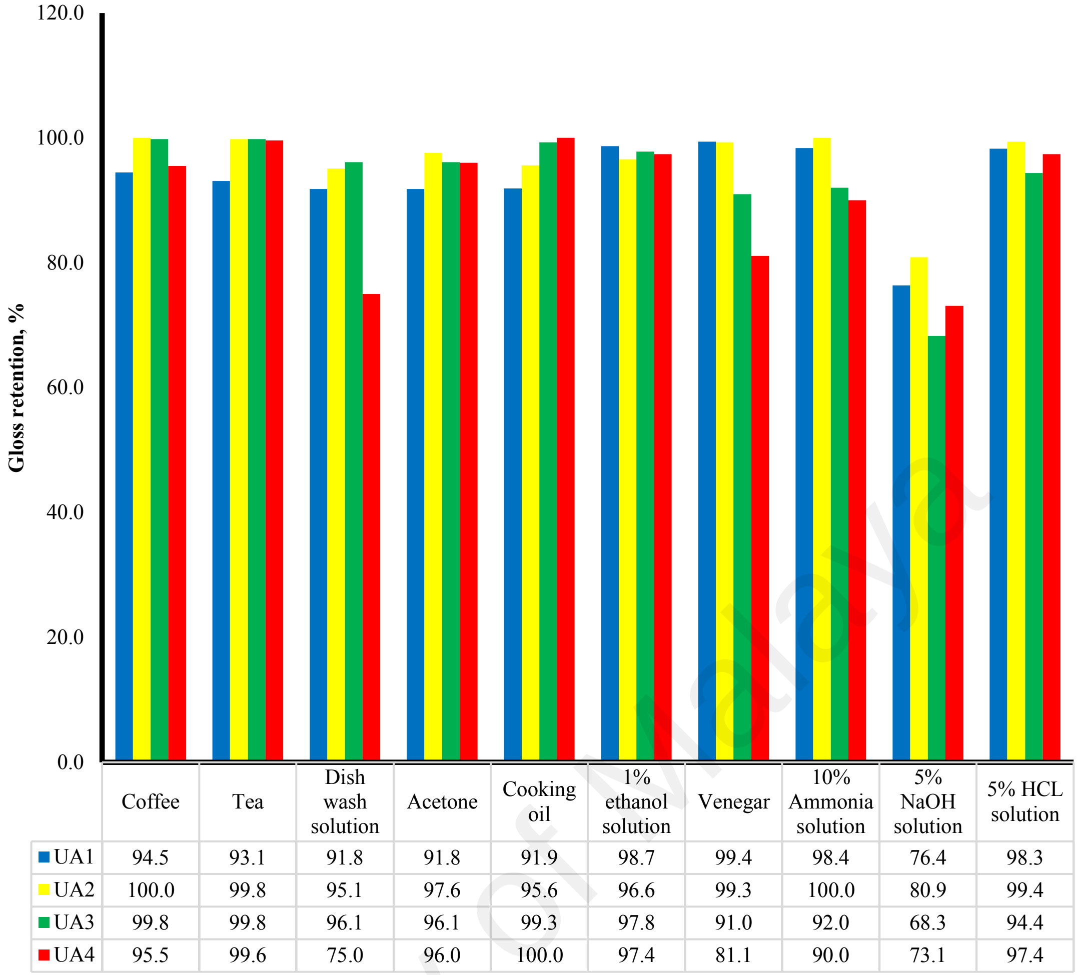

	Coffee	Tea	Dish wash solution	Acetone	Cooking oil	1% ethanol solution	Venegar	10% Ammonia solution	5% NaOH solution	5% HCL solution
🟦 UA1	94.5	93.1	91.8	91.8	91.9	98.7	99.4	98.4	76.4	98.3
🟨 UA2	100.0	99.8	95.1	97.6	95.6	96.6	99.3	100.0	80.9	99.4
🟩 UA3	99.8	99.8	96.1	96.1	99.3	97.8	91.0	92.0	68.3	94.4
🟥 UA4	95.5	99.6	75.0	96.0	100.0	97.4	81.1	90.0	73.1	97.4

Figure 4.28 Gloss retention of UA1 to UA4's UV cured film after 24 hours of chemical aging

Figure 4.28 shows the gloss retention of the films, after 24 h of chemical aging. In general, all cured films have shown very high gloss retention. The films that had performed badly in the 5% NaOH solution test, showed a lower gloss retention ranging from the 68–81%. Except in tea, acetone, cooking oil, and the 5% HCl solution aging test, the UA4 showed the lowest gloss retention in the dish-wash solution, vinegar, the 10% ammonia solution, and the 5% NaOH solution aging, as compared to the other three resins. As shown in Figure 4.28, UA2 showed the highest gloss retention with all chemical aging tests, followed by the UA1 and UA3. The high gloss retention achieved by the UA resins (>90%) is highly desirable for industrial wood-coating applications.

4.3 Synthesis of PFAD Urethane Acrylate with Various Dicarboxylic Acid

The PFAD-UA using different dicarboxylic acids were synthesized for further investigation on their differences in final resin performance. The dicarboxylic acids used in this study include aliphatic, aromatic and acid anhydride types: they are adipic acid, terephthalic acid, isophthalic acid and phthalic anhydride. All the dicarboxylic acids were introduced into the backbone at macromer synthesis and later to copolymerize with TDI and 2-HEA to produce the UV curable PFAD-UA resins from each dicarboxylic acid used.

4.3.1 Synthesis of M-AA, M-IPA, M-TPA and M-PA

The M-AA, M-IPA, M-TPA and M-PA was synthesized using formulation provided in Table 3.18. The plausible macromer structure as shown by the Scheme 4.4.

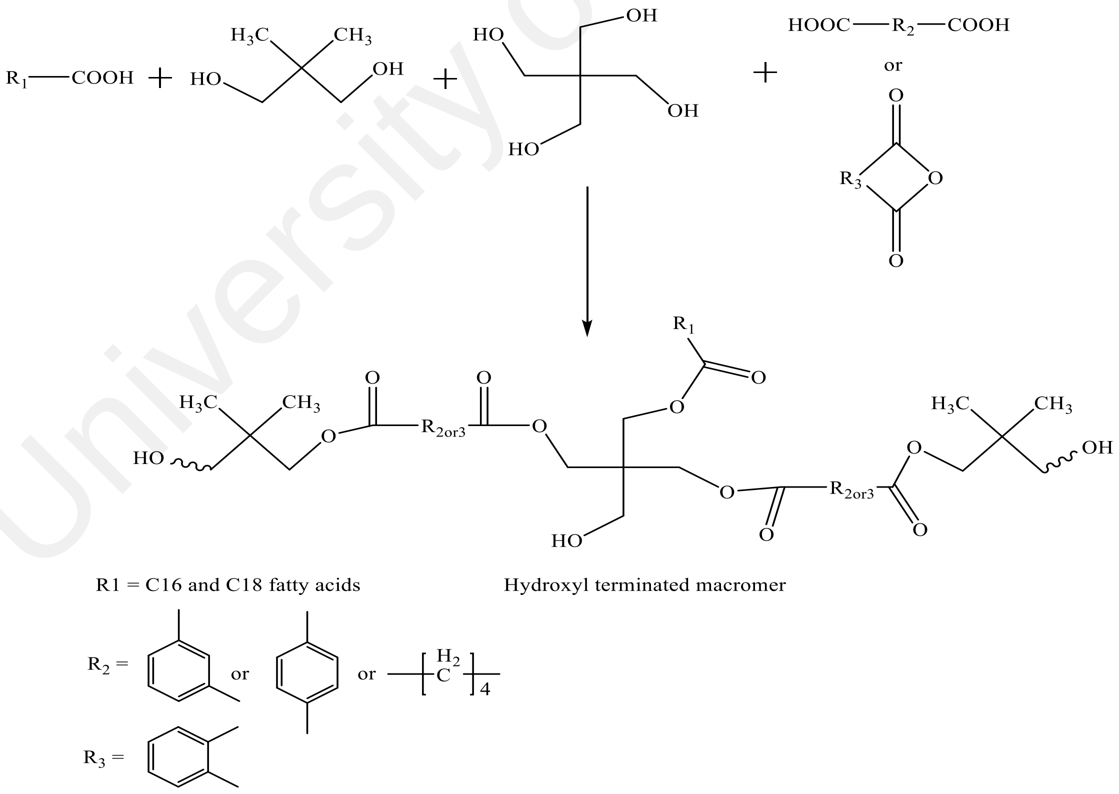

Scheme 4.4 The plausible structure of M-PFAD macromer using different dicarboxylic acids

4.3.1.1 Acid Value and Molecular Weight Analysis for M-AA, M-IPA, M-TPA and M-PA

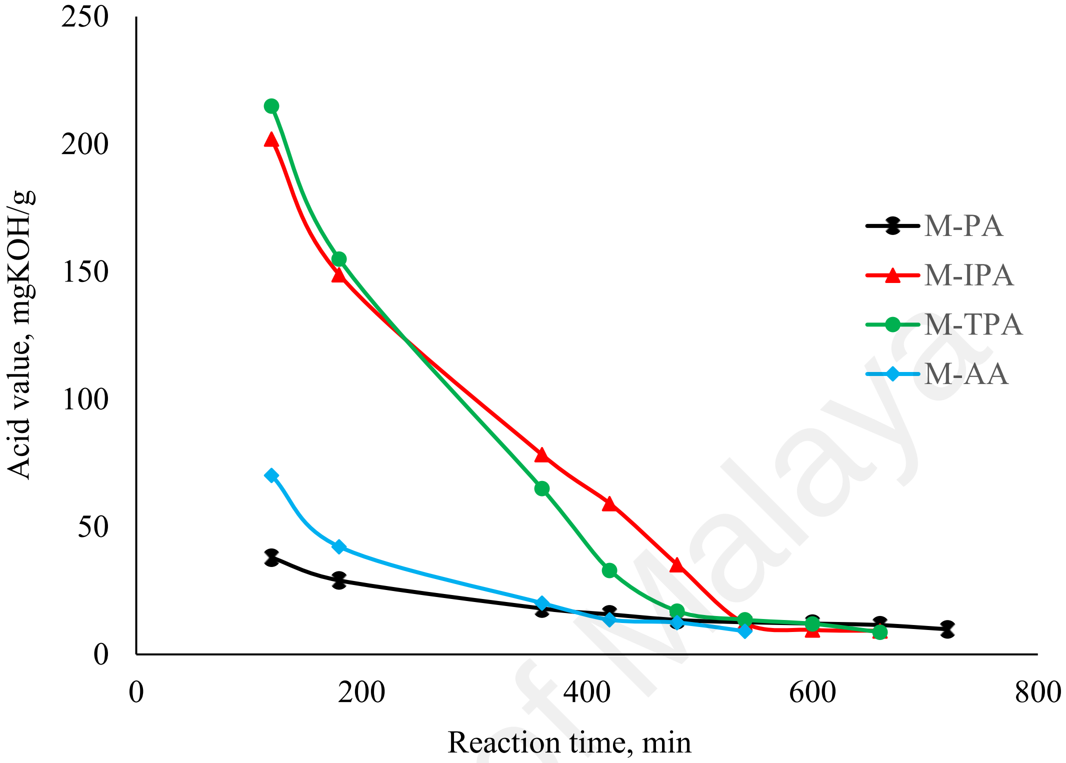

Figure 4.29 Acid value as function of reaction time

Figure 4.29 shows the change in acid value with reaction time during the synthesis of the M-PFAD macromers. With reference to Table 3.18, the polybasic acid used in the macromer synthesis showed different in reaction trend. IPA and TPA being aromatic diacid has showed slower reaction rate as compared to adipic acid and phthalic anhydride. This can be related to the physical properties of the polybasic acid. IPA and TPA have melting points of 345°C and 300°C respectively, thus requiring high esterification temperature ranging from 260-300°C. To avoid sublimation of the diacid during polymerization, the synthesis was carried out at maximum reaction temperature of 240°C that was far below the melting temperature of IPA and TPA and has resulted in slower esterification rate as reflected in the slower initial decrease of the acid value. For adipic acid and phthalic anhydride, their melting temperature are 152°C and 131°C respectively, being lower than the polymerization temperature. The acids were in liquid form at 240°C and having higher mobility for esterification to occurred as compared to IPA and TPA. Thus, the acid value has drop dramatically to 70 and 38 mgKOH/g for AA and PA respectively even at reaction time of 120 minutes. At same reaction time, IPA and TPA were showing acid value of 202 and 215 mgKOH/g respectively. In the case of phthalic anhydride, the acid value decreased at higher initial rate was due to the anhydride group which is more reactive than carboxylic acid, by ring opening reaction of the anhydride group. Subsequent reduction of acid value was becoming slowest among the acids used, which is due to the stearic hindrance effect of the bulky half ester formation.

The M_w each macromer is shown in Table 4.10 and Figure 4.30a and 4.30b show the GPC chromatogram of the macromers.

[Average Molecular Weight]
Number Average Molecular Weight(Mn) 2588
Weight Average Molecular Weight(Mw) 7251
Mw/Mn 2.80222

[Average Molecular Weight]
Number Average Molecular Weight(Mn) 1729
Weight Average Molecular Weight(Mw) 4799
Mw/Mn 2.77586

Figure 4.30a GPC chromatogram of M-AA and M-PA

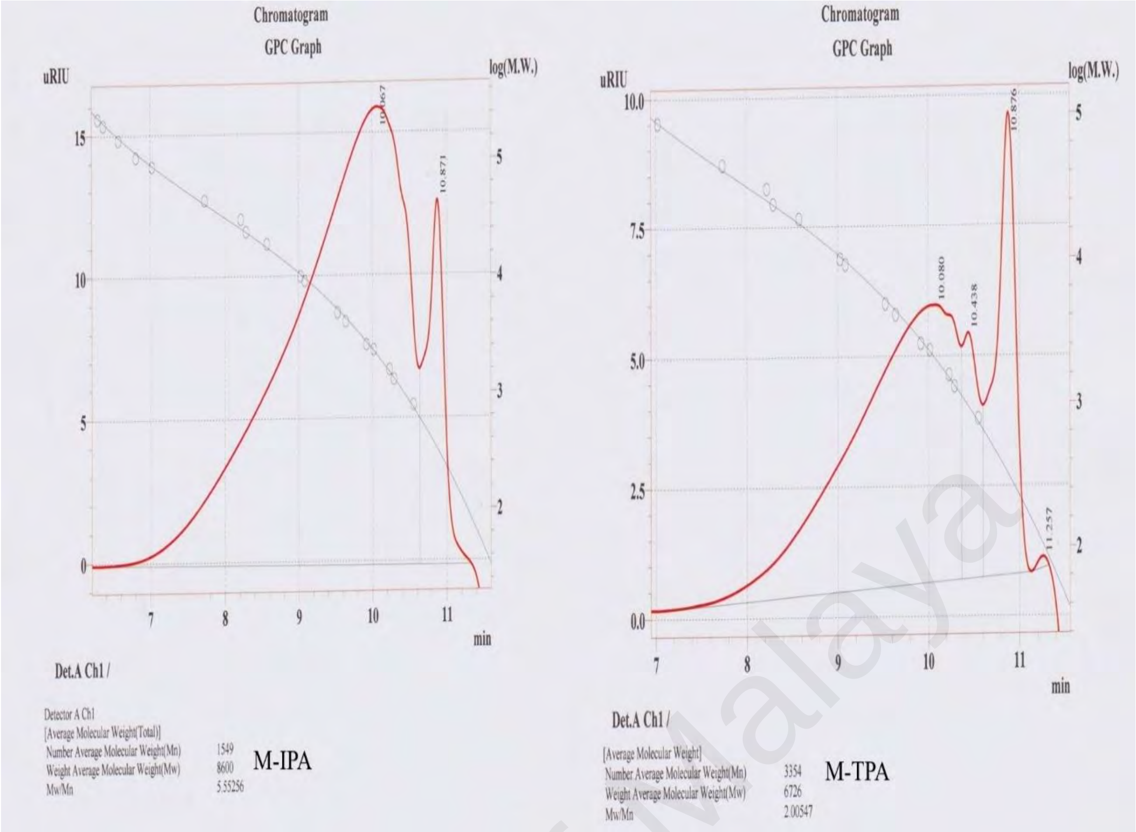

```
Detector A Ch1
[Average Molecular Weight(Total)]
Number Average Molecular Weight(Mn)     1549
Weight Average Molecular Weight(Mw)     8600
Mw/Mn                                   5.55256
```

```
[Average Molecular Weight]
Number Average Molecular Weight(Mn)     3354
Weight Average Molecular Weight(Mw)     6726
Mw/Mn                                   2.00547
```

Figure 4.30b GPC chromatogram of M-IPA and M-TPA

Table 4.10 Molecular weight of M-AA, M-IPA, M-TPA and M-PA

Formulation	Molecular weight (dalton)	Polydispersity, PDI
M-PA	4800	2.78
M-AA	7200	2.80
M-IPA	8600	5.55
M-TPA	6700	2.01

M_w each macromer is shown in Table 4.10. In general, the molecular weight of macromers were between 4800-8600 dalton. The M_w was in the trend of M-PA<M-TPA<M-AA<IPA. M-PA has the lowest M_w. the reaction temperature at 240°C was above the T_m of AA has resulted in faster reaction rate to produce M_w of 7200. The long reaction time for IPA and TPA has produced M-IPA and M-TPA with M_w of 8600 and

6700 dalton respectively. The macromer of phthalic anhydride showed the lowest M_w at 4800 dalton, due to stearic hindrance of the half ester structure that resulted in slower molecular weight growth.

4.3.1.2 FTIR Analysis of M-AA, M-IPA, M-TPA and M-PA

FTIR technique was used to identify the functional group in macromers synthesized. The comparison of the FTIR spectrum for all macromers were shown in Figure 4.31.

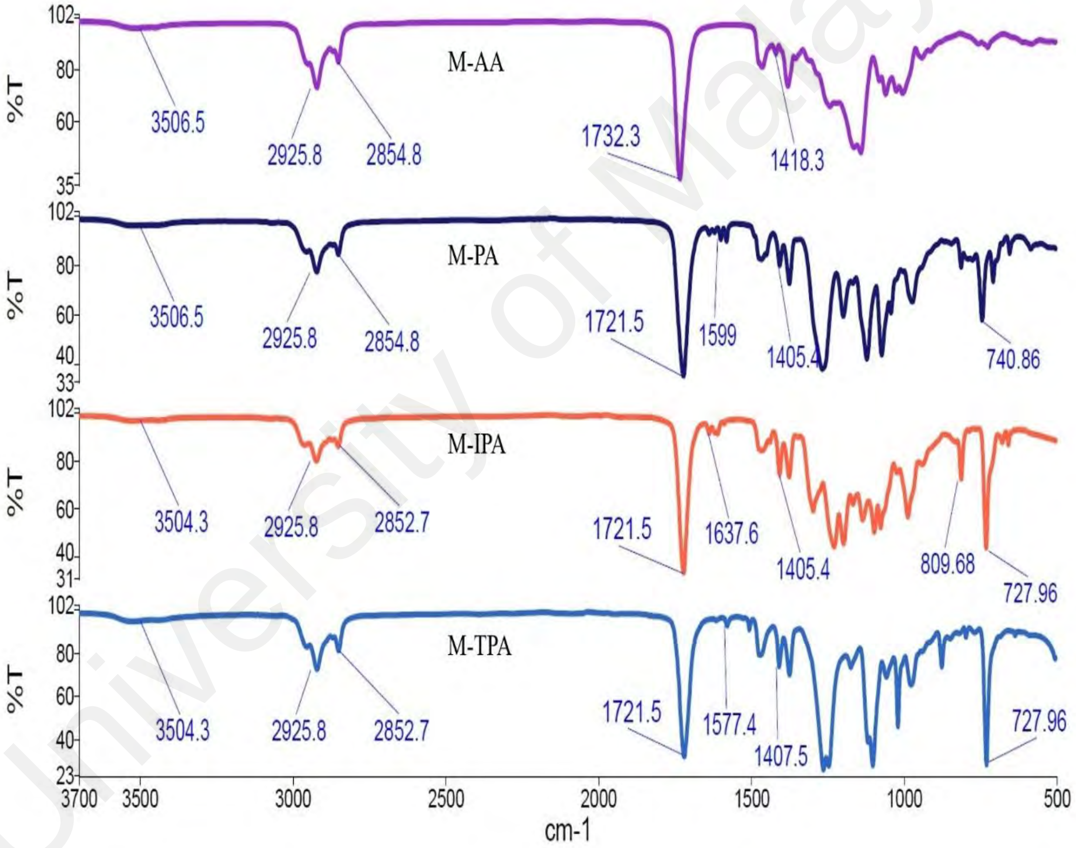

Figure 4.31 Comparison of FTIR spectra for M-AA, M-IPA, M-TPA and M-PA

Figure 4.31 shows spectra of the macromers. Macromer synthesized from aromatic polybasic acids (PA, IPA and TPA) but AA, the aliphatic type of acid shows different particularly in wave number of 500-1700 cm^{-1}. The similarity of the FTIR peaks could be due to the resemblance of the functional groups in the molecular structure of the macromers. The weak and broad peaks at 3507 cm^{-1} could be assigned to the hydroxyl group (Donald L. Pavia et al., 2015, Umare S.S. et al., 2007). The weak peaks between 2927 -2853 cm^{-1} are the stretching of C-H (Umare S.S. et al., 2007). The strong peaks at 1734 cm^{-1} for AA and 1722 cm^{-1} for other aromatic acid is assigned to carbonyl C=O stretching (Donald L. Pavia et al., 2015, Umare S.S. et al.,2007, Zhang J. et al.,2008). The weak peaks within 1602 -1581 cm^{-1} is assigned to C=C stretching (Donald L. Pavia et al., 2015) of in the aromatic rings of PA, IPA or TPA moieties. The peak centered at 745 cm^{-1} is due to out of plane bending of C-H in the ortho di-substituted benzene ring. The strong peaks at 810 and 728 cm^{-1} are out of plane bending of C-H in meta di-substituted benzene ring (Donald L. Pavia et al., 2015) of isophthalic acid moiety. The strong peak at 728 cm^{-1} in the M-TPA spectrum is assigned to C-H bending of para di-substituted benzene ring in terephthalic acid moiety.

The properties of PFAD macromers were summarized in Table 4.11.

Table 4.11 Properties of M-AA, M-IPA, M-TPA and M-PA

Description	M-AA	M-PA	M-IPA	M-TPA
Oligomer content/%	80.0	80.0	80.0	80.0
Reactive diluent/%	20.0	20.0	20.0	20.0
Viscosity@25^{o}C/poise	318.0	220.0	340.0	310.0
Acid value/mgKOHg^{-1}	9.1	9.8	9.3	8.7
Molecular weight (Mw)/dalton	7200	4800	8600	6700
Polydispersity/PDI	2.80	2.78	5.55	2.01

4.3.2 Synthesis of UA-AA, UA-IPA, UA-TPA and UA-PA

The UA-AA, UA-IPA, UA-TPA and UA-PA were synthesized with the corresponding macromers and the feed composition UA-AA, UA-IPA, UA-TPA and UA-PA were provided in Table 3.19. Each macromer was copolymerized with TDI and 2-HEA to produce the corresponding PFAD-UA. The plausible structure of each UA formation is represented in Scheme 4.5.

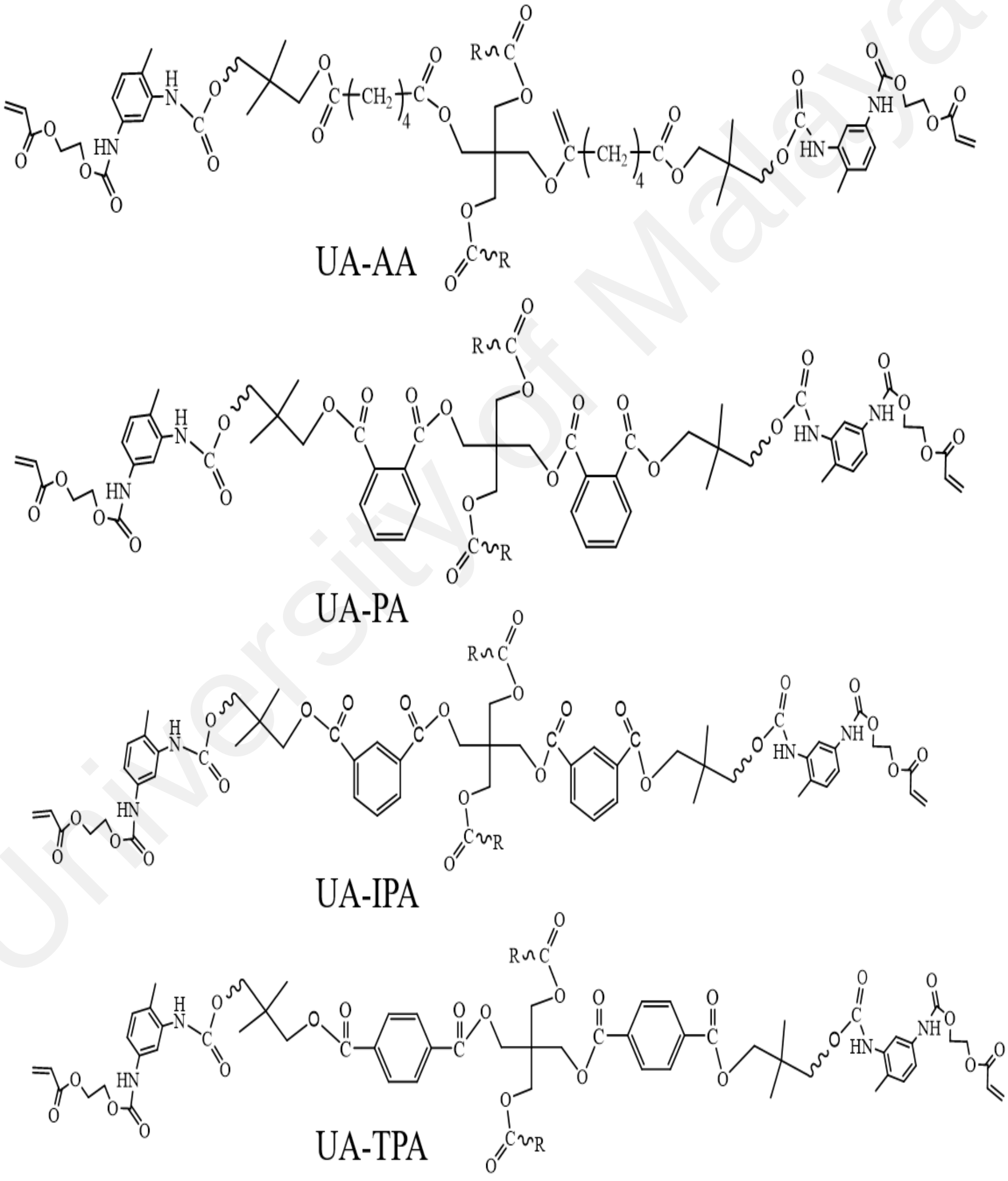

Scheme 4.5 The plausible structure of PFAD urethane acrylate formation from each dicarboxylic acid

4.3.2.1 NCO Content Analysis for UA-AA, UA-IPA, UA-TPA and UA-PA

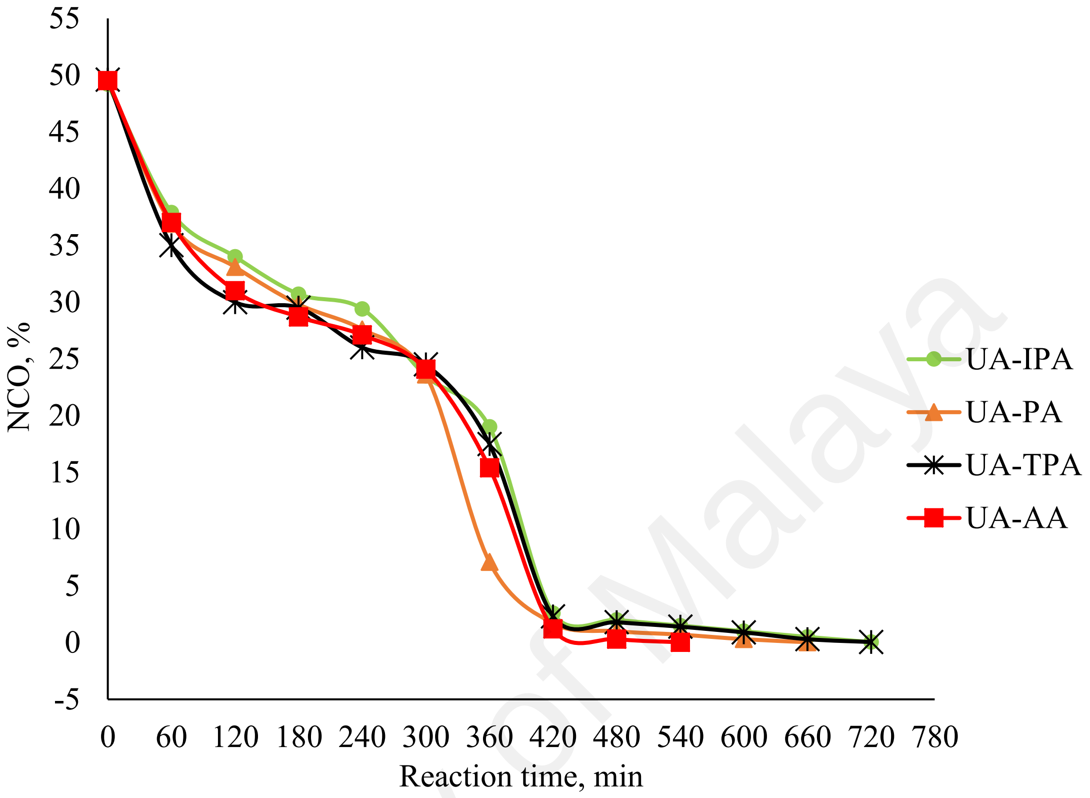

Figure 4.32 The change in NCO values reaction time during synthesis of UA-AA, UA-IPA, UA-TPA and UA-PA

Figure 4.32 shows the change in NCO fraction during synthesis of PFAD urethane acrylate. All macromers show similar trend of NCO reduction during the grafting process. Since the TDI-HEA adducts were reacted at similar conditions, all macromers were show similar rate of initial reduction of NCO content to half of its value at time interval of 300 min. The reduction rate has increased when at interval of 350-420 min. At 360 min, M-PA has showed faster NCO reduction as compared to the other three macromers presumably due to the effect of viscosity. The lower viscosity of M-PA has provided better mobility of reactants during the grafting process and resulted in faster reaction rate as compared to M-IPA, M-AA and M-TPA. The formation of UA-AA was the fastest due to the least steric hindrance in M-AA during the grafting process. Bulky groups in IPA, TPA and PA macromers have higher stearic hindrance and could reduce the reaction rate. Thus M-IPA and M-TPA have taken 720 min to reach 0.05% NCO while M-PA required 660 min to reached 0.03% NCO.

4.3.2.2 FTIR Analysis of UA-AA, UA-IPA, UA-TPA and UA-PA

For illustration, Figure 4.33 shows the FTIR spectra of the macromer M-AA and final urethane acrylate of UA-AA.

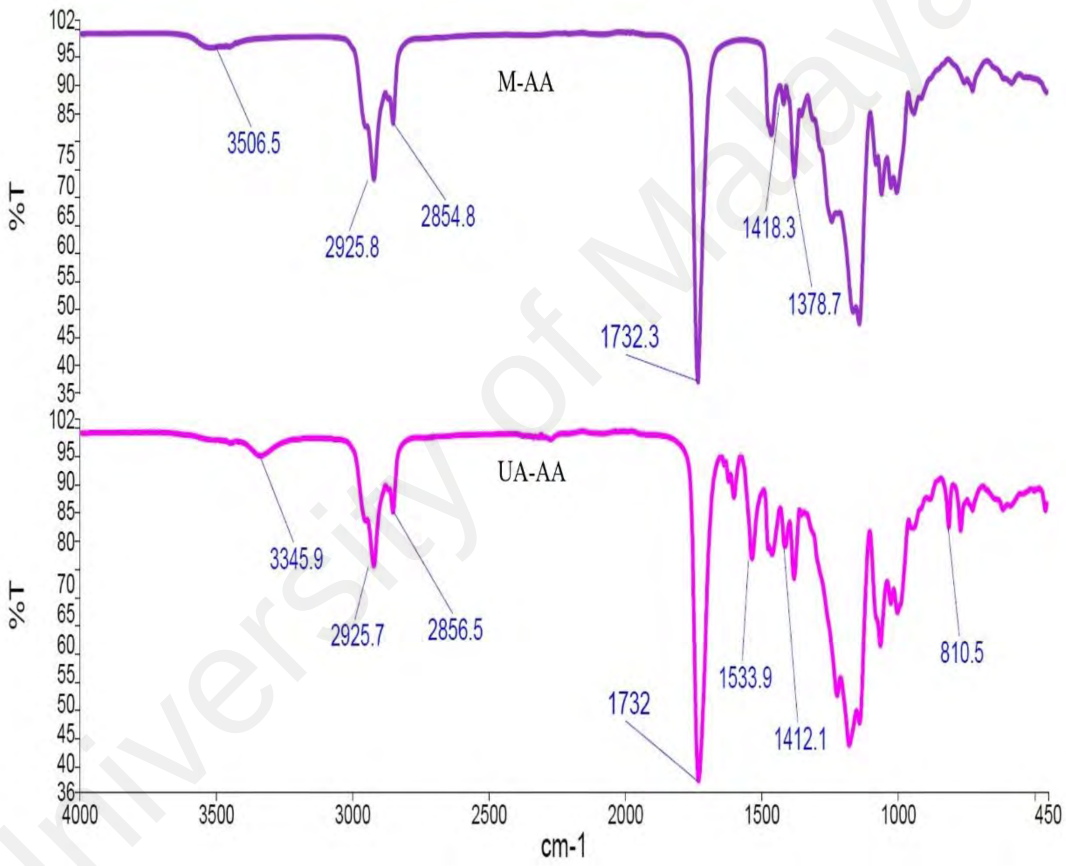

Figure 4.33 Overlaid of FTIR spectra of M-AA and UA-AA

The peak at 3526 cm^{-1} has disappeared due to the reaction of OH and NCO to form the urethane linkage where a new peak at 3344 cm^{-1} appeared due to the NH stretching of urethane group. This NH deformation peak is seen at 1532 cm^{-1}. The acrylate double bond absorption peaks at 808 cm^{-1} was observed on UA-AA but not on M-AA.

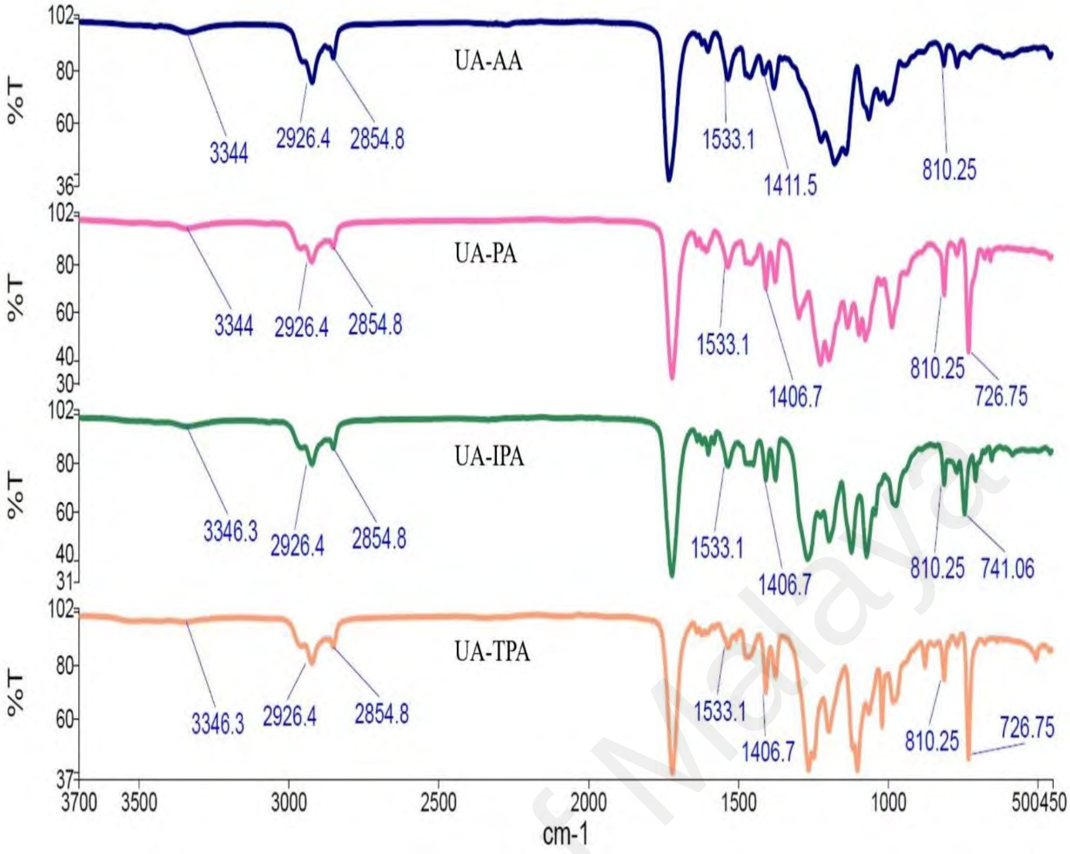

Figure 4.34 Overlaid FTIR spectra of UA-AA, UA-IPA, UA-TPA and UA-PA

Figure 4.34 shows the spectra of all the UA resins. All UA contain similar functional groups, except the strong peaks at 700-800 cm^{-1} due to C-H out of plane bending of di-substituted benzene ring for those aromatic dicarboxylic acid. The 3344 cm^{-1} and 1533 cm^{-1} peaks due to -NH confirms the formation of urethane linkage. The acrylate double bond was successfully introduced onto the resin backbone as evidence from the acrylate peaks at 810 cm^{-1} and -CH_2=CH-R absorption peaks at 1406 cm^{-1}.

4.3.3 UV Irradiation Curing of UA-AA, UA-IPA, UA-TPA and UA-PA

The FTIR technique was used to study the UV curing of the resin with the formulation as provided in section 3.4.1. The composition of UA-AA, UA-PA, UA-IPA and UA-TPA for this study were provided in Table 3.18. The UV curing reaction was monitored by FTIR from the reduction of acrylate double bond at 810 cm^{-1} and the peak area reduction is related to conversion of the acrylate unsaturation by Eqn 3.8, and the results are shown in Figure 4.35.

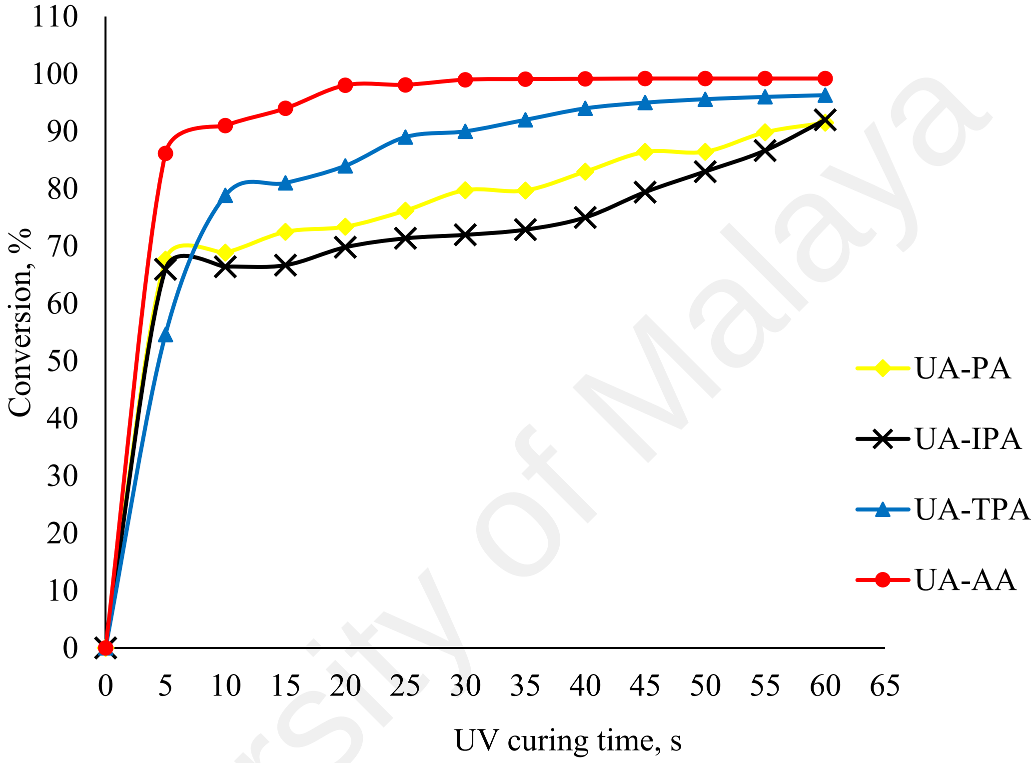

Figure 4.35 Conversion of absorbance 808 cm^{-1} versus UV curing time for all UA

The curing process of the urethane acrylate resin occurred in two steps. In the first stage, there was an accelerated polymerization due to higher initial concentration of double bond and better mobility of the oligomer. After that, the conversion rate has decreased due to viscosity built up and lower amount of unsaturation left. Within 5 s of UV irradiation, the conversion was recorded at 55, 66, 67 and 86% for UA-TPA, UA-IPA. UA-PA and UA-AA respectively. The conversion rate started to show differences among the resins after 20 s. UA-PA and UA-IPA did not continue at higher rate as compared to UA-AA and UA-TPA. In the case of UA-PA and UA-IPA, the two oligomers recorded a very slow increase of conversion rate at 69 and 67% respectively; but UA-AA and UA-TPA have achieved conversion rate of 91 and 79% respectively. UA-PA and UA-IPA were showing slower conversion rate from 20 until 60 s of UV curing time. Both samples reached 92% of total conversion after 60 s. The UA-AA has achieved 99% conversion in just 30 s and remained constant until 60 s. UA-TPA has shown similar trend as with UA-AA. The UA-TPA clear coat had achieved a final conversion of 98% after 60 s of UV irradiation. The differences in conversion rate can be related to stearic hindrance of bulky structure and viscosity of the resin. The lowest reactivity of UA-PA is clearly due to the stearic hindrance. The higher M_w and highest viscosity of UA-IPA has significantly affected and contributed on its low conversion result. These two factors have reduced the mobility of the oligomer resulted in slower conversion rate. The low M_w and viscosity have allowed the UA-AA resin to have the highest mobility and resulted faster conversion. UA-TPA are quite similar in chemical structure as UA-IPA. However, the lower M_w and viscosity of UA-TPA has showed higher conversion rate than UA-IPA.

4.3.4 T_g Analysis of UA-TPA, UA-IPA, UA-PA and UA-AA on UV Curing

Each clear coat was applied onto glass panel by a bar coater to achieve a thickness of 25µm and expose to UV irradiation at specified durations. T_g of the cured film was determined by DSC method. Figure 4.36 shows the change in T_g at different cure time. Figure 4.37 shows the T_g thermogram of the UA before and after 60 s of UV curing.

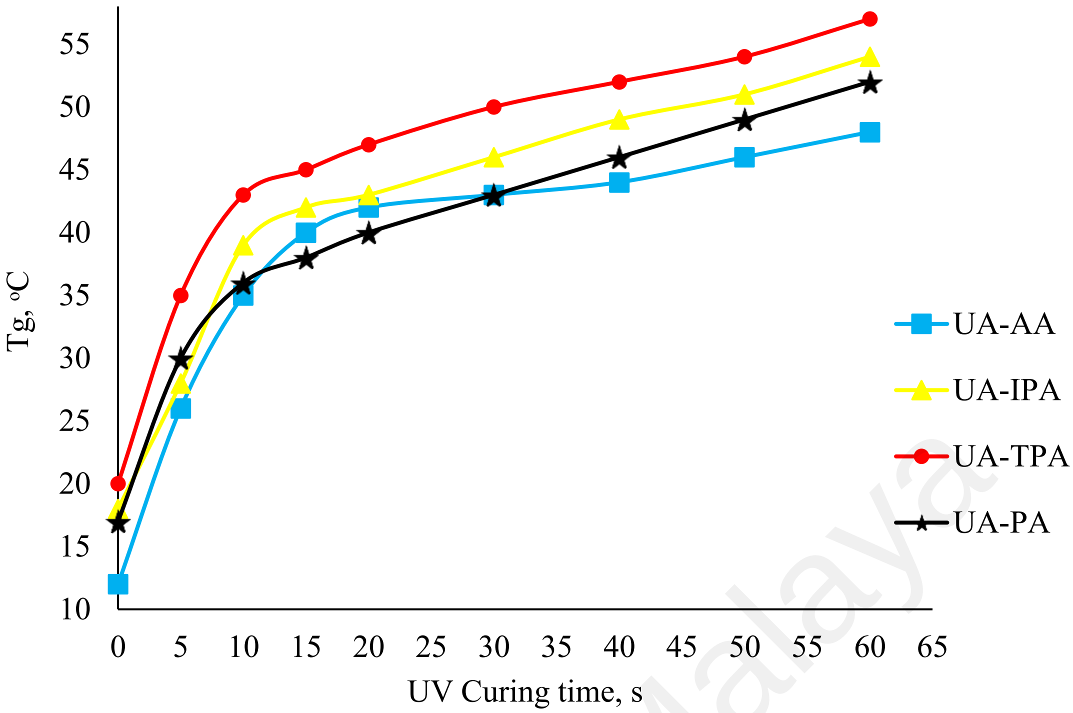

Figure 4.36 T_g of all UA's UV cured film at different UV curing time

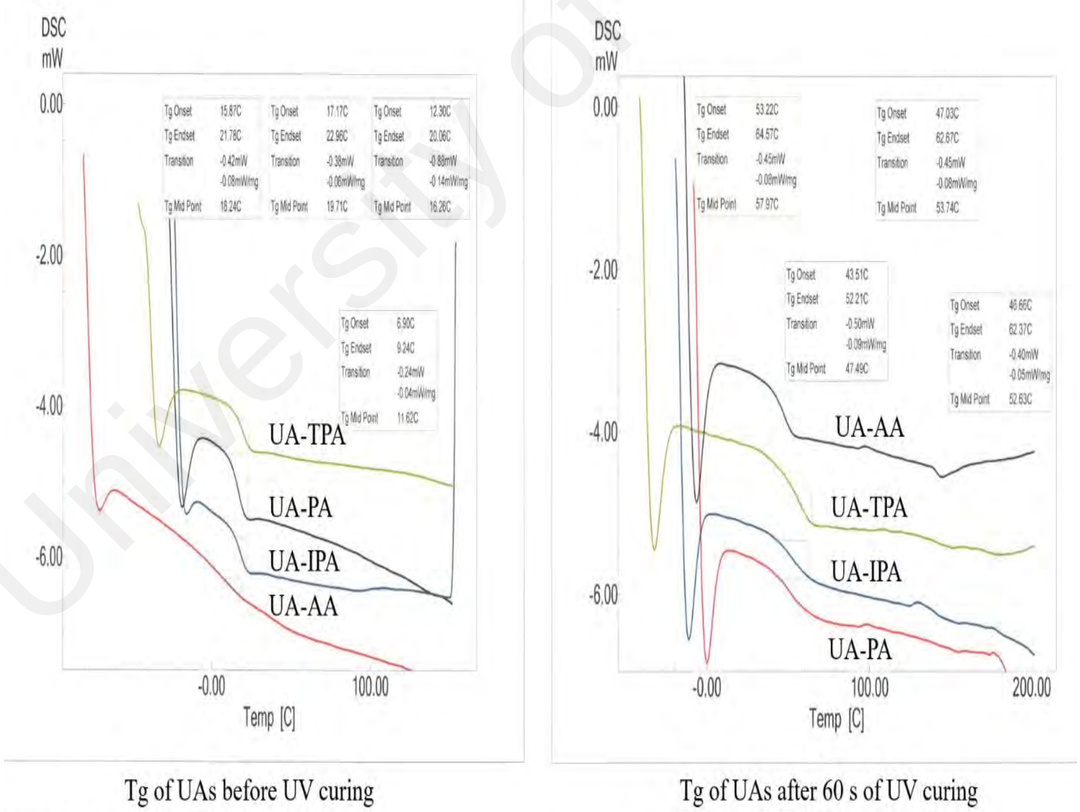

Tg of UAs before UV curing

Tg of UAs after 60 s of UV curing

Figure 4.37 The T_g thermogram of UAs before and after 60 s of UV curing

The initial increase of T_g was fast within the first 5 to 15 s of UV curing time. This could be due to the higher concentration of double bond and lower viscosity at initial conditions, subsequently from 20 to 60 s, T_g has increased slower. Resins of aromatic diacids have showed higher T_g than aliphatic diacid. The UA-PA, UA-TPA and UA-IPA have achieved T_g of 52, 57 and 54 ^{o}C respectively, whereas UA-AA can only achieve 48 ^{o}C at finally. As shown by the double bond conversion in UV reaction study, the UA-AA cured film 98% of conversion within 20 s and subsequently increased further by 1% of conversion. The change in T_g has a great influence on the final film properties, which include flexibility, hardness and solvent resistance, which has been reported in polyester or alkyd study (Stoye D. et al., 1996). Polyesters from monomers with short aliphatic chains as well as aromatic rings are known to result in higher T_g in comparison to polyesters from monomers with long aliphatic chains (Deligny D. 2000). The glass transition temperature would constantly fall as the soft building block such as adipic acid is incorporated into the backbone of the PFAD urethane acrylate. Oligomer modified with TPA producing high T_g of cured is due to increase crystallinity of the oligomer resulting from TPA regular and molecular symmetry structure.

4.3.5 Pendulum Hardness Analysis of M-AA, M-IPA, M-TPA and M-PA UV Cured Film

The film at different stages of UV curing was subjected to the pendulum hardness test by using the Sheen Konig pendulum tester and according to the ASTM 4366. The results are shown in Figure 4.38.

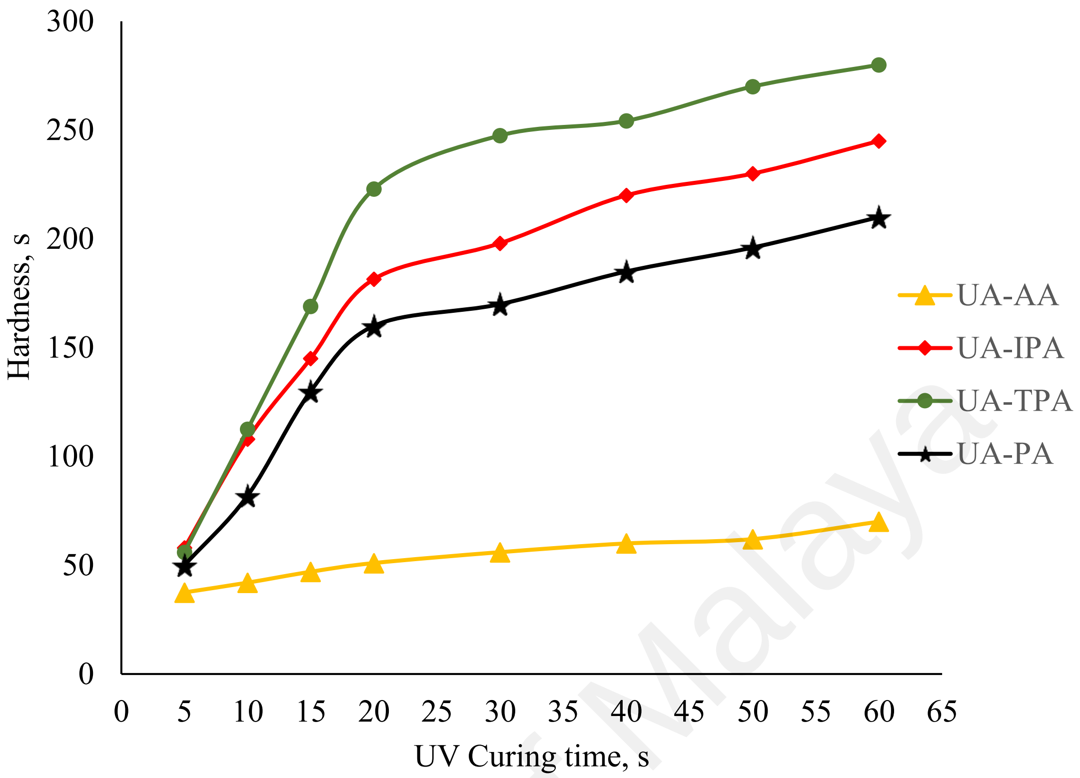

Figure 4.38 Pendulum hardness development of the UA during the UV curing process

In Figure 4.38, the change in hardness versus curing time showing similar trend as T_g changes. The hardness was directly associated with the T_g. All the cured films of urethane acrylate resins derived from the four dicarboxylic acids show satisfactory film hardness after the UV curing process. The UA made from aromatic diacids show faster increase in hardness during initial 20 s of UV irradiation. Subsequent UV curing process showed lower increase of hardness due to the less double bond and higher viscosity. The final hardness of the cured film has achieved 280, 245 and 210 s for UA-TPA, UA-IPA and UA-PA respectively. In case of UA-AA, the low T_g and fast curing rate was due to the soft building block of adipic acid and high mobility of the UA. The film has achieved its pendulum hardness of 51 s within 20 s, and subsequent UV curing only contributed a very small increase in hardness of the final film at 70 s, which was far lower than the aromatic diacid cured films.

4.3.6 Performance of M-AA, M-IPA, M-TPA and M-PA in Metal Coating

The coating formulations were as described in section 3.4.1, and applied on metal panels, and their film performances were tested for mechanical properties, which included film flexibility, impact resistance, durability, solvent, water and corrosion resistance. Figure 4.39 illustrated the UA's coated panel for the testing purpose.

UA's UV cured film coated on pre-primer metal with cross cut salt spray test

UA's UV cured film coated on pre-primer metal without cross cut for other test

Figure 4.39 Illustration of UA's UV cured coated metal panel

4.3.6.1 Physical and Mechanical Performance of UV Cured Film

The test results were summarized in Table 4.12.

Table 4.12 Summaries of UA UV cured film performance

Test Description	Formulation			
	UA-AA	UA-PA	UA-IPA	UA-TPA
60^o Gloss (GU)	94	100	100	98
Crosscut adhesion	5B	5B	5B	5B
Impact (H x W; 100cmX1.8kg)	>100 cm NTO	>100 cm NTO	>100 cm NTO	>100 cm NTO
T-bend	1T	3T	3T	2T
Pencil Hardness	H	3H	3H	3H
MEK double rub	15	45	90	90

NTO= no tape off after adhesion test.

The test results review in Table 4.12, have shown that all the coating exhibited good gloss appearance and excellent cross cut adhesion test outcome. In gloss measurement, the aromatic diacids IPA, TPA and PA have recorded higher gloss of 100 and 98 GU as compared to AA which recorded at 94 GU. All films pass the crosscut adhesion test.

4.3.6.2 UV Cured Film Flexibility Performance by T-bend Method

From the result in Table 4.12 cured film of the UA-AA recorded flexibility of 1T bending, follow by UA-TPA that has recorded 2T, UA-PA and UA-IPA achieving 3T on T-bend test. Flexibility required flexible component in the resin backbone, this can be easily achieved by linearity of AA structure. Incorporation of adipic acid into the UA has positive effect on making the UV cured film flexible after UV curing process. In case of UA-TPA, the cured film has achieved 1T lower than to the other two aromatic diacid PA and IPA. The lower flexibility achieved by TPA derived UA's cured film was due to its symmetry structure of 1,4 substitution of benzene ring. The UA modified with PA and IPA showed least flexibility was due to the presence of the moiety of asymmetry geometry structure of 1,2- and 1,3-disubstitution benzene ring in resin-backbones structure.

4.3.6.3 Cracking Resistance of the UV Cured Film by Impact Deformation

In cured film, the rigidity of aromatic moiety might impart good hardness as shown by the high pencil hardness of IPA, TPA and PA modified UA and recorded at scale of 3H as compared to AA modified UA (Table 4.12). The linearity of AA has resulted in more flexible film with lower pencil hardness of H. Resistance of the UV cured film to cracking after deformation by impact highly depends on both flexibility and good adhesion (Danick C.,2005). It is known that good adhesion of the cured film could be achieved if the coating makes closed contact with surface (Danick C., 2005). In this study, there was no cracking detected for all UV cured films after deformation by impact. Moreover, the cured films did not chip off after the peeling test on the deformed area by adhesive tape. The AA modified UA achieved good adhesion was resulted from the linear structure of AA. The impact results of IPA, PA and TPA modified UA reveal that the aromatic moieties in the resin-backbones result in an effective contact angle between the coating and the substrate, thus imparted good adhesion after deformation by impact.

4.3.6.4 Solvent Resistance of the UV Cured Film

The MEK test was carried out on UV cured film derived from all polybasic acids modified UA to evaluate the degree of curing. Theoretically, it was expected that higher degree of crosslinking would be achieved by higher conversion of double bond of the UA resin, and produce higher resistance to MEK solvent. From the results showed in Table 4.12, UV cured film recorded 15, 45 MEK double rubs for UA-AA and UA-PA modified respectively. Both UA-IPA and UA-TPA recorded 90 MEK double rubs. The resistance to MEK could be related to nature of building block in the backbone rather than crosslinking density. Regardless of the crosslinking density, the nature of hard polybasic acids used in the UAs synthesized had significant influence on the MEK resistance of the cured film. In this respect, soft diacids such as adipic acid and phthalic anhydride has resulted in lower solvent resistance, while inclusion of hard diacids such as isophthalic and terephthalic acid would increase the solvent resistance.

4.3.6.5 Durability of UV Cured Film

The resistant of the coating to the influence of the environment is important physical characteristic, especially for outdoor usage. In this aspect, resistance to environment can be defined as weathering durability. In outdoor conditions, many factors simultaneously influence the lifespan of the coating. The factors could be combined actions of light, heat and moisture, which can cause changes in chemical structure of the polymers (Pospisil J. et al., 2000, B. Singh N. et al., 2008, Malanowski P., 2009). Figure 4.40 shows the gloss retention of the UA's clear coat after the accelerated weathering test.

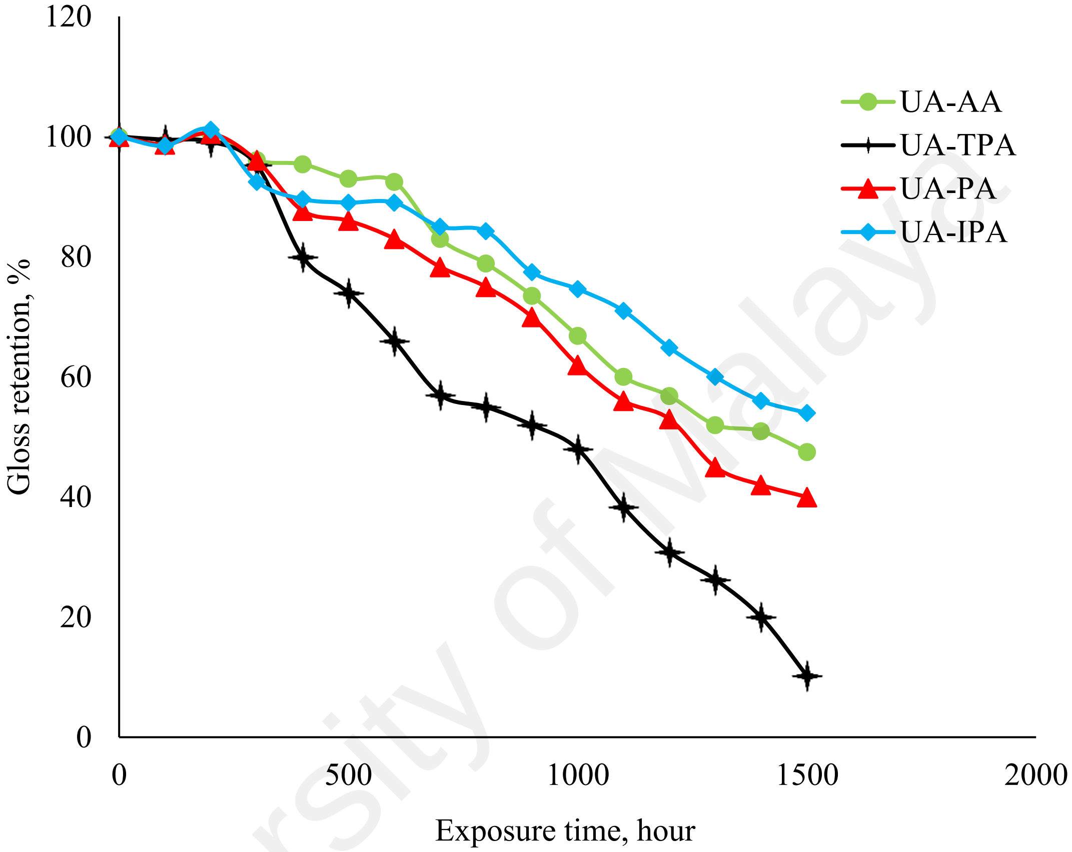

Figure 4.40 Gloss retention of UA's clear coat on accelerated weathering test

The reduction of gloss was resulting from the reactions happening on the surface of the polymeric materials, these include photolysis, hydrolysis and thermal degradation (K. Shanti, 2013). In general, increase in aromatic content will lead to increase in T_g, crystallinity and thermal stability of the UAs. In addition, UAs derived from aromatic diacids are much less electrophilic and thus far less sensitive to hydrolysis than aliphatic diacid modified UA, leading to better weathering result after prolong test schedule. UA-IPA has the best weathering resistant as compared to other aromatic diacids. In previous study, IPA and TPA modified polymer show same degradation mechanism and this could be due to the lower absorption of UV light by IPA as compared to TPA and PA (Maetens D., 2007). It was found that UA-TPA, has the poorest weathering result as compared to other aromatic diacids. In Malanowski P. (2009) study, TPA modified coating absorbs ~95% of UV light at 300 nm whereas IPA modified coating only absorb ~15% of UV light. The higher absorption rate has direct impact on poor weathering resistant of TPA modified coating.

4.3.6.6 Performance of Corrosion Resistance of the UV Cured Film

The corrosion resistance of the coated panels for all UA's coatings was studied by salt spray test method. Visual inspection of the surface was carried out, and the observations were tabulated in Table 4.13. The change of gloss for the exposed cured films have been measured and results shown in Figure 4.41. Figure 4.42 illustrates blistering appearance and corrosion performance of UA-AA UV cured film using digital microscope image.

Table 4.13 Observation and rating of corrosion resistance for UA UV cured film

Description	UA-AA	UA-PA	UA-IPA	UA-TPA
Corrosion rating	7 Blistering	8 Slight blistering	9 No blister	9 No blister

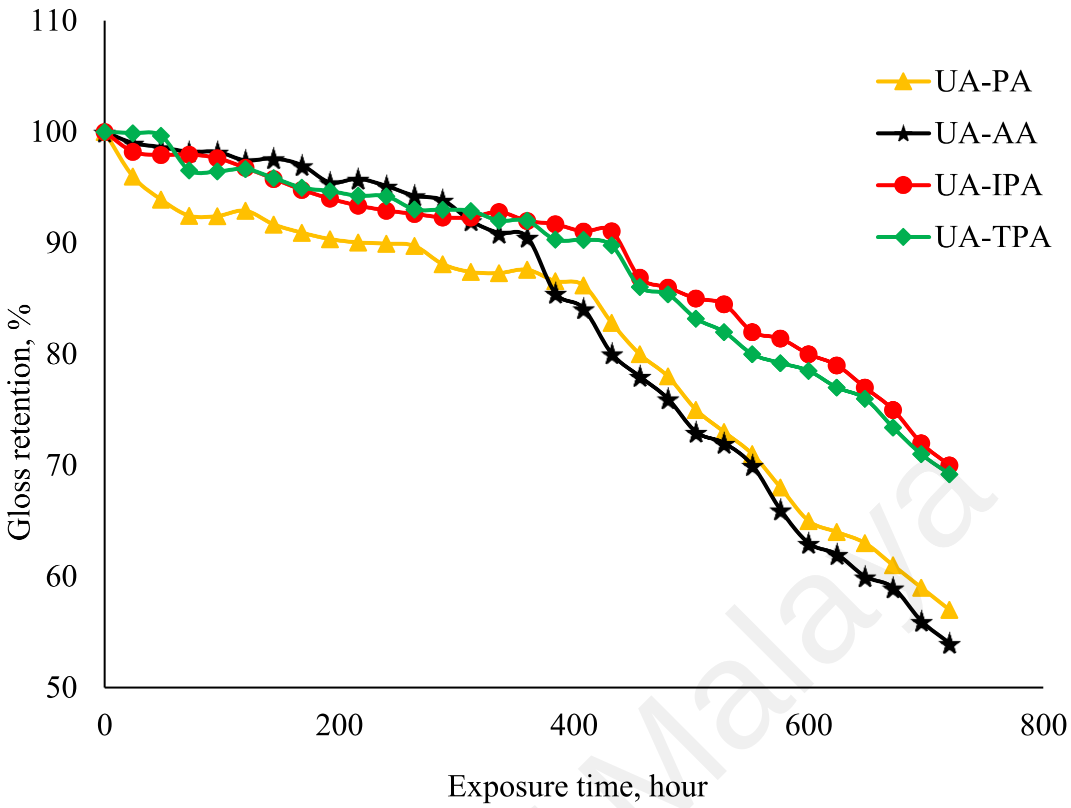

Figure 4.41 Gloss retention of the UA UV cured film by salt spray corrosion test

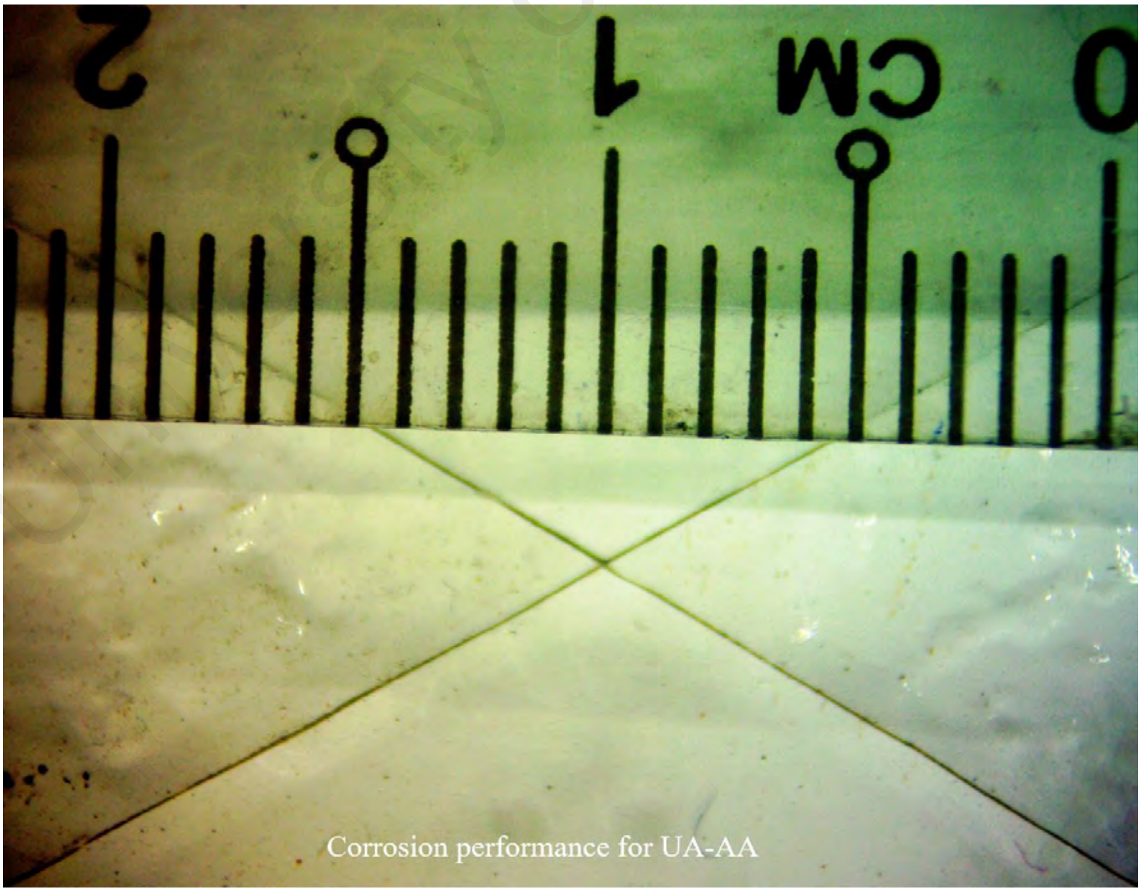

Figure 4.42 Digital image of UA-AA panel after corrosion test

UA-AA has showed the lowest corrosion rating at 7 with blistering observed. UA-PA, UA-IPA and UA-TPA have showed good corrosion resistance at rating of 8 and 9 respectively with only slight blister being observed on UA-PA cured film surface. The soft and low T_g of UV cured film of UA-AA has higher tendency of moisture absorption which may reduce the film strength for possible chloride ion to penetrate into the substrate to cause corrosion. Inclusion of aromatic moieties such as PA, IPA and TPA diacids has impart higher hydrophobicity of the cured film and effectively improved the film corrosion resistance. In Figure 4.41, all UV cured films have shown good corrosion resistant at initial 400 hours with lower rate of gloss reduction. After this point, higher gloss reduction was observed on UV cured film derived from UA-AA and UA-PA, which could maintain final gloss retention at around 60% after 700 hours of corrosion test cycles. The result shows that UA-IPA and UA-TPA cured film show lower gloss reduction. Their films have shown final gloss retention at approximately 70% after 720 hours of cycles test duration.

4.3.6.7 Performance of Water Resistance of the UV Cured Film

The water resistance was performance on the UAs cured film by humidity cycle test technique. The test results were summarised in Table 4.14 and their gloss retention were elaborate as graph in Figure 4.44. Based on the principle, through temperature changes and through relative humidity (RH) changes, stresses can develop within coating film. These internal stresses have an effect on coating degradation. They affected the adhesion and or cohesion of the coating and have an effect on delamination and cracking of the coated film. Figure 4.43 shows the crosscut adhesion performance on UA-AA UV cured panel after 720 hours humidity cycle test. Similar appearance was observed on the other three UV cured panels.

Table 4.14 Physical properties of UV cured film after 720 hours of humidity cycle test

Test Description	Formulation							
	UA-AA		UA-PA		UA-IPA		UA-TPA	
	Initial	Final	Initial	Final	Initial	Final	Initial	Final
60° Gloss (GU)	94.0	86.7	100.0	88.0	100.0	90.5	98.0	92.6
Crosscut adhesion	5B	5B	5B	5B	5B	5B	5B	5B
Pencil Hardness	H	F	3H	2H	3H	3H	3H	3H

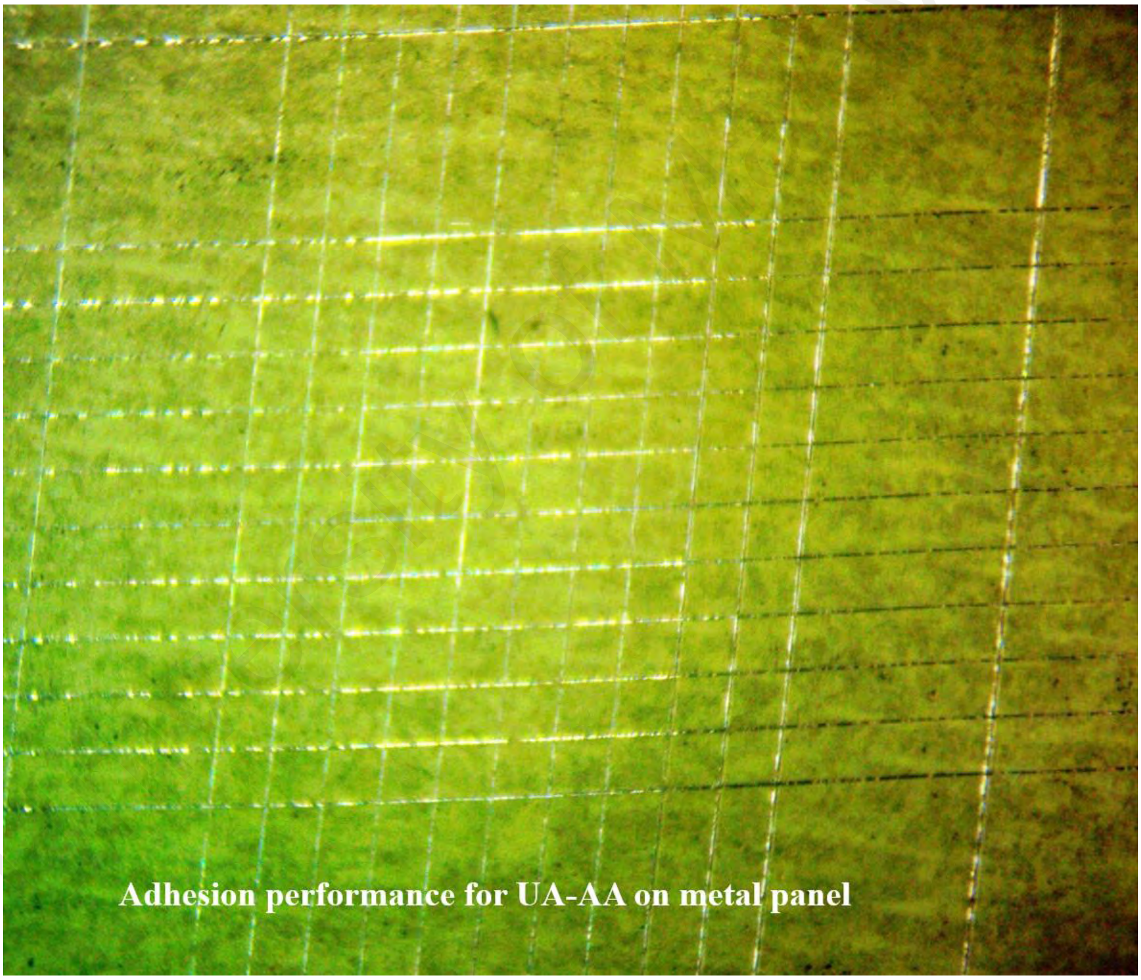

Figure 4.43 Crosscut adhesion performance for UA-AA UV cured metal panel

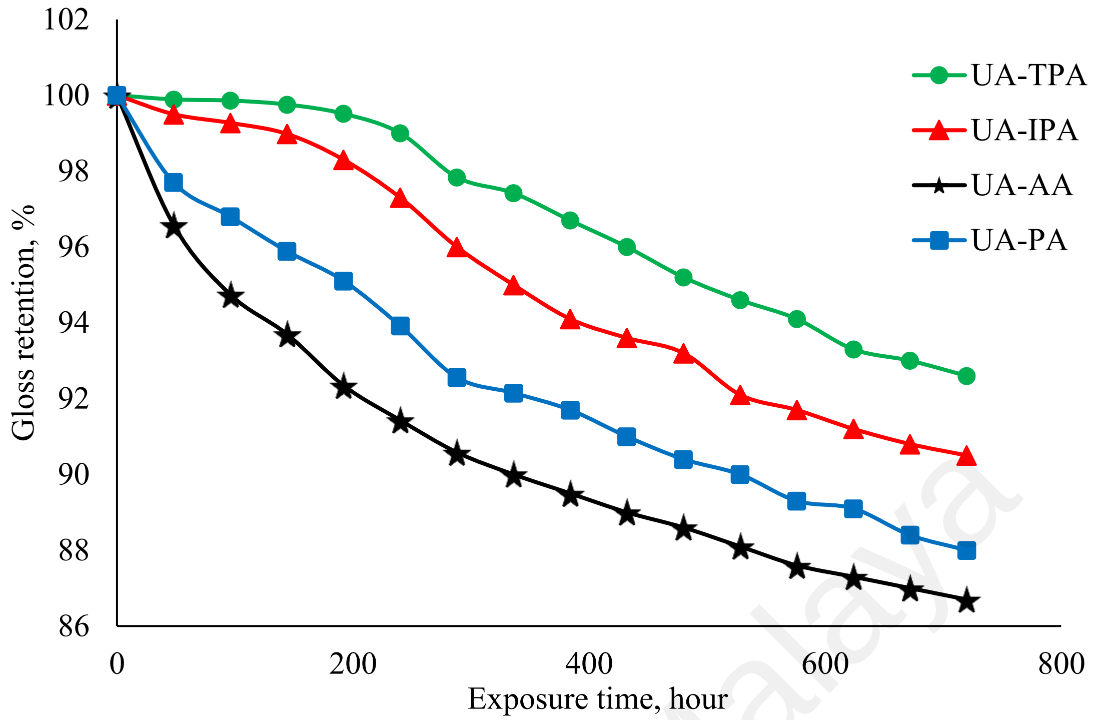

Figure 4.44 Gloss retention of UA UV cured film on humidity cycle test

In Figure 4.44, the change in gloss reduction manage to differentiate the performance among the polybasic acid modified UV cured film. The water resistance of the cured films was of similar trend as the gloss reduction in corrosion resistance test. The difference is the magnitude of changes in water resistant was smaller as compared to those in corrosion test. This could be due to the absence of chloride ion in humidity cycle test and there was no weaker point being created by cross cut on the cured film for humidity test panel. The cured film has successfully prevented moisture from penetrating through, which could result in blistering and delamination. Thus, water resistance of the film is affected by its chemical structure in nature. The inclusion of more hydrophobic moieties such as benzene ring into UA structure, higher water resistance could be achieved as shown by the UA modified with PA, IPA and TPA. Aliphatic diacids such as AA can reduced water resistant performance of the cured film.

CHAPTER 5: CONCLUSION AND SUGGESTIONS FOR FUTURE WORK

5.1 Synthesis of PFAD Urethane Acrylate

PFAD was utilized in the synthesis of UV-curable urethane acrylate resin via two stages. It was first converted to a hydroxyl terminated macromer M-PFAD. Then, followed by reacting the pendant hydroxyl group with TDI and 2-HEA to create a UV curable urethane acrylate resin. The Mw of M-PFAD was 6800 dalton (measured with GPC) and the urethane acrylate resin was 12500 dalton. The urethane acrylate resin has shown good UV curing activity, whereby 76% of its double bonds has reacted after 60 s of UV irradiation using a 225 mW/cm^2 mercury vapour lamp. The PFAD-UA clear coat has showed the increased in T_g of 54 °C after 60 s of UV curing. Its initial T_g was 15°C. The cured film showed good hardness development, where the final recorded a pendulum hardness of 107 s after 60 s of UV exposure.

5.2 Effect of PFAD Content on the PFAD-UA and Its Wood Coating Application

Five hydroxyl terminated macromers were synthesized using 15–70 % PFAD to react with a mixture of isophthalic acid, phthalic anhydride, neopentylgylcol (NPG), and pentaerythritol. Each macromer was then reacted with 2-hydroxylethylacrylate (2-HEA) and a toluene diisocynate (TDI) adduct to generate a urethane acrylic (UA) resin containing acrylate side chains that can be cured by UV irradiation. The content of the PFAD had a significant influence on the final film chemical and mechanical properties. The urethane acrylic oligomers with 15–55% PFAD in the macromers, could be UV-cured satisfactorily to form hard films with a T_g of 35–62°C. UA5 that is made from M5 containing 70% PFAD in the macromer, cured to form a soft film with $T_g < 30$°C. Thus, it can be concluded that urethane acrylate oligomer formulated with macromer containing >70% PFAD would not form a useful UV-cured coating. To obtain a PFAD-based urethane acrylate oligomer with good performances, the M-PFAD should be within the range of 40–55% PFAD. From series of the UV-cured film, the urethane acrylate of macromer containing 45% PFAD has exhibited the best chemical and physical properties, and has shown to be useful and valuable bio-resources for wood-coating applications.

5.3 Effect of Dicarboxylic Acids Building Block on the PFAD-UA and Its Metal Coating Application

A series of PFAD urethane acrylate resins were synthesized using IPA, TPA, PA and AA as polybasic acid building block. The M-PFAD was formulated with hydroxyl value of 91 mgKOH/g with polybasic acid equivalent of 0.32 g/mol in 100 g of resin. Results have demonstrated that the type of polybasic acid has great influences on the UA resin in terms of the mechanical performances of the cured film. In term of UV curing kinetic, all UA derived from the four dicarboxylic acids showed excellent UV curing activity and achieved the double bond conversion ranging from 92-99%. The aromatic type of polybasic acid such as IPA, TPA and PA can produce higher T_g and hardness of UV cured film. Other outstanding mechanical and physical properties that could be achieved include good adhesion, solvent resistance, impact strength and good flexibility on metal coating. The aromatic moieties and hydrophobicity of the aromatic dicarboxylic acid also contributed to the good corrosion and water resistance of the UV cured film performance. The durability of the UV cured film has showed degradation after prolong accelerated weathering test, whereas TPA derived UA has poorest durability performance and showed the gloss retention of 10% after 1500 hours of testing interval. Aliphatic polybasic acid such as AA could imparted good flexibility and soft film formation on the PFAD urethane acrylate cured film.

5.4 Suggestion for Future Works

In future works, the PFAD could be modified using others additives such as silicone intermediate to produce new resins suitable for high durability, good heat resistant coating application. In addition, flame resistance could be introduced into PFAD modified resin through the incorporation of bio-based flame-retardant material such as tannic acid, phytic acid or polydopamine, either through blending or covalent attachments. With the improved flame resistance performance, the coating could be usefully for many industrial applications particularly for those involving wood and plastic composite substrates.

Further modification of PFAD urethane acrylate with di-methylol propionic acid (DMPA) could yield a new polymer which could be dispersed into water base dispersion without using any surfactant. The resin could still be UV curable and used in coating application. Study on its synthesis path, UV curing behavior and coating performance characterization, could yield an interesting and useful project on water-based coating application for PFAD.

Besides that, it would be possible to study the PFAD urethane acrylate in composites application. The incorporation of natural fillers and fibers as reinforcement materials allows tailoring the composites properties to fit the requirements of structural or functional materials. The study could be focused on characterization of PFAD UA UV crosslinking behavior after incorporation of the fillers or fibers used as composites materials using FTIR, DIC, TGA or dynamic mechanical thermal analysis (DMTA) method. The research could be extended into nanocomposites application by using nano size fillers or fibers such as nano clays, nano silica or graphene as functional composites material. With the specific functional filler or fibers incorporated into the PFAD urethane acrylate, the resin application characterization could be extended into possible composite coating and adhesive usage

REFERENCES

Akram, D., Sharmin, E., Ahmad, S. (2008). Synthesis, characterization and corrosion protective properties of boron-modified polyurethane from natural polyol. *Progress in Organic Coatings*, *63*, 25-32.

Akram, D., Sharmin, E., Ahmad, S. (2009). Synthesis and characterization of boron incorporated polyester polyol from linseed oil: a sustainable material. *Macromolecular Symposia*, *277*, 130-137.

Akram, D., Sharmin, E., Ahmad, S. (2010). Development and characterization of boron incorporated linseed oil polyurethanes. *Journal of Applied Polymer Science*, *116*, 499-508.

Alam, M., Ray, A.R., Ashraf, S.M., Ahmad, S. (2009). Synthesis, characterization and performance of amine modified linseed oil fatty amide coatings. *Journal of the American Oil Chemists' Society*, *86*, 573-580.

Alam, M., Akram, D., Sharmin, E., Ahmad, S. (2014). Vegetable oil based eco-friendly coating materials: A review article. *Arabian Journal of Chemistry*, *7*, 469-479.

Armstrong, R.D., Jenkins, A.T.A. and Johnson, B.W. (1995). An investigation into the UV breakdown of thermoset polyester coating using impedance spectroscopy. *Corrosion Science*, *37*, 1615-1625.

Azam, M. A., Ooi, T. L., Salmiah, A., Umaru, S. I. and Ishak, Z. A. M. (2001). New polyester acrylate resins from palm oil for wood coating application. *Journal of Applied Polymer Science*, *79*, 2156-2163.

Belgacem, M. N., and Gandini, A. (Eds.). (2008). *Materials from vegetable oils: Major sources, properties and applications. Monomers, polymers and composites from renewable resources* (pp. 39-66). Oxford OX5 1GB, UK: Elsevier.

Bongiovanni, R., Montefusco, F., Priola, A., Macchioni, N., Lazzeri, S., Sozzi, L., and Ameduri, B. (2002). High performance UV-cured coatings for wood protection. *Progress in Organic Coatings*, *45*, 359-363.

Boyes, S.G., Chaplin R.P., Davis T.P., Viatos J. and Buxton D.P. (2000). Direct esterification of a hydroxyl functional polyester resin with p-hydroxybenzoic acid Part A: investigation of the direct esterification reaction scheme and characterisation of products. *Progress in Organic Coatings*, *39*, 137-143.

Bussell, G.W. (1974). *U.S. Patent No. 3855163*. Washington, DC: U.S. Patent and Trademark Office.

Chaudhari, A.B., Tatiya, P.D., Hedaoo, R.K., Kulkarni, R.D., Gite, V.V., (2013). Polyurethane prepared from neem oil polyesteramides for self-healing anticorrosive coatings. *Industrial & Engineering Chemistry Research*, *52*, 10189-10197.

Chen Guangxue, Xiaoyuan Guan, Ruixin Xu, Junfei Tian, Minghui He, Wei Shen, Jiamwen Yang (2016). Synthesis and characterization of UV-curable castor oil-based polyfunctional polyurethane acrylate via photo-click chemistry and isocyanate polyurethane reaction. *Progress in Organic Coatings*, *93*, 11-16.

Cheong, M. Y., Ooi, T. L., Salmiah, A., Wan Md Zin, W. Y. and Dzulkefly, D K. (2008). Synthesis and characterization of palm-based resin for UV coating. *Journal of Applied Polymer Science*, *111*(5), 2353-2361.

Chester, W. Fitko (1971). *U.S. Patent No.* 3567494. Washington, DC: U.S. Patent and Trademark Office.

Chia-Wei Chang, Kun-Tsung Lu (2013) Linseed oil based waterborne UV/air dual cured wood coating. *Progress in Organic Coatings*, *76*, 1024-1031.

Chittavanich, P., Miller, K., Soucek, M.D. (2012). A photo curing study of a pigmented UV curable alkyd, *Progress in Organic Coatings*, *73*, 392-400.

Choi Joon suk, JongChul Seo, Sher Bahadar Khan, Eui Sung Jang, Haksoo Han (2011) Effect of acrylic acid on the physical properties of UV-cured poly(urethane acrylate-co-acrylic acid) films for metal coating. *Progress in Organic Coatings*, *71*, 110-116.

Claus, E., Weinell, Soeren Nyborg Rasmussen (2007, March). Advancement in zinc rich epoxy primers for corrosion protection. NACExpo 2007 Conference, Nashville, Tennessee: *NACE international*.

Clayton A May. (1988). Epoxy resins-chemistry and technology. 2nd edition, New York, USA: *Marcel Dekker Inc.*

Crepy, L., Chaveriat, L., Banoub, J., Martin, P., and Joly, N. (2009). Synthesis of cellulose fatty esters as plastics-influence of the degree of substitution and the fatty chain length on mechanical properties. J*ournal of Chemistry and Sustainability, Energy and Materials*, *2*(2), 165-70.

Cunningham, A., Yapp, A. (1974). *U.S. Patent No. 3827993*. Washington, DC: U.S. Patent and Trademark Office.

Danick, C. (2005). Improving flexibility and impact resistance. *Focus on Powder Coatings*, *2005* (1), 4-5.

Deligny, P. (2000). Polyester resins: alkyds & polyesters. P.K.T Oldring (ed.) Second Edition, Exeter, UK: *John Wiley and Sons Ltd in Association with SITA Technology Ltd.*

Dinwoodie, J. M. (1989). Wood, nature's cellular, polymeric, fibre-composite. London, England: *Institute of Metals, The University of Michigan*.

Donald L. Pavia, Gary M. Lampman, George S. Kriz, James R. Vyvyan (2015). Introduction to spectroscopy: A guide for students of organic chemistry. (pp. 14-28) 5th Edition, Washington, USD: *Cengage Learning*.

Dr. Llham Ulkem, Mike Winter (2010). Understanding inorganic zinc rich primers and specification. *Journal of Protective Coatings and Linings*, December 2010, 40-48.

Eckersley, S., A. Rudin. (1990). Mechanism of film formation from polymer latexes. *Journal of Coating Technology, 62* (780), 89-100.

Embong, N.H., Maniam, G.P., Rahim, M.H.A., Lee, K.T., Huisingh, D. (2016). Utilization of palm fatty acid distillate in methyl esters preparation using /TiO_2–SiO_2 as a solid acid catalyst. *Journal of Cleaner Production*, *116*, 244-248.

European Coil Coating Association (1996). Resistance to salt spray fog. EN 13523-8 (2014). Retrieved from https://prepaintedmetal.eu/890/European_test_standards

Force, C. G., F. S. Starr, (1988). *U.S. Patent No. 4740367*. Washington, DC: U.S. Patent and Trademark Office.

Gandini, A. (2009). Epoxy polymers based on renewable resources, in epoxy polymers: New materials and innovation. J.P. Pascault and R.J.J. Williamd (Eds), Weinheim, Germany: *Wiley - VCH Verlag GmbH.*

Gan Seng Neon, Wan Haliza Binti Abd Majid, T.S. Velayutham, A. B. Ahmad (2009). The physical and mechanical properties of polyurethanes from oleic acid polyols, *Journal of Applied Polymer Science*, *112*(6), 3554-3559

Gapor, A.B., Top, M.D., Leong, W.L., Ong, A.S.H., Kawada, T.,Watanabe, H., Tsuchiya, N. (1988). Production of high concentration tocopherols and tocotrienols from palm oil by-product. (Australian Patent No. AU 1989031360). IP Australia.

http://pericles.ipaustralia.gov.au/ols/auspat/applicationDetails.do? Application No =1989031360.

Gapor, A.M.T. (2000, July). In Proceedings of the 2000 national seminar on palm oil mining, refining technology, quality and environment. (pp. 146-151). Pahang, Malaysia. Retrieved from https://mpob.gov.my/printed_publication

Ghosal, A., Shah, J., Kotnala, R.K., Ahmad, S., (2013). Facile green synthesis of Nickel nanostructures using natural polyol and morphology dependent dye adsorption properties. *Journal of Materials Chemistry*, *A 1*, 12868-12878.

Global wood coating market 2018 by manufacturers, regions, type and application, forecast to 2023 ID: PD027177 June 2018 GIR (Global Info Research). Retrieved from https:// www.globalinforesearch.com (accessed on 2 December 2018).

Gummeson, J.J. (1990). Acrylates melamine in UV curable coating. *Journal of Coatings Technology*, *62*(785) 43-49.

Gunstone, F. (1996). Fatty acid and lipid chemistry. London: *Blackie Academic & Professional*.

Haiyan Gu, Kangtai Ren, Dustin Martin, Thomas Marino, Douglas C. Neckers (2002). Cationic UV-cured coatings containing epoxidized soybean oil initiated by new onium salts containing tetrakis(pentafluorophenyl) gallate anion. *Journal of Coatings Technology*, *74*(927), 49-52.

Hanrahan, M. J. (1990). Oxygen inhibition: causes and solutions. *RadTech Report*, March/April, 14-19

Hazimah, A.H., Tuan Noor Maznee, T I., Mohd Norhisham S., Hoong S.S., Ooi T L., Salmiah A., Kosheela Devi P. P. and Cheong, M Y (2008). *U.S. Patent No. 0293913 A1*. Washington, DC: U.S. Patent and Trademark Office.

Hazmi, A.S.A., Aung, M.M., Abdullah, L.C., Salleh, M.Z., Mahmood, M.H. (2013). Producing jatropha oil-based polyol via epoxidation and ring opening. *Industrial Crops and Products*, *50*, 563-567.

Hermas, A.A. (2008). XPS analysis of the passive film formed on austenitic stainless steel coated with conductive polymer. *Corrosion Science*, *50*, 2498-2505.

Hindley Walker, J. & Co. (1965). *U.S. Patent No. 1006587*. Washington, DC: U.S. Patent and Trademark Office.

Hodakowski L.E., Osborn C.L., Harris E.B. (1975). *U.S. Patent No. 4119640*. Washington, DC: U.S. Patent and Trademark Office.

Hohne, G.W.H., Hemminger W.F, and Flammersheim H.J. (2003). Differential scanning calorimetry (pp. 1-8). Second edition. Berlin, Germany: *Springer*.

Hojabri , L. , Kong , X. , and Narine , S.S. (2009). Fatty acid-derived diisocyanate and biobased polyurethane produced from vegetable oil: synthesis, polymerization, and characterization. *Biomacromolecules*, *10*, Article#884.

Holman, R. (1984). UV&EB curing formulation for printing inks coatings & paints. London, England: *SITA Technology Ltd*.

Hoong, S. S., Mazalan, N. M., Mohd Norhisham, S., Tuan Noor Maznee, T. I., Hazimah, A. H., Ooi, T. L., Salmiah, A., Mohd Basri, W., and Yusof, B. (2009). *U.S. Patent No. 7629478 B2*. Washington, DC: U.S. Patent and Trademark Office.

Husbands, M.J., Standen, C.J.S, and Hayward, G. A. (1987). Manual for resins of surface coatings vol III (pp. 153-155). Second Edition. London, England: *SITA Technology Ltd.*

Islam, M. R., Beg, M. D. H., and Jamari, S. S. (2014). Development of vegetable-oil-based polymers. *Journal of Applied Polymer Science*, *131*, Article#40787

Issam, A. M. and Cheun, C.Y. (2009). A Study of the effect of palm oil on the properties of a new alkyd resin. *Malaysian Polymer Journal*, *4*(1), 42-49.

Ivanov, Dušica S., Lević, Jovanka D., Sredanović, Slavica A. (2010). "Fatty acid composition of various soybean products". *Journal of the Institute for Food Technology in Novi Sad*, *37*(2), 65-70.

Jeong, W., Mauldin, T.C., Larock, R.C., and Kessler, M.R. (2009). Bio-based rubbers by concurrent cationic and ring-opening metathesis polymerization of a modified linseed oil. *Macromolecular Materials and Engineering*, *294*, Article#756.

Joseph Edwards (1997). Coating and surface treatment systems for metals: A comprehensive guide to selection. Technology & Engineering, Digitized 2007, Materials Park, Ohio: *ASM International*.

Joseph Francis Ackerman, Cedar Grove, Joseph Weisfeld, Fair Lawn, Robert Georg Savageau, Pompton Lakes, George Beerli, North Arlington, (1972). *U.S. Patent No. 3673140*. Washington, DC: U.S. Patent and Trademark Office.

Kapor, N.Z.A.; Maniam, G.P.; Rahim, M.H.A.; Yusoff, M.M. (2017). Palm fatty acid distillate as a potential source for biodiesel production a review. *Journal of Cleaner Production*, *143*, 1-9.

Kearne, J.D. Ed. (1983). Steel structure painting manual. Vol. I, Good painting practices, 2nd ed., vol. II, System and specifications. 6th ed., (1991). Pittsburgh, USA: *Steel structure painting council.*

Kienle, R. H., Meulen, P. A. van der., Petke, F. E. (1939). The polyhydric alcohol-polybasic acid reaction. IV. Glyceryl phthalate from phthalic acid. *Journal of The American Chemical Society*, *61*(9), 2268-2271.

Kim, H. B., M. Winnik (1995). Factor affecting interdiffusion rate in film prepared from latex particle with a surface rich in acid groups and their salts. *Macromolecules*, *28*, 2033-41.

Kim Teck Teo, Gan, S.N. (1997). Novel water reducible alkyds from palm stearin. *Paint and Ink International*, *October*, 26-30.

Kim Teck Teo, Gan, S.N. (1999). Curing and film properties of palm stearin alkyds. *Pigment and Resin Technology*, *28*, 283-292

Kim Teck Teo, Gan, S.N. (1999). Effects of composition variations and curing conditions on the gloss of water reducible clear coatings prepared from palm stearin alkyds. *Jocca-Surface Coating International*, *82*(1), 31-36.

Knobbe, A.J. (1996). Powder spray guns. *Metal Finishing*, *94* (5A), 225-228.

Kosheela, D. P. P., Hazimah, A. H., Tuan Noor Maznee, T. N., Yeong, S. K., Hoong, S. S., Kushairi, A. and Choo, Y. M. (2015). Optimisation on synthesis of acrylated epoxidized palm olein using response surface methodology. *Journal of Oil Palm Research*, *27*(4), 366-376.

Landry, V., Blanchet, P., and Riedl, B. (2010). Mechanical and optical properties of clay-based nanocomposites coatings for wood flooring. *Progress in Organic Coatings*, *67*, 381-388.

Lee, L.H. (1965). Mechanisms of thermal degradation of phenolic condensation polymers. II. Thermal stability and degradation schemes of epoxy resins. *Journal of Polymer Science*, *3* (3), 859-882.

Lee and Neville (1967). Handbook of epoxy resin. New York, USA: *McGraw-Hill*.

L.F.F. Jacques (2000). Accelerated and outdoor/natural exposure testing of coating. *Progress in Polymer Science*, *25*, 1337-1362.

Liberto, N. (1996). Powder coating equipment. *Metal Finishing*, *94*(5A), 213-224.

Lowe, C., Simmons G.S., (2004). A study on the adhesion and flexibility in radiation-cured coil coatings. *Surface Coatings International Part B: Coatings Transactions*, *87*, 33-39.

Lowe, C. (1994). Test method for UV and EB curable systems. London, England: *SITA Technology Ltd.*

Maetens, D. (2007). Weathering degradation mechanism in polyester powder coatings. *Progress in Organic Coatings*, *58*(2-3), 172-179.

Mahapatra, S.S., Karak, N. (2004). Synthesis and characterization of poly (ester amide) resins from Nahar seed oil for surface coating applications. *Progress in Organic Coatings*, *51*, 103-108.

Malanowki, P. (2009). Weathering of aromatic polyester coatings. Eindhoven: *Technische Universiteit Eindhoven*. https://doi.org/10.6100/IR639672

Meshram, P.D., Puri, R.G., Patil, A.L., Gite, V.V. (2013). Synthesis and characterization of modified cottonseed oil based polyesteramide for coating applications. *Progress in Organic Coatings, 76*, 1144-1150

McConnell, J.A., F.K. Willard (1990). Structure performance relationships of urethane acrylates. Radiation curing of polymeric materials (pp. 272) Hoyle, C.E., Kinstle, J. E., (Eds). ACS symposium series 417, Washington D.C., USA: *American Chemical Society.*

McKee, M.G, Unal, S., Wilkes, G.L., and Long, T.E. (2005). Branched polyesters: recent advances in synthesis and performance. *Progress in Polymer Science*, *30*, 507-539.

Min Min Aung, Zahira Yaakob, Luqman Chuah Abdullah, Marwah Rayung (2015). A comparative study of acrylate oligomer on Jatropa and palm oil-based UV curable surface coating. *Industrial Crops and Products*, *77*, 1047-1052.

Misev, T.A. (1991) Powder caotings: Chemistry and technology. New York, USA: *John Wiley & Sons, Inc.*

Mishra, A.K., Jena, K.K., and Raju, K.V.S.N F. (2009). Synthesis and characterization of hyperbranched polyester-urethane-urea/K10-clay hybrid coatings. *Progress in Organic Coatings*, *64*, 47-56

Mongkolbovornkij, P., Champreda, V., Sutthisripok, W., Laosiripojana, N. (2010). Esterification of industrial-grade palm fatty acid distillate over modified ZrO_2 (with WO^{3-}, $SO^{4-}$and TiO^{2-}): Effects of co-solvent adding and water removal. *Fuel Processing Technology*, *91*, 1510-1516.

Montarnal, D., Cordier, P., Souli e -Ziakovic, C., Tournilhac, F., and Leibler, L. (2008). Synthesis of self-healing supramolecular rubbers from fatty acid derivatives, diethylene triamine, and urea. *Journal of Polymer Science Part A: Polymer Chemistry*, *46*, Article#7925.

Morawetz, H. (1987). Difficulties in the emergence of the polymer concept-An essay. *Angewandte Chemie*, *26*(2), 93-160.

MPOB (2019). *About palm oil*. Official palm oil information source. Retrieved from http://www.palmoilworld.org/about_palmoil.html

Nang, H.L.L., Wafti, N.S.A., May, C.Y. (2009). Production technology of biodiesel from palm fatty acid distillate (PFAD). MPOB TT No. 430. Retrieved from http:// www.palmoilworld.org (accessed on 1 June 2009).

Narin Thanamongkollit, Kent, R. Miller, Mark, D. Soucek (2012). Synthesis of UV curable tung oil and tung oil alkyd. *Progress in Organic Coatings*, *73*, 425-434.

Nurshafiza Shahabudin, Rosiyah Yahya, Seng Neon Gan (2016). Microcapsules filled with a palm oil-based alkyd as healing agent for epoxy matrix. *POLYMERS*, *8*, Article #125.

Ogunniyi, D.S. (2006). Castor oil: a vital industrial raw material. *Bioresource Technology*, *97*, Article #1086.

Okamoto, G., Shibata, T. (1978). The Electrochemical society monograph series, (Chapter 6). New Jersey: *Pennington Publish.*

Ooi, T. L. and Hazimah, A. H. (2001). Oleochemicals and non-food applications of palm products. Lectures on palm oil and its uses on 21st palm oil familiarisation programme (POFP) (pp. 297-305). Hisamuddin, M A and Johari, M (Eds.). Kuala Lumpur: *MPOB.*

Patton T.C., (1962). Alkyd resin technology Vol 20. New York and London: *Interscience.*

Paul, J. Flory (1971). Principles of polymer chemistry. London, England: *Cornell University Press Ltd.*

Paul, S. (1986). Surface coating science and technology. New York, USA: *John Wiley & Sons.*

Perou, A.L., and Vergnaud, J.M. (1997). Correlation between the state of cure of a coil coating and its resistance to liquids. *Polymer Testing*, *16*, 19-31.

Pfister, D. P., Xia, Y., and Larock, R. C. (2011). Recent advances in vegetable oil-based polyurethanes. *Journal of Chemistry and Sustainability, Energy and Materials*, *4*, 703-717.

Pilati, F., Tosselli, M., and Messori, M. (1999). Principles of step polymerisation. In: D. Sanders (Ed.), Waterborne and solvent based saturated polyesters and their end user applications. London, UK: *John Wiley and Sons Ltd in association with SITA Technology Ltd.*

Ping, B.T.Y., Yusof, M. (2009). Characteristics and properties of fatty acid distillates from palm oil. *Oil Palm Bulletin*, *59*, 5-11.

Piper, R. (1965). The hazards of painting and varnishing. *British Journal of Industrial Medicine*, *22*, 247-260.

P.K.T. Oldring, G. Hayward (1995). Resin for surface coatings. Vol I & II. London, England: *SITA Technology Limited*.

Pospisil, J., S. Nespurek (2000). Photo-stabilization of coatings. Mechanisms and performance, *Progress in Polymer Science*, *25*, 1261-1335.

Pramanik, S., Sagar, K., Konwar, B.K., Karak, N. (2012). Synthesis, characterization and properties of a castor oil modified biodegradable poly (ester amide) resin. *Progress in Organic Coatings, 75*, 569-578.

Pranali, P. Chiplunkar, Vinita, V. Shinde, Amit, P. Pratap (2017). Synthesis and application of palm fatty acid distillate-based alkyd resin in liquid detergent. *Journal of Surfactants and Detergents*, *20*(1), 137-149.

Remy van Gorkum, Elisabeth Bouwman (2005). The oxidative drying of alkyd paint catalysed by metal complexes. *Coordination Chemistry Reviews*, *249*, 1709-1728.

Richard Wool, Xiuzhi Susan Sun (2005). Bio-based polymers and composites. Amsterdam; Boston: *Elsevier Academic Press*.

Robison, T. (1994). Thermoplastic powder coatings. *Products Finishing*, *59*(2A), 48-55.

Rochmadi, Budhijanto, Mohammad Fahrurrozi1 (2017, July). Investigation on palm fatty acid distillate (PFAD) based alkyd resin and styrene as a coating material. *Materials Science Forum*, *901*, 173-181.

Rosli, W. D. W., Kumar, R. N., Zah, S. M. and Mohd Hilmi, M (2003). UV radiation curing of epoxidized palm oil-cycloaliphatic diepoxide system induced by cationic photoinitiators for surface coatings. *European Polymer Journal*, *39*, 593-600.

Rossi, S, Deflorian, F, and Fiorenza, J. (2007). Environmental influences on the abrasion resistance of a coil coating system. *Surface Coatings & Technology*, *201*, 7416-7424.

Roussel, P. A. (1984). Technological maturity proves a valid and important concept. *Research Management*, *27*(1), Article #29.

Salmiah, A., Partiban, S. and Dieter, W. (1995). *Singapore patent No. 55223*. Singapore: IPOS; *Malaysian patent MY-114189-A*. Kuala Lumpur: MyIPO.

Schultze, J.W., Lohrengel, M.M. (2000). Stability, reactivity and breakdown of passive films. Problems of recent and future research. *Electrochimica Acta*, *45*, 2499-2513.

Schurr, G.G. (1981) Paint. In: Mark, H.E., Othmer, D.F., Overberger, C.G., Seaborg, G.T. & Grayson, M. (Eds), Kirk-Othmer Encyclopedia of chemical technology (pp. 742–761), 3rd edition Vol. 16, New York, USA: *John Wiley & Sons.*

Shahla Ataei, Yahya, R., Gan, S.N. (2011). Fast physical drying, high water and salt resistant coatings from non-drying vegetable oil. *Progress in Organic Coatings*, *72*, 703-708.

Shakina, J., Sathiya, K. Lekshmi and Allen Gnana Raj, G. (2012). Synthesis and characterisation of novel cross linked biopolyesters from olive oil as eco-friendly biodegradable materials, *E-Journal of Chemistry*, *9*(1), 181-192.

Shanti, K. (2013). Degradation of polymers. *International Journal of Mathematical Sciences, Technology and Humanities*, *82*, 937-940.

Sharmin, E., Ashraf, S.M., Ahmad, S. (2007). Epoxidation, hydroxylation, acrylation and urethanation of Linum usitatissimum seed oil and its derivatives. *European Journal of Lipid Science and Technology*, *109*, 134-146.

Sharmin, E., Zafar, F., Akram, D., Alam, M., and Ahmad, S. (2015). Recent advances in vegetable oils-based environment friendly coatings: A review. *Industrial Crops and Products*, *76*, 215-229.

Singh, B., Sharma, N. (2008). Mechanistic implications of plastic degradation. *Polymer Degradation and Stability*, *93*, 561-584.

Siti Nur Amalina Ramlana, Wan Jefrey Basiruna, Sook-Wai Phangb, Desmond Teck-Chye Ang, (2017). Electrically conductive palm oil-based coating with UV curing ability. *Progress in Organic Coatings*, *112*, 9-17.

Solomon, D.H. (1977). The chemistry of organic film formers. Krieger Publishing Co.

Stoye, D., Freitag, W., and Beuschel, G. (Eds), (1996). Resins for coatings: Chemistry, properties and applications. Cincinnati, Ohio, USA: *Hanser Gardner Publications*.

TA instruments (1997). Modulated DSC compendium, basic theory & experimental considerations. TA-210. New Castle, USA: *TA Instruments*. Retrieved from http://www.tainstruments.com /pdf/ literature/TA210.pdf

Tang, J., Zhang, Z., Song, Z., Chen, L., Hou, X. and Yao, K. (2006). Synthesis and characterization of elastic aliphatic polyesters from sebacic acid, glycol and glycerol. *European Polymer Journal*, *42*, 3360-3366.

Trecker, D.J., Borden, G.W., Smith, O.W. (1976). *U.S. Patent No. 3979270.* Washington, DC: U.S. Patent and Trademark Office.

Tsai, C.J., Chang, W.C., Chen, C.H., Lu, H.Y. and Chen, M. (2008). Synthesis and characterisation of polyesters derived from succinic acid, ethylene glycol and 1,3-propanediol. *European Polymer Journal*, *44*, 2339-2347

Umare, S.S., Chandure, A.S., and Pandey, R.A., (2007). Synthesis, characterization and biodegradable studies of 1,3-propanediol based polyesters. *Polymer Degradation and Stability*, *92*, 464-479.

Uzoh, C. F., Onukwuli, O. D., Odera, R. S., Okey-Onyesolu, C. F. (2013). Synthesis and Characterization of palm oil-based air-drying alkyd resin for surface coating. *Research Journal in Engineering and Applied Sciences*, *2*(3), 187-191.

Vashist, A., Shahabuddin, S., Gupta, Y.K., Ahmad, S. (2013). Polyol induced interpenetrating networks: chitosan–methyl methacrylate based biocompatible and pH responsive hydrogels for drug delivery system. *Journal of Materials Chemistry*, *B 1*, 168-178.

Verhé, R.G. (2004). Industrial products from lipids and proteins in Renewable bioresources: Scope and modification for non-food applications (Chapter 9, pp. 208 – 250). Stevens C.V. and Verhé R.G. (Eds). New York: *John Wiley & Sons, Ltd, Chichester.*

Wick, Z.W., Jones F.N., Pappas, S.P. (1994). Powder coatings. In organic coatings: Science and technology Vol II. New York: *John Wiley & Sons, Inc*.

Wilkes, G.L., McKee, M.G., Unal, S., and Long, T.E. (2005). Branched polyesters: recent advances in synthesis and performance. *Progress in Polymer Science*, *30*, 507-539.

Wypych, G. (1993). Handbook of material weathering. 3rd ed. Toronto: *ChemTec Publishing.*

Wypych, G. (1999). Weathering of plastic testing to mirror real life performance. Norwich, NY: *William Andrew Publishing/Plastics design library*.

Yang Xuejuan, Chunpeng Wang,ab Shouhai Li, Kun Huang,ab Mei Li, Wei Mao, Shan Caoa and Jianling Xia (2017). Study on the synthesis of bio-based epoxy curing agent derived from myrcene and castor oil and the properties of the cured products. RSC Advances, *The Royal Society of Chemistry*, *7*, 238-247.

Zafar, F., Sharmin, E., Ashraf, S.M., Ahmad, S. (2004). Studies on poly(styrene-co-maleic anhydride) modified polyesteramide-based anticorrosive coatings synthesized from a sustainable resource. *Journal of Applied Polymer Science*, *92*, 2538-2544.

Zafar, F., Sharmin, E., Ashraf, S.M., Ahmad, S. (2008). Ambient cured polyesteramide-based anticorrosive coatings from linseed oil—a sustainable resource. *Journal of Applied Polymer Science*, *97*, 1818-1824.

Zengshe Liu, Kenneth M. Doll and Ronald A. Holser (2009). Boron trifluoride catalysed ring opening polymerization of epoxidized Soyabean oil in liquid carbon dioxide. *Journal of Green Chemistry*, *11*, Article#1774.

Zeno W. Wicks, Jr., Douglas A. Wicksb, James W. Rosthauser (2002). Two package waterborne urethane systems. *Progress in Organic Coatings*, *44*, 161-183.

Zhang, J. and Hu, C.P. (2008). Synthesis, characterization and mechanical properties of polyester-based aliphatic polyurethane elastomers containing hyperbranched polyester segments. *European Polymer Journal*, *44*, 3708-3714.

LIST OF PUBLICATIONS AND PAPER PRESENTED

PUBLICATIONS

1. **Kim Teck Teo**, Aziz Hassan, Seng Neon Gan (2018). UV curable urethane acrylate resin from palm fatty acid distillate. *Polymers*, *10*, Article #1374.

2. **Kim Teck Teo,** Aziz Hassan, Seng Neon Gan (2020). Effects of different dicarboxylic acid on the UV-curable urethane resins made from palm fatty acid distillate. *Journal of Coatings Technology and Research*. DOI : 10.1007/s11998-020-00379-4

PAPER PRESENTED

1. **Kim Teck Teo**, Aziz Hassan, Seng Neon Gan. (2016). Synthesis of urethane acrylate from palm fatty acid distillate. Paper presented at International Symposium of Advance Polymeric Materials (IMTCE-ISAMP 2016) under auspices of 10th International Materials and Technology Conference and Exhibition, 16th-19th May 2016, Kuala Lumpur, Malaysia.

   Kim Teck Teo, Aziz Hassan, Seng Neon Gan (2016). Synthesis of urethane acrylate from palm fatty acid distillate. *Polymers Research Journal*, *10*(3), 129-140.

polymers

MDPI

Article

UV-Curable Urethane Acrylate Resin from Palm Fatty Acid Distillate

Kim Teck Teo, Aziz Hassan and Seng Neon Gan *

Chemistry Department, University of Malaya, 50603 Kuala Lumpur, Malaysia;
ktteo@polymerictechnology.com (K.T.T.); ahassan@um.edu.my (A.H.)
* Correspondence: sngan@um.edu.my; Tel.: +603-79674241; Fax: +603-79674193

Received: 15 November 2018; Accepted: 6 December 2018; Published: 11 December 2018

Abstract: Palm fatty acid distillate (PFAD), is a by-product of the crude palm oil refining process. It comprises mainly of free fatty acids—around 45% palmitic and 33% oleic acids—as the major components. Ultra-violet (UV) curable urethane acrylate (UA) oligomers could be synthesized from PFAD, by the following procedure. A hydroxyl terminated macromer was first prepared by reacting PFAD with a mixture of isophthalic acid, phthalic anhydride, neopentagylcol (NPG), and pentaerythritol. The macromer was then reacted with 2-hydroxylethylacrylate (2HEA) and toluene diisocynate (TDI) to generate a resin, containing acrylate side chains for UV curable application. A series of UA resins were prepared by using 15, 25, 45, 55, and 70% of PFAD, respectively. The UA resin has M_w in the range of 3,200 to 27,000. They could be cured by UV irradiation at an intensity of 225 mW/cm^2. Glass transition temperature (T_g) of the cured film was measured by differential scanning calorimeter (DSC), and hardness of the film was determined by a pendulum hardness tester, according to American Society for Testing and Materials (ASTM)4366. The resins were used in a wood-coating application. All of the cured films showed good adhesion, hardness, and chemical resistance except for the one using the 70% PFAD, which did not cure properly.

Keywords: PFAD; urethane acrylate; crosslinking; UV curing; chemical resistance; T_g; pendulum hardness

1. Introduction

The coating industry has always been searching for technological improvements, to achieve greater efficiency, productivity, and lower cost. There are significant contributions that have been made by the resin industry and its ancillaries, particularly, to improve the curing rates and film properties. A coating system without a solvent would be cheaper in cost and more environment-friendly. Thus, radiation curing techniques offer many advantages, such as an energy-saving, VOC (volatile organic compounds) free, and fast curing cycle. One pack UV-curable resin system is a rapidly growing technology within the coating, adhesive, and related industries. It has found a large variety of applications, due to its high efficiency, environment-friendliness, and energy-saving nature [1–3]. The main components in the UV-curable formulation are the unsaturated oligomer, active diluents, and photoinitiator.

Most commercial UV-curable formulations are based on a combination of acrylic oligomers and monomers [4,5], urethane acrylate [6,7] polyester acrylate [8], and epoxy acrylate [9,10]. Properties of the UV-curable coatings are determined by the type of oligomers employed in the formulation. Currently, most available resins are petroleum-based and lacking in natural materials and sustainability.

Depletion of petroleum reserves and increasing environmental concerns have stimulated the revolution to explore materials from readily-available, renewable, and inexpensive natural resources, such as carbohydrates, oils, fats, and proteins. These renewable materials are going to play noteworthy

Polymers **2018**, *10*, 1374; doi:10.3390/polym10121374 www.mdpi.com/journal/polymers

Polymers Research Journal
Volume 10, Number 3

ISSN: 1935-2530

SYNTHESIS OF URETHANE ACRYLATE FROM PALM FATTY ACID DISTILLATE

Kim Teck Teo, Aziz Hassan, and Seng Neon Gan*
Chemistry Department, University of Malaya,
Kuala Lumpur, Malaysia

ABSTRACT

Palm fatty acid distillate (PFAD) is a by-product from the refining of crude palm oil. It comprises mainly of free fatty acids, having around 45% of palmitic and 33% oleic acid as the major components. It has been used as raw material in the making of soap, oleo chemicals and animal feed. This paper reports the synthesis of a urethane acrylate resin from PFAD. A hydroxyl terminated PFAD-based macromer was first prepared with molecular weight (Mw) around 6800 and acid value of **9.8** mgKOH/g and then copolymerized with 2-hydroxylethyl acrylate (2HEA) and toluene diisocynate (TDI). The urethane acrylate resin was produced from further reactions with TDI and characterized by Gel Permeation Chromatography (GPC) and % isocyanate (NCO) by titration. The urethane acrylate resin has Mw 12500 and less than 0.03% NCO. The resin could be cured by Ultra Violet (UV) irradiation using metal halide lamp at intensity of 225mW/cm^2. The reactions could be followed by Fourier transform infrared spectroscopy (FTIR) equipped with Attenuated Total Reflectance (ATR) by monitoring the peak at 810 cm^{-1} due to the unsaturation of the acrylate group. Glass transition temperature (T_g) of the cured film was measured by differential scanning calorimeter (DSC), and hardness of the film was determined by pendulum hardness tester according to ASTM4366. Crosslinking reactions initiated by UV irradiation have caused the decrease in unsaturation, while Tg has increased from 15° to 54°C and pendulum hardness of the film has increased from initial 15 to 105 s. The materials could potentially be applied as industrial wood coatings.

Keyword: PFAD, Urethane acrylate, UV curing kinetic, Tg, Pendulum Hardness

1. INTRODUCTION

Depletion of petroleum reserves and increasing environmental concerns have stimulated the revolution in coating industry to explore the application of polymeric materials from readily available, renewable and inexpensive natural resources, such as carbohydrates,

---

[*] Corresponding author. Tel:+603 79674241; Fax:+603 79674193, Email Address: sngan@um.edu.my

UNIVERSITY OF MALAYA

SENG NEON GAN <sngan@um.edu.my>

Your article in Journal of Coatings Technology and Research (379): Information Required

1 message

Springer <springerauthorquery@springeronline.com> Tue, Jun 16, 2020 at 5:30 AM
Reply-To: customerservice@springer.com
To: sngan@um.edu.my

Springer

Springer: My Publication 15.06.2020

visit us at springer.com

Important Announcement

Dear Author,

Thank you for publishing with Springer. This message is to let you know that your article

- Article title: Effects of Different Dicarboxylic Acid on the UV-curable Urethane Resins Made from Palm Fatty Acid Distillate
- DOI: 10.1007/s11998-020-00379-4

has gone into production. Before we can send you your proofs, we have to ask you to provide some additional information. Please go to the following website (you may need to copy and paste the URL into your browser): https://www.springer.com/home?SGWID=0-0-1003-0-0&aqId=4061659&checkval=926e4c2d1717c18721087aeb50775c42

Please indicate if you would like to:

- order Open Choice, i.e. publish the article as open access. The published version will then become freely available for anyone worldwide in exchange for payment of an open access charge.
- order paper offprints or e-offprints of your article upon issue publication